ELECTROCHEMICAL ETCHING AMPLIFICATION OF LOW-LET RECOIL PARTICLE TRACKS IN POLYMERS FOR FAST NEUTRON DOSIMETRY

A THESIS

Presented to

The Faculty of the Division of Graduate

Studies and Research

by

Mehdi Sohrabi

In Partial Fulfillment

of the Requirements for the Degree

Doctor of Philosophy

in the School of Nuclear Engineering

Georgia Institute of Technology

November, 1975

ELECTROCHEMICAL ETCHING AMPLIFICATION OF LOW-LET RECOIL PARTICLE TRACKS IN POLYMERS FOR FAST NEUTRON DOSIMETRY

Approved:

Karl Z. Morgan, Chairman

Geoffrey G. Eichholz

Don S. Harmer

Date approved by Chairman: Nov. 14, 1975

ACKNOWLEDGMENTS

It is a pleasure to have this opportunity to acknowledge and express thanks for the invaluable support and contributions of many organizations and individuals which made the progress in this work possible. Above all, I wish to express my sincere and deep gratitude to my distinguished thesis advisor, Dr. Karl Z. Morgan, Neely Professor of Nuclear Engineering, for the honor of his invaluable guidance, interest, support, encouragement and patient understanding during the entire course of this study, and for his careful review and valuable editorial and technical comments on this dissertation.

I would like to extend my sincere appreciation to Professor G. G. Eichholz, who has advised me since I joined this institution, for his advice, interest, encouragement, and support, and for his valuable review and comments on this dissertation.

I am sincerely indebted to the other members of my reading committee, Professors F. W. Chambers, R. H. Fetner, D. S. Harmer, and C. J. Roberts, for their advice, interest and encouragement, to Dr. Lynn E. Weaver, Director of the School of Nuclear Engineering for his continuous support, cooperation and understanding, to Dr. P. H. McGinley for his cooperation especially in high energy x-ray irradiations, and to the School of Biology, especially Dr. Fetner, for being generous in lending me some laboratory equipment for long-term use.

I am sincerely grateful to many staff members of the Health Physics Division of Oak Ridge National Laboratory, especially to Dr. J. A.

Auxier, Director of the Division, to Dr. J. W. Poston, and to Mr. F. F. Haywood, who generously gave me valuable advice and assistance during the last five years of close cooperation with them. I am most grateful to Dr. K. Becker for his invaluable guidance, support, and association during our joint research at Oak Ridge National Laboratory. Without this early association with Dr. Becker, it is doubtful that I would have continued my interest in this direction of research.

I would like to express my sincere appreciation to Messrs. D. R. Ward, F. F. Haywood, H. W. Dickson and W. F. Fox (ORNL) for the numerous days of kind cooperation and assistance during the HPRR operation; to Dr. E. W. Thomas (School of Physics, Georgia Tech) for generous cooperation in the use of Georgia Tech's Van de Graaff accelerator; to Dr. J. B. Smathers (Grant No. 12542, Texas A&M University), Dr. J. Eenmaa (University of Washington), and Dr. P. Shapiro (Naval Research Laboratory) for their kind cooperation by providing neutron beam time from their medical cyclotrons and for performing the irradiations; and to Georgia Tech Research Reactor Operations Group and Health Physics Group for their valuable cooperation.

I wish to express my sincere thanks to many individuals in the School of Nuclear Engineering, especially Mr. B. D. Statham for his cooperation and assistance in the design and construction of the high voltage power supply systems, to Mr. W. B. Jeter and Mr. J. M. Burke for their fine machining of the parts used in this study, to Mr. P. D. Field (Nuclear Research Center) for providing some equipment on loan, to Mrs. Lydia Geeslin for her patience and very professional typing of this dissertation and other publications prepared during this study, to Mrs. Phyllis

Frost for the financial management of this project and for her cheering comments which brightened the days, and to my many fellow graduate student friends for their fellowship and association, especially Mr. J. J. Shonka, for his cooperation and willing assistance, Mr. P. S. Stansbury, for his cooperation especially in supplying bone-equivalent fluid, and Dr. T. A. White for his interest and part-time assistance during Summer, 1975.

Special thanks are due to the School of Nuclear Engineering which gave me continuous support and authority to establish and continue this research program, the U. S. Energy Research and Development Administration, Division of Biomedical and Environmental Research, for the support of this project under Contract No. AT-(40-1)-4814, the Health Physics Division, Oak Ridge National Laboratory, which was considered a home laboratory for the author and for partial equipment and facility support under Subcontract No. 3921.

Special thanks are also due to my many colleagues in the University of Tehran and the Atomic Energy Organization of Iran, the International Atomic Energy Agency, and the U. S. National Academy of Sciences for cooperation in permitting the continuation of my studies toward this degree.

Finally, and most importantly, I wish to give special thanks to my parents, especially my mother, and to my brothers and sisters for their support and confidence in me which always inspired my studies.

TABLE OF CONTENTS

TABLE OF CONTENTS (Concluded)

LIST OF TABLES

LIST OF ILLUSTRATIONS

LIST OF ILLUSTRATIONS (Continued)

LIST OF ILLUSTRATIONS (Continued)

LIST OF ILLUSTRATIONS (Continued)

LIST OF ILLUSTRATIONS (Continued)

LIST OF ILLUSTRATIONS (Continued)

LIST OF ILLUSTRATIONS (Concluded)

SUMMARY

Neutron dosimetry is a problem of concern in many areas of health physics and radiotherapy. Considering the present state-of-the-art of fast neutron dosimetry, new developments and improvements in this area seemed desirable and justified a detailed experimental investigation. Among the numerous methods being studied are various track-etch methods in which the damage regions left by the passage of heavy charged particles in appropriate insulators are enlarged by subsequent etching procedures to make them more readily visible.

An electrochemical etching method for the amplification of fast-neutron-induced recoil particle tracks in polymers was investigated. The technique gave superior results over those obtained by conventional etching methods especially when polycarbonate foils were used for recoil particle track amplification.

Electrochemical etching systems capable of multi-foil processing were designed and constructed to demonstrate the feasibility of the technique for large-scale neutron dosimetry. Electrochemical etching parameters were studied including the nature or type of the polymer foil used, foil thickness and its effect on etching time, the applied voltage and its frequency, the chemical composition, concentration, and temperature of the etchant, distance and angle between the electrodes, and the type of particles such as recoil particles including protons. Recoil particle track density, mean track diameter, and optical density as functions of the mentioned parameters were determined. Each parameter was found to

have a distinct effect on the etching results in terms of the measured responses.

Several new characteristics of this fast neutron dosimetry method were studied especially for personnel dosimetry using various radiation sources such as nuclear reactors, medical cyclotrons, and isotopic neutron sources. The dose range, neutron energy dependence, directional response, fading characteristics, neutron threshold energy, etc. were investigated.

The neutron dosimetry technique under this investigation is relatively insensitive to high doses of x- and gamma rays (e.g. 10^4 rad); it has dose-equivalent response (rem) and it provides high spatial resolution. It was used for measurement of dose-equivalent of fast neutron contamination in high energy x-ray beams from medical betatrons and some results are reported here. Also some studies were conducted to compare the response of this dosimeter as a function of depth in bone-equivalent fluid and plastic and tissue-equivalent fluid inside an elliptical phantom. Both bone-equivalent materials performed equally well for fission neutrons; however, bone-equivalent fluid provides more flexibility for heterogeneity effect studies. Some results on the neutron dose distributions near bone-tissue and air-tissue interfaces inside a cubical phantom are reported also.

In conclusion, a neutron dosimetry technique is presented in which sensitivity and track diameter can be controlled simply by some of the parameters governing the electrochemical etching results. This neutron dosimetry approach provides simplicity, flexibility, and feasibility for large-scale neutron dosimetry. It has promising applications, especially for fast neutron personnel dosimetry since it provides many advantages

over proton track registration in nuclear track emulsions and fission fragment registration techniques. As another approach, spark counting of recoil particle tracks in conventionally-etched thin polycarbonate foils (six μm) was also investigated and did not prove to be as feasible as the above approach.

CHAPTER I

INTRODUCTION

Due to the vast increase in the number and scope of nuclear power operations, high voltage accelerators, and intense isotopic neutron sources, there is a great need for the development of improved neutron dosimetry techniques for many health physics and radiotherapy areas. One problem of considerable interest is the monitoring of personnel working with these facilities, especially with fast neutron sources. Therefore, a neutron dosimeter that avoids many shortcomings associated with nuclear track emulsions such as post-irradiation fading, fogging by other types of radiation, tedious microscopic counting, limited dose range, etc. is badly needed.

There are also many areas in radiotherapy, human radiography, and radiobiology where there is a need for a small, low cost, tissue-equivalent, neutron-sensitive dosimeter that would be insensitive to x, beta, and gamma radiations and that would have a high spatial resolution. Obtaining information on neutron dose distributions near biological interfaces such as bone-tissue and air-tissue interfaces is of growing concern to many health physicists and biomedical researchers. Monitoring of patients undergoing neutron therapy is of great importance to medical physicists. Furthermore, growing applications such as output measurements of neutron sources, dosimetry intercomparisons, area monitoring, fast neutron contamination measurements in high energy x-ray beams produced

by betatrons and linear accelerators all point to the need for an integrating instrument having some of the features mentioned above.

No single and simple integrating fast neutron dosimetry technique is available to satisfy all the requirements of a good dosimeter for the above applications. Among the various existing techniques having the potential of being improved, it appeared that track-etch methods are among the most promising. In this method, charged particles bombarding a sensitive insulator (especially polymers) produce a narrow trail of damage along their trajectory. These damaged regions can be made visible by a chemical method so that they are etched more readily than surrounding undamaged material, leading to enlarged holes or tracks. These tracks can be detected and counted by various methods such as visual counting, densitometry, and many other methods described in Chapter III.

In this dissertation, a new electrochemical etching method proposed by Tommasino (1970) is studied for the amplification of fast-neutron-induced recoil particle tracks in polymers (Sohrabi and Becker, 1971; Sohrabi, 1974). This appears to be a superior technique leading to amplified tracks in many polymers, especially in Lexan polycarbonate. The characteristics of this technique including parameters affecting the etching of recoil particle tracks and its capability for large-scale neutron dosimetry were studied and are discussed in this manuscript. These results help to provide a better understanding of the physics of the technique as well as to provide some knowledge on how best to control the electrochemical parameters for dosimetry applications. Also, the characteristics of the dosimeters developed in this investigation were determined as applied to various neutron dosimetry problems. As another

approach, a preliminary investigation of spark counting of recoil particle tracks in conventionally-etched thin polycarbonate foils (6 μm) has also been explored.

1.1 Technological Considerations

1.1.1 Development of Neutron Dosimeters

The discovery of neutrons by Chadwick (1932) attracted the interest of many scientists and technologists in employing neutrons in many radiobiological and physical studies. This led to a rapid development in nuclear technology and for devices to generate beams of neutrons and charged particles capable of producing intense ionization. Thus the prospect for large-scale neutron research, nuclear power operations, accelerators producing high energy particles, and intense isotopic neutron sources, etc. grew significantly in a relatively short time. This rapid development increased also the potential for excessive irradiation of a growing number of radiation workers. Therefore, a need for the measurement of mixtures of neutrons, gamma rays, and other newly discovered particles was obvious. A number of techniques was developed and many devices were designed and placed in service to measure beam output and energy spectrum and for dosimetry in problems arising in area monitoring, personnel monitoring, accident dosimetry, and a variety of other health physics and biomedical related applications.

Of particular concern is neutron dose measurement because of the high biological effectiveness of neutrons. Here one needs to determine the neutron absorbed dose, D, or dose equivalent, H, at a point of interest in a radiation field to relate the biological damage it causes to the human body or a particular organ. This process is called neutron dosimetry.

Although there is a superficial similarity between neutrons and gamma rays, dosimetry of either type in the presence of the other causes some difficulties. Gamma dosimetry is simpler because some gamma dosimeters are relatively neutron insensitive and in many practical situations gamma fields are neutron free. However, in the case of neutron fields, gamma rays almost always accompany them with varying intensity depending on the nature of the source and its geometry, shielding conditions, etc. Therefore, a suitable dosimetry system must be capable of determining both neutron and gamma absorbed doses separately as well as the dose equivalent of the mixture.

Many neutron dosimetry methods including ionization, scintillation, activation, and solid state dosimetry methods have been developed for various applications. Discussion and detailed information on all existing techniques deserving of mention are beyond the scope of this brief review and are given in many textbooks such as those by Morgan and Turner (1973), Attix et al. (1969), and Becker (1973). Therefore, a brief discussion of some methods used for neutron beam measurements and depth dose studies, area monitoring, spectrum measurements, and especially neutron personnel dosimetry are given in the following.

The oldest, most widespread, and useful method of neutron dose measurement in a beam, inside a phantom or in many other areas of application, has been the use of ionization chamber techniques. In this method, the ionization produced inside a gas-filled chamber is measured and is converted to dose. Gray and Read (1939) described the use of tissue-equivalent ionization chambers for neutron dose measurements in their biological experiments. Stone and Larkin (1942) carried out the measure-

ments of their neutron beam by a condenser type ionization chamber. Many developments have been made since then in the design of ionization chambers to satisfy better the Bragg-Gray conditions (Burlin, 1968) that the cavity should be a small fraction of and the wall thickness be greater than the range of the charged particles which cross the chamber. Therefore, in practical dosimetry small and homogeneous ionization chambers with a wall thicker than the range of secondary charged particles have been designed for neutron and gamma dosimetry in a radiation field.

Rossi and Failla (1956) introduced a paired ionization chamber to separate neutron and gamma dose in a mixed field of neutrons and gamma rays. This dosimetry system consists of two chambers, one which is sensitive to both neutrons and gamma rays and is constructed of tissue-equivalent (TE) materials and filled with tissue-equivalent gas. The other chamber is much less sensitive to neutrons having a graphite wall filled with CO_2 gas; therefore, both chambers maintain their homogeneity. Because of the differing sensitivity of the two chambers to neutrons and gamma rays, the dose components cannot be obtained directly, but from a pair of equations given in terms of reading the two calibrated chambers. The error in the measurements may be quite large, especially when the neutron dose and gamma dose are comparable. Therefore, in some experiments the gamma dose can be measured separately by a single-ion detector (Wagner and Hurst, 1961), or by neutron-insensitive solid state integrating devices such as CaF_2 : Mn, or ^7LiF, etc. (Bewley and Parnell, 1969; McGinley, 1971; Attix et al., 1973), while the total dose can be measured by the tissue-equivalent ionization chamber. Another shortcoming of the Rossi-Failla paired chamber method is that the graphite chamber responds

not only to gamma radiation but also to neutron production of recoil carbon ions and this response depends on the energy of the neutrons. Therefore, for accurate measurements the neutron energy spectrum must be known (Hurst, 1973).

Measurement and compensation of gamma dose can also be done by the use of compensated ionization chambers consisting of a concentric pair of cylindrical chambers, the inner having a hydrogenous and the outer a non-hydrogenous wall (Bewley and Parnell, 1969). This system is insensitive to gamma rays and has been used for depth dose studies. However, again the energy dependent carbon recoil response of the graphite chamber introduces an error in the measurement.

Proportional counters relying on fast-neutron-induced proton recoil measurements have been designed by Hurst and Ritchie (1953). One design (the Hurst count-rate dosimeter) makes use of a combination of proton radiators, aluminum absorbers, and methane counting gas such that the count rate is directly proportional to the neutron dose. Another chamber (the Hurst absolute proportional counter) uses a polyethylene inner wall with a thickness greater than the range of the most energetic protons and is filled with ethylene gas to satisfy Bragg-Gray theory. The appropriate neutron energy response is obtained by use of an especially designed binary scalar circuit or a multichannel analyzer. The chambers can discriminate against gamma rays and a neutron dose rate of one mrad per hour can be measured in the presence of 100 rads per hour of gamma radiation. These chambers are large and a smaller counter has been designed for neutron dose measurements in phantoms. This is called a "phantom counter" (Hurst and Ritchie, 1953; for details see Morgan and

Turner, 1973).

Special types of proportional counters have been designed to obtain neutron dose in radiation fields and in phantoms and to provide information on the LET spectrum of secondary charged particles produced by neutrons, which is of immediate interest for planning radiobiological experiments as well as for radiation protection purposes (Rossi and Rosenzweig, 1955). The counters have a wall of TE plastic and are filled with a counting gas at a certain pressure. By obtaining the pulse height spectrum and utilizing a mathematical relation, one can obtain neutron dose and information on dose as a function of LET.

Organic scintillators having tissue-like compositions are detectors of interest for neutron dosimetry. Lawson and Watt (1964) and Watt et al. (1967) designed and used an "NE 102" organic scintillator between two hydrogenous materials to establish charged particle equilibrium and to satisfy the Bragg-Gray principle. The dosimeter has many advantages and disadvantages that have been reviewed by Tochilin and Shumway (1969).

Although the neutron dosimeters reviewed above have useful characteristics for a variety of applications, they do not provide adequate spatial resolution for neutron depth dose studies at biological interfaces unless uniquely arranged dosimeters are designed or other special methods are applied. An elaborate method of this kind is the extrapolation ionization chamber consisting of an adjustable sensitive volume permitting one to measure the ionization produced per unit volume for a range of electrode gap spacings extrapolated to zero (Failla, 1937; Wingate et al., 1962). Extrapolation chambers constructed of tissue-equivalent and bone-equivalent materials have been used also to measure

neutron absorbed dose in tissue and bone at bone-tissue interfaces in a heterogeneous phantom (Poston, 1971). Another especially designed chamber is a disk-shaped TE plastic ionization chamber having various thicknesses. It has been used to investigate the manner in which charged particle equilibrium takes place in a human phantom (Goodman, 1969a).

Some other techniques have been developed which give additional information about dose and/or the neutron spectrum. For thermal neutron detection boron-lined or BF_3 gas filled proportional counters have been used for dosimetry in and around biological phantoms (Boot and Dennis, 1968). Inorganic scintillators such as ^{6}LiI(Eu) are highly sensitive thermal neutron detectors. These detectors have been made useful for fast neutron dosimetry by using polyethylene spheres around the detectors (Bramblett et al., 1960). Foils such as ^{235}U-insulator, or ^{10}B-insulator combinations based on track-etch methods may also be placed in the center of a polyethylene sphere or a water container for fast neutron area monitoring (Rago et al., 1974). Changing the radii of the spheres discriminates neutrons of different energies thus providing some information on the neutron spectrum which is essential in estimating the dose. For example, indium foils inside spheres of different radii have been used to measure the neutron contamination spectrum of a 25 MV x-ray beam produced by a betatron (Briden and Ice, 1972). Such combinations of spheres are usually bulky; this limits their applications to areas such as neutron monitoring around facilities where there is no space limitation. Also some of these systems are little better than fast neutron detectors or flux meters because of their failure to take into proper account the energies of the neutrons.

For spectrum measurements inside fast neutron beams, techniques such as time-of-flight measurements have been used (Theus et al., 1974). For neutron dosimetry and spectral information on neutron beams from reactors or in criticality accidents, the Hurst threshold detector system is used (Hurst and Ritchie, 1959). This detection system is based on activation of many elements including ^{239}Pu, ^{237}Np, ^{238}U, and ^{32}S foils, enclosed in a ^{10}B sphere where they have threshold energies of 10 keV, 0.6 MeV, 1.5 MeV, and 3.0 MeV, respectively. Fission fragment track recorders have also been incorporated into the Hurst threshold system for reactor spectrum measurements (Kerr and Strickler, 1966). Combinations of S, Al, Fe, Ag, Mg, and Cu having different neutron energy detection thresholds have been used also for spectrum measurements inside a human phantom (Field and Parnell, 1965).

For neutron personnel dosimetry, an integrating dosimetry technique which can accumulate the neutron dose over a period of time is required. A good neutron personnel dosimeter should be:

1. sensitive to neutrons over a wide dose range to cover routine and accidental dosimetry (i.e. from 0.001 to 1000 rad);

2. insensitive to non-ionizing radiation and to other types of ionizing radiations such as x, beta, and gamma radiations, or it should have at least a good compensation system included in the design;

3. provided with a wide energy response to follow kerma or rem curves recommended by appropriate legislative authority;

4. independent of the orientation of the radiation impinging on the dosimeter since the direction of incident neutrons is not always known;

5. possessed of nil or at least tolerable post-irradiation fading rates, i.e. it must retain the radiation induced effect for the period of interest;

6. simple, rugged, inexpensive, and easily available;

7. inexpensive and easy to read rapidly;

8. designed to require minimal training for its operation; and

9. capable of providing the possibility for dosimetry intercomparison by mail and being applied to other areas of applications.

The specifications listed above for neutron personnel dosimeters also can be considered for neutron dosimeters to be used in other applications. However, in some cases there are further requirements and in others certain requirements may be ignored. For example, depth dose studies, in particular at biological interfaces such as at bone-tissue interfaces, require a dosimeter of high spatial resolution. Furthermore, if many of these dosimeters can be placed simultaneously inside the phantom, this eliminates uncertainties associated with beam fluctuations and machine time provided that the dosimeters do not disturb the radiation field. Patient monitoring requires a dosimeter capable of measuring high neutron doses in the beam and low neutron doses outside the beam. In practice, activation of aluminum foil or silicon diodes are dosimetry methods used to monitor a patient under a neutron therapy trial. An example of an extreme condition is the neutron contamination dose measurement in the presence of high photon doses such as in high energy x-ray beams. Such contamination usually contributes only a very low percentage of the total dose under normal operating conditions.

Up to the time of this investigation, no neutron dosimeter existed

which satisfied the above mentioned requirements. However, proton track registration in special nuclear track emulsions has been the only method of widespread use for neutron personnel monitoring for over thirty years (Morgan, 1946; Cheka, 1947, 1954). The number of knock-on proton tracks produced by elastic scattering of fast neutrons with hydrogen atoms present in the emulsion or surrounding materials is a measure of fast neutron flux to which the person is exposed. Thermal neutrons interacting with nitrogen atoms present in the emulsion and its surroundings also produce some tracks due to protons by the reaction $^{14}N(n,p)^{14}C$. Discrimination of these tracks from those of fast-neutron-induced protons is necessary by shielding some portion of the film by cadmium filters. However, the emulsion detection method indicates the flux and not the absorbed dose and is insensitive in the energy range from thermal to 0.7 MeV. There are some variations in this threshold energy reported by different investigators which are due mainly to the skill of the track reader and gamma contamination of the beam.

Neutron dosimetry by nuclear track emulsions has a number of drawbacks (Vallario and Hankins, 1973). These drawbacks mainly include serious fading of the latent "image," tedious microscopic counting which usually requires magnifications of 500 to 900 times, fogging by other types of radiations which affects both fast neutron energy threshold and dose range and makes track counting impossible in some cases, insensitivity to neutrons from thermal to 0.7 MeV, failure to respond closely to the appropriate energy loss in tissue when taking into account the element distribution in soft tissue and the quality factors, low sensitivity and lack of accuracy at low neutron doses, and limited dose range. Due to

these shortcomings some have gone so far as to recommend that the nuclear track emulsion technique be discontinued even if there were no replacement technique (Becker, 1973). Therefore, in recent years many attempts have been made to develop an alternative method to the nuclear track emulsion method for neutron personnel dosimetry. The alternative methods can be categorized into four groups:

1. albedo neutron dosimetry methods,
2. fission fragment registration methods,
3. recoil particle registration methods, and
4. other methods.

Albedo neutron dosimetry is based on detection of thermalized neutrons reflected from the body of a person under neutron exposure. It generally consists of one or two pairs of ^{6}LiF and ^{7}LiF TLD dosimeters covered in such a way as to detect only thermal neutrons backscattered from the body. A successful dosimeter of this kind designed by Hoy (1972) is in use at the Savannah River Laboratory. Hankins (1973) has reviewed the design and characteristics of different albedo neutron dosimetry systems investigated at different laboratories. This class of neutron dosimetry is very sensitive in the energy range in which nuclear track emulsions are insensitive, i.e. from thermal to 0.7 MeV. However, it has many characteristic disadvantages. Hankins (1973) has reviewed some of the sources of error associated with the use of these types of dosimeters, such as errors caused by the effect of varying the distance of the dosimeter from the body, TLD reading errors, etc. The main disadvantage of this type of dosimeter, however, is its neutron-energy dependence, i.e. response decreases with increase in neutron energy. Although methods

have been applied to improve this energy dependence (Piesch and Burgkhardt, 1973), albedo neutron dosimetry techniques are generally complex and, because of their poor energy dependence, they are accepted only in areas where the neutron energy spectrum is known. They have some sensitivity to gamma radiations which can be compensated by the use of ^{7}LiF dosimeters. The TLD dosimeter has the added disadvantage that a reading can be carried out only one time. The application of this system is limited mainly to personnel dosimetry.

Fission fragment and fast-neutron-induced recoil particle track registration techniques have shown considerable promise for neutron dosimetry, especially for fast neutron personnel dosimetry. Although their applications to personnel dosimetry show great promise, they are only mentioned here to avoid undue repetition since they are described in some detail in section 1.2.

Many attempts have been made to develop other alternative neutron personnel dosimetry methods. These methods have been concerned mainly with solid state dosimetry techniques such as thermoluminescent dosimeters (TLD), radiophotoluminescent glass dosimeters (RPL), thermally-stimulated exoelectron emission dosimeters (TSEE), and pocket-size ionization chambers. Each of these dosimetry methods consists of a wide variety of materials and methods and has provided means for gamma, beta, x-ray, and neutron dosimetry (for reviews see Auxier, 1967; Becker, 1973; Attix et al., 1966). Some of these dosimeters contain isotopes such as ^{10}B or ^{6}Li (e.g. in the form of ^{6}LiF) or materials which can produce induced activity to increase the sensitivity for thermal neutron dosimetry. However, they generally lack hydrogen which makes them insensitive to fast

neutrons. Thus, either thermal neutron sensitive meters such as ^{6}LiF are used in albedo neutron dosimeters as stated above or some hydrogenous materials have been incorporated into or in contact with some TLD or TSEE dosimeters (Becker, 1973) to enhance fast-neutron sensitivity. The albedo dosimetry methods have attracted a limited amount of interest for routine use; although the other approaches have been the subject of some preliminary investigations, nevertheless they have not provided satisfactory results to be applied in routine use.

Pocket-size ionization chambers are in widespread use for gamma ray dosimetry and when they are boron-lined, they provide sensitive dosimeters for thermal neutrons. Polyethylene-lined chambers with built-in gamma ray compensation have been studied for fast neutron dosimetry (Tymons and Cooper, 1975). These dosimeters, whether used for gamma rays or for neutrons, are usually intended for short-term dosimetry (e.g. to monitor dose received on an eight hour shift).

For high neutron dose levels such as might occur during a criticality accident, neutron personnel dose can be assessed by many means. The common method is to incorporate in the personnel badge activation foils such as indium or gold (both bare and cadmium-covered) and sulfur pellets (Gupton and Davis, 1973). Materials such as rhodium-103 foils have been studied also and proposed for use in a personnel badge which gives a kerma response to fast neutrons similar to that in soft tissue providing some neutron energy independence in the range from 0.75 MeV to 10 MeV (Ing and Cross, 1973). Dosimeters such as RPL phosphate glasses relying on activation of silver and phosphor in the glass have been studied for accident dosimetry (Piesch, 1972). Activation of body elements such as sodium

contained in the human body and sulfur contained in human hair can be used also for a rapid estimation of thermal and fast neutron dose to various parts of the human body (Hurst and Ritchie, 1959). This requires a separate measurement (or estimate) of the neutron energy distribution.

1.1.2 Charged Particle Track Etching in Solid Insulators

In this method heavy charged particles passing through certain solid insulators produce thin trails of damage along their trajectories. The damaged region can be chemically etched so that the tracks may be observed by a light microscope or they may be observed easily by the unaided eye after a suitable development.

Charged particle track etching in solid insulators including certain minerals (e.g. mica, quartz), inorganic glasses, and organic polymers provides a number of attractive features for many applications. The most attractive features of this technique are insensitivity to low-LET radiations such as x, beta, and gamma radiations, and flexibility for adaptation to applications in many fields including nuclear physics, chemistry, biology, space research, geochronology, neutron radiography, and neutron dosimetry (for review see Becker, 1973; Fleischer et al., 1975), which is of particular interest in this investigation.

The advancement in this field has been so rapid that within fifteen years over a thousand papers investigating basic mechanisms of track formation, etching of damage sites, track counting methods, and many applications have been published (Griffith, 1974). This new research area was made after the discovery of Young (1958) who observed fission fragment tracks in lithium fluoride crystal etched in mixtures of hydrofluoric and acetic acids. In 1959, Silk and Barnes observed fission fragment tracks

in mica by electron microscopy. However, the pioneering work and discoveries of Fleischer, Price, and Walker on the preferential etching of charged particle tracks in solid insulators paved the way for rapid advancement in this field (Price and Walker, 1962; Fleischer and Price, 1963; Walker et al., 1963; Fleischer et al., 1965a).

Experimentally, in order to observe and count particle tracks in insulators two main steps are followed:

1. bombardment of a suitable insulator by heavy charged particles or fast neutrons to produce induced recoil tracks, and

2. enlargement of the damaged sites by an etching method to a point such that they can be detected by many methods.

Although more detailed information on the above steps is given in Chapter III a brief review of the above is given in the following as applied to the neutron dosimetry problem.

Two bombardment methods (i.e. external and internal) are usually applied depending on the application and type of particles of interest. External bombardment of an insulator takes place from heavy charged particle bombardment from accelerators or by particles produced by conversion screens in contact with the insulator. Internal bombardment of a sensitive polymer (e.g. polycarbonate, cellulose nitrate, etc.) results when particles such as fast neutrons bombard a polymer leading to secondary recoil particle and (n,α) tracks induced in the polymer.

External bombardment methods using conversion screens have been used in many dosimetry applications. Examples of such conversion screens include fissionable materials resulting in (n,f) reactions under neutron exposure and materials such as ^{6}Li and ^{10}B to produce alpha particles

under thermal neutron irradiations. The fission fragment registration method proposed by Walker et al. (1963) has been the subject of many aplications, in particular in radiobiology (Bleaney, 1969; Jee et al., 1972; Cole et al., 1970) and in neutron dosimetry (Kerr and Strickler, 1966; Becker, 1967; Prêtre et al., 1968; Sohrabi, 1969; Sohrabi and Becker, 1971, 1972; Gold et al., 1974; Cross and Tommasino, 1968; Cross and Ing, 1975a). Alpha particle registration in sensitive polymers has been incorporated in radon progeny dosimeters (Auxier et al., 1970). Converters using ^{6}Li or ^{10}B have also been applied for the detection of thermal and intermediate energy neutrons (Becker, 1969a; Tymons et al., 1973).

The fission fragment registration method for neutron dosimetry is an attractive alternative to the use of NTA emulsions. Its sensitivity, stability, energy response, dynamic range, directional response, insensitivity to x, beta, and gamma radiations are far superior to those of NTA films. The fission fragment registration method meets many requirements of a satisfactory neutron personnel dosimeter and fission fragment track counting can be automated easily by a spark counting method (Cross and Tommasino, 1970). However, utilization of fissionable materials on the human body adds considerably to the cost, contamination risk, and complexity of the system as a personnel dosimeter.

Several fissile materials have been investigated for neutron personnel dosimetry including ^{239}Pu, ^{238}U, ^{232}Th, ^{237}Np, and ^{235}U. The high radiotoxicity of ^{239}Pu and long-term alpha exposure causing damage to the polymer foils in contact with ^{239}Pu make this method impractical and it would be likely to result in regulatory and administrative problems if used for personnel monitoring. The high spontaneous fission rate of ^{238}U

causes a considerable background increase over long periods of time as usually is the case in personnel dosimetry. From the point of view of spontaneous fission, ^{232}Th with a spontaneous fission half-life of 10^{21} years is superior to ^{237}Np ($> 10^{18}$y), ^{235}U ($\sim 2 \times 10^{17}$y), and ^{238}U ($> 6.5 \times 10^{15}$y) (Sohrabi and Becker, 1971).

Characteristics of ^{232}Th and ^{237}Np as components of fast neutron personnel dosimeters have been the subject of some studies (Cross and Ing, 1975a; Sohrabi and Becker, 1971). Neptunium-237 having a neutron threshold energy of 0.6 MeV for (n,f) reactions compared to 1.5 for ^{232}Th, and a fission cross section about 12 times larger than that of ^{232}Th, gives a superior performance. Cross and Ing (1975a) carried out extensive studies on the energy response and sensitivity of the ^{237}Np-polycarbonate foil method. Neptunium-237 has an energy response which is nearly proportional to tissue kerma or dose equivalent (Cross and Ing, 1975a). However, both ^{237}Np and ^{232}Th have attracted interest for fast neutron personnel dosimetry and are in routine use for personnel monitoring and for finger dosimetry in glove boxes in some laboratories (see Becker, 1973).

By diluting or reducing the amount of fissionable materials the technique can be applied for emergency personnel dosimetry. By using alloys of two or three fissionable materials the response of the detector system also can be adjusted to follow the energy response curves given by ICRP (Prêtre et al., 1968). An alloy consisting of 0.5 percent (by weight) of natural uranium and 99.5 percent ^{232}Th has been applied for this purpose.

In most neutron environments measurement of dose of fast neutrons having energy below one MeV and epithermal neutrons is essential. Gold

et al. (1974) have developed a personnel dosimeter consisting of two thick ^{235}U foils (93.1% enriched) in contact with two pre-etched mica foils to be used in routine monitoring of personnel around the ZPR facility at the Argonne National Laboratory. One set of fission foil-mica combinations is covered with aluminum and the other is totally enclosed in cadmium to separate the thermal neutron component of the dose. The tracks can be counted by a computer controlled microscope (Cohn and Armani, 1974).

A second irradiation method, i.e. registration of tracks induced directly inside the polymers by particles such as fast neutrons, is more attractive since it does not require use of any fissionable material or any other conversion screens and is the subject of this dissertation. This can be accomplished by exposing polymers such as polycarbonate $(C_{16}H_{14}O_3)_n$ or cellulose nitrate $(C_6H_8O_9N_2)_n$ directly to fast neutrons. The tracks observed are due to recoil carbon, oxygen, nitrogen, and alpha particle tracks from threshold reactions such as $^{16}O(n,\alpha)^{13}C$ and $^{12}C(n,n,\gamma)3\alpha$. Very importantly also, we believe it is shown in this research that tracks are observed which are produced by hydrogen atoms that are elastically scattered by the fast neutrons. This technique has been known for a decade (Medveczky and Somogi, 1966) and has been the subject of some fast neutron flux and dosimetry studies (Becker, 1967; Tuyn, 1969; Piesch, 1970; Price et al., 1971; Sohrabi and Becker, 1971; Frank and Benton, 1970).

Unlike fission fragment tracks which are formed by external radiators only on the surface of the insulator, recoil particle tracks induced by fast neutrons are distributed throughout the polymer foil. However,

only those in contact with the etchant will be developed. By increasing the etching time the number of tracks increases reaching an equilibrium between the tracks which are etched away near the surface and those freshly etched deeper below the surface.

Although elastic scattering with the elements in the polymer occurs at all neutron energies, only recoil particles causing a damage density above a threshold value can be registered (see Chapter III). Since polymers have various energy thresholds for charged particle track registrations, depending on their composition, they show different neutron sensitivities (tracks/neutron) and different neutron energy thresholds. For example, the sensitivity of some polymers is 0.5 to 3 x 10^{-5} tracks/neutron depending on the neutron energy and etching conditions (Becker, 1967). These sensitivities are comparable to those of the fission fragment registration techniques mentioned above. The neutron energy dependence of some polymers such as cellulose acetate appears to follow the first collision tissue dose quite well down to a threshold between about 0.5 to 1.2 MeV, depending on the sensitivity of the material (Becker, 1969b).

Polycarbonate foils which have many good characteristics for dosimetric applications have a threshold energy around one MeV (Jozefowicz, 1971, 1973). It has been estimated that most sensitive polymers have threshold energies around 0.3 to 0.7 MeV (Becker, 1973). The higher sensitivities in these polymers, for example in cellulose nitrate, seem to be due to lower energy threshold for registration of lower LET recoil particles including protons which have been observed in some investigations (Varnagy et al., 1970; Carpenter and LaFleur, 1972; Lück, 1974; and this investigation). However, there has been some doubt expressed as to

whether or not proton track registration really takes place in polycarbonates.

Neutron dosimetry by fast-neutron-induced recoil particle tracks in polymers is very simple, inexpensive, and attractive for practical applications and avoids problems associated with using fissionable conversion screens. However, neutron personnel dosimetry by this method has been hampered by the fact that the tracks developed by previously developed methods are small and tedious to count by a microscope making dosimetry in general difficult and impractical at low neutron fluences. Therefore, prior to this publication, this technique has been recommended only for fast neutron personnel dosimetry in criticality accidents (Piesch, 1970). Furthermore, recoil particle track registration in NTA film backing has been studied and recommended for use in criticality accidents above the upper limit of sensitivity commonly encountered for NTA photographic films (Jasiak and Piesch, 1975; Sohrabi and Becker, 1971), which can be etched by removing the emulsion. Also, polymer foils can be incorporated in dosimetry belts to obtain an indication of the direction of the beam (Piesch, 1970). This becomes important since fission neutrons are attenuated very rapidly by the human body.

The size distribution of etch pits depends on the energy of the perpendicularly incident neutrons and it has been suggested that this characteristic be used for obtaining some information on the neutron spectrum (Tuyn, 1970). The etch pit diameter distribution depends also on the direction of neutron incidence and coupled with the small size of the tracks makes this approach somewhat impractical and too time consuming.

Several etching methods have been advanced. The most common etching

method, referred to as "conventional etching" in this dissertation, can be carried out by immersing the irradiated foils into a chemical solution of certain concentration and temperature (see Chapter III). These etching methods are convenient means of track amplification and give more detailed information on the charged particle trajectory. The tracks obtained by this technique are small and are observed usually by a light microscope. For example, fission fragment track diameters in polycarbonate foils are of the order of 6 μm after being etched for six hours in 5N potassium hydroxide solution at 60°C (Dutrannois, 1971) or 20 μm when red-dyed cellulose nitrate (Kodak-Pathé LR-115) is etched in 10% NaOH for 100 minutes at 60°C (Sohrabi and Becker, 1971). However, a spark counting method has greatly simplified automatic counting of these tracks especially for fission fragment tracks (Cross and Tommasino, 1970).

Fission fragments cause densely damaged regions and are usually relatively simple to locate under a microscope. However, recoil particle tracks which are produced by much lower LET particles lead to small tracks which, when conventionally etched, are usually more difficult to locate and count visually. Spark counting of recoil particle tracks has been carried out recently after extended etching in thin polycarbonate foils (Becker and Abd-el Razek, 1974; and this investigation). Also there has been some improvement in etching recoil particle tracks induced in red-dyed cellulose nitrate (Kodak-Pathé LR-115) by etching the foils in 2.5N NaOH solution at 38°C for 10-20 hours depending on the neutron dose (Tripier et al., 1975). Tracks in this case appear as clear spots on a dark red background and are similar to those observed by fission fragments and alpha particles (Barbier, 1970; Sohrabi and Becker, 1971; Costa-Ribeiro

and Lobão, 1975).

Some other more complex etching methods have also been proposed to enhance etching speed, sensitivity, and/or the size of the etched region. These methods include detection of charged particle tracks by polymer grafting (Monnin and Blanford, 1973) and electrochemical etching (Tommasino, 1970). This latter approach gives superior results and has been the subject of this study. Electrochemical etching is based on conductive energy loss along the tracks obtained by applying an alternating electric field of sufficient strength which is most conveniently of sinusoidal waveforms. This results in enhanced local etching at the damaged sites and leads to an etching speed along the tracks which is much greater than that of undamaged bulk surfaces. This enhanced and more rapid etching of the tracks seemed advantageous especially for low LET charged particle tracks such as fast-neutron-induced recoil particle tracks. The original work was concerned with the enhancement of alpha and fission fragment tracks (Tommasino, 1970) and an earlier investigation by this writer and Becker (1971) led to amplified recoil tracks in NTA photographic film backings which were larger than those obtained by conventional etching but not as well-defined as fission fragment tracks. Figure 1 shows a micrograph of fast-neutron-induced recoil particle tracks in NTA film backing enlarged by three hours of electrochemical etching in 28 percent KOH solution at 25°C by applying 650 V at one kHz. This finding attracted the interest of this writer and led him to believe the electrochemical etching technique warranted further investigation. The present dissertation reports on work done in this area which is aimed at improving the usefulness of fast-neutron-induced recoil particle track amplification in polymers by

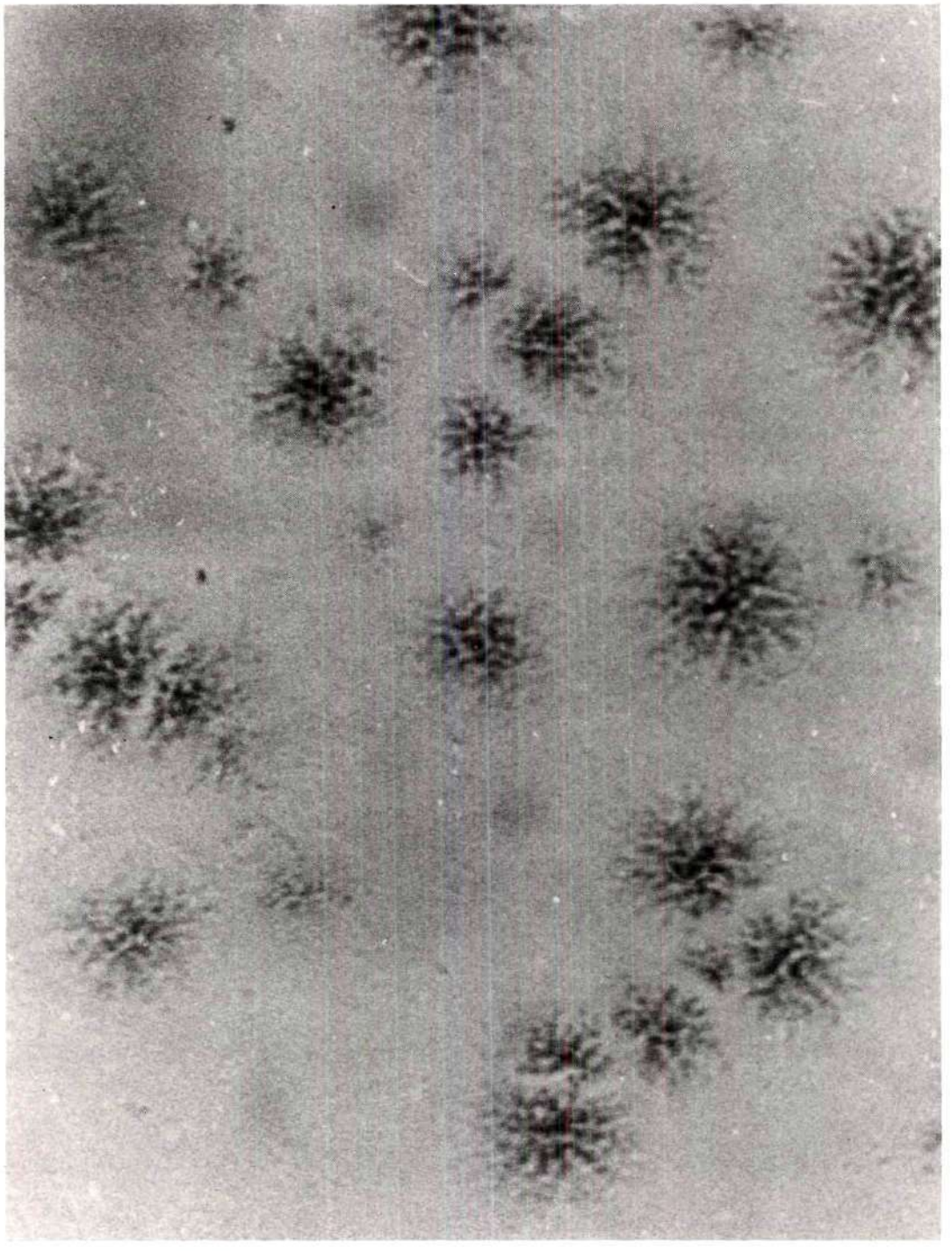

Figure 1. Microphotograph of Recoil Particle Tracks in NTA Film Backing (cellulose acetobutyrate) Enlarged by 3 Hours of Electrochemical Etching in 28% KOH Solution at 25°C Applying 650 Volts at 1 kHz (after Sohrabi and Becker, 1971)

electrochemical etching and in establishing performance parameters of such methods.

1.2 Neutron Depth Dose Studies

When an object as heterogeneous as the human body containing organs of different compositions and structures is under irradiation, the distribution of absorbed dose and dose equivalent through the body differs considerably from that obtained in homogeneous phantoms. In most of the early calculations and measurements of neutron depth dose, the phantom simulating the human trunk or other organs was considered to consist of homogeneous soft tissue (Snyder and Neufeld, 1955; Barr and Hurst, 1954; Mills and Hurst, 1954; Smith and Booth, 1962; Lawson et al., 1967; Booth and Dennis, 1968; Auxier et al., 1968; Zolotukhin et al., 1971; Jones et al., 1971; Jones and Auxier, 1971) and pioneering work of Snyder and Neufeld (1955) has been the main source of comparisons for depth dose studies by other investigators and has served as a guideline for radiation protection purposes.

The assumption of homogeneity of human phantoms has led to a simplified version of the human trunk. The presence of body cavities and air spaces (e.g. in the lungs), and of tissues of high density (e.g. bone) causes the actual distribution of absorbed dose through the phantom to differ considerably from point to point from that of homogeneous phantoms. This deviation was first discussed in x- and γ-ray therapy (Spiers, 1951). Due to the increasing use of fast neutrons in radiotherapy and human radiography as well as the need for reliable information for radiation protection purposes, this area of neutron dosimetry has been attracting considerable current interest (Wilkie, 1970; Poston, 1971; McGinley, 1971). Of particular concern is the fact that certain tissues adjacent to or en-

closed by bone (e.g. red bone marrow and endosteal and preosteal tissues) have a high radiation sensitivity and doses received by these tissues are of special importance in setting appropriate radiation protection standards, in radiotherapy and in radiography. Neutron dose to these tissues is of particular significance since it is here that many of the radiation induced malignancies (i.e. leukemia, bone sarcoma, bone carcinoma, etc.) have their origin.

Previous studies of dose received by these tissues have been limited to a few calculational treatments and experimental measurements; however, no detailed or adequately localized experimental values have been published. Randolph (1963) has calculated the absorbed dose to the compact bone under equilibrium condition for various fission neutron spectra. Lawson (1967) has calculated also the recoil proton dose at a bone-tissue interface consisting of two parallel slabs of bone surrounded by tissue when irradiated by 14 MeV neutrons. The calculational technique is similar to that developed by Charlton and Cormak (1962) on the dissipation of energy by electrons in finite cavities.

More recently, Prasad et al. (1971) have further modified Lawson's studies by assuming non-isotropic scattering of protons. They have calculated also the distribution of dose due to neutron elastic scattering by O, C, and N and extended their studies to slabs and cylindrical tissue cavities. Their investigations indicated an increase in neutron dose as one goes into tissue from a bone-tissue interface and a decrease in neutron dose as one goes into bone from a tissue-bone interface.

Another theoretical study of neutron dose in tissue and bone has been carried out by Budinger et al. (1971) to analyze the neutron

depth dose through a simulated human arm including bone and marrow for fission neutrons and for 1 keV, 120 keV, and 14 MeV monoenergetic neutrons. Also, ICRU (1969) has discussed the dose to the soft tissue in and near mineral bone exposed to two MeV neutrons. The discussion was brought up as an example of the use of kerma in biological problems. It was concluded that for two MeV neutrons the kerma in bone is less than that of soft tissue because of the lower hydrogen concentration in bone. If the dose in soft tissue away from the bone is assumed to be one rad, i.e. a kerma of 100 ergs/g, the kerma in bone is 43 ergs/g. The ICRU report (1969) also commented that, with a kerma of one rad in soft tissue, the dose at the bone-tissue interface is 1.8 (the ratio of the mass stopping powers) having a higher dose on the tissue side, and the dose in a 5 μm osteocyte is 0.77 rad, which is the product of 1.8, the mass stopping power ratio, times 0.43 (the kerma in bone) (ICRU, 1969).

Turner et al. (1968) have reported the calculated dose for high energy neutrons and protons of 100, 250, and 400 MeV energy in targets of dimensions approximating a small primate or human torso. The results are of interest in radiation protection but they are beyond the energy range of interest in this dissertation.

The only extensive neutron dose measurements at bone-tissue interfaces are those carried out by Poston (1971) for broad beams of neutrons with a fission spectrum, at 14 MeV, and from isotopic neutron sources. The phantom used was a cube filled with tissue-equivalent liquid. Neutron dose distributions were obtained as a function of depth near bone-tissue and tissue-bone interfaces using extrapolation ionization chambers made of tissue-equivalent and bone-equivalent plastics. The results were

extensive and interesting; however, the finite thickness of the electrode facing the interface prevented measuring the neutron dose gradients very near the bone-tissue interface.

Neutron dose measurement at the air-tissue interface also is of interest to the radiotherapist. The dose build-up curves for different neutron energies have been reported by Goodman (1969a) and Bewley (1971). The dose increases to a maximum at depths of several millimeters underneath the skin, the depth of which depends on the neutron energy.

In the light of previous experiences in the estimation of dose at biological interfaces and the difficulties encountered and discrepancies in published estimates of detailed and localized dose distributions, we were motivated and led to further investigation. Part of the limitation in obtaining such distributions of dose is due to the fact that a neutron dosimeter suitable for these types of applications should have certain characteristics that have been difficult to obtain. It should be neutron-sensitive, gamma-insensitive, tissue-equivalent in composition, and compact enough to have high spatial resolution capable of measuring the absorbed dose at the point of interest.

Perhaps tissue-equivalent extrapolation ionization chambers are in some respects a near ideal detector for interface studies provided that the shortcomings mentioned by Poston (1971) can ever be overcome. However, even with his suggested improvements they would be lacking in terms of small size, simplicity and flexibility, and they would have a response to gamma radiation. Solid state dosimeters show some promise for these measurements. Among them, thermoluminescent and thermally stimulated exo-electron emission dosimeters have been used for interface

studies (Ennow, 1973). However, their applications seem limited for neutron dosimetry at interfaces because of high sensitivity to gamma rays which always accompany neutrons. Therefore, recoil particle track registration in polymers which have been the subject of some depth dose studies (Becker, 1969b; Tuyn and Broerse, 1970; Piesch and Sayed, 1974a) seemed to offer the best promise for the measurement of neutron dose distribution near bone-tissue and air-tissue interfaces.

1.3 Objectives of This Research

The main objectives of this research were:

1. Design and construction of a practical electrochemical etching system that would be simple and capable of etching a number of foils simultaneously for large-scale neutron dosimetry.

2. Investigate electrochemical etching amplification of fast-neutron-induced recoil particle tracks in those polymers that will provide best etching results.

3. Optimize the electrochemical etching parameters for the amplification of recoil particle tracks in Lexan polycarbonate.

4. Develop a fast neutron personnel dosimeter to cover dose ranges of interest in routine and accidental dosimetry and study its characteristics.

5. Investigate the performance of the dosimeters for measurement of output of neutron sources, neutron contamination of high energy medical x-ray beams produced by betatrons and linear accelerators, and depth-dose studies near biological interfaces in heterogeneous phantoms.

6. Compare the results with previous experimental and theoretical

data.

7. Spark counting of recoil particle tracks in very thin polycarbonate foils (6 μm) when conventionally etched as an approach for recoil particle track counting.

CHAPTER II

PHYSICAL AND BIOLOGICAL CONCEPTS

This chapter presents the physical and biological concepts related to the area of this research. It includes some neutron production methods and gives some detail on the interaction of radiation in general and neutrons in particular with tissue and tissue-like materials. Tissue masses and tissues adjacent to or enclosed by bone are reviewed and some radiation quantities and units are discussed where relevant.

2.1 Sources of Neutrons

For over thirty years, neutron sources have served as useful tools for many applications, for example, in health physics studies, radiobiology, therapy, geology, industry, and agriculture. Numerous neutron production methods have been developed including reactors, accelerators directing high-energy charged particle beams on to target materials, and isotopic neutron sources. Depending on the technical characteristics of the source, neutrons of different energy spectra are produced often over a wide energy range. The neutrons are generally categorized in terms of their energy as thermal, intermediate (or epithermal), fast, and relativistic neutrons. Briefly, thermal neutrons are those in equilibrium with the surrounding medium at a given temperature and the energy spectrum has a Maxwellian distribution. Intermediate energy neutrons (or epithermal) extend from about 0.5 eV to approximately 10 keV above which protons resulting from elastic scattering of neutrons begin to ionize matter sig-

nificantly. Fast neutrons extend from about 10 keV to 10 MeV where inelastic scattering and nuclear reactions become significant. Above this energy, neutrons are sometimes referred to as relativistic neutrons (Tochilin and Shumway, 1969).

For dosimetric applications of these sources some basic information on their characteristics is needed. These characteristics include energy spectrum, output, gamma emission rate, etc. Based on this information some additional values such as mean neutron energy ($\bar{E}$), and fluence-to-kerma factors ($\bar{k}$) can be obtained. Therefore, in the following some neutron sources of relevance to this research as well as some of their characteristics will be discussed.

Table 1 summarizes some characteristics of the most common isotopic neutron sources including (α,n), (γ,n), and spontaneous fission sources based on data given by DePangher and Tochilin (1969). Sources making use of the (α,n) reaction are mixtures of an alpha emitter (such as ^{238}Pu, ^{239}Pu, ^{210}Po, ^{226}Ra, ^{241}Am) and Be powder or some other suitable light element, or a select isotope such as ^{7}Li, ^{10}B, ^{19}F, ^{18}O, etc. Sources with a Be target provide a higher yield than the others but they usually have also a higher gamma emission rate and complex spectra. Neutron sources utilizing targets other than Be are of particular interest mostly because of their well-resolved energy spectra which makes them more suitable for calibration of neutron detectors.

Sources of the (γ,n) type, including α-shielded ^{226}Ra-γ-Be and ^{124}Sb-γ-Be, produce neutrons of energies lower than one MeV. The ^{226}Ra-Be sources have a long half life, thus a constant emission rate. The ^{124}Sb-Be sources have a short half life of 60 days which is a disadvantage of

Table 1. Some Characteristics of Isotopic Neutron Sources*

Type of Neutron Source	Reaction	Half-life	Neutron Yield $\frac{n/sec \times 10^6}{Ci}$	Calculated Values $\bar{E}$ (MeV)	Calculated Values $\bar{k}$ $(rad/n/cm^2) \times 10^{-9}$	Averaged Values $\bar{E}$ (MeV)	Averaged Values $\bar{k}$ $(rad/n/cm^2) \times 10^{-9}$
^{239}Pu-Be	α,n	2.44×10^4y	2.2	3.9	3.52	4.1	3.73
^{241}Am-Be	α,n	458y	2.7	4.5	3.86	4.3	3.77
^{210}Po-Be	α,n	138.4d	2.5	4.3	3.85	4.0	3.78
^{226}Ra-Be	α,n	1620y	20	5.1	4.16	4.5	3.82
^{210}Po-B^{10}	α,n	138.4d	0.185	2.2	2.97	---	---
^{210}Po-B^{11}	α,n	138.4d	0.818	2.9	3.48	2.8	3.30
^{210}Po-O^{18}	α,n	138.4d	1.1	2.3	3.15	---	---
^{210}Po-F^{19}	α,n	138.4d	0.1	1.3	2.45	---	---
^{210}Po-Li^7	α,n	138.4d	0.05	0.36	2.26	---	---
^{239}Pu-F^{19}	α,n	2.44×10^4y	---	1.1	1.23	---	---
^{252}Cf	Spontaneous Fission	2.65y	2.3 per μg	2.35	3.111	---	---
^{124}Sb-Be	γ,n	60d	1.3	0.024	0.218	---	---
^{226}Ra-Be	γ,n	1620y	1.257	0.12	0.640	---	---

*Data from DePangher and Tochilin (1969).

this source; however, if they are used for reactor start ups, the short half life can be compensated by reactivation of the antimony (Murray, 1961). Both types of gamma sources suffer for dosimetric studies because of their high gamma emission rates.

Neutrons are produced also by photon-neutron reactions in high energy photon beams from betatrons and linear accelerators of interest for radiotherapy applications. These reactions occur at high photon energies. For example, photon threshold energies for ^{208}Pb and ^{63}Cu are 7.4 and 10.8 MeV, respectively (Wilenzick et al., 1973). However, these neutrons produced in high energy x-ray beams are usually considered only as sources of undesirable neutron contamination in the beam.

Spontaneous-fission sources are attractive and are of interest for many applications. Many elements such as $^{240}Cm(Ts=1.9 \times 10^{6}y)$, ^{242}Cm $(Ts=7.2 \times 10^{6}y)$, $^{248}Cm(Ts=4.6 \times 10^{6}y)$, $^{250}Cm(Ts=1.1 \times 10^{4}y)$, $^{246}Cf(Ts=2.1y)$, $^{248}Cf(Ts=7 \times 10^{3}y)$, $^{250}Cf(Ts=1.7 \times 10^{4}y)$, $^{252}Cf(Ts=85.5y)$, $^{254}Cf(Ts=60.5d)$. $^{254}Fm(Ts=228d)$, $^{256}Fm(Ts=3h)$, $^{257}Fm(Ts=100y)$, $^{255}Es(Ts=2440y)$ etc. have been considered as common spontaneous fission sources. (Note: In the above Ts = spontaneous fission half-life.) Among these sources, californium-252 with characteristics shown in Table 1 and an almost ideal Ts of 85.5 years, is the most common neutron source of this kind in use and is produced by fourteen successive neutron captures in high flux reactors. Its exceptionally high yield and reasonably long radioactive half life, Tr = 2.5y, make it a point source far superior to the other available neutron sources for use as implants in interestitial or intracavity therapy.

By far the most prolific source of neutrons is the nuclear reactor. The fast neutrons produced in the fission reaction are thermalized making

thermal neutrons available in quantity from research reactors in many nuclear research centers. Fast neutrons produced by reactors for biomedical and dosimetry applications are limited for the most part to thermal neutron reactor facilities utilizing fission converter plates or ^{6}Li-D targets which provide neutron beams having fission spectra and 14 MeV energy, respectively. For example, the Janus reactor at Argonne National Laboratory makes use of plates that are 93 percent enriched in ^{235}U (Williamson et al., 1965). There are also some reactor facilities especially designed to obtain directly usable fluxes of fast neutrons. As an example, the Health Physics Research Reactor (HPRR) at Oak Ridge National Laboratory (ORNL) is a bare, unmoderated reactor facility having a fission neutron leakage spectrum of 1.5 MeV neutron average energy. It is designed as a neutron source for health-physics-related research such as radiation dosimetry and biomedical studies (Auxier, 1965). Examples of other fast-neutron irradiation facilities are given by Tochilin and Shumway (1969).

For most dosimetric and biomedical studies monoenergetic neutrons are usually required. Accelerators can produce monoenergetic beams of neutrons by allowing accelerated beams of charged ions to bombard a suitable thin target. Depending on the ion and its energy and target material and its thickness, neutrons of different characteristics can be obtained.

Neutron generators are flexible and an economical means of producing neutrons. They have relatively large outputs at accelerating voltages of 100-400 kV. Common neutron generators employ a Cockcroft-Walton voltage generator to produce accelerating potentials of the order of 150-200 kV. Neutrons of ~ 3 MeV and ~ 14 MeV are obtained by reactions ^{2}H(d,n)^{3}He

and $^{3}H(d,n)^{4}He$, respectively. The latter reaction is of particular interest for radiotherapy applications. Other reactions such as $^{3}H(p,n)^{3}He$ may also be used for low monoenergetic neutron production.

Most of the neutron generators of the above mentioned types do not supply sufficient outputs or life times of interest for radiotherapy or other similar applications mainly because of limitations on target construction. However, some progress has been made in this field by several investigators (Haywood et al., 1973; Brennan et al., 1973) in obtaining a neutron dose rate of 10 rad/min at 125 cm from the target with a constant output of over 100 hours of operation.

Cyclotrons can produce high intensity fast neutron beams by bombarding a Be target with accelerated particles such as deuterons or protons. In many cyclotrons in common use for biomedical applications, deuterium ions of different energies are used to produce high neutron yields through the reaction $^{9}Be(d,n)^{10}B$. As the bombarding energy increases total neutron yield and mean neutron energy increase. Figure 2 shows typical neutron spectra of three different cyclotrons used in this investigation, i.e. the University of Washington Cyclotron at Seattle, Washington; the Naval Research Laboratory Cyclotron at Washington, D. C., and the Texas A&M University Cyclotron at College Station, Texas. Although such machines produce high neutron yields of the order of 20-60 rad/min at target-to-skin distances (TSD) of about one meter, their cost, complexity, and lack of flexibility limit their availability for many laboratories.

In practice, fluence-to-kerma factors are required for any conversion of neutron fluence to kerma or vice versa. Table 1 shows calculated

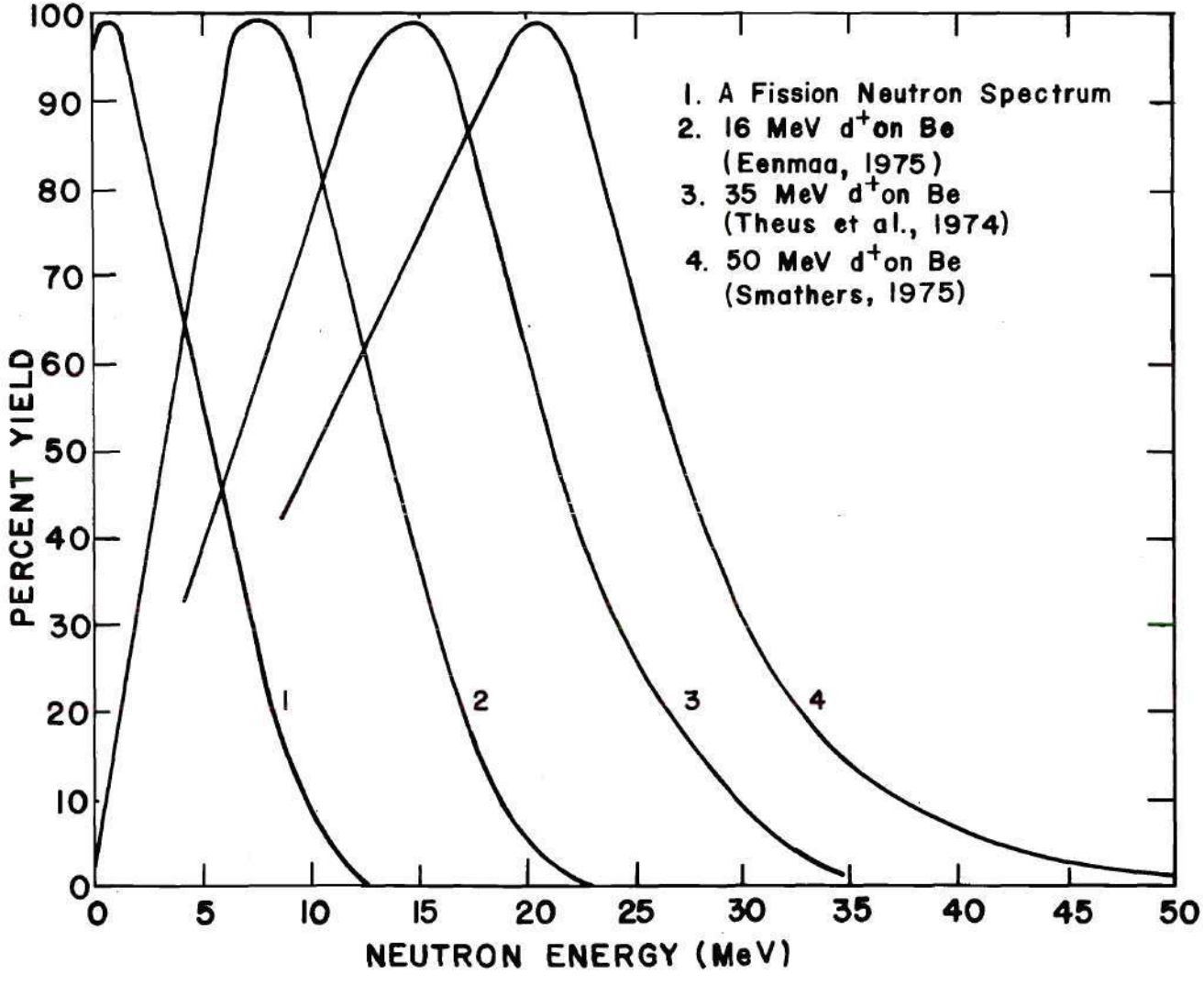

Figure 2. Fission Neutron Spectrum and Neutron Spectra Obtained by Deuterium Ions of Various Energies on a Beryllium Target at Three Different Cyclotron Facilities

and average values of neutron energy and kerma factors for sources given in the table based on calculations of Bach and Caswell, and Nachtigal (DePangher and Tochilin, 1969). The kerma factors for neutrons up to 18 MeV of energy (calculated by Bach and Caswell) are reported also by ICRU (No. 13, 1969).

2.2 Radiobiologically Important Tissues in Bone

Tissues in general and tissues adjacent to or enclosed by bone in particular are discussed in many texts (e.g. see Elias and Pauly, 1966; Hollinshead, 1967; Spiers, 1969; ICRP, No. 11, 1967). In particular, Spiers (1969) has discussed radiobiologically important tissues in bone that are subject to radiation damage.

Tissue histologically is referred to as the assemblage of similar cells with a specific function. Tissue, however, is more complex than implied by such a simple definition since even a small portion of muscle or any other tissues may contain one or more of the four tissue categories including epithelial, connective, muscular, and nerve tissues each containing cells with varying functional and morphological characteristics. The difference between cell characteristics exhibits a pronounced order of sensitivity to any type of damage produced by ionizing radiations.

The criteria for cell sensitivity were generalized by Bergonie and Tribondeau (Cassaret, 1968) stating that cells are more sensitive if:

(1) they have a high mitotic rate,

(2) they have a long mitotic future, and

(3) they are of primitive type.

These criteria have been known as a law for predicting cell sensitivity in different tissues although there are some exceptions (e.g. white blood

cells or the lens of the eye). Based on these criteria, it is evident that tissues adjacent to or enclosed by some other tissues may exhibit different sensitivities to radiation. It should be noted also that even similar cells of a certain tissue, e.g. tumor cells, may exhibit a pronounced differential cell sensitivity because of their supply of blood and oxygen. It has been shown that the well oxygenated cells are much more sensitive than cells with oxygen shortage. In fact, a rapid increase in cell sensitivity occurs as the oxygen concentration rises from zero to a maximum, beyond which the sensitivity remains unchanged (Gray et al., 1953). In some cases this is one of the objectives of using high LET radiations in therapy, since they eliminate to some extent this differential cell sensitivity. This is a practical problem of irradiating certain tissue and at the same time protecting the adjacent tissue. One of the tissues of special concern here is bone which is an elaborate tissue of a number of different structures containing living tissues each of which responds differently to radiation and has different susceptibilities to radiobiological damage, and each of which can have a particular malignant tumor associated with it.

Bone or osseous tissue is a connective tissue consisting of a non-living matrix of calcium in which biologically important tissues live and function. The non-living part of hard bone consists mainly of cortex (the bone wall) and trabeculae (the spongy bone) and has a high density and relatively higher effective atomic number. This is due to the presence of calcium and the calcium-phosphorus compound hydroxyapatite embedded in a matrix of collagen fibrils and a ground substance.

In the hard bone there exist somewhat organized units called

Haversian systems or osteons. Each osteon consists of a central canal containing nutrient blood vessels and is surrounded by mature bone cells (osteocytes) occupying small spaces called lacunae. Osteocytes have small processes on their bodies joining them together and to a central canal for nutrient supply. These cells and others in the Haversian canal constitute the living cells inside the hard bone and are responsible for maintenance of bone and its repair after damage.

There are also living cells which can be found near the external and internal bone surfaces. The external surface is covered with a periosteum, a tissue containing a thick external layer of fibrous connective tissue and a thin layer of cells called osteoblasts. The interior surface is lined with endosteal tissue consisting of osteoblasts and another type of cells called osteoclasts. Since bones are small at birth, their growth and turnover is due to the activities of osteoblasts and osteoclasts. Osteoblasts build up bone on the external surfaces by putting down layers of hydroxapatite and become mature osteocytes. On the other hand, osteoclasts break down bone in the internal layer by gradually dissolving the hydroxyapatite and feeding it to the blood stream. Therefore, through the activities of these types of cells, bone grows in diameter until adulthood is reached and repairs any damage which may occur to it.

Another important tissue which fills all the bone cavities within the cortex and the trabecular bone network is marrow. At birth all the marrow distributed throughout the bones is a blood forming organ. As the individual grows, the red marrow in some cavities within the cortex of some bones (e.g. humerus, femur, etc.) is replaced by a fatty tissue (yellow marrow), so that by the time the individual becomes a young adult, red

marrow will be limited only to bone extremities where the trabecular bone cavities are filled.

The living tissues within the bone (active or red marrow) and on the surfaces (endosteum and periosteum) constitute what are considered to be the radiosensitive components of the bone that are most susceptible to radiation damage and care should be taken in the amount of dose received by these tissues so that bone is relatively undamaged or damaged to an extent that permits repair (Spiers, 1966). Therefore, depending on the criterion of concern, dose received by these tissues may be regarded as the limiting dose subject to any biological damage to bone. This is true whether the dose is from internal emitters such as ^{226}Ra and ^{239}Pu, which are bone seekers and can deliver a large dose to tissues adjacent to the bone, or from external radiation which deposits its energy through the secondary charged particle production as discussed in the next section.

2.3 Energy Deposition in Tissue by Ionizing Radiations: Units and Definitions

Ionizing radiations are divided by ICRU into two categories: (1) directly ionizing radiations such as electrons, protons, alpha particles, and other similar particles, and (2) indirectly ionizing radiations such as photons and neutrons.

2.3.1 Directly Ionizing Radiations

Charged particles including electrons, protons, alpha particles, etc. can transfer their energy directly to tissue or tissue-like materials. Their energy transfer is mainly by elastic and inelastic collisions with atoms or molecules forming that particular matter. The particle loses its

kinetic energy usually by inelastic electronic collisions with atomic electrons along its path. However, at the end of the path of a heavy particle (i.e. excluding beta particles or electrons) elastic collision with the nucleus becomes predominant leading to heavy recoil particles.

Electrons having a small mass can transfer a large fraction of their energy by a single collision with atomic electrons; also they are deflected through large angles. Therefore, their energy deposition is not usually localized. On the other hand, heavier charged particles such as protons or alpha particles lose only a small fraction of their energy in each electronic collision and are deflected at very small angles which do not alter their paths significantly. This leads to highly localized damage along the particle path, thus more local biological damage (Bichsel, 1968).

In order to quantify the localization of energy deposition of each type of radiation, the term linear energy transfer (LET) or restricted stopping power, L_Δ, was introduced (Zirkle et al., 1952). The most recent definition of LET is given by ICRU (1971):

> The linear energy transfer (LET) or restricted linear collision stopping power, L_Δ, of charged particles in a medium is the quotient of dE by dl where dl is the distance traversed by the particle and dE is the energy loss due to collisions with energy transfer less than some specified value Δ.

$$L_\Delta = \left(\frac{dE}{dl}\right)_\Delta$$

Although the definition of LET specifies an energy cut off and not a range cut off, the energy losses are sometimes called "energy locally imparted." Furthermore, to bring about uniformity, it is recommended that Δ can be expressed in electron volts. Thus, L_{100} is the linear energy transfer

for an energy cut off at 100 electron volts (ICRU, 1971).

Due to increased applications of high LET radiations during the fifties ICRU recognized the need for concepts to correlate any ionizing radiations to their biological or related effects and expressed energy deposition in terms of energy absorbed per unit mass (ergs per gram) of the irradiated material at the point of interest (Roesch and Attix, 1968). Soon afterward, it established a new quantity, absorbed dose, which represents a real step forward in improving dosimetry terminology. It is defined as (ICRU, 1971):

> The absorbed dose, D, is the quotient of $d\bar{E}$ by dm, where $d\bar{E}$ is the mean energy imparted by the ionizing radiation to the matter in a volume element and dm is the mass of the matter in that volume and can be written as:
>
> $$D = \frac{d\bar{E}}{dm}$$
>
> The special unit of absorbed dose is the rad
>
> $$1 \text{ rad} = 10^{-2} \text{ J kg}^{-1}$$

ICRU (1971) specifies the term "energy imparted" to be the net amount of the sum of energies (excluding rest energies) of all directly and indirectly ionizing particles which have entered the volume of mass dm and of all energies released, minus the sum of all the energies expended, in any transformations of nuclei and elementary particles which occurred within the volume of mass dm minus the sum of energies (excluding rest energies) of all those directly and indirectly ionizing particles which have left the volume (ICRU, 1971).

Based on LET and dose concepts, it is evident that heavy charged particles having higher LET lead to more localized energy depositions, thus more severe localized biological damage in tissue. This is true since damage produced in living tissues increases with energy density up

to the point of saturation. In addition, the ability to repair damage is less as the LET increases and is believed to be essentially zero at LET values characteristic of alpha particles (Shapiro, 1972). As a result, for certain forms of damage, the relative biological effectiveness of energy imparted by alpha particles is found to be as much as 10 times greater than that of an equivalent amount of energy transferred by beta particles or secondary electrons produced by x or γ radiation. Therefore, in biological studies one attempts to establish a meaningful relationship between dose and effect by introducing a weighting factor to take into account the biological effectiveness of different types of radiations. This is called "relative biological effectiveness" (RBE) and is a function of LET of radiation of concern, absorbed dose, dose rate, dose protraction, oxygen concentration, type of damage considered, etc. (Sinclair, 1969), and is defined as the ratio of dose in rads of the standard radiation (250 keV x-rays) to produce a certain effect to dose in rads of radiation of interest to produce the same effect. It should be stated that the irradiation conditions should be the same for both radiations. Since 250 keV x-ray is the reference radiation, the RBE for 250 keV x-rays is one.

The RBE concept is defined in biological terms. However, for radiation protection purposes a modifying factor based on physical terms, i.e. a function of LET, is often used. It is called "Quality Factor," Q, a factor of substantial importance in radiation protection. Table 2 lists the recommendation of ICRU (1971) for the relationship between Q and L_{∞}.

Table 2. L_∞ - Q Relationship

L_∞ in water (keV/μm)	Q
3.5 and less	1
7.0	2
23.0	5
53.0	10
175.0 and above	20

When the Q factor and other weighting factors N are used to weight the absorbed dose, the result is dose equivalent, H, which is defined by ICRU (1971) as: The dose equivalent is the product of D,Q and N at the point of interest in tissue, where D and Q are as defined above and N is the product of any other modifying factors. Therefore,

$$H = D \cdot Q \cdot N.$$

The special unit of dose equivalent is the rem.

ICRU recommends that the quantity Q should be limited to radiation protection applications when H is in the region of or below the applicable maximum permissible dose equivalent and should not be used for high level accidental exposures. It has been noted also that in the usual case when D is delivered by particles which have a range of L values, an average value for Q, $\overline{Q}$, should be used.

Although the above describes RBE, Q, H, and N as given by ICRU, it should be mentioned that there have been some practical difficulties in applying these definitions and therefore many objections have been raised regarding inconsistencies in the system of quantities and units (Neufeld, 1973). Perhaps the most serious difficulty in this system is that dose equivalent, H, is supposed to be the quantity expressed in rem units that

is most closely related to the biological damage that might be expected to result in a small fraction of a population exposed at a maximum permissible dose, MPD. Historically Q in the above equation is the quantity most closely related to RBE and now QN → RBE so that, for example, in the case of neutrons the dose equivalent $H_n \rightarrow D_x$ in which D_x is the absorbed dose in rad of 250 keV x-rays which would be expected to produce the same damage as H_n(rem) of neutrons.* Thus N depends on many things among which we might mention: (1) type of damage (leukemia, life shortening, genetic mutation, etc.), (2) age, (3) sex, (4) state of health of exposed individual, (5) dose, (6) dose rate, (7) oxygen tension, (8) other concurrent body insults, (9) radiosensitivity of exposed tissue, (10) localization of dose, and (11) essentialness of damaged tissue (Morgan, 1973).

2.3.2 Indirectly Ionizing Particles

Indirectly ionizing particles such as photons or neutrons interacting with tissue or tissue-like materials liberate directly ionizing particles or can initiate nuclear transformation (ICRU, 1971). Therefore, they deposit energy to the medium of concern through a two step process: (1) production of directly ionizing particles plus indirectly ionizing particles, and (2) the charged particles impart energy to the medium (ICRU, 1969). Although the term "absorbed dose" has been established for any type of radiation, a new term was introduced by Roesch (1958) to act as a bridge between the energy of the indirectly ionizing particles and the absorbed dose, i.e. the kinetic energy of charged particles

*This relationship follows since

$$RBE = \frac{D_x(\text{rad})}{D_n(\text{rad})} \text{ and } QN = \frac{H_n(\text{rad})}{D_n(\text{rad})} \text{ or } H_n(\text{rem}) = \frac{QN}{RBE} \times D_x.$$

released (in step one) per unit mass, called "KERM." This term was further refined by ICRU to be called Kerma, kinetic energy released in matter. The most recent definition of this term is given by ICRU (1971).

> The kerma is the quotient of dE_{tr} by dm, where dE_{tr} is the sum of initial kinetic energies of all charged particles liberated by indirectly ionizing particles in a volume element of a specified material and dm is the mass of the matter in that volume element.
>
> $$K = \frac{dE_{tr}}{dm}$$ (ICRU, 1971)

It should be noted that the energy which these charged particles radiate in bremsstrahlung and the energy of any charged particles which are produced in secondary processes (e.g. Auger electrons) are also included in dE_{tr} (ICRU, 1971). ICRU also recommends that kerma can be a useful quantity in dosimetry when charged particle equilibrium exists in the material at the point of interest and also bremsstrahlung losses are negligible; kerma is then equal to the absorbed dose at that point.

For photons charged particles contributing to kerma are mainly electrons. They are produced by a number of processes the most important of which are: (1) photoelectric effect, (2) Compton effect, and (3) pair production. These processes are strongly dependent on photon energy and atomic number of the medium of concern.

Neutrons, however, have a rest mass approximately equal to that of protons and they primarily interact with atomic nuclei in which one or more charged particles, photons, and/or neutrons may be released. Therefore, in this case electrons and heavy charged particles contribute to the kerma value. Depending on their energy, neutrons may interact with elements (C,O,H,N) in tissue or tissue-like materials in a number of ways

such as elastic scattering, inelastic scattering, non-elastic scattering, inelastic capture, and spallation. An excellent and comprehensive explanation of these processes is given by Auxier et al. (1968); however, because of relevance to the area of this research, a brief review of the mentioned processes follows.

Elastic scattering is the most important interaction of fast neutrons with tissue elements in the energy range up to 10 MeV. The kinetic energy and momentum are conserved and neutron energy is distributed between the neutron and the struck nucleus. Among the tissue elements, hydrogen (H) is the element of primary importance in tissue dosimetry leading to recoil protons which contribute between 85 and 95 percent of the absorbed dose depending on the neutron energy (Fitzgerald et al., 1967). This is because hydrogen, although only 10 percent by weight of soft tissue, has the highest atomic concentrations per gram of tissue, highest elastic cross section, and a neutron may lose all of its energy in one single collision with a hydrogen atom. Elastic scattering with other tissue elements (C,O,N) contributes less than 10 percent of the total absorbed dose in the energy region where the elastic scattering predominates (Fowler, 1967). These reactions lead to recoil particles which can be registered in some polymers used in this research by a suitable etching technique.

At thermal and epithermal neutron energies, the main reactions responsible for energy deposition in tissue are the inelastic "capture" processes in which a neutron is absorbed by the target nucleus and a new isotope is formed. The important target nuclei for these processes are H and N resulting in reactions $^{1}H(n,\gamma)^{2}H$ and $^{14}N(n,p)^{14}C$. In the former

reaction a 2.2 MeV gamma ray is emitted which has a high chance of escaping from the reaction site and even from the body; therefore, it makes only a minor contribution to the local absorbed dose. In the latter reaction about 0.62 MeV energy is transferred to the recoil nucleus and proton, of which 0.58 MeV is the kinetic energy of the proton. Therefore, this amount of energy is absorbed locally.

Inelastic scattering is the process in which a neutron is captured by the nucleus and reemitted, usually altered in direction and reduced in energy. In this process the nucleus is raised to an excited state and the compound nucleus subsequently decays by photon emission, frequently of high energy. Inelastic scattering cannot occur unless the incident neutron has kinetic energy greater than the first excited state of the target nucleus (Auxier et al., 1968). This process does not contribute to the local absorbed dose in tissue significantly.

In non-elastic scattering a neutron is absorbed by the nucleus and one or more particles such as neutrons, protons, alpha particles, and de-excitation gamma rays are emitted. The cross sections for this reaction have a threshold around 5 MeV and generally, but not always increase as neutron energy increases (Auxier et al., 1968). As was discussed in Chapter I, reactions such as the $^{12}C(n,n,\gamma)3\alpha$ reaction are important at high neutron energy (> 11 MeV) and can be seen easily by sensitive track recorders (Frank and Benton, 1970).

Finally, another reaction of importance at energies greater than 100 MeV is spallation. In this process a neutron is absorbed by the nucleus and the compound nucleus is fragmented ejecting several particles and nuclear fragments. Several neutrons are usually produced in this

process plus the excitation gamma rays which escape the local reaction site (Auxier et al., 1968).

Depending on the neutron energy, all the reactions may occur either in tissue or polymers. However, the tracks observed in polymers are mainly due to elastic scattering, non-elastic scattering, and spallation products produced in polymer elements and the contribution from each reaction depends on the neutron energy (e.g. neutrons of energy greater than 100 MeV produce tracks of spallation products). In materials containing nitrogen such as cellulose nitrate, the capture reaction of thermal neutrons by nitrogen may contribute substantially to track density. It is interesting to note that polymers usually have the same elements as those in tissue, and charged particle tracks which occur in them can be etched by a suitable etching technique as will be discussed in the next chapter.

CHAPTER III

PRINCIPLES OF TRACK ETCHING

In Chapter I, general irradiation and etching procedures regarding charged particle track registration in insulators were discussed. For useful applications of this method proper selection of an insulator and etching method as well as optimized etching conditions are essential. Furthermore, if the technique is applied for dosimetry or other related applications, need for track density evaluation for conversion to fluence, dose, or dose equivalent is required. Therefore, this chapter deals with mechanisms of track formation in different insulators, etching and track density evaluation methods. The principles of track etching have also been reviewed in the literature (Becker, 1972, 1973; Fleischer et al., 1975; Sohrabi and Becker, 1971).

3.1 Mechanisms of Track Formation

Charged particle tracks can be formed in many insulating materials such as minerals, inorganic glasses, and organic polymers. Fleischer et al. (1964), in their earlier work, proposed that etchable tracks may be formed by any charged particle whose energy loss per unit path length is greater than a critical value which is a characteristic of the recording material. Based on this criterion cellulose nitrate appears to require the lowest critical energy loss, thus the most sensitive material for track registration of charged particles including protons.

Because of some problems in predicting the dependence of track

formation on ion velocity, an improved criterion was proposed (Fleischer et al., 1967). The new criterion was based on primary specific ionization rate, i.e. the number of primary electrons formed per unit path length. The authors (Fleischer et al., 1969), utilizing the Bethe formula, obtained the radiation damage densities for different track recorders and different ions. In Figure 3 the thresholds for three common track detectors, muscovite mica, polycarbonate (Lexan), and cellulose nitrate of different sensitivites are indicated as well as the radiation damage densities for various particles as a function of their velocities (energy per nucleon) (Fleischer et al., 1969). As can be seen, for etchable track formation in insulators the particle should cause sufficient damage density along its path, i.e. the energy of the particle should be in the range causing the most damage density. For example, according to Figure 3, protons should have an energy lower than about 0.5 MeV to cause sufficient damage density for track formations in most sensitive cellulose nitrates and no tracks would be expected in Lexan. However, this energy range does not depend only on the characteristics of the material itself but also on the etching method and etching conditions applied which will change the indicated thresholds.

Another important factor which governs the visible track formation after etching is the angle of incidence at which the charged particle enters the surface of the detecting material (i.e. the angle between the particle path and the plane of the surface). The particles entering the surface at angles less than a critical value will not become visible but are etched away. The sine of this critical angle ($\sin\phi_c$) has been found by geometric relations to be the ratio of the etching speed (or etching

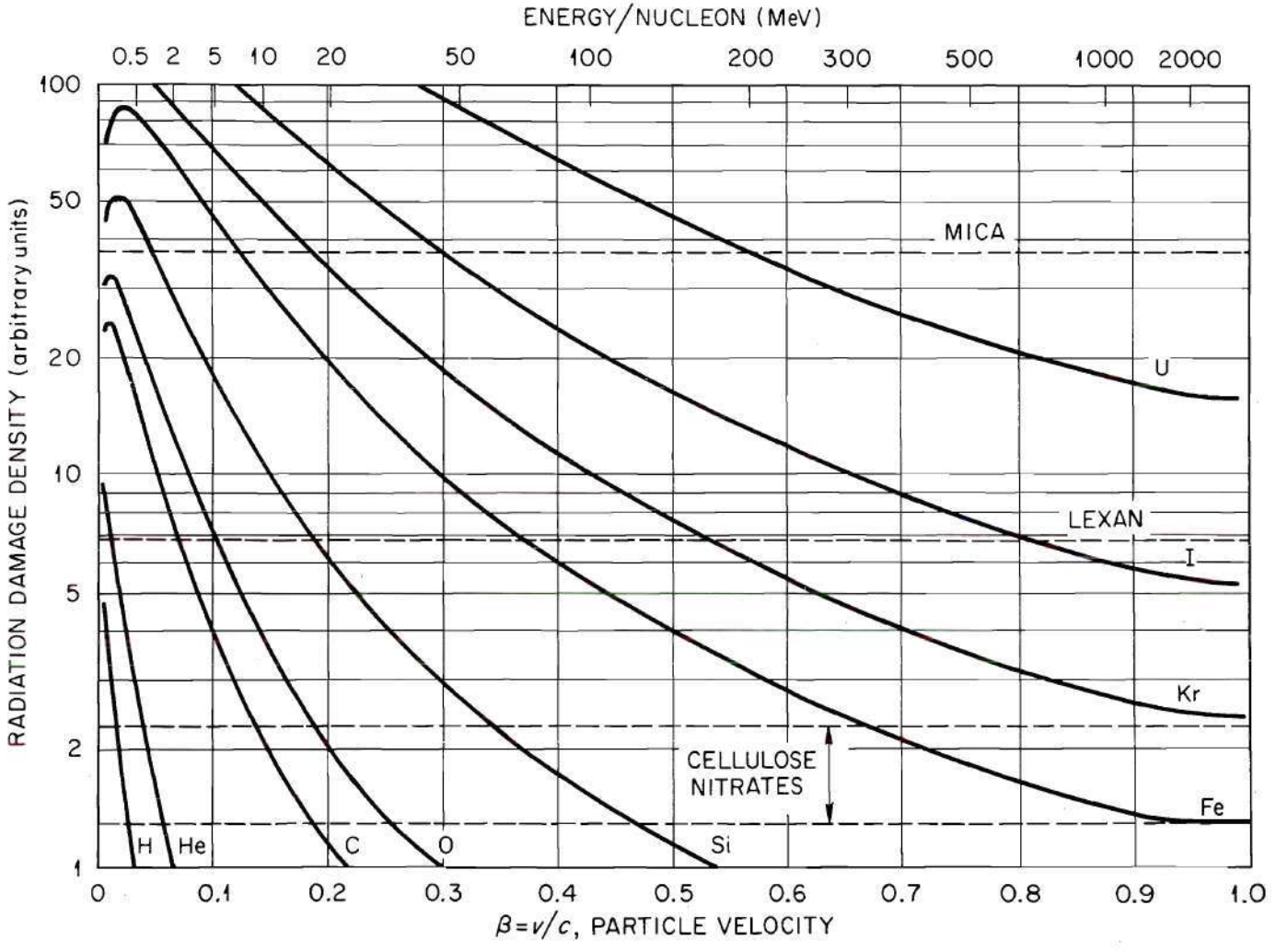

Figure 3. Detection Threshold of Three Widely Used Track Detectors for Charged Particles of Different Atomic Number and Energy (after Fleischer et al., 1969)

rate) along the surface to that along the track itself (Tuyn, 1970). This angle determines the registration efficiency of the material and governs the shape of the track. If the etching speeds along the surface and along the charged particle path are comparable, the tracks appear circular, if the speed is faster along the particle trajectory, the track appears cylindrical or needle like. Moreover, since etching speed along the track and along the surface determines the efficiency, many factors mainly type of insulator, etching method and its conditions, and type and speed of particle govern the efficiency.

Several other track formation mechanisms have been proposed to explain the damage region immediately surrounding the track and its relevance to the higher etchability of this region than that of the undamaged surface. Different mechanisms come from the two modes of interaction, i.e. elastic and inelastic collisions, when a charged particle passes through a material. A "displacement spike" model, relying on elastic scattering of a charged particle with the atomic nuclei is not believed to be the cause of track formation in solids because no tracks have been observed in conductors and at the end of a particle range where elastic scattering with atomic nuclei predominates (Fleischer et al., 1965b). Another proposed mechanism of track formation is the "thermal spike" model in which the energy given to the electrons is partially dissipated by the lattice atoms in a small region around the particle path raising local temperature to a point above the decomposition temperature of the track recorder, thus causing a region of imperfections which will be attacked by the etchant more than the undamaged surrounding region (Maurette, 1970). This model is more promising than that described above (displace-

ment spike) but suffers from the lack of correlation between the sensitivity of the materials in terms of their decomposition temperatures or melting temperatures (Fleischer et al., 1975).

An alternative is the "ion explosion spike" model proposed by Fleischer et al. (1965b), which has shown the most promise for track formation in minerals. This model suggests that a cylindrical region of positive ions is produced along the path of heavy charged particles due to the ejection of electrons and a mutual repulsion of the primary heavy positive ion results in atomic displacements in the crystal lattices. This process causes a cylindrical region of imperfections which is more readily attacked by an etching reagent than the surrounding, undamaged surface, the process that ultimately leads to microscopically visible etch pits or tracks.

The ion explosion model explains all the features of track formation and is consistent with the primary specific ionization criterion; however, the model is unsatisfactory for offering a complete explanation of the formation of the etchable tracks in organic polymers. In this case a theory based on a radiochemical damage mechanism (Benton, 1968; Boyett et al., 1970; Monnin, 1968) states that etchable tracks are formed when a long polymer chain is broken into shorter fragments by passage of a charged particle. These lower molecular weight radiolytic fragments are highly reactive which makes them more easily attacked by a chemical reagent than the surrounding undamaged region. Here, both primary and secondary events contribute to the damage density around the track core since the energy required to break a chemical bond in polymers is less than the ionization potential of atoms (Fleischer et al., 1965b). Thus,

the energy loss of short-range delta rays causes additional bond breakage around the central core which enhances the etchability of the tracks. The more energetic delta rays can escape to considerable distances from the formation site. It is recognized that this discussion is similar to that of LET, i.e. by taking into account different delta ray energy cut offs total energy deposited at the damage site will differ.

Another model for formation of etchable tracks in insulators has been proposed to account for spatial distribution of microdose (Katz and Kobetich, 1968). Depending on the range cut off of the delta rays, different doses will be delivered. Thus for a certain radial distance from the primary ion path the energy loss by the secondary electrons in this critical distance causes a minimal dosage to be considered as the threshold for that material for the appearance of visible tracks. For example, taking 2×10^{-7} g/cm^2 as a critical distance an energy deposition of about 8×10^{8} erg g^{-1} has been determined to be minimal dosage in Lexan polycarbonate. The critical dose is about 3×10^{8} and 3×10^{9} erg g^{-1} in cellulose nitrate and mica, respectively.

Unlike the "ion explosion" model which is based only on the primary events in the track core, the above model by Katz and Kobetich has taken into account only the effect of secondary events in both minerals and polymers. Since no etchable region has been induced in mica by doses of electrons much higher than the dose delivered by the passage of a heavy ion, there has been some discussion of the validity of this model (Fleischer et al., 1975). Another model which takes into account the effect of both primary and secondary events seems more tenable (Monnin, 1970; Fain et al., 1974)

Based on the detailed justification of track formation mechanisms by Fleischer et al. (1975) and this review, a track formation mechanism which justifies and predicts all the track formation features has not yet been advanced.

According to the above, even very insensitive insulators can register tracks of high LET particles such as fission fragments. However, lower LET particles such as fast-neutron-induced recoil particles or similar ions from particle accelerators can be registered only in sensitive polymers. Further, the lightest charged particles considered for their registration have been protons. It has been shown both theoretically and experimentally that protons can be registered in the most sensitive polymers such as cellulose acetate (Varnagy et al., 1970), cellulose nitrate (Carpenter and LaFleur, 1972; Lück, 1974), and red-dyed cellulose nitrate under this investigation. The dependence of track diameter on proton energy has been used also as a sensitive system of proton and alpha energy spectrometry (Lück, 1975). However, there have been some doubts expressed regarding the possibility of registration of proton tracks in polycarbonate which is a less sensitive polymer compared to cellulose nitrate.

3.2 Etching Methods

The damage region along a charged particle track can be etched readily by a suitable etching method as previously stated. Many parameters control etching characteristics of each method. Description of parameters affecting conventional etching and electrochemical etching are discussed below.

3.2.1 Conventional Etching Methods

Etching is usually carried out by immersing the irradiated foils

in a chemical solution (etchant) under pre-selected conditions (Price and Walker, 1962; Fleischer and Price, 1963). In order to make charged particle tracks observable after etching, the etching speed (or etching rate) along the track, V_t, should be greater than that of the undamaged surface or bulk etching rate, V_b. Therefore, any etchant under known etching conditions as regards concentration and temperature to meet the above requirement can be used as etchant. The most common etchants for charged-particle track etching in polymers are alkali halide solutions, mainly potassium hydroxide (KOH) and sodium hydroxide (NaOH) solutions. Many other etchants for selected etching conditions have been recommended for fission fragment track etching of insulators (Blanc, 1970; Fleischer and Hart, 1970; Becker, 1973). However, in practice, depending on the type of charged particle, material and its applications, etching conditions must be optimized for a particular application. Etching speed for a given material depends on:

(1) type and velocity of the charged particles,

(2) type of the etchant, its concentration, and its temperature,

(3) pre- or post-irradiation treatment of track recorders.

The sensitivity of less sensitive insulators (e.g. mica) compared with the most sensitive insulators (e.g. cellulose nitrate) for different ions having different velocities has already been shown in Figure 3. The high LET heavy particles such as fission fragments can be registered in all track recorders with high sensitivity, and simple etchants such as hydrofluoric acid (HF) and potassium or sodium hydroxide solutions provide suitable etchants for track registration in, for example, mica and polymers, respectively. All the tracks appear almost at the same time and

additional etching time increases the diameter linearly with time (Dutrannois, 1971; Sohrabi and Becker, 1971; and others). Alpha particles, however, having lower LET's usually have a wider energy spectra especially if they are emitted from a thick source. Therefore, their registration should be made in the more sensitive polymers. They first appear at different times and the etching rate is much slower than that of fission fragments in the same material. Figure 4 illustrates a micrograph of alpha particles (small holes) and fission fragment tracks (large holes, 17 μm in diameter) in cellulose nitrate film (Kodak-Pathe LR-115) etched by the conventional method in 10 percent NaOH solution at 60°C for 90 minutes (Sohrabi and Becker, 1971). Tracks produced by direct interaction of fast neutrons with polymers (i.e. fast-neutron-induced recoil particle tracks) as previously stated are a rather more complex function of etching time because the induced tracks are due to recoil particles of differing LET's and are distributed throughout the polymer. In this case the track density increases with etching time and reaches a plateau where equilibrium exists between the development of tracks from a greater depth in the detector and the disappearance of overetched shallow pits.

Generally, in any type of track etching, only tracks in touch with the etchant are developed. Since fast-neutron-induced recoil particle tracks (as stated above) are distributed throughout the polymer, techniques for etching volume tracks from deeper layers have been advanced (Benton, 1971; Khan, 1975a). In this case, etchant will be conducted through some source channels. These channels are produced in the polymer by bombardment of heavy charged particles such as 9.6 MeV/nucleon $^{56}Fe^{+22}$ ions prior to fast neutron irradiation. By such methods, sensitivity for re-

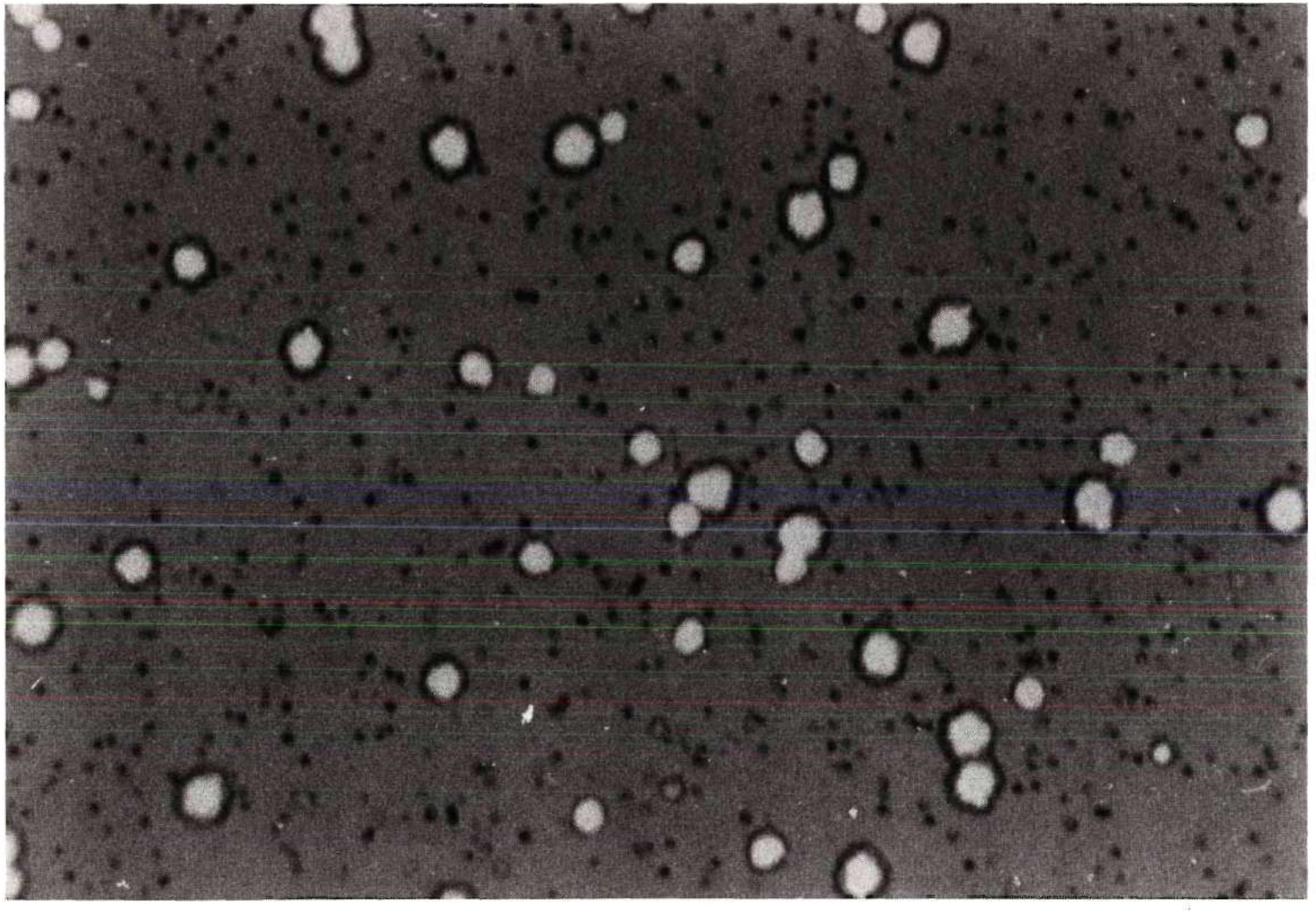

Figure 4. Microphotograph of Alpha Particle (small holes) and Fission Fragment (large holes) "Tracks" in LR-115 after Etching (after Sohrabi and Becker, 1971)

coil particle registration has been increased by two orders of magnitude (Khan, 1975a).

Effects of chemical composition and concentration of some etchants, in particular alkali halide solutions, have been studied for different polymers by some investigators (Blanford et al., 1970a; Dutrannois, 1971; Enge et al., 1974). Figure 5 shows fission fragment track etching rate of different polymers as a function of NaOH concentration (Blanford et al., 1970a). As can be seen the concentration dependence of the track diameter etching rate takes on quite different forms for different track recorders such as polycarbonate, cellulose acetate, cellulose nitrate, and cellulose acetobutyrate in a decreasing order, with the Lexan curve displaying the steepest slope, and the cellulose nitrate curve the flattest slope (Blanford et al., 1970a). In fact in cellulose nitrate the bulk etching rate reaches a plateau after a certain concentration (Enge et al., 1974).

Etching temperature is perhaps the most critical parameter affecting the etching rate. For example, the etching rate of silicon polycarbonate in 6.25 N NaOH solution has been shown to be an exponential function of etching temperature (Fleischer et al., 1972). A tenfold increase in the fission fragment track diameter (from 2.5 to 25 μm) has been observed when etching temperature was increased from 30 to 60°C for some track recorders (e.g. cellulose acetate) (Blanford et al., 1970a). This critical temperature dependence reveals a necessity for its control in cases where optical density or spark counts are measures of track density. However, for track counting by a microscope, small variations in temperature do not cause any significant changes in the results such as track density.

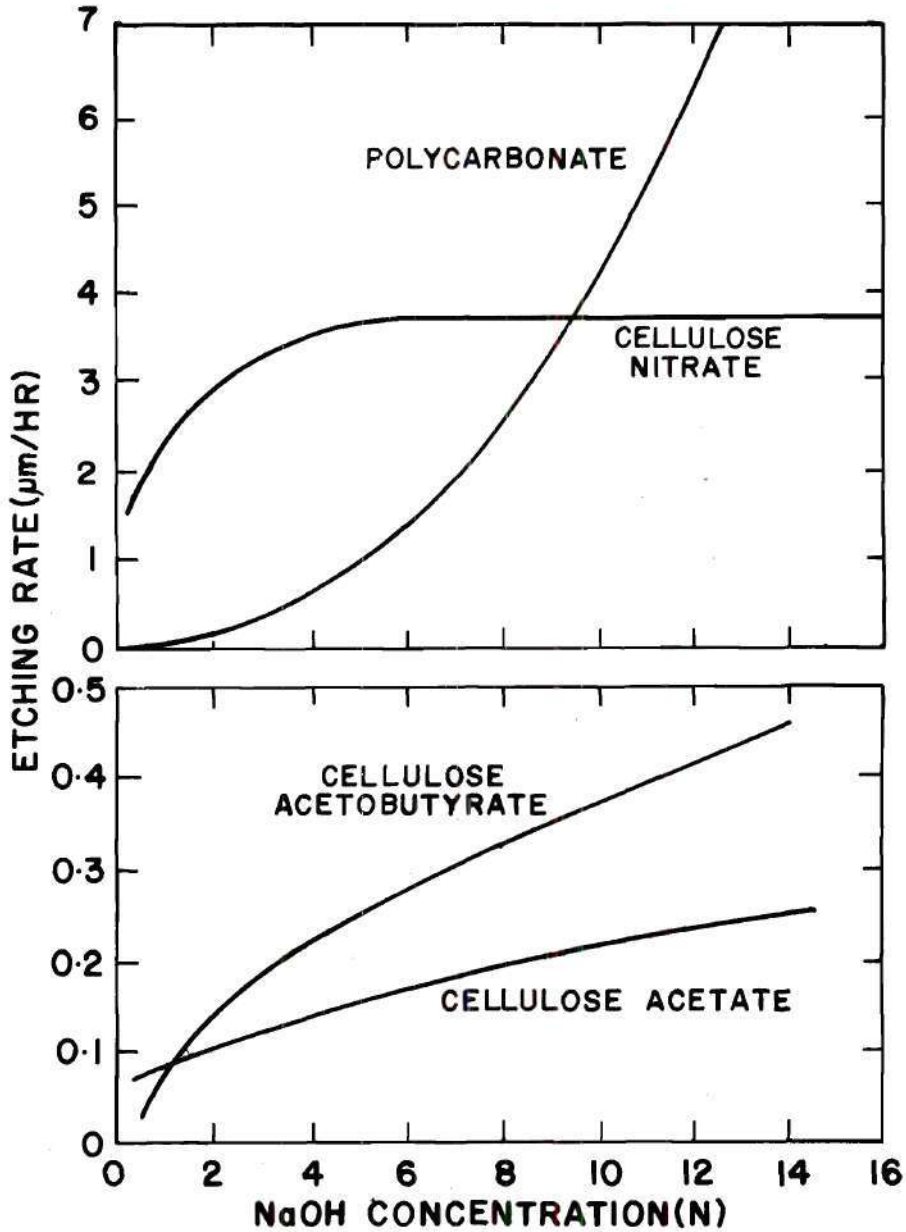

Figure 5. Etching Rate (rate of increase in track diameter) as a Function of NaOH Concentration in Different Polymers (after Blanford et al., 1970a)

The physical and chemical pre- or post-irradiation treatment of detector materials such as hardening of polymers by aging or preheating changes the etching kinetics particularly at high temperatures and in more sensitive polymers. For example, the etching kinetics of cellulose nitrate were changed dramatically when it was preheated to temperatures up to 145°C for an hour, while no changes occurred in polycarbonate foils up to 180°C (Somogi, 1972a). On the other hand, Khan (1975b) reported some changes in maximum track length of fission fragment tracks and registration efficiency of polycarbonate and cellulose nitrate materials by short term (10 minute) pre-irradiation annealing at different temperatures. Long term post-irradiation storage (three months) of 10 micron thick polycarbonate foils in a tropical climate (30°C, 95 percent humidity) after being irradiated with fission fragments from an uncapsulated ^{252}Cf source has increased the required etching time for perforation of all fission tracks before spark counting (Sohrabi, 1971). Softening of polymers by chemical reagents such as H_2O_2 (Becker, 1968) and UV light in different gaseous environments (Henke et al., 1970), oxidation by O_3 (Somogi, 1972b), and spark discharge in the irradiated foils before etching (Blanford et al., 1970b) also change the etching rate either along the track or along the unirradiated bulk surface. Many other pre- or post-irradiation treatments such as environmental, thermal, mechanical, electrical, photochemical, and irradiation effects have been reviewed and discussed by Becker (1973) and Fleischer et al. (1975) and have been shown to change track etching characteristics.

For good reproducibility in ultimate track density or track dimensions, etching conditions must be carefully controlled; in particular,

this is essential if counting methods, as will be seen below, such as spark counting or optical densitometry, are applied. In addition, for spark counting techniques, foils having uniform thicknesses must be used. However, if visual track counting is employed, foil thickness is not very critical. It must not be overlooked that foil materials obtained from different vendors or from batch to batch might differ significantly. Therefore, individual calibration of each batch under controlled etching conditions is sometimes essential.

The stability of "latent" damage under different temperatures and humidities differs from material to material (for review, see Becker, 1973). After etching, no fading of tracks can be observed except in polymers at temperatures close to their melting points. Before etching in some materials such as mica and quartz, temperatures as high as 600 to 800°C are required to anneal fission fragment tracks (Khan, 1974). In sensitive polymers such as cellulose nitrate, complete annealing of the tracks occurs by overnight storage at 80°C (Johnson and Becker, 1970). However, polycarbonate is more stable in retaining charged particle tracks for both fission fragments and fast-neutron-induced recoil particles (see Chapter VI).

3.2.2 Electrochemical Etching Methods

Perhaps the most elegant etching method is that introduced by Tommasino (1970). Detailed information on the electrochemical etching system as well as etching procedure will be given in Chapter IV. Briefly, the technique is based on conductive energy loss along the tracks by applying a high voltage at a frequency having square or sinusoidal waveforms in an etchant at room temperature (or at a higher temperature if desired which

results in preferential local etching along the track This leads to an etching rate along the track which is much greater than that of undamaged surrounding surface leading to very large tracks usually round in shape. Figure 6 shows fission fragment tracks from a ^{252}Cf source in gamma film backing (Sohrabi and Becker, 1971). These tracks were developed in succession by electrochemical etching and conventional etching at room temperature in an electrochemical etching chamber by simply turning the high voltage on and off in different periods of time. Different regions shown in the tracks indicate different processing events.

In electrochemical etching, a high voltage at a certain frequency is applied across an etching chamber (see Figure 9) filled with the etchant. The diffused ions in the etchant each experience a force which is equal to

$$\vec{F} = Z_i \, e \, \vec{E}$$

where $\vec{F}$ = the induced force, Z_i = the number of elementary charges, e = the unit electric charge, and $\vec{E}$ = the electric field at the location of the ions. This force is superimposed on the random walk of the diffused ions. Thus a positive ion is accelerated toward and away from an electrode as its potential oscillates from minus to plus, respectively. Likewise, the negative ion is accelerated to and from an electrode as it alternately becomes an anode or cathode, respectively. A steady ion movement occurs in one direction when a steady dc voltage is applied; however, in case of ac voltage, the direction of motion of the ions is changed twice each cycle. To better visualize the behavior of electrochemical etching, at least in part, the following steps may be considered:

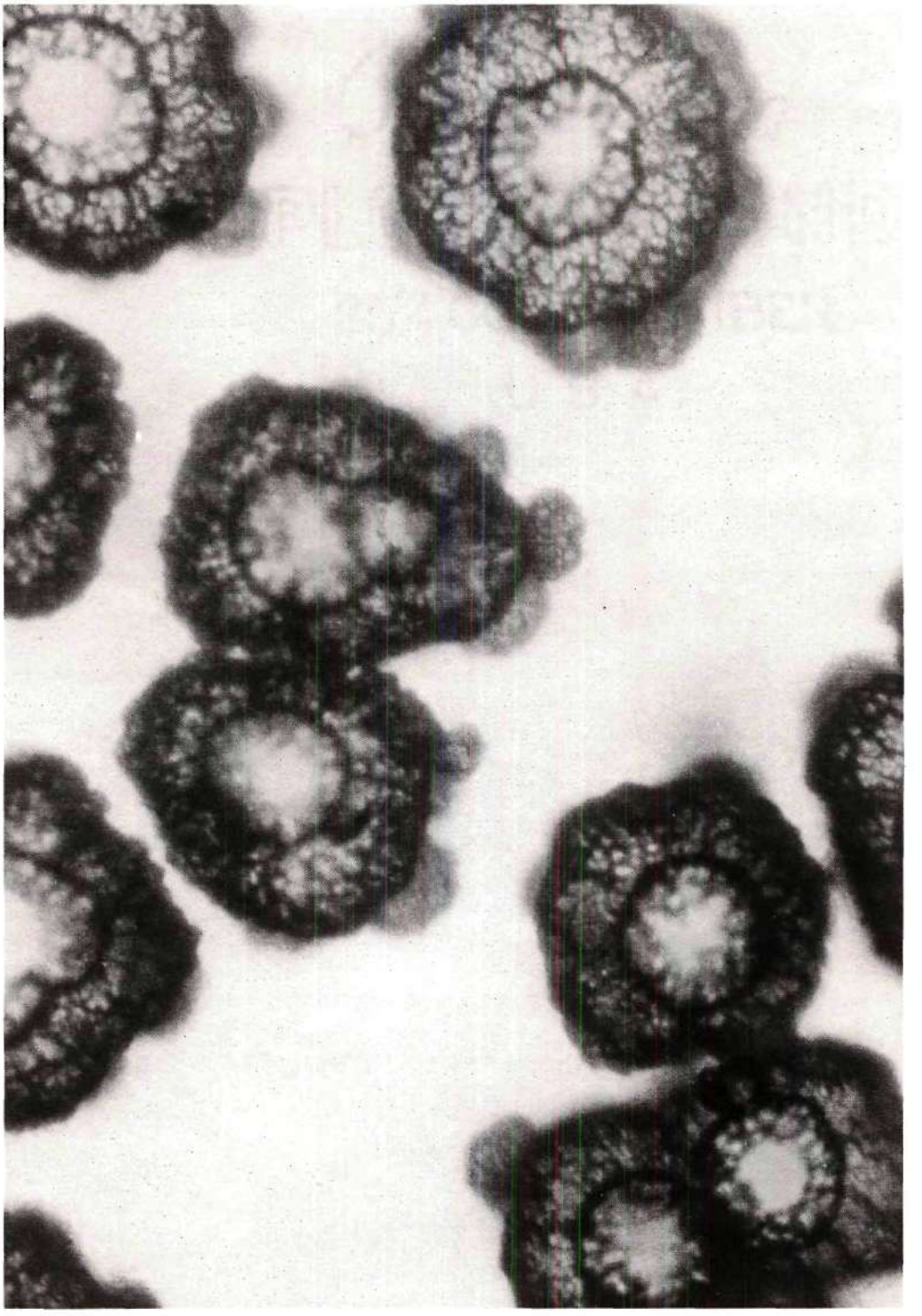

Figure 6. Fission Fragment Tracks from ^{252}Cf in Gamma Film Backing by Consecutive Treatment of Electrochemical and Conventional Etching

(1) When no foils are present between the containers, under a dc or ac voltage, an ionic current will flow across the chamber if the electrical impedance is finite; it is steady in the former case and alternative in the latter. This ionic flow in the solution is equal to the electron flow in the external circuit.

(2) When a dielectric foil is incorporated between the two containers of the chamber, a capacitance is introduced in the circuit. The capacitive reactance of the current is therefore $X_c = 1/2\ \pi fC$ where f is the frequency and C is the capacitance. In this case, with a steady dc voltage applied, f equals zero and the capacitive reactance is infinite so that no current can pass through the chamber. Therefore, it performs like an open circuit and electrochemical etching is not effective.

(3) When an ac voltage is applied across the chamber with foils of optimum thickness present, the electrochemical etching becomes effective even at one Hz (Tommasino, 1970). The ions in the etchant experience a force which changes their direction two times per cycle. In this case the impedance and capacitive reactance are finite leading to a small current through the chamber which depends strongly on the foil thickness. Figure 7 shows measured capacitance and current through the chamber as functions of polycarbonate foil thickness. The currents for different polycarbonate foil thicknesses were measured in the chamber filled with 28 percent KOH solution at 25°C applying 800 V at two kHz using the power supply of Figure 10. As can be seen, the capacitance and the current follow each other as hyperbolic functions of foil thickness. The current decreases with thickness reaching a small value corresponding to a thickness beyond which electrochemical etching becomes ineffective as will be

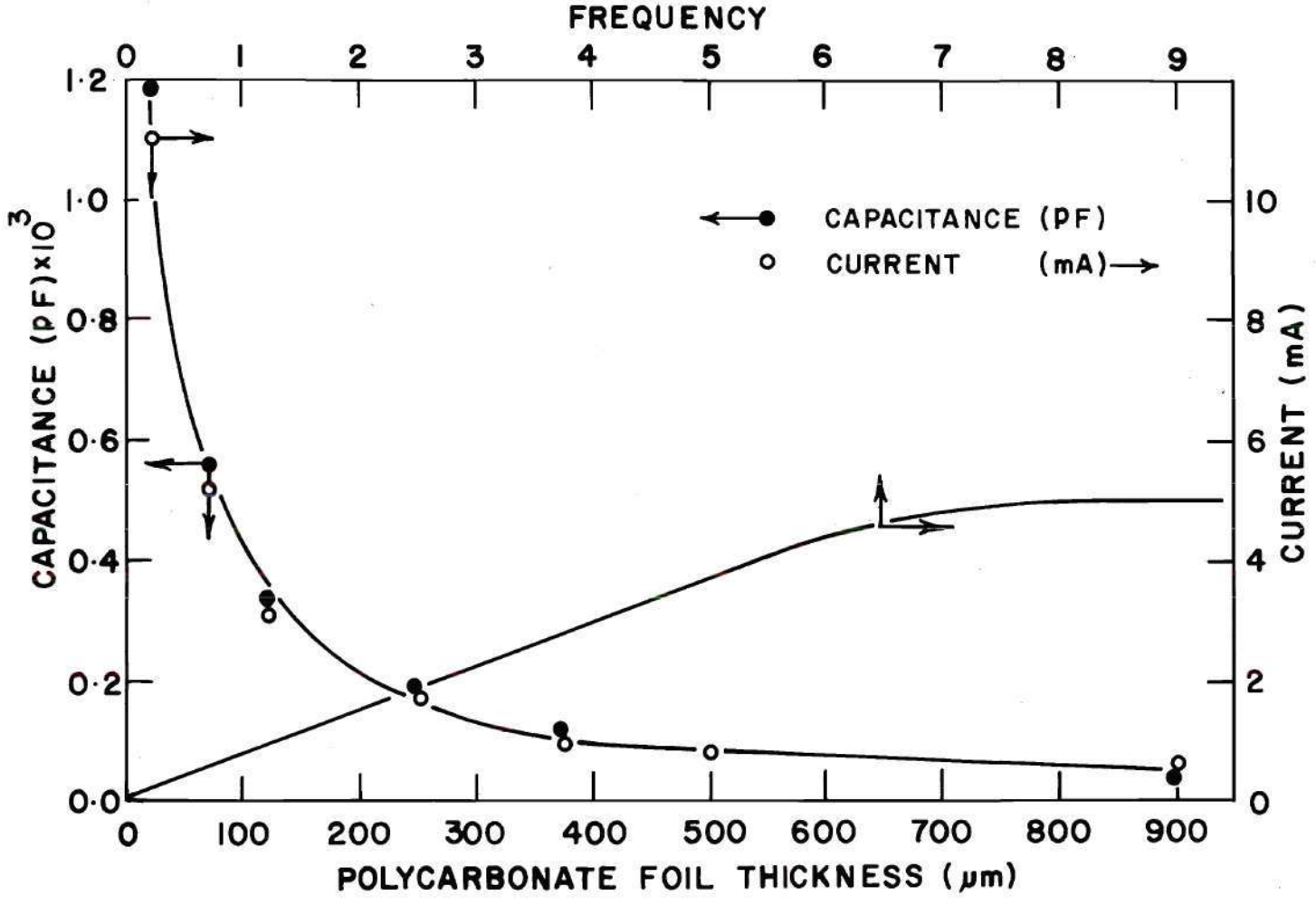

Figure 7. Measured Capacitance (pF) and Current (mA) as Functions of Polycarbonate Foil Thickness (μm) Introduced in the Electrochemical Etching Chamber Shown in Figure 9, and Measured Current as a Function of Frequency for 250 μm Polycarbonate Foils Etched in 28% KOH Solution at 25°C Applying 800 V

discussed in Chapter V. On the other hand, as the frequency increases the capacitive reactance decreases, thus the current (measured for 250 μm polycarbonate foils at the above etching conditions) increases to a point reaching a plateau, as shown also in Figure 7, determined by the ohmic resistance, R, of the circuit. If there is an inductive reactance $X_L = 2\pi fL$ in the circuit, resonance or a maximum current is reached when $f = 1/2\pi\sqrt{LC}$. In any case the absolute value of the total impedance, $|Z|$, is given by $|Z| = \sqrt{(X_L - X_C)^2 + R^2}$. Based on the experimental results obtained during this investigation, it was found that, although the current through the chamber controls the overall effectiveness of etching in different foil thicknesses, local oscillation of the ions at the damaged sites leads to currents which seem to be responsible for sensitivity (tracks/cm^2·rad) control for each foil thickness (see Chapter V).

Like any other etching method etching conditions must be controlled for best results. Unlike conventional etching techniques, however, many parameters govern the effectiveness of electrochemical etching in terms of sensitivity and track diameter. Some of the more important parameters include:

1. nature or type of the dielectric material used,
2. thickness of the dielectric material and its dependence on the duration of the etching process,
3. applied voltage and its frequency,
4. chemical composition, concentration, and temperature of the etchant,
5. size of the electrodes, distance, and angle between them,
6. type and energy of the charged particle.

These parameters were studied in some detail in this investigation as applied to fast-neutron-induced recoil particle track amplification in polycarbonate foils and will be discussed in Chapter V.

3.3 Track Detection Methods

It is a basic requirement in dosimetric application of solid state nuclear track detectors to determine the number of tracks per unit area of detector surface or any change in the detector characteristics, such as optical density, which is a measurable parameter varying as a function of dose delivered by the particles bombarding the foil. A large number of techniques has been proposed and used for track detection. For the purpose of this section some track counting techniques will be discussed based on conventional etching of tracks unless otherwise indicated where relevant to electrochemical etching. The counting methods are divided into four categories:

(1) microscopic or visual counting method,

(2) optical densitometry,

(3) spark counting techniques, and

(4) other techniques.

Visual track counting with a microscope has been the most common technique in studying track structure and track density determination. It is a unique technique for studying track structure and dimension measurements, but a tedious method for counting purposes. It is also a slow and inaccurate process subject to systematic errors especially when tracks are small and not well defined. This is particularly true when the track density is either very low or high where increased error in counting is

unavoidable.

Attempts have been made to simplify visual track counting under a microscope. For example, some especially developed films, such as Kodak Pathé LR-115 consisting of a thin film (8 μm) of red-dyed cellulose nitrate coated on a clear polyester base have been used for track detection (Barbier, 1970). In this case tracks become visible under a microscope as transparent holes on a red background which easily can be counted visually (see Figure 4). The technique has been further applied to alpha particle detection (Costa-Ribeiro and Lobão, 1975) and recoil particle detection (Tripier et al., 1975). Other methods such as interference-contrast techniques provide additional contrast by producing different interference colors around the etch pits (Piesch, 1970; Sohrabi, 1969).

There are other visual counting techniques especially for low track densities. One technique utilizes thin polymer films coated with aluminum on one side. The etchant passes through the fission fragment trajectory to the other side of the foil, thus making holes in the aluminum coating which can be seen by the unaided eye (Fleischer et al., 1966). An alternative method is placing the etched perforated foil against a membrane filter and forcing a solution of dye through the perforations making a dyed spot on the membrane which is large enough to be observed by the unaided eye (Cross and Tommasino, 1970). A rather similar method is the dyeing of the tracks after etching by red ink for contrast amplification (Khan, 1971). All these methods are usually time consuming but useful for low track density counting.

Prior to development of electrochemical etching, conventionally-etched fission fragment track counting by a microscope was considered the

simplest because these tracks can be distinguished easily from other particle tracks such as alpha or recoil particle tracks (see Figure 4) and because fission fragment tracks are usually developed more easily by conventional etching and appear very well defined. However, by electrochemical etching such a discrimination between different types of tracks no longer exists. Both fission fragment and recoil particle tracks can be amplified by electrochemical etching as very well-defined tracks which can be observed easily under a microscope at low magnifications (X40) or projected on a white screen or observed by a microfilm screen or even detected easily by the unaided eye. Thus, at low track densities the whole area of the foil (e.g. two cm^2) can be counted with minimum counting errors.

Another category of track counting methods is optical densitometry (Tuyn, 1969). Optical density in general depends on many factors such as track density, etching conditions, and foil thickness. Therefore, if the other parameters are fixed and the first factor (track density) is the only variable parameter, then the optical density can be an indication of track density or particle fluence. The red-dyed cellulose nitrate as mentioned above can be subjected to optical densitometry, particularly if the wavelength chosen for the densitometry is adjusted to the optical absorption peak of the dye. Figure 8 shows optical density as a function of etching time in 10 percent NaOH solution at 60°C for red-dyed cellulose nitrate irradiated to fission fragment (from ^{252}Cf) and for different track densities (Sohrabi and Becker, 1971). Optical densitometry with other track detectors such as phosphate glasses and polycarbonate foils have

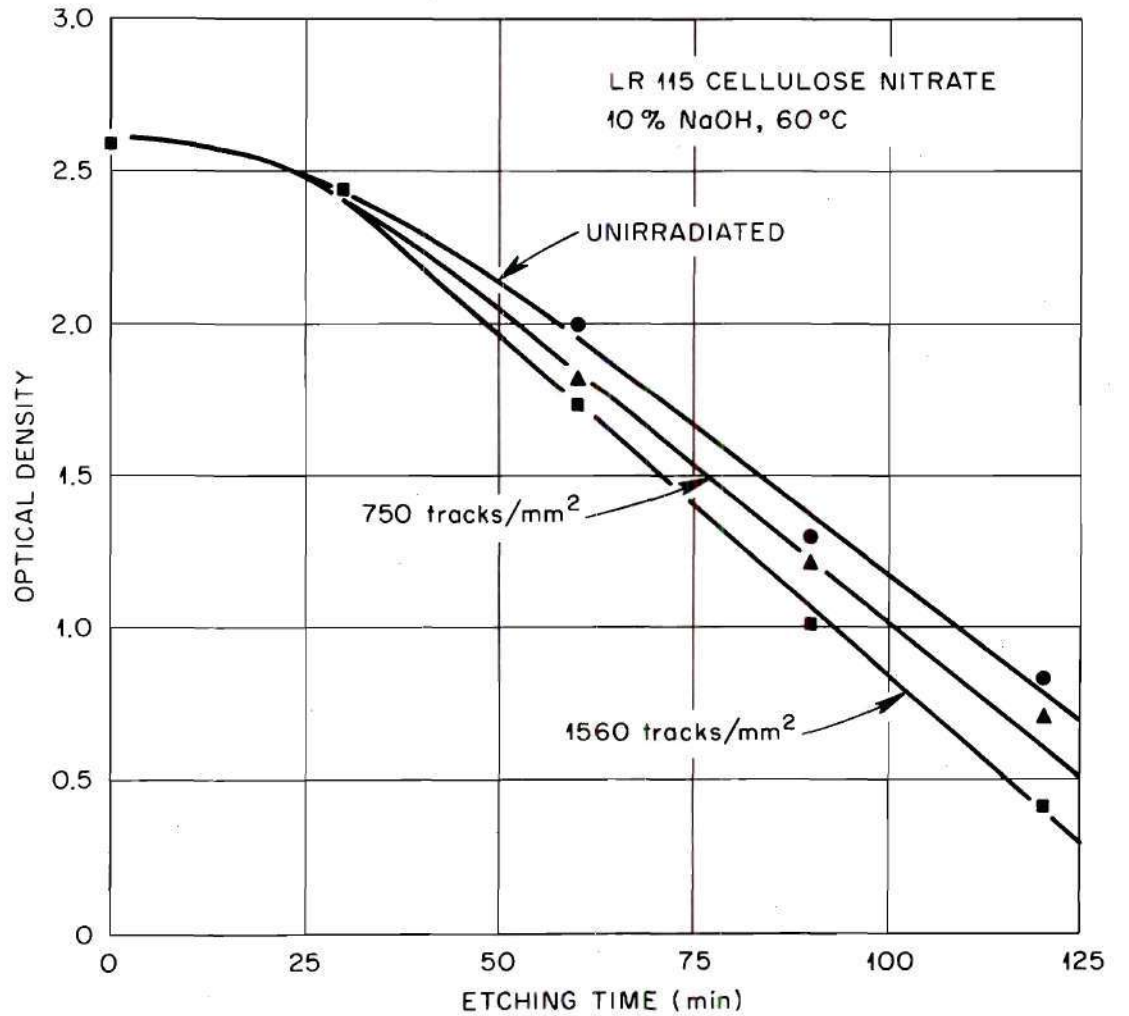

Figure 8. Optical Density of Unexposed and Fission Fragment (from ^{252}Cf) Irradiated LR-115 as a Function of Etching Time in 10% NaOH at 60°C for Indicated Track Densities

been applied in a few applications (Tuyn, 1969; Tuyn and Broerse, 1970). Generally, optical density measurements can be used at high track densities. However, if tracks are large and have good contrast at low track densities, visual counting is preferable.

The availability of thin plastic foils also opened up new methods for automatic determination of track density. Conventional etching of thin foils irradiated by fission fragments or alpha particles leads to perforations through the foils so that one can produce sparks through them. One method is to place the etched foil against a grounded plane electrode and scan across it with a knife-edge at high potentials (Cross and Tommasino, 1968; Lark, 1969). Whenever the knife edge passes a hole, a spark occurs which enlarges the hole and also darkens the whole path so that the darkened spots can be observed by the eye. This technique is limited to relatively low track densities because there are difficulties in resolving perforations that are close together.

An improved sparking method developed by Cross and Tommasino (1970) is based on the same principle but instead the moving parts are avoided during the counting process. The technique is extremely simple, fast, and capable of counting low and intermediate track densities. The etched foil is placed as an insulator on a central electrode and is covered in close contact with a piece of aluminized Mylar with the aluminized side facing the etched film and making contact with an outer grounded electrode. When a positive voltage is applied between ground and the central electrode, a spark passes through one of the holes, and the heat of the spark causes an evaporated spot on the aluminum electrode. Thus the electrical resistance through this hole increases preventing the counter from multi-

ple sparking through the same hole. Thereafter, the spark jumps from one hole to another until all the holes have been sparked (and burned evaporized spots have been produced opposite each hole), then the counting stops.

The counting process can be done by coupling the counter to a scaler through a simple, GM-type quenching circuit so that each spark is recorded by the scaler. The number of counts or sparks obtained depends on applied voltage, etching conditions, foil thickness, etc. The number of counts as a function of applied voltage increases reaching a plateau between 500 and 800 volts for 10 μm polycarbonate foils (Burger et al., 1970). Therefore, the operating voltage often used is usually around 500 volts with a precounting at 600 volts to cause complete perforations in those tracks which are about to perforate through the foil.

The spark counting technique has been applied successfully to fission fragment and alpha particle track counting in polycarbonate and cellulose nitrate films, but it had not proven to be very efficient in counting recoil particle tracks (Johnson and Becker, 1970). Two investigations by Becker and Abd-el Razek (1974) and by this author have shown that recoil particle tracks can be spark counted easily if the foils are properly etched. This method is based on extended etching of 10 μm polycarbonate foils (Kimfol) to a point comparable to the range of recoil particle tracks as used by Becker and Abd-el Razek or by using thinner foils such as 6 μm polycarbonate as are discussed in section 4.4. Spark counting of fission fragment tracks is linear up to 3000 tracks/cm^2; however, as will be seen, the range has been extended to higher track densities when recoil particle tracks are being spark counted. Also,

spark counting of fission fragment tracks in thin mica foils has been reported (Becker, 1975). The spark counting technique has found worldwide interest and has been the subject of many investigations (Prêtre, 1973; Nishiwaki et al., 1973; and others).

There are also numerous other techniques for track density determination; however, they have not found wide applications. One method is to pass gas through the perforations in the foil and detect the gas on the other side (Block et al., 1969) or to irradiate etched samples with short wavelength UV light and detect the photons passing through the holes by a photomultiplier tube (Prêtre et al., 1968).

Another method is based on the fact that the etched holes under dark field illumination of a microscope appear as bright spots on a dark field background where the integral amount of scattered light can be detected by a photomultiplier tube located at the microscope eyepiece (Becker, 1966).

Fission fragment track counting can be performed also by placing the perforated foil between an alpha source and a surface barrier detector (Khan and Durrani, 1972) or any other sensitive alpha detecting device. The number of alpha particles detected after passing through the holes is a sensitive measure of fission fragment track density. Measurement of scattered light from the fission fragment track sites by a photomultiplier tube is another method for high track density determinations (Schultz, 1968).

Among the mentioned techniques, visual track counting and studying track structure under a microscope, and spark counting methods have been widely used in many investigations. In particular, the spark counting

technique is good for low and intermediate track densities and has been used in many laboratories for track density determinations for research and routine neutron personnel dosimetry services.

CHAPTER IV

INSTRUMENTATION, EQUIPMENT, AND PROCEDURES

This chapter describes instrumentation, equipment, facilities, and procedures used in this investigation. The main portion of instrumentation and equipment required for track amplification was the electrochemical etching system designed and constructed in our laboratories during the course of this study. It consists of an etching chamber and a high voltage supply to maintain the voltage across the chamber at frequencies of interest. Phantoms also were constructed and used for depth dose studies. In addition, many gamma and neutron facilities used for foil irradiations in phantom or in air are discussed in this chapter.

4.1 Electrochemical Etching Instrumentations

An electrochemical etching system for large-scale foil etching applications requires an especially designed chamber capable of processing a large number of foils simultaneously. An electrochemical etching chamber was designed and constructed so that six foils could be etched simultaneously to demonstrate the feasibility of multi-foil etching. Figure 9 shows the electrochemical etching chamber used in most of this study. As can be seen, it consists of two cylindrical Lucite containers each having dimensions of 11 cm in diameter and 11 cm in length. The overall length of the chamber is therefore 22 cm. A slit was made on top of each container for placing and replacing the electrodes.

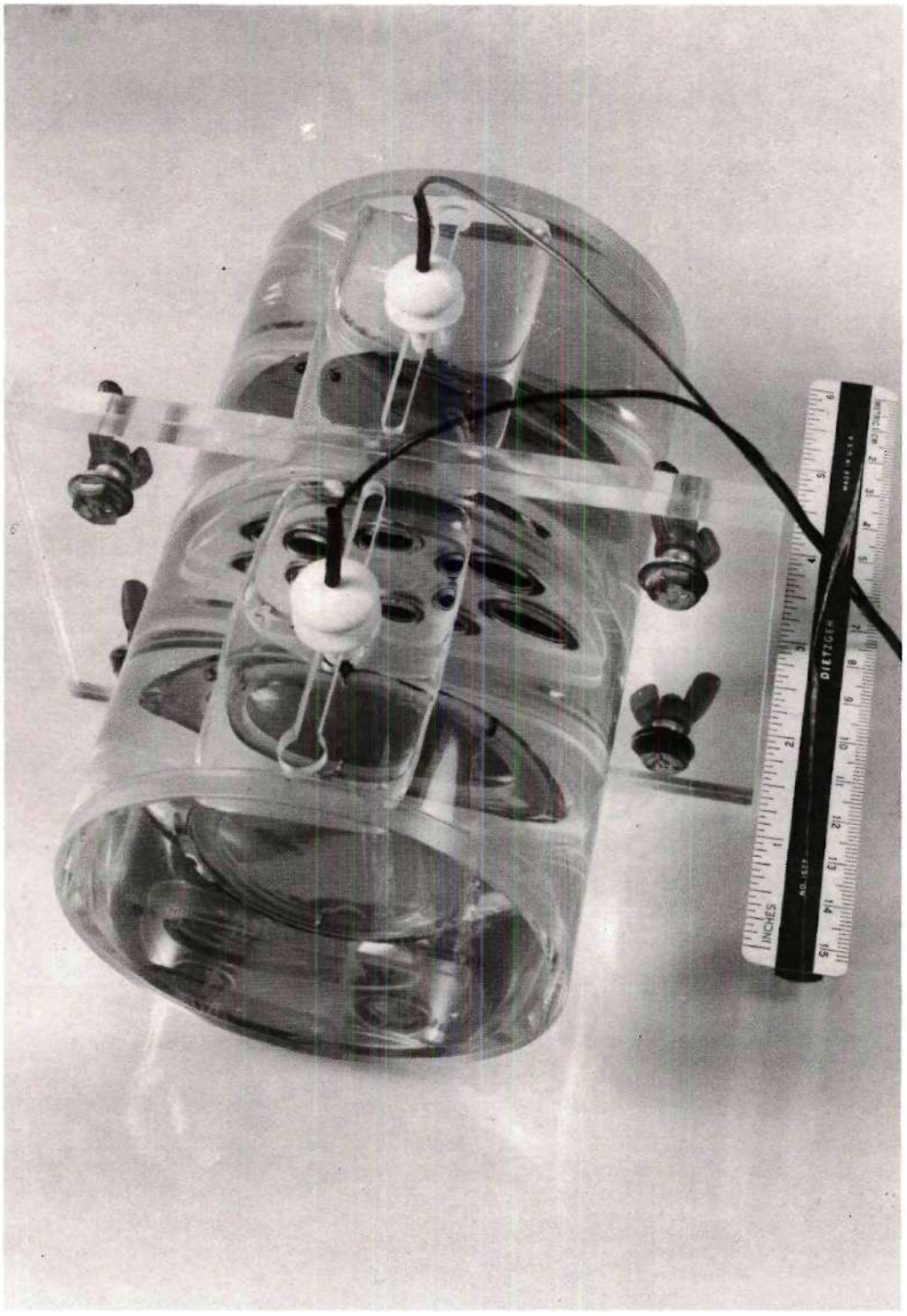

Figure 9. An Electrochemical Etching Chamber

The foils to be etched (each two cm in diameter) were placed in windows between the containers to isolate them electrically when the high voltage is applied. Each foil is held firmly in place by means of two rubber "O" rings. The containers, as can be seen from Figure 9, are held together by means of four wing nuts. Special precautions were taken to prevent any etchant leakage through or around the foils which would automatically stop the electrochemical etching process.

After the chambers were set up with foils in place, they were filled with the etchant at a preadjusted temperature. Then two electrodes each six cm in diameter were placed in the etchant as they are shown in Figure 9. Platinum, palladium, and stainless steel were each used as satisfactory electrodes during the course of this study. Platinum and stainless steel electrodes were found to be thick enough to be used without added support. However, the palladium electrodes were thin (125 μm) and difficult to handle, so they were supported by a Lucite "O" ring having the same diameter (six cm). Stainless steel electrodes were preferred because of negligible cost and ready availability. The electrodes were kept parallel to the plane of the foils for better reproducibility, although the angle did not seem to be very critical.

4.1.1 High Voltage Supply Systems

Electrochemical etching amplification of charged particle tracks requires a high voltage power supply having variable output voltages ranging from 100 to 1500 volts, or higher if desired, at variable frequencies of square or sinusoidal waveforms ranging from 1 Hz to 10-20 kHz. Such a power supply permits one to study the effects of applied voltage and frequency over a wide range.

To obtain the desired frequency, a high frequency generator is required. Two audiofrequency generators (Jackson, Model No. 652 and Heathkit, Model No. 1G-72) were available for this investigation. These types of audiogenerators usually do not supply sufficient power and voltage for electrochemical etching amplification of charge particle tracks. Therefore, their outputs had to be further amplified to maintain the necessary voltages at the desired frequencies.

Two power supplies were constructed and used in this investigation. In one system, the output of the Jackson audiogenerator (which was of the order of 80 volts at two kHz) was further amplified by means of a home-made push-pull power amplifier. Figure 10 shows the circuit diagram of such an amplifier connected to the frequency generator and the etching chamber. It was used in almost the entire investigation. The maximum voltage obtained by this power supply system was about 1500 volts. The current passing through the chamber depends on a number of factors including the applied voltage and its frequency, foil material and its thickness, total foil area, etchant concentration and its temperature, etc. For example, currents of the order of 11 mA and two mA were obtained using Lexan polycarbonate foils of thicknesses 25 μm and 250 μm, respectively, when the chamber was filled with 28 percent KOH at 25°C by applying 800 V at two kHz.

Another power supply was designed and used in some of the investigations. In this case the output of a Heathkit audiofrequency generator was amplified through a 70 watt Heathkit push-pull amplifier followed by further amplification by an audiotransformer to supply a maximum output of about 2500 volts at two kHz.

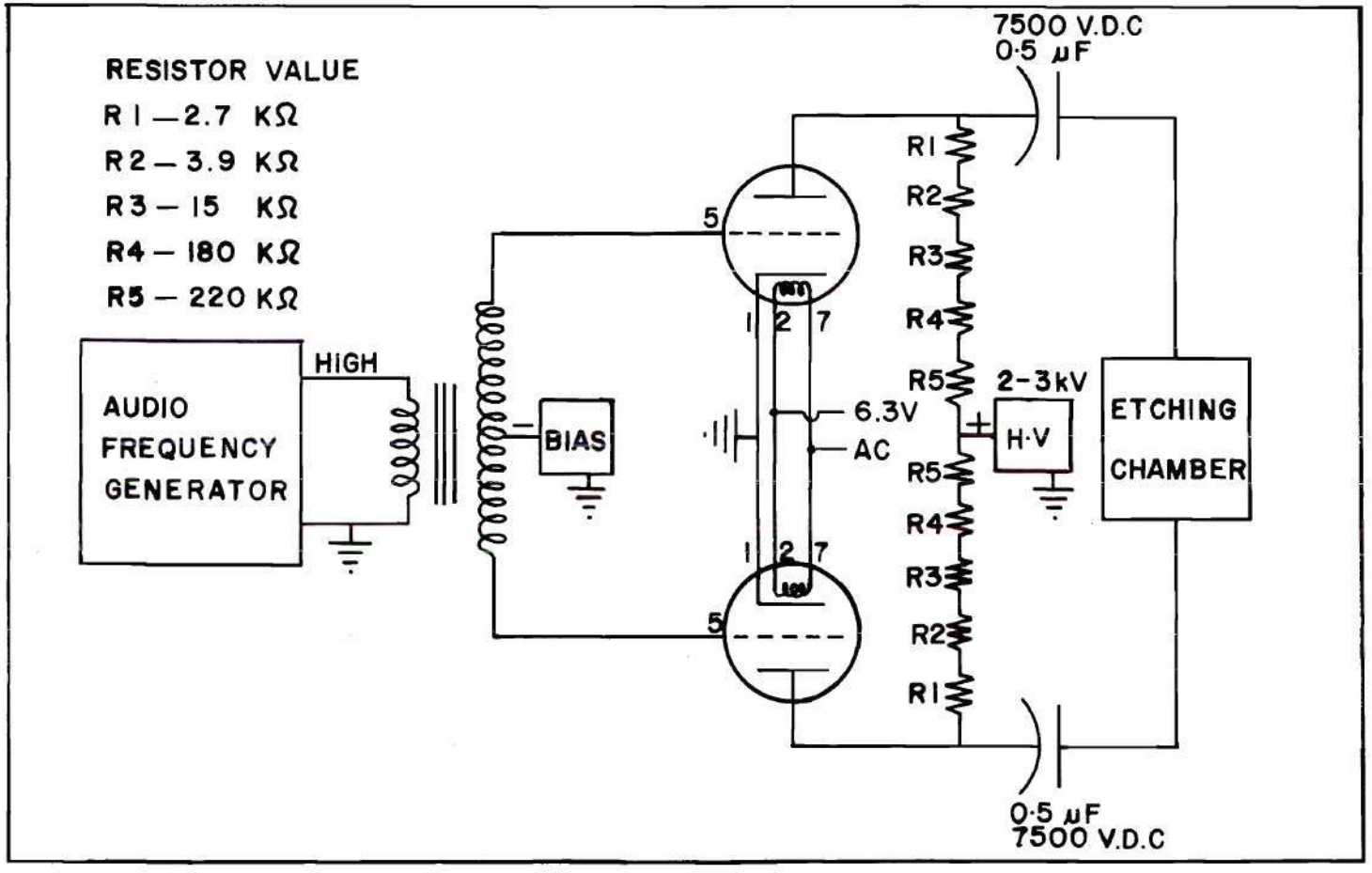

Figure 10. Diagram of Electrochemical Etching System Used in This Study

Both power supplies were tested for frequency and voltage stability. Under similar electrochemical etching conditions they both performed satisfactorily in the amplification of fast-neutron-induced recoil particle tracks. The sensitivities (tracks/n·rad) obtained with the two systems were the same within experimental errors. However, because of the larger power output of the second power supply, it was more suitable for etching large numbers of foils. Nevertheless, the first power supply was used mostly in these investigations.

4.2 Electrochemical Etching Procedure

Etchant solution ("etchant") of a certain concentration is required for any type of etching technique. Etchants having appropriate percent by weight were prepared by adding known amounts of potassium hydroxide or sodium hydroxide into known amounts of distilled water in a beaker. This process was carried out slowly followed by gentle stirring of the combination. The beaker was covered to prevent the collection of dust or loss of water by evaporation. The solution was allowed to cool down to room temperature (usually 24.5 ± 0.5°C); however, the temperature is reported as 25°C.

Polymer foils used in most parts of the study were 2 cm in diameter. They were punched out of a plain sheet of irradiated or unirradiated polymers. Care should be taken in this process to prevent the foils from being scratched unless they are masked by the manufacturer. Each foil was labeled by a strip of transparent tape attached to the foil and numbered by a marking pen.

The foils to be etched were placed between the containers comprising

the chamber as described in section 4.2.1. The containers were then filled with the etchant having the desired temperature and concentration. The electrodes were placed in the containers at fixed positions about 8.5 cm apart and parallel to each other. Then a high voltage at a selected frequency was applied across the chamber through the electrodes. The voltage across the chamber was continuously monitored by a voltmeter for any unexpected voltage changes since the voltage will drop if there is any perforation through the foil or etchant leak between containers. Etching then proceeds for a time which depends mainly on the foil thickness when other parameters are fixed.

After an optimum etching time in each process, the high voltage was disconnected and cleanup begun, i.e. removing the electrodes, pouring out the etchant, washing to remove any residual etchant from the foil surfaces, etc. Then the foils were removed and dried at ambient room conditions, often by blowing air over them. The total time for these steps was 20 to 30 minutes.

4.3 Recoil Particle Track Counting

A number of counting techniques was discussed in Chapter III. Some of the methods included visual track counting under a microscope and on a microfilm screen, optical densitometry, scattered light measurements, and spark counting techniques. It should be mentioned that spark counting was applied only to those tracks induced in very thin polycarbonate foils (six μm) when conventionally etched (discussed in the following section).

Some of the good characteristics of fast-neutron-induced recoil particle track amplification by electrochemical etching compared to tracks

obtained by conventional etching methods are large track sizes and sharp contrast against an undamaged transparent surface. This is to the extent that the unaided eye can provide a rough track density determination when the observer is experienced. Hence, dose determination by the eye can be considered as the simplest and fastest method for routine and accidental fast neutron dosimetry cases.

For visual track counting under a microscope, a Nikon light microscope Model No. 74890 was used. The microscope was used extensively for both track density determination and track diameter measurements. For track diameter measurements a filar micrometer was placed on the microscope eyepiece. Tracks can be observed under different illumination conditions, e.g. under light field or dark field. Figures 11 and 12 show the appearance of the tracks under the two illumination conditions, respectively, in 125 μm polycarbonate foils etched in 28 percent KOH solution at 25°C by applying 700 V at one kHz for 2.5 hours. As can be seen, tracks are amplified on both sides of the foil with a ratio which depends on the neutron energy and etching conditions applied. Therefore, for consistency, tracks on both sides of the foils were counted under each field of view and reported track densities are the averaged values of 10-12 field areas randomly scanned. For low neutron doses encountered in routine personnel monitoring the whole area of the foil can be scanned by projecting the tracks on a microfilm screen thus reducing counting errors significantly.

For optical density measurements, an Ansco-McBeth densitometer, Model No. TD100A, was used. The input voltage to the densitometer was maintained constant by a voltage regulator. The optical appearance of the

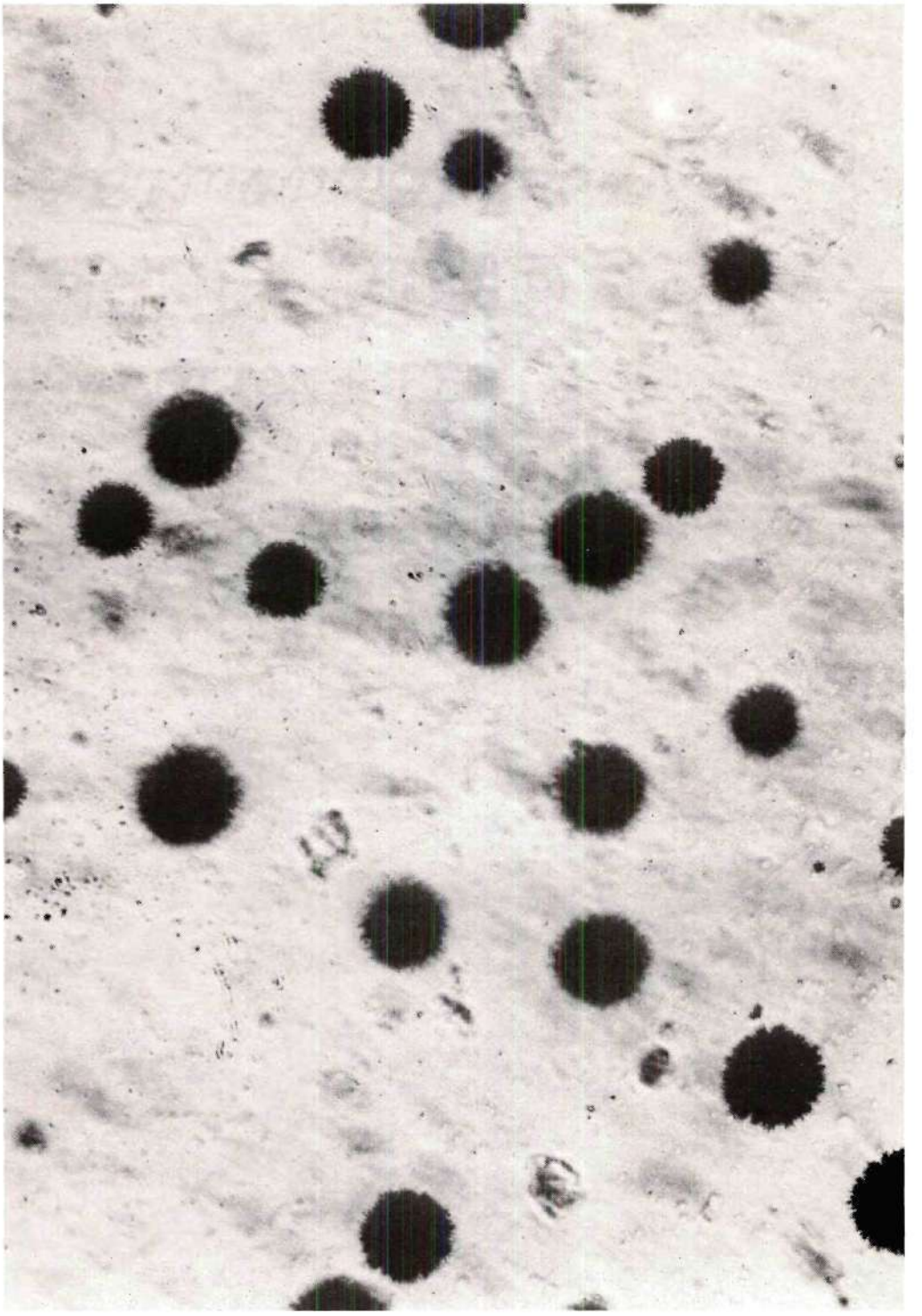

Figure 11. Micrograph of Recoil Particle Tracks in 125 μm Thick Polycarbonate Foil Etched in 28% KOH Solution at 25°C Applying 700 V at 1 kHz for 2.5 Hours

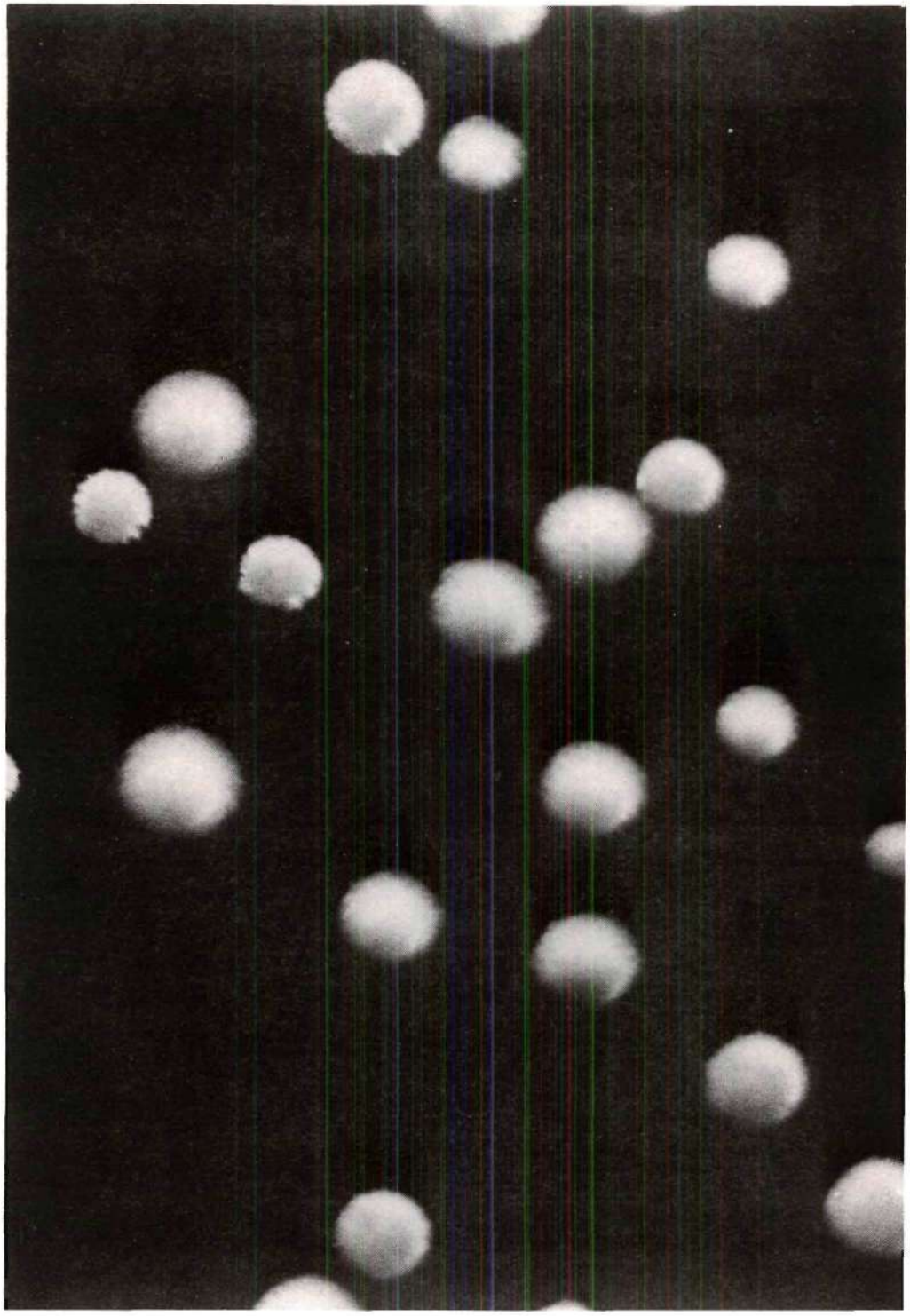

Figure 12. Micrograph of Recoil Particle Tracks in 125 μm Thick Polycarbonate Foil Etched in 28% KOH Solution at 25°C Applying 700 V at 1 kHz for 2.5 Hours

tracks is so pronounced that the optical density reading becomes significant at doses as low as 10 rads of fission neutrons.

A Bausch and Lomb microprojector was used both for track projection on a screen and for a light scattering measurement experiment. The projector consists of a 100 watt bayonet-base bulb with condensers and heat absorbing glass which prevents heating the sample. This microprojector was adopted for track density evaluation by measuring either the scattered or transmitted light from the foil. The scattered or transmitted light can be measured by a photovoltaic cell mounted on a circular Lucite shell in such a fashion that the cell can detect the scattered light at different angles. The system was isolated and painted black so that no stray light can reach the detector and only the scattered light can be measured. The intensity of the light was controlled by a variable transformer. This system was only used in some preliminary investigations.

4.4 Spark Counting of Conventionally Etched Recoil Particle Tracks

It has been shown that conventionally-etched recoil particle tracks due to their short range do not lead to efficient perforations through the foil for spark counting (Johnson and Becker, 1970). In a preliminary investigation in the early stage of this research it was shown that recoil particle tracks can be spark counted by using thin foils with a thickness close to the range of recoil particle tracks in the polymer using conventional etching methods. A similar investigation was reported by Becker and Abd-el Razek (1974) who used extended etching in 10 μm polycarbonate foils and stripable cellulose nitrate films. Our present report

describes briefly the techniques used and conditions applied and presents some preliminary results on response as a function of fission neutron dose. To avoid confusion, the etching technique used here was a conventional method as discussed beofre. The spark counter was constructed similar to the one used in a previous investigation (Sohrabi and Becker, 1971).

In this conventional etching method, six μm thick aluminized polycarbonate foils (Kimfol) were used. They were irradiated by fission neutrons according to the procedure described in the following sections. Each foil had been punched and glued to a Lucite "O" ring following a similar procedure applied in a previous investigation (Sohrabi and Becker, 1971). The ring had a 1.8 cm internal diameter. The advantage of the aluminized side was to provide extra support in handling the foils before etching. The aluminized side was dissolved after dipping in the etchant.

The etchant solution in this conventional etching system was contained in a dish and placed in a low temperature oven. The etchant temperature was controlled within ± 1°C. The stirring conditions could be controlled by a small magnetic rod in the solution and a magnetic plate underneath the dish. The dish had a Lucite top so that mounted foils could be placed in the solution by small alligator clips in a circular fashion to provide reproducible uniform etching of all foils. After etching, the foils were removed from the etchant with care, washed gently in running water, and dried in an oven at 40°C.

Etching time was optimized by etching several unexposed and exposed foils and observing the results using various etching times. By etching the foils in 28 percent KOH solution at 60 ± 1°C under very gentle

stirring conditions, etching time was optimized at 74 minutes. This time is slightly lower than the time after which the spark density becomes significant in etched unexposed foils. However, due to poor reproducibility, this time did not seem reliable.

Satisfactory spark counting of these foils is a very critical function of polymer thickness, etching conditions, neutron dose, sparking voltage, etc. After the exposed foils were etched under the mentioned etching conditions they were presparked at 600 volts followed by sparking at 500 volts. This routine was based on previous experiences with fission fragment track spark counting. It was observed that spark count density increases by successive sparking. Furthermore, slight movement of a foil over the electrode causes significant changes in the spark counts. Therefore, somewhat arbitrarily the third spark count density (without any movement of foil over the electrode) was chosen as the spark count density corresponding to a neutron exposure.

Figure 13 shows spark counts as a function of HPRR (Health Physics Research Reactor) fission neutron dose under the mentioned etching and sparking conditions at three different etching times. Under the applied conditions, the spark count density was a critical function of any variations in etching conditions such as temperature, etching time, etc. Therefore, the reproducibility and precision were not very satisfactory. Attempts were made to improve the mentioned etching conditions by using a 20 percent NaOH solution at 50°C. By this approach, better reproducibility and more uniform sparking were obtained although the etching time for satisfactory sparking had to be increased to seven hours.

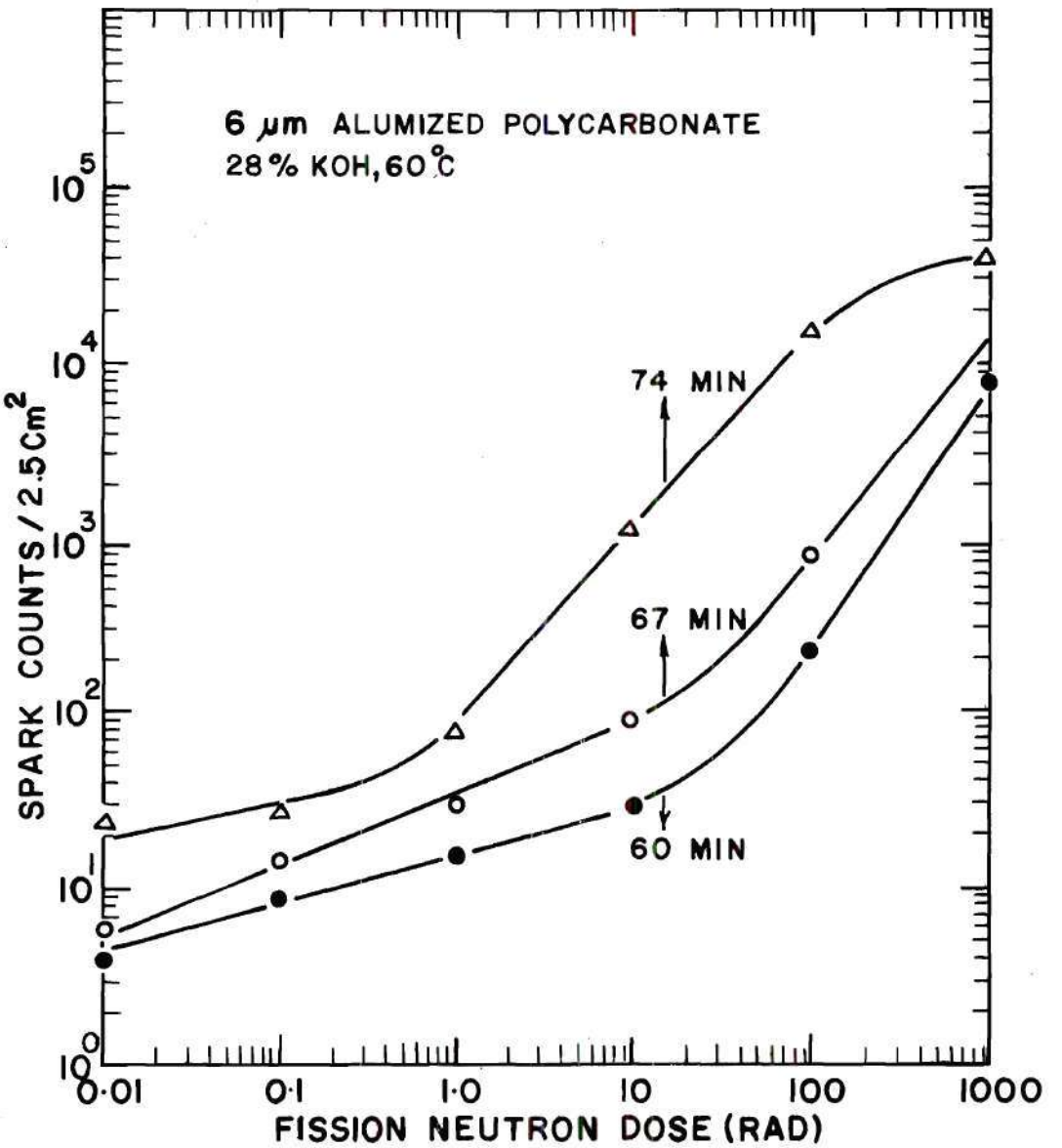

Figure 13. Recoil Particle Spark Counts as a Function of Fission Neutron Dose in 6 μm Aluminized Kimfol at Different Etching Times Etched in 28% KOH Solution at 60°C

4.5 Tissue-Equivalent Materials

Because of the complicated histological structure of tissue a simplified composition of tissue is applied in tissue dosimetry. This is because of difficulty in duplicating the exact composition and structure of tissue which are variable from tissue to tissue. Furthermore, experimental depth dose determination of a human body in vitro is an impossible task. Therefore, in practice, to simulate soft tissue or bone, equivalent solids or liquids are often used. To simulate the human body, simple phantoms consisting of cylindrical, elliptical, and cubical containers filled with tissue-equivalent materials are commonly used to obtain depth dose information. To study the effect of heterogeneity of a human body such as the presence of lungs or bones, usually lung phantoms and bone-equivalent materials are introduced inside the phantom. Recently, a sophisticated simulation of a theoretical anthropomorphic phantom proposed and studied by Snyder and Fisher (Fisher and Snyder, 1967) has been constructed for some external and internal dosimetry studies (Garry et al., 1973).

Table 3 summarizes some tissue and bone-equivalent compositions commonly used for dosimeter and phantom constructions. Additional information on tissue-equivalent liquids, solids, and gases is given also by Poston (1971). As can be seen from Table 3, the tissue-equivalent (TE) liquid of Goodman (1969b) is closest to the tissue composition recommended by NCRP (No. 38, 1971) and is often used in practice. It has only three components, i.e. urea, glycerin, and water. Bone-equivalent (BE) plastic (B-100) also has been used in many dosimetry investigations. Recently, bone-equivalent (BE) liquid used for the bone component of the anthropo-

Table 3. Elemental Composition of Tissue and Some Equivalent Materials

Element	Whole Body[1] %	Adipose Tissue[1] %	Muscle[1] %	Bone[1] %	Skeleton[1] %	TE Fluid[2] %	TE Fluid[3] %	TE Plastic[4] %	BE Plastic[5] %	BE Liquid[6] %	Polycarbonate* %	Cellulose Nitrate† %
Oxygen	61	23	75	43	49	71	74.2	5.0	3.06	53.0	18.9	57.1
Carbon	23	64	11	16	23	15.6	12.0	77.1	53.41	19.1	75.6	28.6
Hydrogen	10	12	10	4.1	7.1	9.8	10.2	9.9	6.39	6.5	5.5	3.2
Nitrogen	2.6	0.80	2.6	4.3	3.9	3.6	3.6	4.4	2.67	3.9	-	11.1
Calcium	1.4	0.0022	0.0031	21	10.0	-	-	-	17.69	10.3	-	-
Phosphorus	1.0	0.016	0.18	10	7.0	-	-	-	-	6.8	-	-
Sulfur	0.20	0.073	0.23	0.31	0.17	-	-	-	-	-	-	-
Potassium	0.20	0.032	0.30	-	0.15	-	-	3.6	-	-	-	-
Sodium	0.14	0.050	0.075	0.62	0.32	-	-	-	-	0.2	-	-
Chlorine	0.12	0.12	0.078	-	0.14	-	-	-	-	-	-	-
Magnesium	0.027	0.0020	0.019	0.22	0.12	-	-	-	-	0.2	-	-
Fluorine	-	-	-	-	-	-	-	-	16.77	-	-	-
TOTAL	99.687	100.09	99.48	99.55	100.9	100.0	100.0	100.0	99.99	100.0	100.0	100.0

[1]NCRP No. 38 (1972; [2]Rossi and Failla (1956); [3]Goodman (1969b); [4]Shonka et al. (1958); [5]Wingate et al. (1962); [6]Garry et al. (1974); *$(C_{16}H_{14}O_3)_n$; †$(C_6H_8N_2O_9)_n$

Abbreviations: Bone-Equivalent (BE); Tissue-Equivalent (TE)

morphic phantom mentioned above is attracting interest in some investigations. The mentioned equivalent materials (TE liquid, BE plastic, and BE liquid) were, therefore, used in this investigation.

4.6 Irradiation Facilities and Experimental Arrangements

Many facilities producing neutrons, protons, gamma rays, and high energy x-rays were used in these studies for foil irradiations in air and in phantoms. Some characteristics of these sources and facilities were discussed in Chapter II. However, the experimental arrangements including some characteristics of each source will be discussed below in more detail.

4.6.1 Neutron Irradiations in Air

Table 4 summarizes some characteristics of neutron sources used for air and phantom studies. The Health Physics Research Reactor was the neutron source used most extensively in this study. Polymer sheets of about 20 x 20 cm were supported in air using tape. The distances between the reactor core and the target samples varied according to the neutron dose to be delivered. For these exposures the reactor power was varied from a few watts up to several kilowatts at each reactor run depending on the neutron doses of interest. The neutron doses delivered were the values reported by the HPRR operation group (Fox, 1974). The reactor core was at the level of the samples during the operation, usually 1.5 meter above the floor.

A five Ci Pu-Be source (Georgia Tech) was used to irradiate samples with neutrons of this energy spectrum. A stand was constructed to support both the source and the samples at the same level. Polymer strips could

Table 4. Some Characteristics of Fast Neutron Sources Used in This Study

No.	Source	Facility	Neutron Energy at Maximum Yield (MeV)	Gamma Contamination (percent total dose)	Dose Range Used (Rad)	Distance between Target and Samples
1	Fission Neutrons	HPRR ORNL	1	~ 10[1]	0.001-1000	1-15 (m)
2	5 Ci Pu-Be	Ga. Tech Atlanta, Ga	4.1*	8[2]	1-15	12 (cm)
3	16 MeV d^+ on Be target	Texas A&M Univ. Cyclotron	7	~ 5[3]	1-1000	140 (cm)
	50 MeV d^+ on Be target		20	~ 5[3]	1-1000	140 (cm)
4	16 MeV d^+ on Be target	Univ. of Washington Cyclotron	7	~ 5[3]	1-1000	106 (cm)
5	35 MeV d^+ on Be Target	Naval Research Lab.	15	~ 3[4]	1-1000	100 (cm)

*Mean Energy

(1)Auxier (1965); (2)Nachtigal (1967); (3)Smathers (1974); (4)Attix et al. (1973)

be irradiated in a circular fashion around the source at a distance of 11.9 ± 0.2 cm from the center of the source. The neutron fluence and kerma dose were calculated from the neutron emission rate of the source.

Three neutron sources from three medical cyclotrons were also used for foil irradiations. Some characteristics of these neutron sources were given in section 2.1 and some are reported in Table 4. The polymer sheets were each supported by a 10 x 10 cm Lucite frame approximately the size of the collimated beam. The neutron doses delivered were varied from 1 to 1000 rads tissue kerma in air. The neutron doses delivered to the samples were the values supplied by Smathers (1974), Shapiro (1975), and Eenmaa (1975). In all samples, the center portion of the samples was punched for energy response studies to avoid any nonuniformity in the neutron dose in the outer portions of the samples.

4.6.2 Neutron Irradiations of Phantoms

Some neutron depth dose studies were carried out in an elliptical cylinder having a minor axis of 22 cm, a major axis of 32 cm, and a height of 35 cm. It was filled with tissue-equivalent fluid recommended by Goodman (1969b). In this part of the study, three different tissue- and bone-equivalent media (i.e. tissue-equivalent (TE) fluid, bone-equivalent (BE) plastic, and bone-equivalent (BE) fluid contained in cylindrical tubes of five cm internal diameter and 21 cm in length) were incorporated into the elliptical cylinder along the minor axis. The cylinders (one at a time) were completely aligned along the minor axis of the phantom. By this setup neutron depth doses were measured in the three mentioned media by using polycarbonate foils as dosimeters held parallel to each other by a sample holder inside the cylindrical tubes. Each foil was numbered ac-

cording to depth in the phantom. When BE plastic was used as the media of interest, foils were supported between the BE slabs without using any sample holder.

Another phantom was constructed consisting of a plexiglass cube 30 x 30 x 30 cm with 0.5 cm walls. A cylindrical plexiglass tube 0.4 cm thick having five cm internal diameter and 31 cm in length was fixed along the central axis of the cube connecting centers of two opposite walls to isolate the phantom liquid from that of the tube. By this design, sample holders supporting the foils could be placed in the tube from outside the phantom. Both ends of the tube could be closed from outside the phantom by screw caps. One cap had a small feeding tube along with a 50 cm rubber tube connected to a polyethylene bottle. By this mechanism, the cylinder could be filled easily with TE fluid just be raising the bottle (filled with TE fluid) above the levels to fill the tube. To prevent any air bubble in the central tube, the air could be evacuated by a Lucite tube (one cm in diameter) joining the central tube vertically to the top of the phantom. This set-up permitted rapid change of the irradiated foils without disturbing the phantom TE fluid.

For air-tissue and bone-tissue interface studies, sample holders were used which were especially designed to hold the 250 μm polycarbonate foils parallel to each other with a 250 μm thick gap between the foils. By this approach, fluid could fill the gaps. Each sample holder was placed in the front or in the rear of a four cm thick BE plastic for bone-tissue interface studies, or near the air-tissue interface, or in BE fluid.

An elliptical thorax water phantom, 20 x 20 x 40 cm, was also used

to study orientation dependence of the dosimeter when it is worn on the human body. Also strips of polycarbonate foils were used on the phantom as a belt. After irradiation, foils to be etched were punched out of the belt.

4.6.3 Neutron Exposure in High Energy Photon Beams

In order to study changes in fast-neutron-induced track registration in Lexan polycarbonate for high doses of photons, polycarbonates were irradiated by different doses of gamma rays from a Georgia Tech cesium-137 source. The dose range used varied from 10^3 rads to 6×10^6 rads as given in Table 5. A visible color change was observed at high doses. (For example, at six Mrads the foils turned brownish color; this coloration may be used for gamma dosimetry in the Mrad regions.) Then the irradiated and unirradiated foils were exposed to equal fluences of Pu-Be neutrons from the source described above.

4.6.4 Proton Irradiations

Polycarbonate foils of 250 μm thickness were irradiated in broad beams of monoenergetic protons produced by the Georgia Tech one MeV Van de Graaff accelerator. The protons had energies from 100 keV to 900 keV in 100 keV intervals. The beam current was roughly on the order of 2×10^{-8} amperes. The irradiation times were a few seconds. The irradiated foils were about five cm in diameter and covered by nickel mesh to distribute any charge build up on or around the foil surface and prevent sparking which might damage the foil.

Another proton irradiation method was used which was similar to that employed by Carpenter and LaFleur (1972). Protons were produced by the reaction $^{14}N(n,p)^{14}C$ under thermal neutron irradiations of a nitroge-

Table 5. Some Characteristics of Gamma and High Energy X-Ray Sources Used in This Research

No.	Source	Accelerator	Expected Neutron Energy	Field Size (cm)	TSD (cm)	Photon Dose Range (rad)
1	(γ,n) neutrons by 10 MV x-rays	Emory University Linear Accelerator	---	20 x 20	100	1 to 2000
2	(γ,n) neutrons by 25 MV x-rays	Emory University Betatron (25 MeV)	Similar to Cf-252 Spectrum[1]	10 x 10	100	1 to 2000
3	(γ,n) neutrons by 45 MV x-rays	Atlanta West Hospital Betatron (45 MeV)	Estimated to be > 3 MeV[2]	10 x 10	110	1 to 2000
4	Cesium-137 0.66 MeV gamma rays	Georgia Tech	---	---	---	10^3 to 6×10^6

[1] Briden and Ice (1972); [2] Axton and Bardell (1972)

nous compound rich in nitrogen such as urea. The cross section for this reaction is 1.81 barns for thermal neutrons. Urea pellets were prepared by pressing 300 mg powder in a pellet die under a hydraulic press using 7,000 lb/sq inch. The prepared pellets were 13 mm in diameter.

Thermal neutron exposures were carried out in the Biomedical Exposure Facility of the Georgia Tech Research Reactor (GTRR). The beam portal is about 10 cm in diameter and the neutron flux at this portal was approximately 1.0×10^{10} n/sec at one MW. Urea pellet/polycarbonate and urea pellet/red-dyed cellulose nitrate foils were irradiated at the beam portal with the pellets facing the thermal neutron beam. By this approach protons of about 0.5 MeV energy are produced and permitted to strike the foils. The exposure time was five minutes.

CHAPTER V

OPTIMIZATION OF ELECTROCHEMICAL ETCHING PARAMETERS FOR THE AMPLIFICATION OF FAST-NEUTRON-INDUCED RECOIL PARTICLE TRACKS IN POLYMERS

Electrochemical etching parameters affecting the etching results and a brief discussion of the etching mechanism were given in Chapter III. Detailed experimental studies on the effect of each mentioned parameter on the amplification of fast-neutron-induced recoil particle tracks to obtain maximum sensitivity, for a minimized etching time, as well as variations in mean track diameter and shape of the tracks are given here. Sensitivity (tracks/cm^2·rad), mean track diameter, and optical density as functions of each mentioned parameter, when the other parameters were fixed, are reported.

5.1 Effect of Polymer Type

Many polymers such as cellulose acetate, cellulose acetobutyrate, cellulose tri-acetate, cellulose nitrate, and polycarbonate have been of interest for heavy charged particle track registration especially for fast-neutron-induced recoil particle tracks. As previously stated, the characteristics of these polymers for track registration vary from one polymer to another. These variations are due to many inherent characteristics such as molecular weight, composition, mechanical and electrical properties, manufacturing, and permeability to many gases and water vapor. For example, polycarbonate has high mechanical strength, high electrical

strength (155 kV/mm) compared to cellulose tri-acetate (100-120 kV/mm), high specific volume resistance (~ 10^{17} ohm·cm) compared to cellulose tri-acetate (~ 10^{14} ohm·cm), lower water absorption (~ 0.35 percent for 24 hours) compared to tri-acetate and acetate having water absorptions of two to four percent and one to two percent, respectively, for 24 hours, high melting point (213°C), and low permeability to gases such as O_2, N_2, CO_2, and water vapor (Mayofis, 1966; Sweeting, 1971). Electrochemical etching seems to be most critical in relation to the mechanical and electrical properties of these materials. It was essential in this study to select a material of high performance and with good dosimetric characteristics for registration of fast-neutron-induced recoil particle tracks to study the electrochemical etching parameters listed in section 3.2.2 and for some fast neutron dosimetry applications.

The above mentioned polymers of various thicknesses were irradiated by fast neutrons of equal doses and foils of 250 μm were used in a comparison study. All the foils were etched in a 28 percent KOH solution at 25°C applying 700 V at one kHz for three hours. All the amplified tracks after etching were larger in size than those obtained by conventional etching methods. Figure 1 (in Chapter I) showed the appearance of tracks in cellulose acetobutyrate obtained in a previous study (Sohrabi and Becker, 1971). Tracks in acetate and tri-acetate had the same appearance as those in Figure 1. In cellulose nitrate the tracks appeared slightly better in appearance than those in acetobutyrate. However, in polycarbonate foils the tracks were registered so that each individual track could be observed with high contrast against the undamaged transparent surface of the polymer and they were very well identified either by the unaided

eye or under a microscope as stated before and shown in Figures 11 and 12. Figure 14 shows a single recoil particle track in polycarbonate that was enlarged by electrochemical etching in 375 μm polycarbonate foil in comparison with one that was enlarged by conventional etching methods. This direct visual comparison of the results obtained by the two etching methods makes it self-evident why it was of interest to further investigate electrochemical etching of recoil tracks in polycarbonate and to optimize the parameters that are of importance in controlling the sensitivity and track diameter, both of which are of interest for dosimetric studies.

In addition to variations in different polymers, there are variations observed in commercial polycarbonates which represent differences in molecular weight, additives and stabilizers, minor addition of co-reactants and fillers, etc. Even a large difference exists between molecular weights of cast-grade and extruded-grade polycarbonate foils leading to different performance under different electrochemical etching treatment (Sweeting, 1971). For example, 250 μm polycarbonate foils obtained from West Lake Plastics (WLP), Lenni, Pennsylvania, could stand etching treatment up to 6.5 hours before a hole or holes broke through the foil and etching stopped and they had higher background track density. On the other hand, similar foils obtained from Rowland Products, Inc., Kensington, Connecticut, could stand etching treatment under the same etching conditions up to five hours and had fairly low background. Thus, although no significant variation in sensitivity was observed in the mentioned foils, individual calibration for each brand or even each batch is highly recommended. The foils that were used as described in this chapter

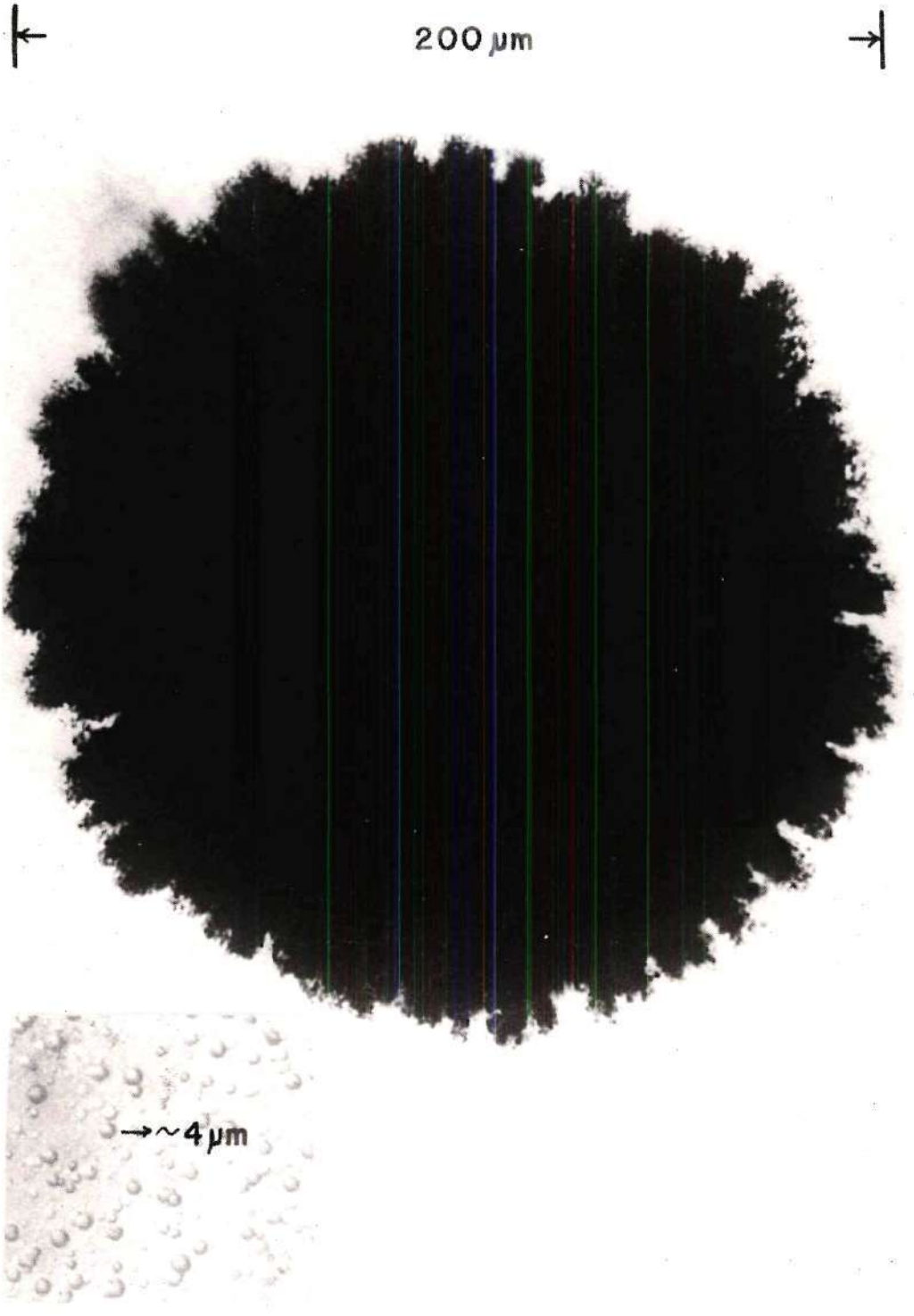

Figure 14. A Single Fast-Neutron-Induced Recoil Particle Track Amplified by Electrochemical Etching in 375 µm Lexan Polycarbonate Compared to Those Tracks Conventionally Etched in the Same Material

were WLP brand in the case of 125 and 250 μm foils and RP brand in the case of 75, 375, and 500 μm foils. Foils of 250 μm thickness of both brands were used in some cases and are indicated in the text.

5.2 Dependence of Etching Time on Foil Thickness

In conventional etching techniques, the etching time required to obtain optimum track density is independent of foil thickness (unless spark counting techniques or other similar approaches are applied for track density evaluations). For electrochemical etching techniques, however, the sensitivity (tracks/neutron) or track density and corresponding optimum etching time depend strongly on foil thickness. Figure 15 shows sensitivity and mean track diameters as functions of polycarbonate foil thickness from 75 μm to 500 μm. As can be seen, for the optimum etching times (upper scale) which depend strongly on foil thickness, sensitivity decreases and mean track diameter increases as the foil thickness increases up to a thickness in which electrochemical etching becomes practically ineffective, as discussed below. This decrease in sensitivity with increase in thickness can be explained by the capacitive nature of the polymer material incorporated in the chamber. Referring back to Figure 7 in section 3.2.2, as the foil thickness increases the capacitance decreases, thus the current passing through the chamber decreases. This leads to longer etching times in thicker foils and shorter etching times in thinner foils. Furthermore, it seems that the current should be above a threshold value below which the track of a particle of certain LET (below a threshold) will not be amplified. Therefore, the sensitivity decreases with increase in foil thickness which is due to decreasing currents which are capable of amplifying only the higher LET particles.

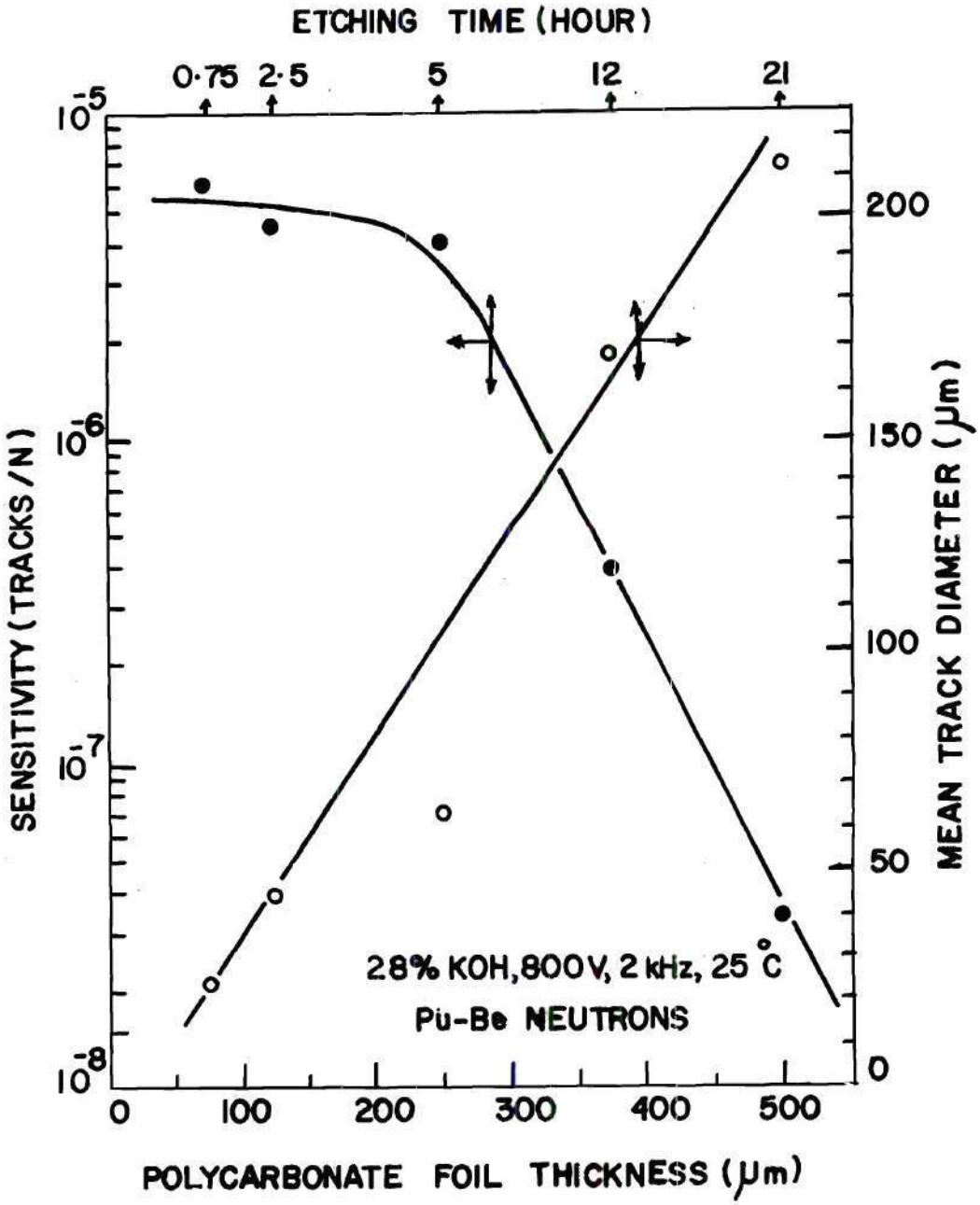

Figure 15. Sensitivity and Mean Track Diameter as Functions of Polycarbonate Foil Thickness at Optimum Etching Times in 28% KOH Solution at 25°C Applying 800 V at 2 kHz

The large size of the tracks in thicker foils, however, seems to be due to two factors: (1) low current which amplifies only the higher LET tracks, and (2) long etching time, i.e. it is shown in these studies that the track diameter increases linearly with time (see below).

Figures 16, 17, and 18 show sensitivity (tracks/n·rad), mean track diameter, and optical density as functions of etching time for 125 μm polycarbonate foils etched in 28 percent KOH solution at 25°C applying 650 V at one kHz. Figures 16 and 17 also show the results when 125 μm foils have been etched under optimized conditions which will be discussed below. As can be seen in Figure 16 (upper curve), some recoil particle tracks will be developed after about 30 minutes of etching reaching a plateau in about two hours. It seems that the amplified tracks under these etching conditions are due only to the surface tracks because of low surface etching at this temperature. It can be concluded that the tracks due to high LET recoils will be developed first followed by lower LET recoil tracks, reaching a plateau when all the tracks on the surface are amplified. It seems logical to accept the opinion that, if there were not an etching time limit due to perforations through the foils (which stops etching), the track density would tend to rise again after this plateau since more tracks would be developed from deeper layers. Figures 17 and 18 show that mean track diameter and optical density are linear functions of etching time over a wide range of time.

Similar studies were carried out for 250, 375, and 500 μm thick polycarbonate foils. Sensitivity, mean track diameter, and optical density as functions of etching times followed the same general pattern as that of 125 μm foils. However, as mentioned above, the optimum etching

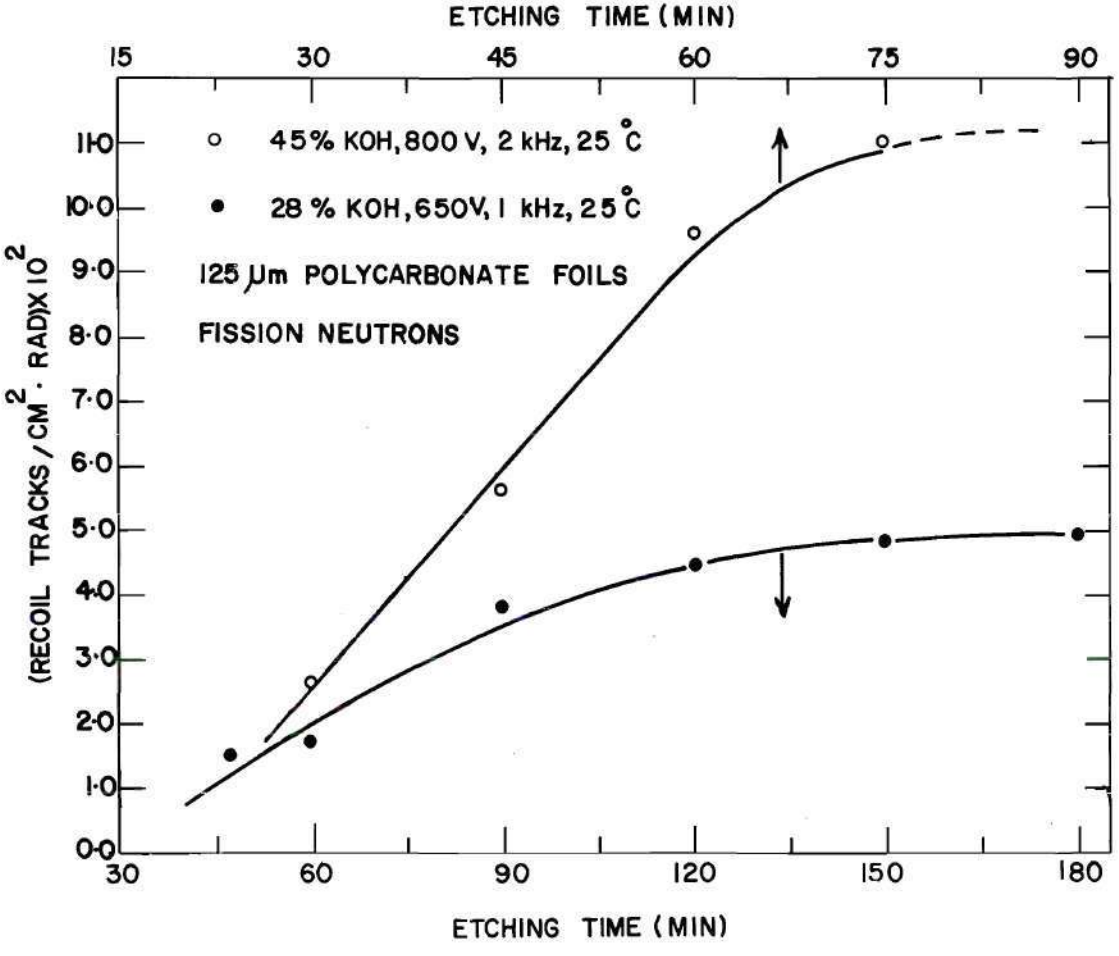

Figure 16. Recoil Track Density per Rad of Fission Neutrons in 125 µm Thick Polycarbonate Foils as a Function of Etching Time at Two Different Etching Conditions (as indicated) before and after Optimization of Etching Conditions

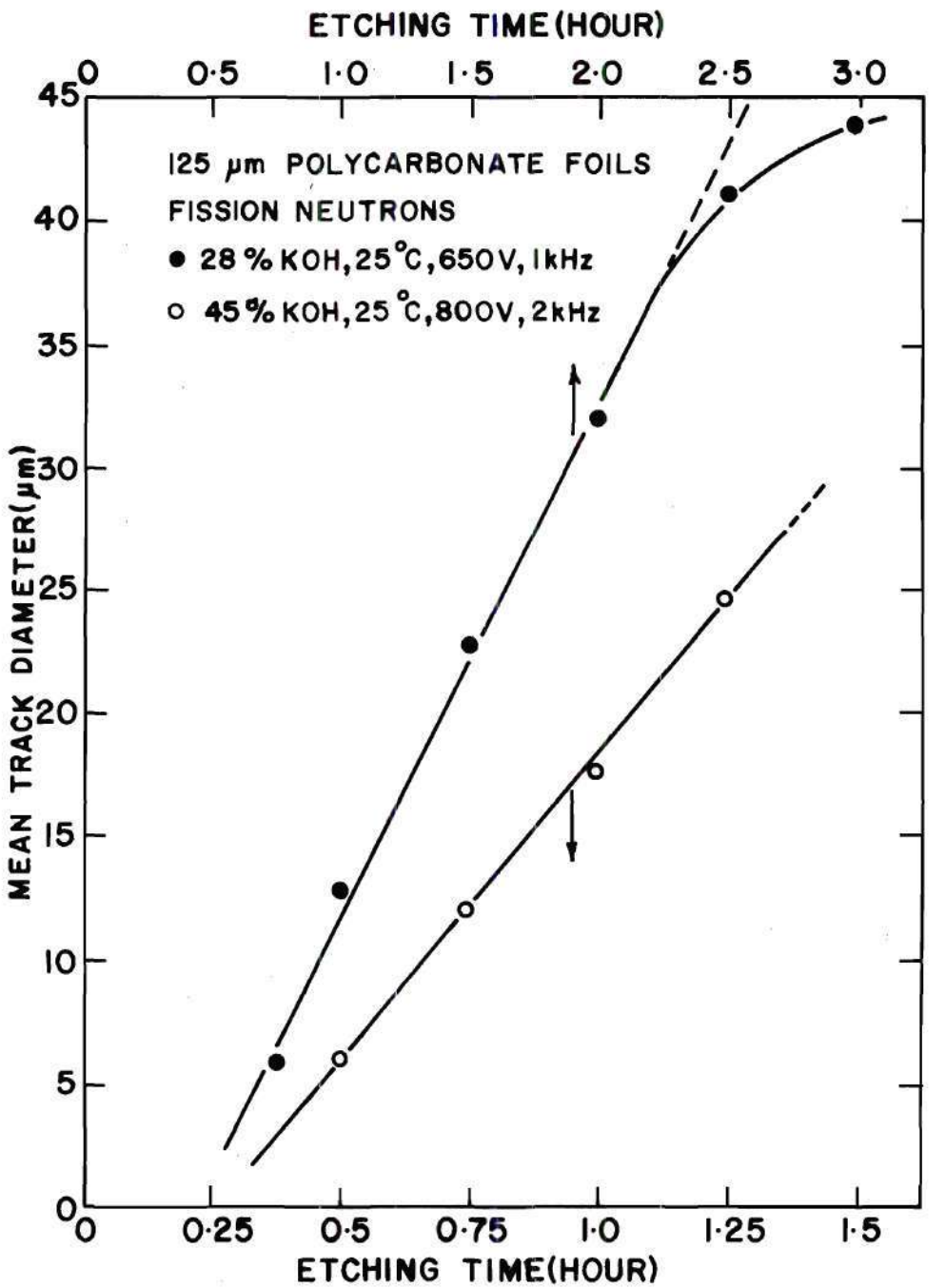

Figure 17. Mean Recoil Track Diameter as a Function of Etching Time in 125 μm Polycarbonate Foils Under Two Different Conditions (as indicated) before and after Optimization of the Etching Conditions

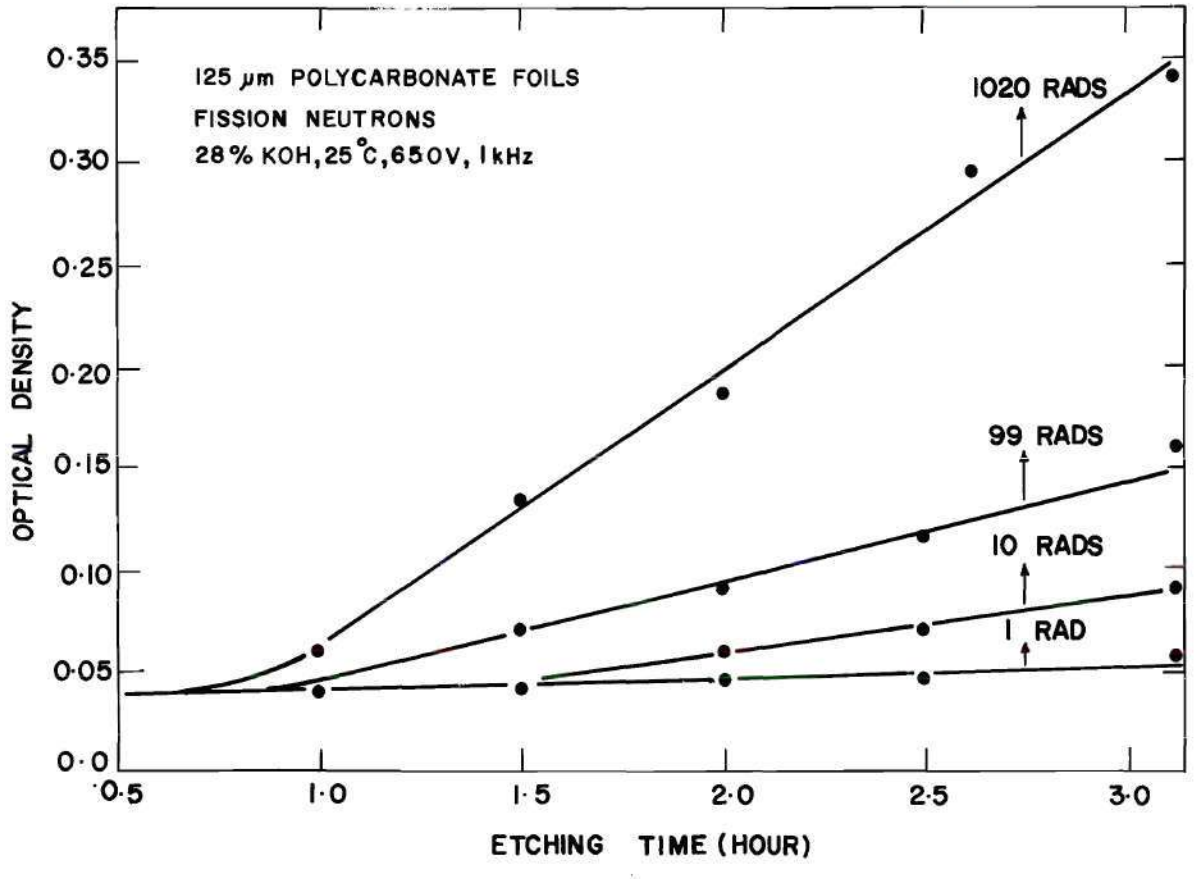

Figure 18. Optical Density as a Function of Etching Time in 125 μm Polycarbonate Foils, Irradiated to Different Fission Neutron Doses, Etched in 28% KOH Solution at 25°C Applying 650 V at 1 kHz

time will be increased and the sensitivity will be decreased as the foil thickness increases.

Etching time dependence on foil thickness was further studied under optimized electrochemical etching conditions (after all the parameters had been studied), i.e. etching the foils in 45 percent KOH solution at 25°C applying 800 V at two kHz. Figures 19 and 20 show, respectively, track density per rad and mean track diameter for fission neutrons as functions of etching time for four different foil thicknesses, i.e. 125, 250, 375, and 500 μm. It should be noted that the time scales in this figure are multiplied by the time factors shown; for example, 3.0 hours on the time scale represents 1, 3, 9, and 15 hours for 125, 250, 375, and 500 μm thicknesses, respectively. As expected, the 125 μm thick foil provided the highest sensitivity among the four thicknesses and 500 μm showed the lowest sensitivity. Furthermore, as can be observed in Figure 16, the sensitivity (tracks/cm^2·rad) of the 125 μm foils etched in 45 percent KOH solution at 25°C applying 800 V at two kHz is about twice as high as that of foils etched in 28 percent KOH solution at 25°C applying 650 V at one kHz while the optimum etching time decreased by a factor of two from two hours to one hour as can be seen by comparing the upper and lower scales. Similarly, it is noted in Figure 17 that the track diameter decreases by a factor of about two when making the above changes in etching conditions. The optical density as a function of etching time in different thicknesses under the optimized etching conditions (shown to be similar to those of Figure 18) are given in Appendix A.

Figure 20 indicates that the mean track diameter can be written approximately by the equation:

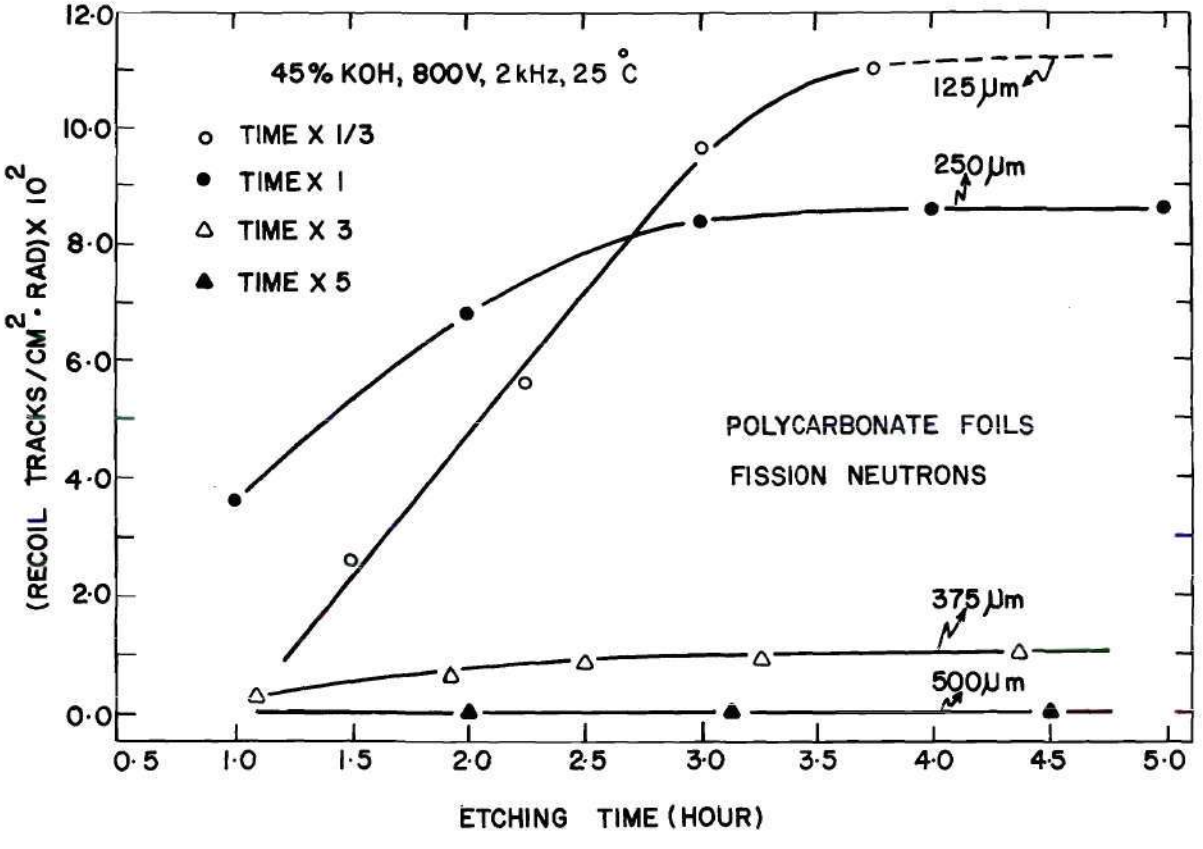

Figure 19. Track Density per Rad as a Function of Etching Time in Polycarbonate Foils of Different Thicknesses Etched in 45% KOH Solution at 25°C Applying 800 V at 2 kHz

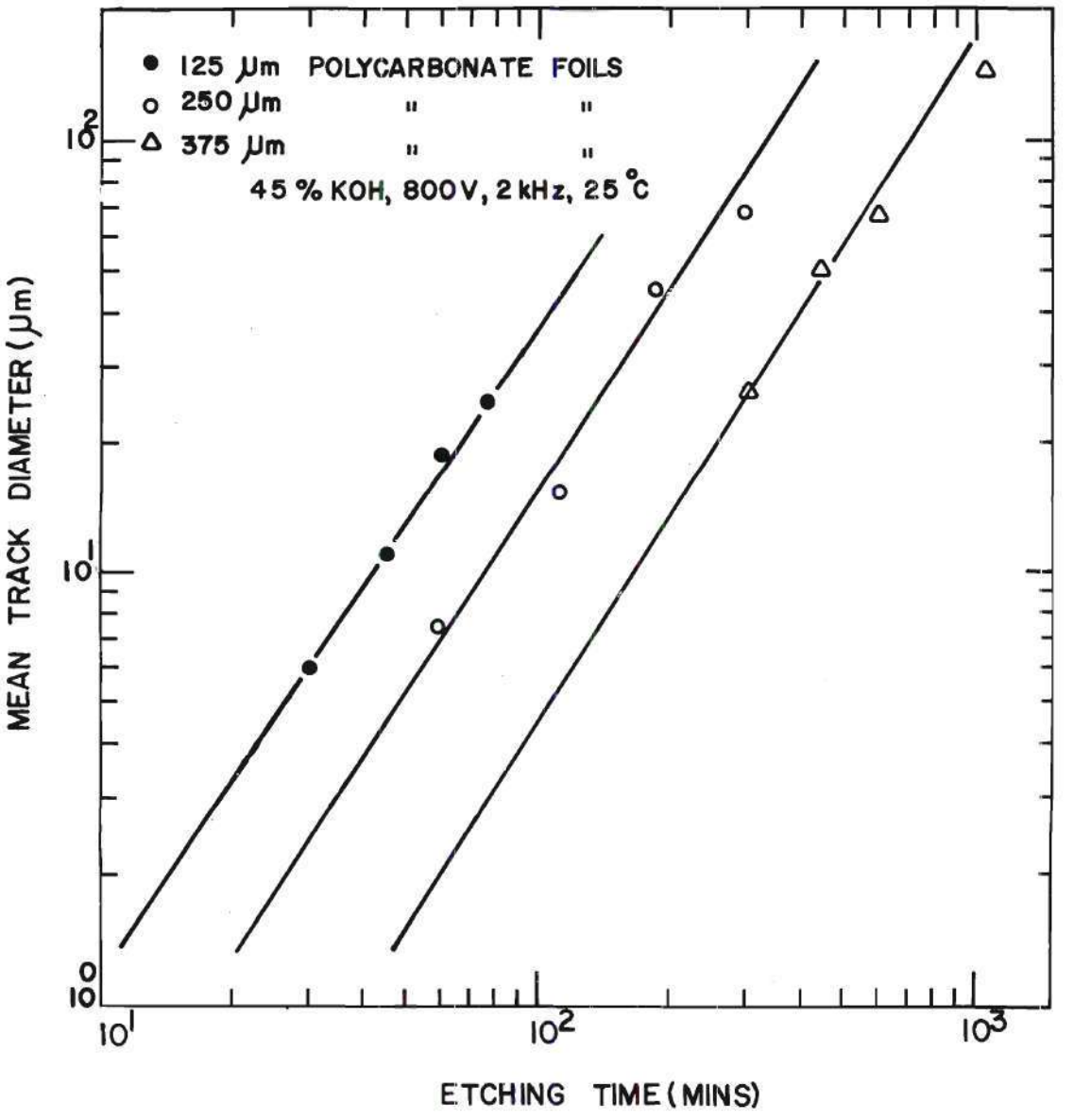

Figure 20. Mean Recoil Track Diameter as a Function of Etching Time in Polycarbonate Foils of Three Different Thicknesses (125, 250, and 375 μm) Etched in 45% KOH Solution at 25°C Applying 800 V at 2 kHz

$$D = C_1 \, t^{1.5}$$

in which D = track diameter (μm), t = time (minutes), and C_1 has values of 0.033, 0.014, and 0.0046 for foils of thickness 125, 250, and 375 μm, respectively.

The above observations reveal that electrochemical etching, under the electrochemical etching conditions applied, is inefficient for thick foils (e.g. Figure 15 indicates an etching time of 21 hours is required for the 500 μm foils). Nevertheless, the following observation seems to be worth mentioning. Figure 21 shows a fast-neutron-exposed (1000 rads of fission neutrons) 500 μm thick foil etched for 21 hours in a 45 percent KOH solution at 25°C applying 800 V at two kHz. It can be seen from the data of Figures 15 and 19 that electrochemical etching is impractical for thick foils, e.g. 500 μm when using these applied electrochemical etching conditions because of the low current (which is not enough to amplify tracks) and very long etching time. On the other hand, the foils are still in contact with the etchant so that recoil tracks can be etched in the same manner as conventional etching regardless of the applied field. Thus, the small dots in Figure 21 are recoil tracks revealed under the effect of only the etchant (i.e. conventional etching). The larger tracks are obviously due to the amplification by electrochemical etching and their density was neutron dose dependent. These very infrequent large tracks might be due to the existence of some traces of fissionable materials in the foils (Eichholz, 1975).

Based on the above mentioned experiences on the electrochemical etching conditions, foils having thicknesses of 125 and 250 μm were pre-

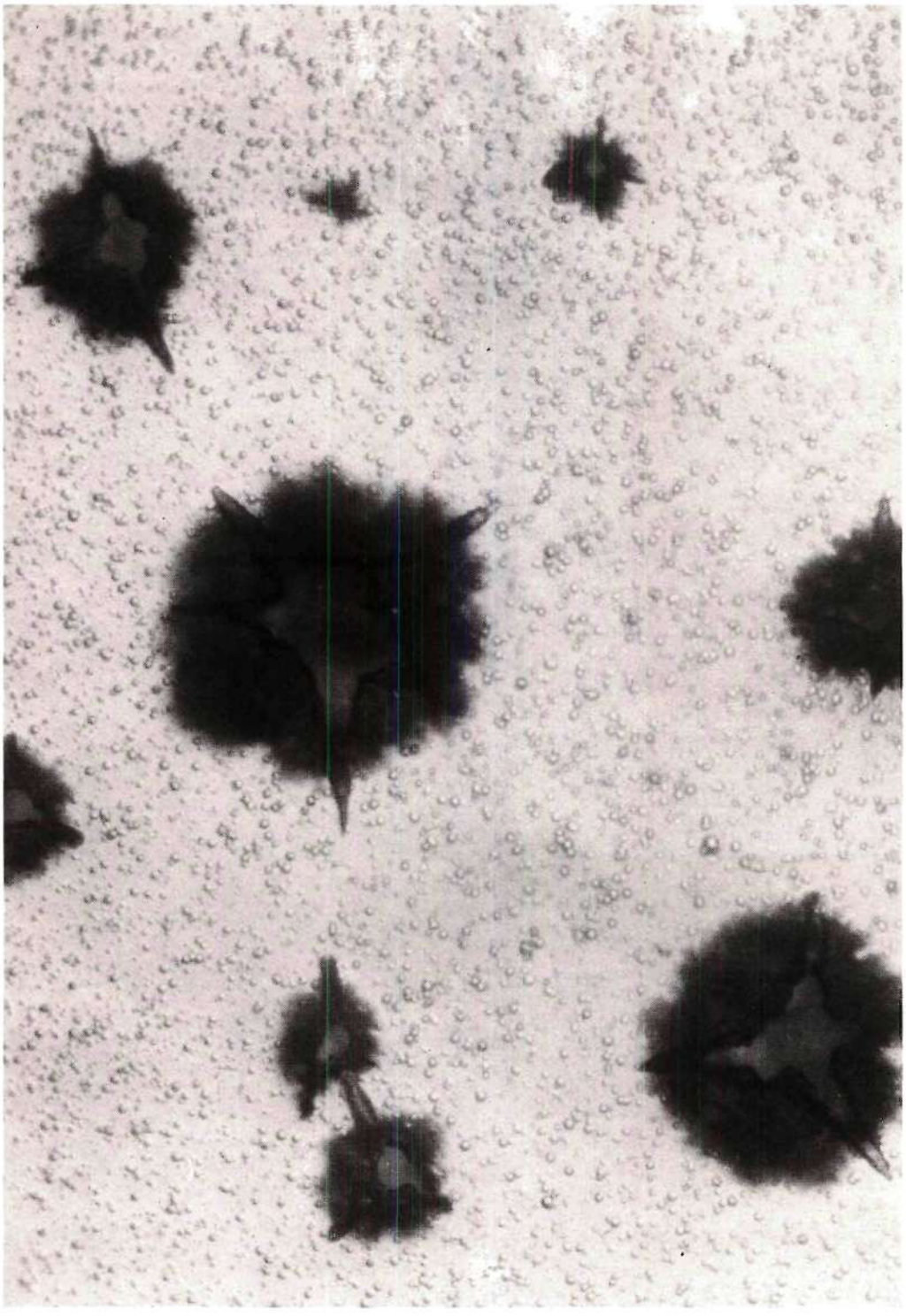

Figure 21. Micrograph of Fast-Neutron-Induced Recoil Particle Tracks in 500 μm Polycarbonate Foils Etched in 45% KOH Solution at 25°C Applying 800 V at 2 kHz for 21 Hours

ferred in most of this present study. They have a reasonable sensitivity, flexibility, lower cost, and a relatively short etching time (one to five hours).

5.3 Dependence on Applied Voltage and Its Frequency

The applied voltage imposes a force on the ions of the etchant so that they are attracted towards the electrode having the charge opposite that of the ions. The alternating nature of the applied voltage, i.e. its frequency, changes the directions of the ions twice each cycle leading to an alternating current through the chamber. For maximum sensitivity at a lower etching time, the electric potential and frequency must be chosen carefully.

5.3.1 Applied Voltage

Figures 22, 23, and 24 are typical sets of data showing the variation with the applied voltage across the electrodes of sensitivity (tracks per $cm^2 \cdot rad$), track diameter, and optical density, respectively, when other parameters (as shown on the graphs) are maintained constant. As can be seen, these three variables tend to reach a semi-plateau above about 600 volts where the voltage of the system is much less critical and does not require unusual circuitry for regulation. Satisfactory and reproducible results were obtained at any fixed potential between 600-1000 V; however, at lower voltages, etching time must be increased.

5.3.2 Frequency

Proper operation of the electrochemical-etching technique depends critically upon the frequency of the electrical potential applied to the etching chambers and across the foils that separate the chambers. Figures 25, 26, and 27 indicate a resonant frequency exists at which we

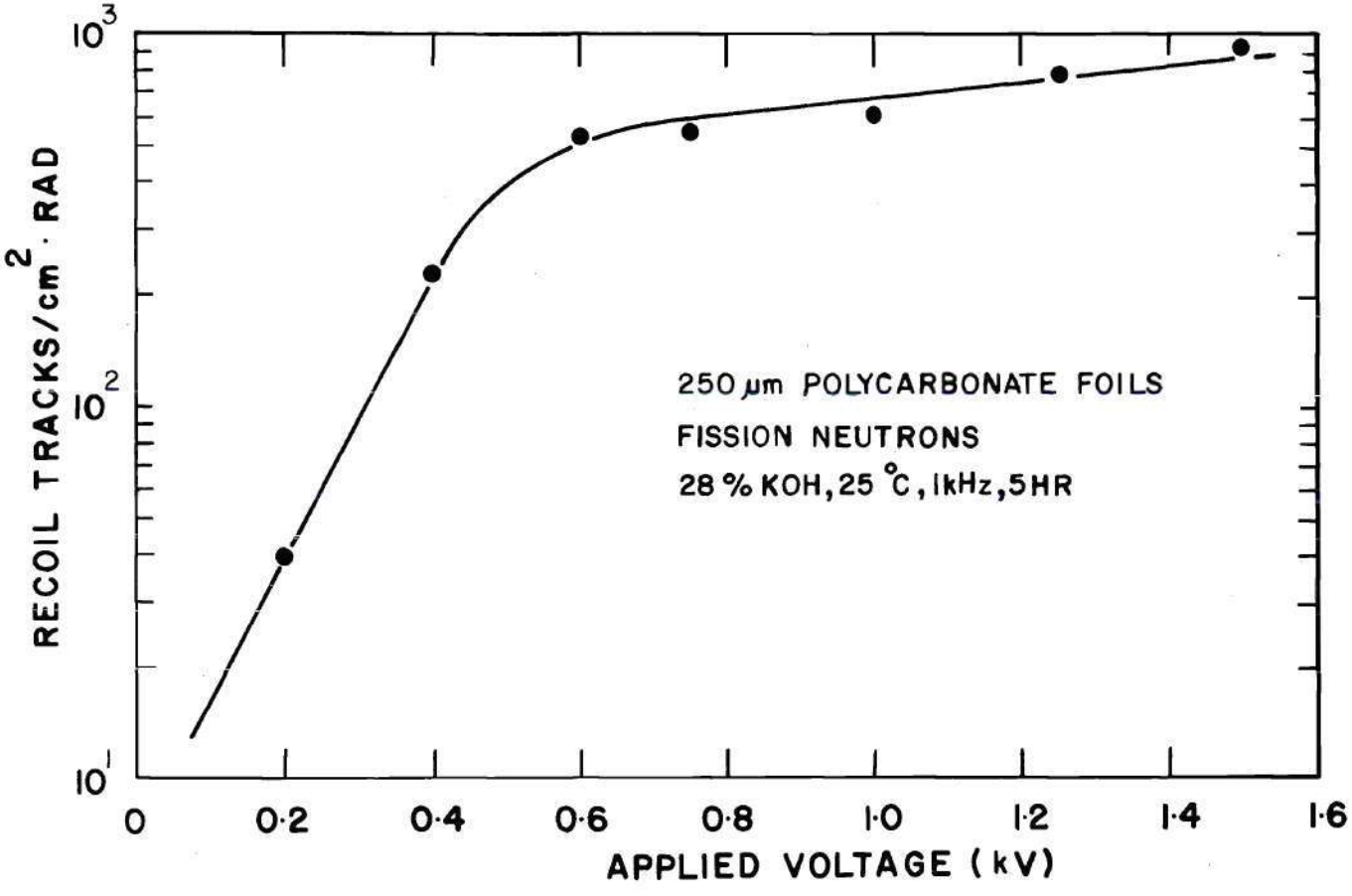

Figure 22. Track Density per Rad as a Function of Applied Voltage in 250 μm Polycarbonate Foils Etched in 25% KOH Solution at 25°C Applying a Frequency of 1 kHz for 5 Hours

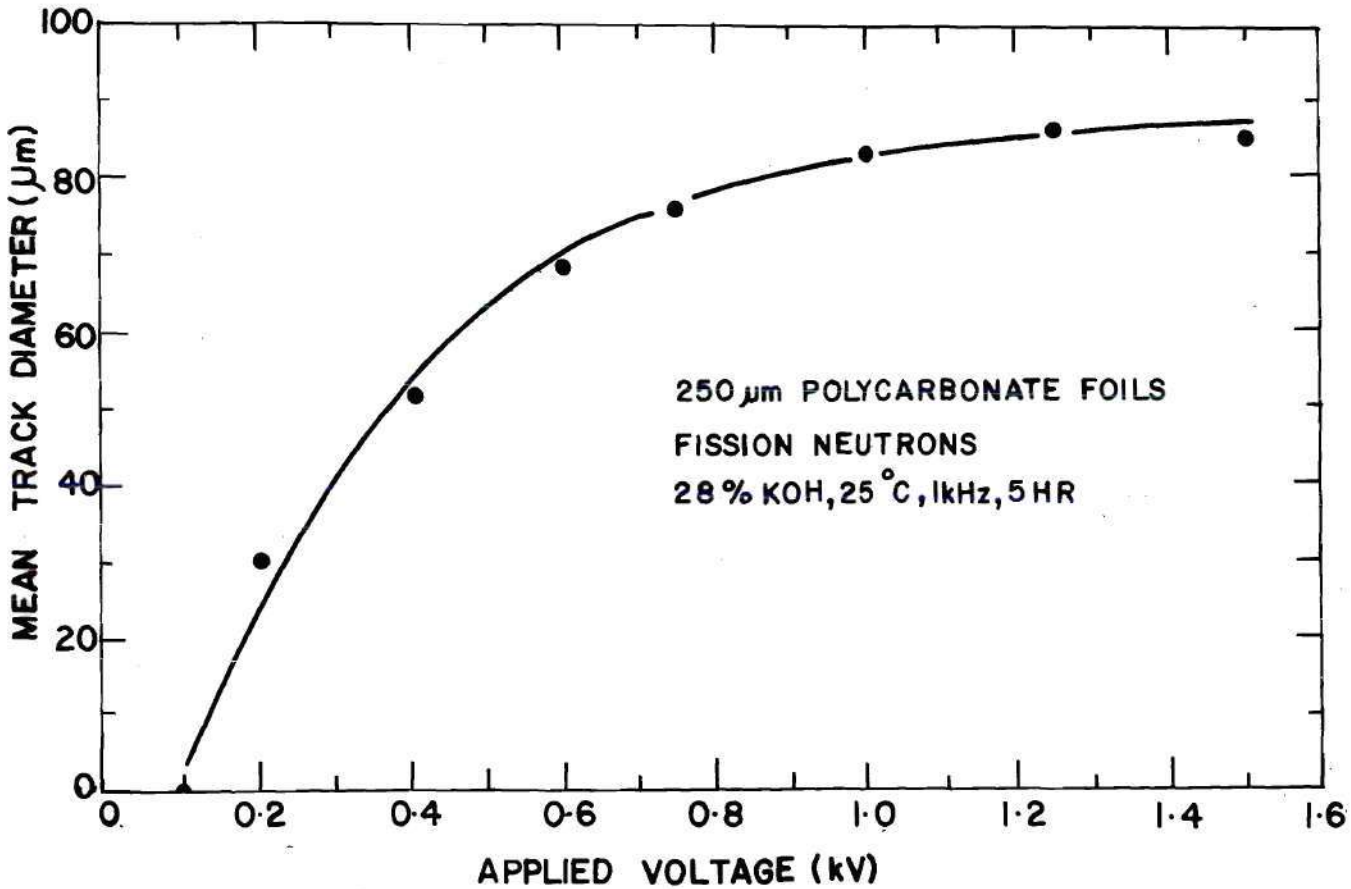

Figure 23. Mean Track Diameter as a Function of Applied Voltage in 250 μm Polycarbonate Foils Etched in 28% KOH Solution at 25°C at 1 kHz for 5 Hours

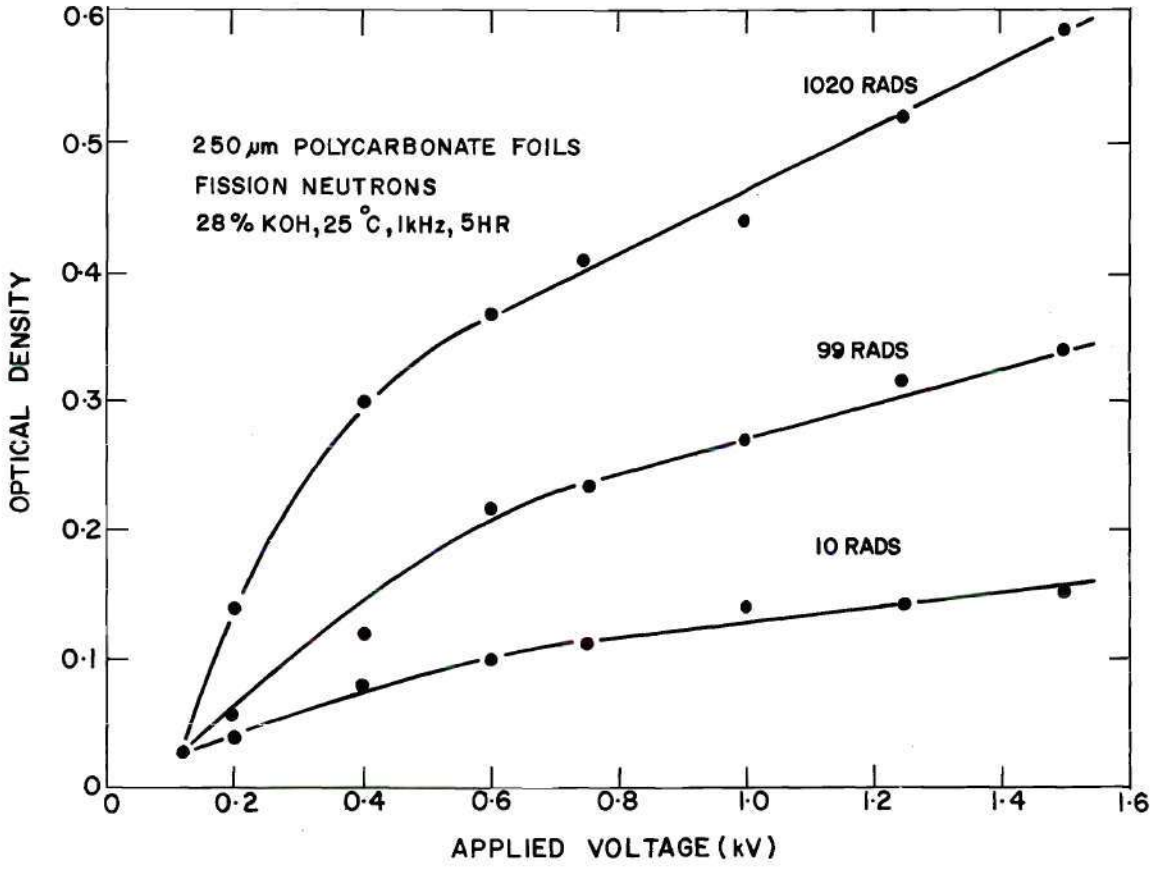

Figure 24. Optical Density as a Function of Applied Voltage for Different Fission Neutron Doses Delivered to 250 μm Polycarbonate Foils and Etched in 28% KOH Solution at 25 °C Applying a Frequency of 1 kHz for 5 Hours

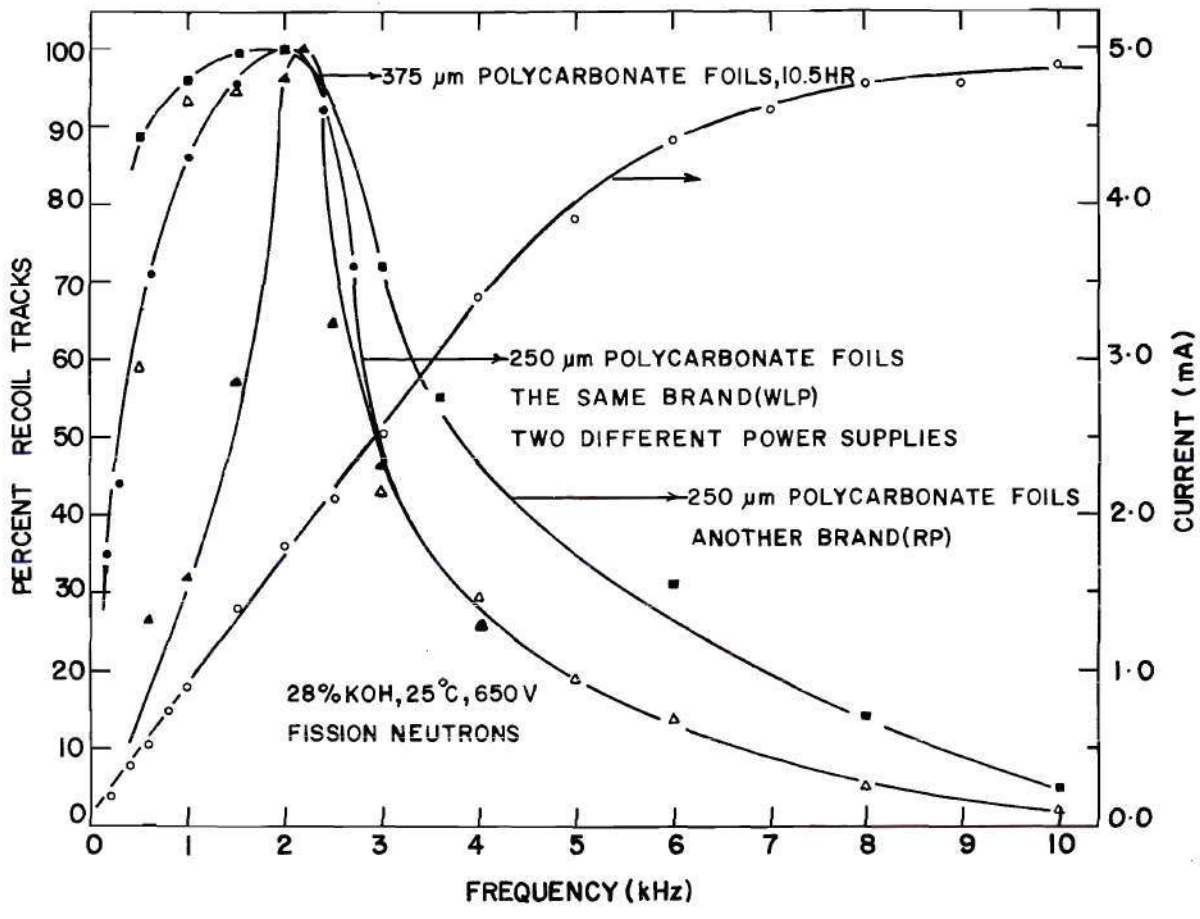

Figure 25. Percent Recoil Tracks and Current as Functions of Frequency of the Applied Voltage in Polycarbonate Foils of Different Thicknesses, Different Brands, and Using Two Different Power Supplies When Foils Etched in 28% KOH Solution at 25°C Applying 650 V for 4 Hours

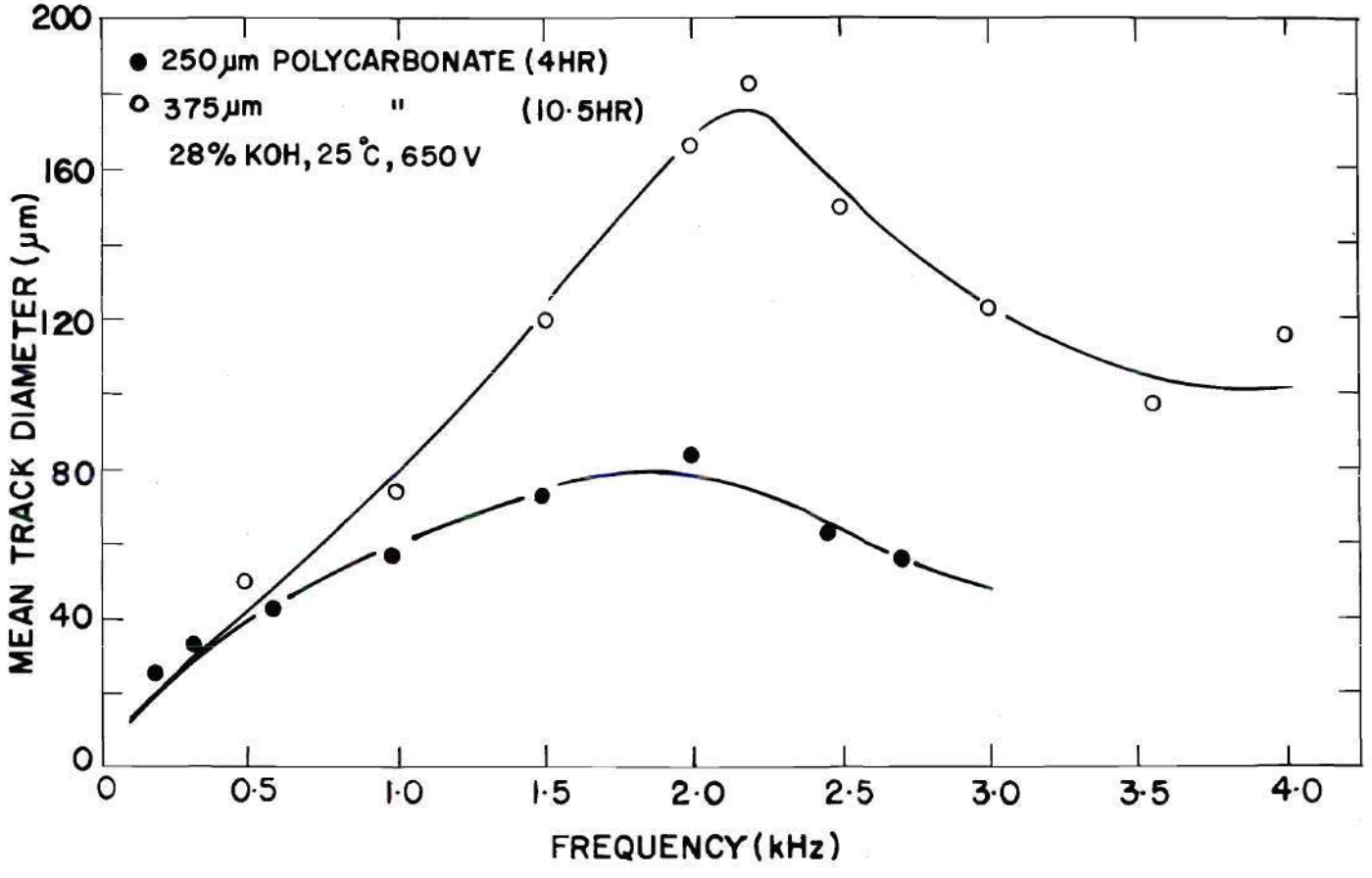

Figure 26. Mean Track Diameter as a Function of Frequency of the Applied Voltage in 250 and 375 μm Polycarbonate Foils Etched in 28% KOH Solution at 25°C for 4 and 10.5 Hours, Respectively

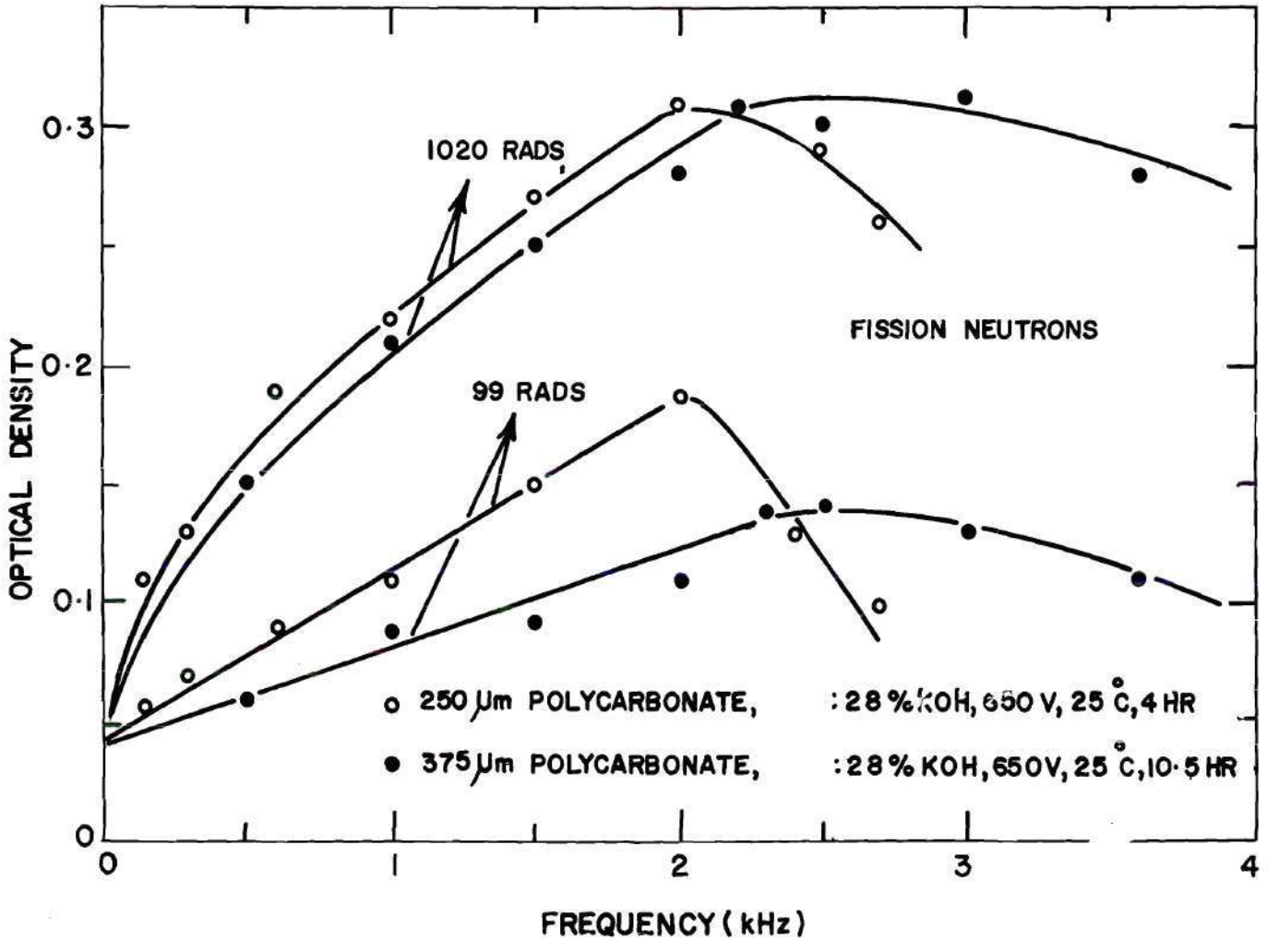

Figure 27. Optical Density as a Function of Frequency of Applied Voltage in 250 and 275 μm Polycarbonate Foils, for Different Fission Neutron Doses, Etched in 28% KOH Solution at 25°C Applying 650 V for 4 and 10.5 Hours, Respectively

obtain maximum etching effectiveness, i.e. maximum sensitivity and maximum track diameter. Under these conditions the resonant frequency is at about two kHz where we obtain a maximum sensitivity, track diameter, and optical density as shown in Figures 25, 26, and 27, respectively. The first thought seems to be that these resonance peaks occur at the electrical resonance frequency given by $f = 1/(2\pi\sqrt{LC})$ in which f is frequency in hertz, L is inductance in henries, and C is capacity in farads. This would have provided a very simple explanation because at resonance the current I_o is a maximum and at any frequency is given by

$$\bar{I}_o = \frac{\bar{V}_o}{\sqrt{R^2 + \left(2\pi fL - \frac{1}{2\pi fC}\right)^2}}$$

in which the potential $\bar{V}_o$ is in volts and current $\bar{I}_o$ is in amperes. However, upon checking the values of L and C and measuring the current $\bar{I}_o$ as plotted also in Figure 25, it became evident that the resonant peak for maximum etch efficiency (~ 2 kHz) occurs far to the left of the very broad electrical resonance peak and the current $\bar{I}_o$ at maximum etching efficiency is only about 1/3 of the current at electrical resonance. Therefore, a semi-quantitative explanation for this resonance based on results obtained in the etch efficiency curves was developed.

Due to the alternating nature of the applied voltage the diffused ions in the etchant move back and forth changing direction twice each cycle. This leads to a current through the chamber which depends strongly on the foil thickness as was illustrated in Figure 7. Figure 25 shows also the increase in the current by increasing the frequency of the applied voltage. By comparing this current curve with sensitivity curves shown on

the same graph, it seems that under conditions applied for each foil thickness the variation in sensitivity with frequency is controlled by the local current at the track site.

At low frequencies (below the sensitivity peak) the average distance or amplitude of motion of the ions in each half cycle is much greater than the path length of the charged particle registered in the polymer. For example, at one Hz, the range of oscillations (amplitude) of the ion is approximately 300 μm or many times the track length in the foils before etching. In other words, the ion flux (ions/cm^2·sec) is low leading to a small local current which may or may not amplify the tracks under the conditions applied. At high frequencies, for example at 10 kHz, the ions are relatively fixed in position or have a range of oscillation of about 0.03 μm per half cycle or only a small fraction of the length of tracks in the foil. Although at this frequency the current through the chamber is the highest (Figure 25), the ion drift is only about 10^{-4} times that at one Hz. Therefore, the ions at this frequency seem to stay essentially stationary leading to a very low local ionic current along a track which amplifies only the highest LET recoil tracks among the distribution of the tracks. However, at a frequency corresponding to the peak in the sensitivity curve, i.e. two kHz, the ions are displaced about 0.2 μm per half cycle and this amplitude seems to provide the highest local ionic current along the recoil tracks (range < 5 μm) leading to maximum energy deposition thus maximum etching at the track site. This current seems to be enough to amplify the tracks of both low and high LET recoil particles in the foil and leads also to maximum mean track diameter at this frequency, thus maximum optical density (Figures 26 and 27).

Figure 25 also indicates similar variations of sensitivity as a function of frequency in polycarbonate foils of thickness 375 μm, 250 μm in the same batch (WLP) and 250 μm from another supplier (RP) keeping the other parameters the same in the three cases. All the foils performed in the same fashion; however, the width at half maximum is much smaller in 375 μm foils. Foils having 250 μm thickness from the same batch (WLP) produced similar results using different power supplies under the same etching conditions. Foils having 250 μm thickness obtained from Rowland Products (RP) show a larger width at half maximum. For all practical purposes, however, the two kHz frequency can be applied for optimum results with all thicknesses.

5.4 Dependence on the Chemical Composition, Concentration, and Temperature of the Etchant

5.4.1 The Chemical Composition of the Etchant

Etchant composition is critical for effective etching of charged particle tracks when other parameters are fixed. A number of different etchants have been recommended and used by many investigators as reviewed in Chapter II when conventional etching is applied. Alkali halide solutions and in particular sodium hydroxide (NaOH), and potassium hydroxide (KOH) solutions have been the main etchants because of their availability, low cost, effectiveness, etc. They were used for electrochemical etching of recoil tracks in the following study.

Figures 28 and 29 show sensitivity (tracks/cm^2·rad) and mean recoil particle track diameter as functions of etching time for sodium hydroxide and potassium hydroxide when other electrochemical etching parameters have been fixed. As expected, the KOH solution is more effective in

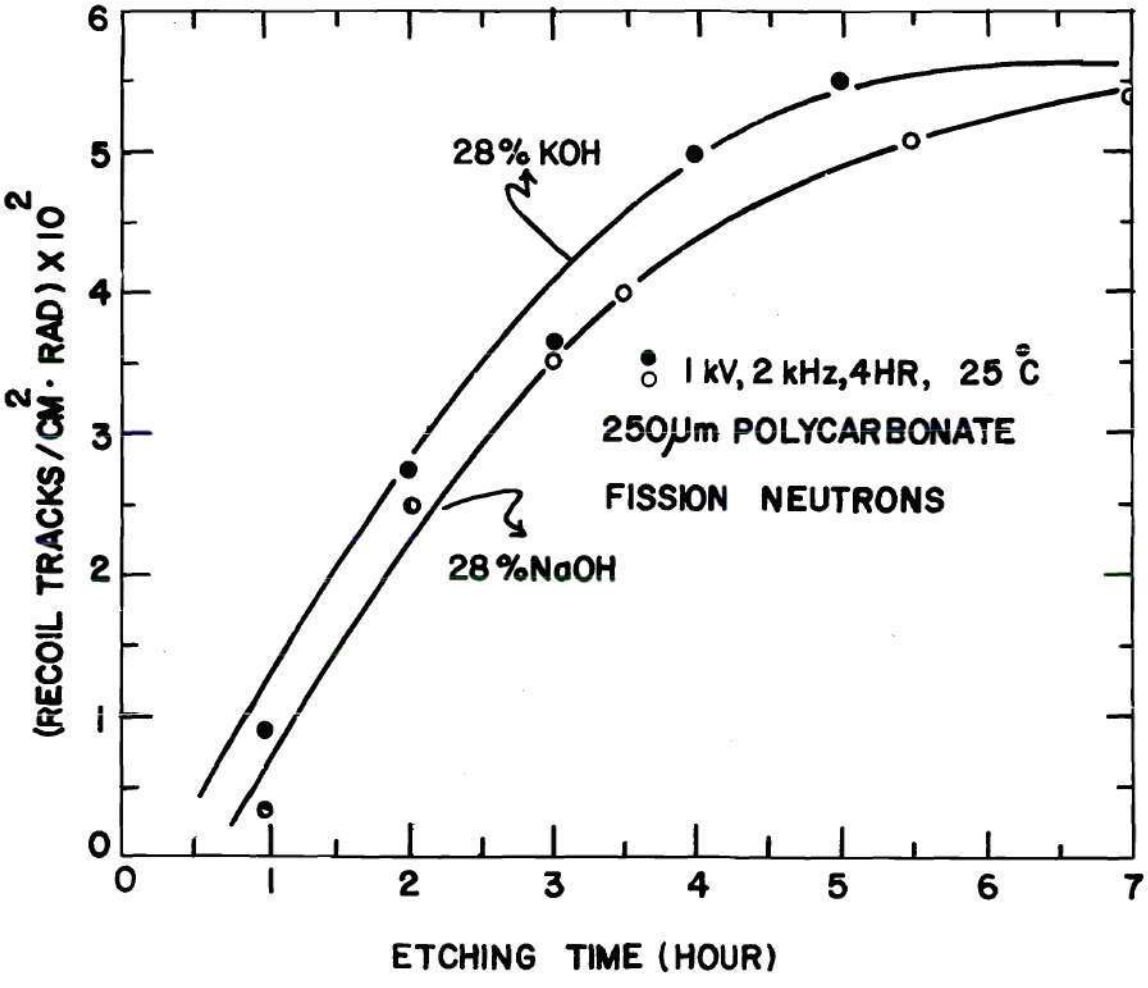

Figure 28. Recoil Track Density per Rad as a Function of Etching Time in 250 μm Polycarbonate Foils Using NaOH and KOH Solutions of 28% by Weight Concentration at 25°C Applying 1 kV at 2 kHz for 4 Hours

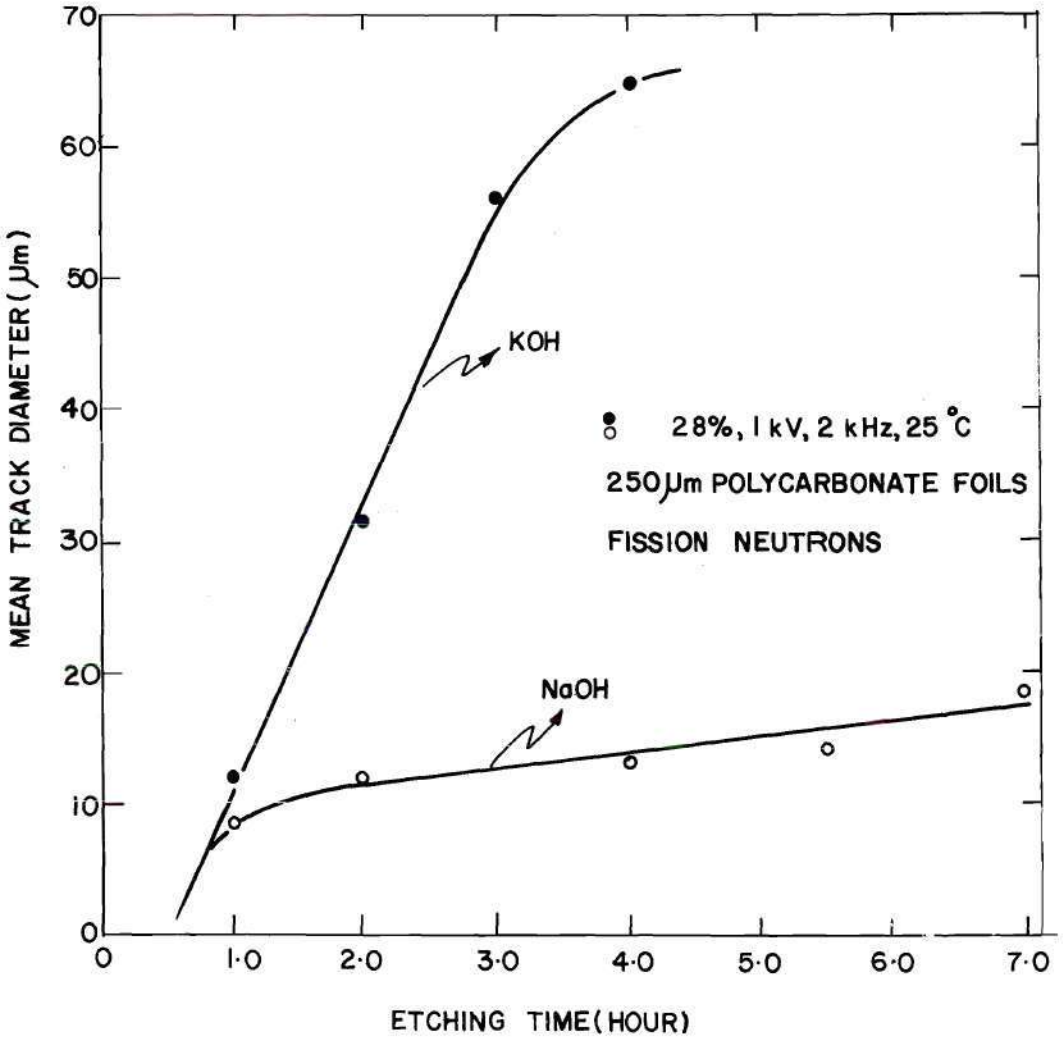

Figure 29. Mean Recoil Track Diameter as a Function of Etching Time in 250 μm Polycarbonate Foils Using NaOH and KOH Solutions of 28% by Weight Concentration at 25°C Applying 1 kV at 2 kHz for 4 Hours

electrochemical etching of charged particle tracks if larger track diameter and higher track density in a shorter etching time is required. Figure 29 shows that mean track diameters using potassium hydroxide solution are about four times larger than those obtained by sodium hydroxide after about three hours of etching. However, the sensitivities seem to reach the same level by extended etching time in the sodium hydroxide solution (Figure 28).

It is expected from these studies and those of others (Blanford et al., 1970; Dutrannois, 1971) using conventional etching techniques that the etching rate (increase in track diameter, μm/hour) will increase with molecular weight of alkali halides, i.e. increase in going from LiOH to NaOH to KOH to RbOH to CsOH. The radii of the alkali ions in aqueous solution increase in the above order while the hydration numbers (number of water molecules attached to an ion) decrease with this order (Kortüm, 1965; Enge et al., 1974). Thus Li^+ with the highest hydration number has the least mobility of the above ions and appears to have the least etching rate of the above etchants. Therefore, for the purpose of this research, potassium hydroxide was used as the principal etchant.

5.4.2 The Etchant Concentration

Etchant concentration (which in this case refers to KOH concentration) plays an important role in the control of sensitivity for recoil particle registration in polymer foils under electrochemical etching treatment. As it increases, surface etching increases leading to amplification of a larger number of tracks from deeper layers as will be shown below. Surface or bulk etching rates of 0.06 and 0.3 μm/hour (corresponding to etching both sides of the foil) were obtained when 250 μm polycar-

bonate unexposed foils were etched for four hours applying 800 V at two kHz, respectively, in 28 percent and 45 percent KOH solutions (by weight) at 25°C. These were found by weighing the samples before and after etching. The etching rate is neutron dose dependent and increases by increasing neutron dose. Surface etching rates for irradiated foils are rather difficult to find since the weight loss at the track sites also contributed to the total weight loss. Therefore, assuming that the weight loss is only to the surface etching, bulk etching rates of 0.45 and 1.2 μm/hr were found for 28 percent and 45 percent KOH solution, respectively, at 1000 rads. In any case, these surface etching rates are much lower than those obtained by conventional etching methods which are commonly carried out at higher temperatures. For example, with conventional etching recoil particle tracks in polycarbonate foils are etched in 28 percent KOH solution at 60°C for four hours (Piesch, 1970). This leads to an increased surface etching and more tracks will be revealed from deeper layers to a point of equilibrium. This is one of the reasons that a lower sensitivity (tracks/n) is obtained by electrochemical etching compared to conventional etching methods as will be discussed in section 6.1.

The concentration dependence of etchant has given interesting results. Figure 30 indicates how the sensitivity increases with concentration of potassium hydroxide when other parameters are maintained constant. Each error bar indicates the standard error of the mean. The relationship (for the least squares fit) in this case is given by the equation

$$S = 25.08C_2 - 207.2$$

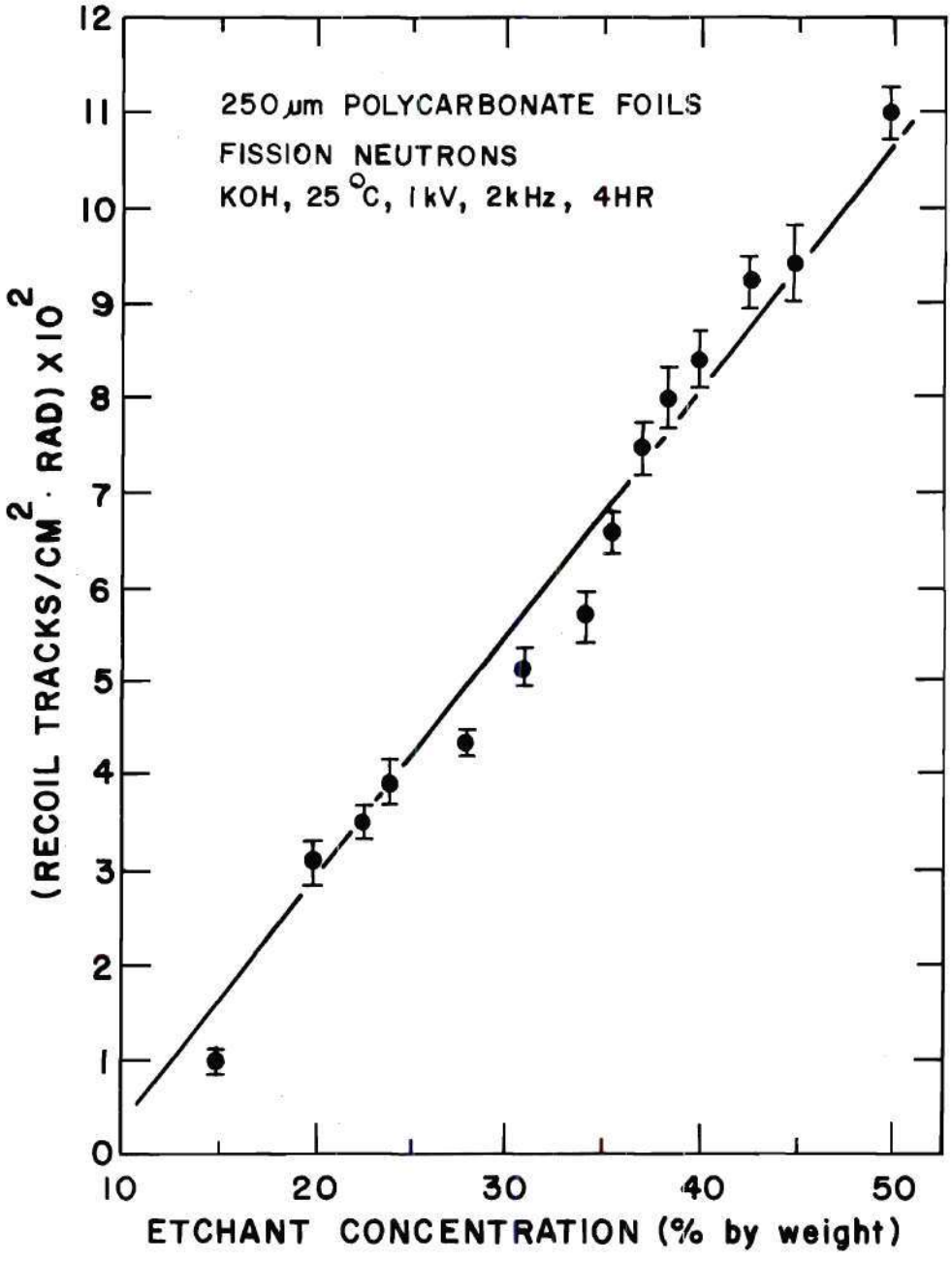

Figure 30. Recoil Track Density per Rad as a Function of Potassium Hydroxide Concentration at 25°C (% by weight) in 250 μm Thick Polycarbonate Foils Etched by Applying 1 kV at 2 kHz for 4 Hours

in which S = sensitivity (tracks/cm^2·rad) and C_2 = the etchant concentration (percent by weight). This recoil particle track density increase is due to the increased surface etching as the concentration increases as mentioned above. For example, the surface etching rate in unexposed foils is about five times higher when etched in 45 percent KOH than 28 percent KOH solutions. However, it leads to only two times the increase in sensitivity. Variations of the data from the linear fit curve in Figure 30 might be considered to be real and should not be overlooked. As was shown in Figure 20, the track density reaches a plateau after a time which depends on the foil thickness (e.g. after three hours for 250 μm) when other parameters are fixed. In Figure 30, two semi-plateaus are observed by a careful look at the data points. If these plateaus are real, they might be due to the etching of tracks from different layers in the foil. For example, the first plateau showing the tracks on the surface (i.e. range of concentrations from ~ 24 to ~ 32 percent KOH). For the purposes of this discussion, it is assumed that within this concentration range, a plateau similar to those of Figure 16 is obtained. As concentration increases, tracks from a deeper layer start to show up and the same process might be repeated. Such tantalizing observations (speculations) will require more experimental research, however, before they can be established as real.

Figures 31 and 32 show mean track diameter and optical density as functions of potassium hydroxide etchant concentration, respectively. As can be seen, there is a cyclic variation in mean track diameter and optical density as a function of etching concentration under the applied etch-

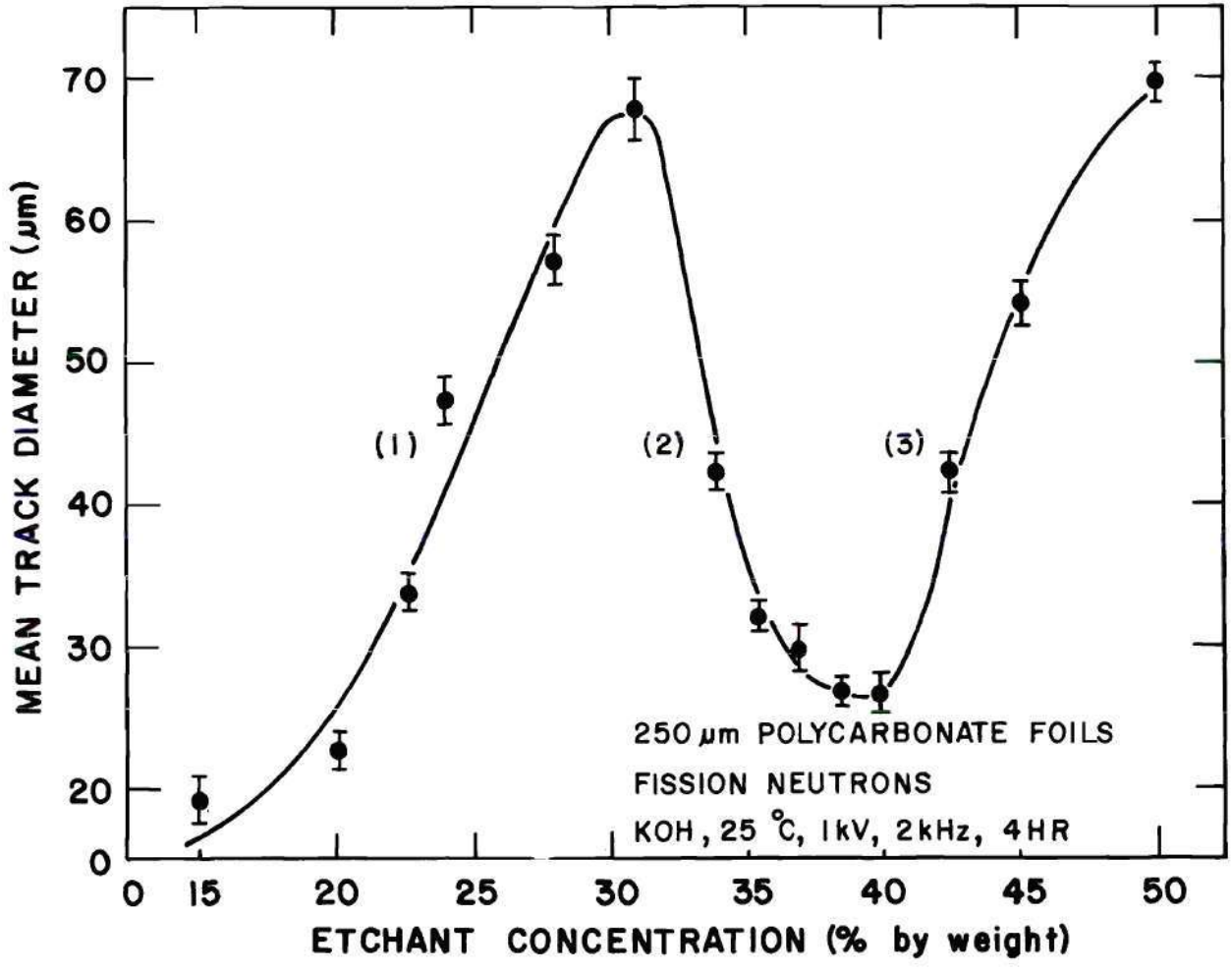

Figure 31. Mean Recoil Track Diameter as a Function of Potassium Hydroxide Concentration in 250 μm Polycarbonate Foils Etched at 25°C Applying 1 kV at 2 kHz for 4 Hours

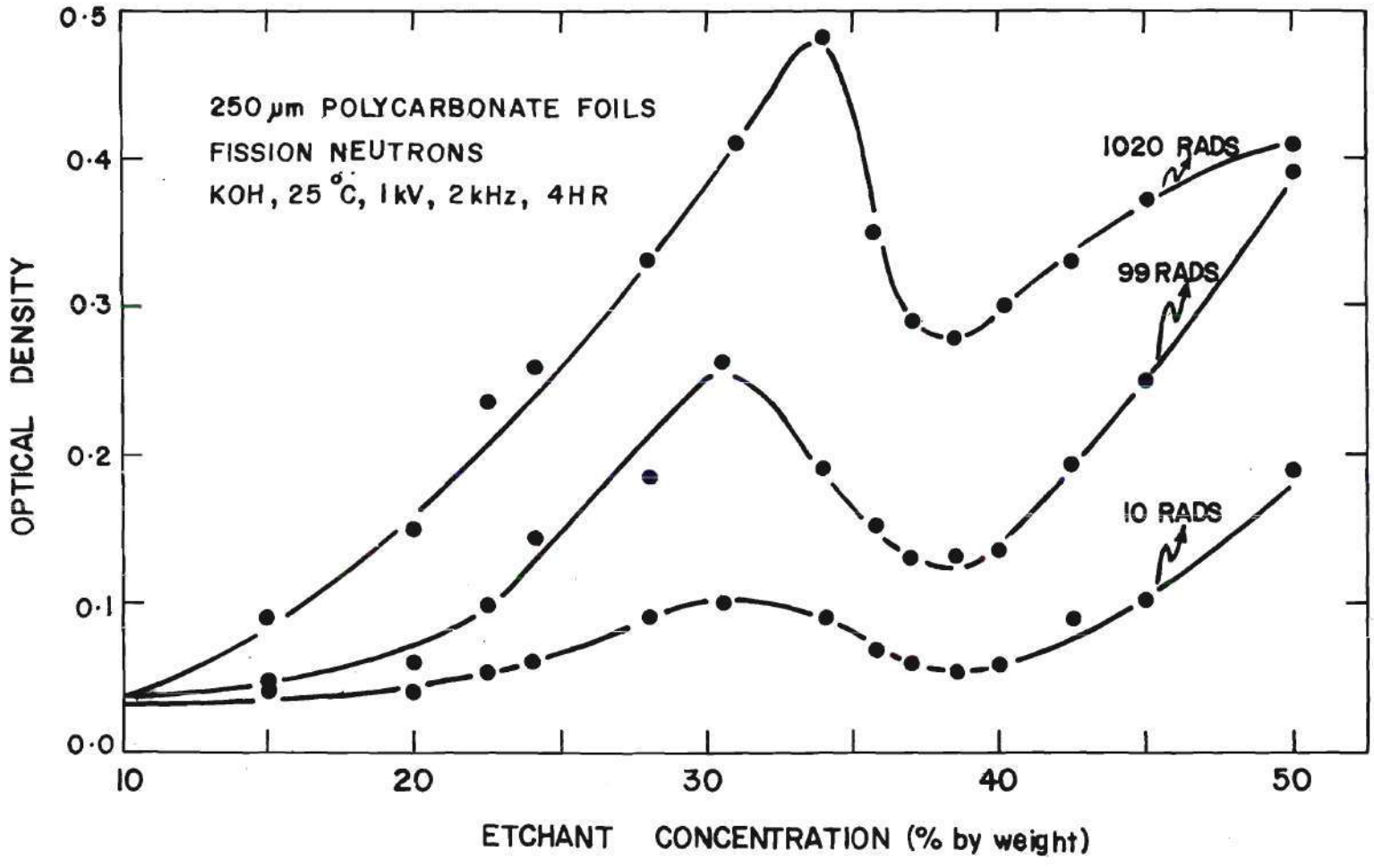

Figure 32. Optical Density as a Function of Potassium Hydroxide Concentration for Different Neutron Doses in 250 μm Polycarbonate Foils Etched at 25°C Applying 1 kV at 2 kHz for 4 Hours

ing conditions. Within the limited data, a complete and convincing explanation is impossible. However, a qualitative explanation may be followed by dividing the curve into three regions. Also, the pattern of the curve in Figure 30 might provide some assistance in explaining these cyclic variations.

Region (1) extends from about 10 to 31 percent concentration of KOH (Figure 31). In this region tracks may be considered to be due only to surface tracks, thus leading to an increase in track diameter and a plateau in track density in a similar fashion to tracks obtained by increasing etching time as discussed above. Tracks in this region are completely round as shown in Figure 32.

Region (2) extends from about 31 to 38 percent concentration of KOH. In this region it is assumed that bulk etching rate becomes significant washing out some portion of the tracks at the original foil surface so that the shape of the tracks becomes irregular as shown in Figure 33. Mean track density increases in this region. In the middle of this region tracks are quite nonuniform in shape becoming regular at the end of this region.

Region (3) is above 37 percent concentration of KOH. In this region a semi-plateau is assumed again in track density leading to an increase in track diameter. The tracks in this region appear circular again but not with sharp contrast as they look in Figure 34. Figure 35 shows tracks etched in 45 percent KOH solution under the indicated etching conditions.

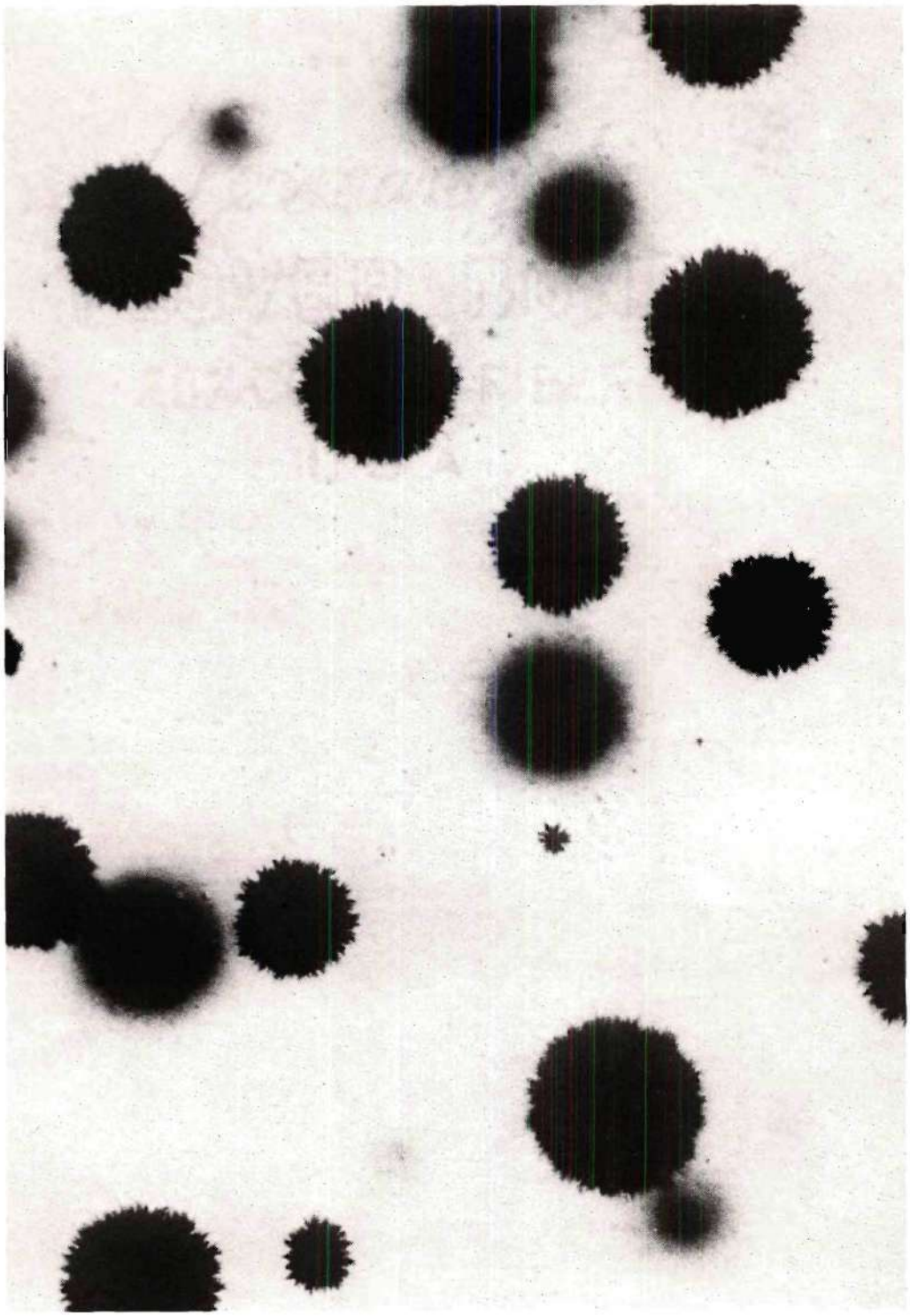

Figure 33. Fission-Neutron-Induced Recoil Particle Tracks in 250 μm Polycarbonate Foils Etched in 28% KOH Solution at 25°C Applying 1 kV at 2 kHz for 4 Hours

Figure 34. Fission-Neutron-Induced Recoil Particle Tracks in 250 μm Polycarbonate Foils Etched in 34% KOH Solution at 25°C Applying 1 kV at 2 kHz for 4 Hours

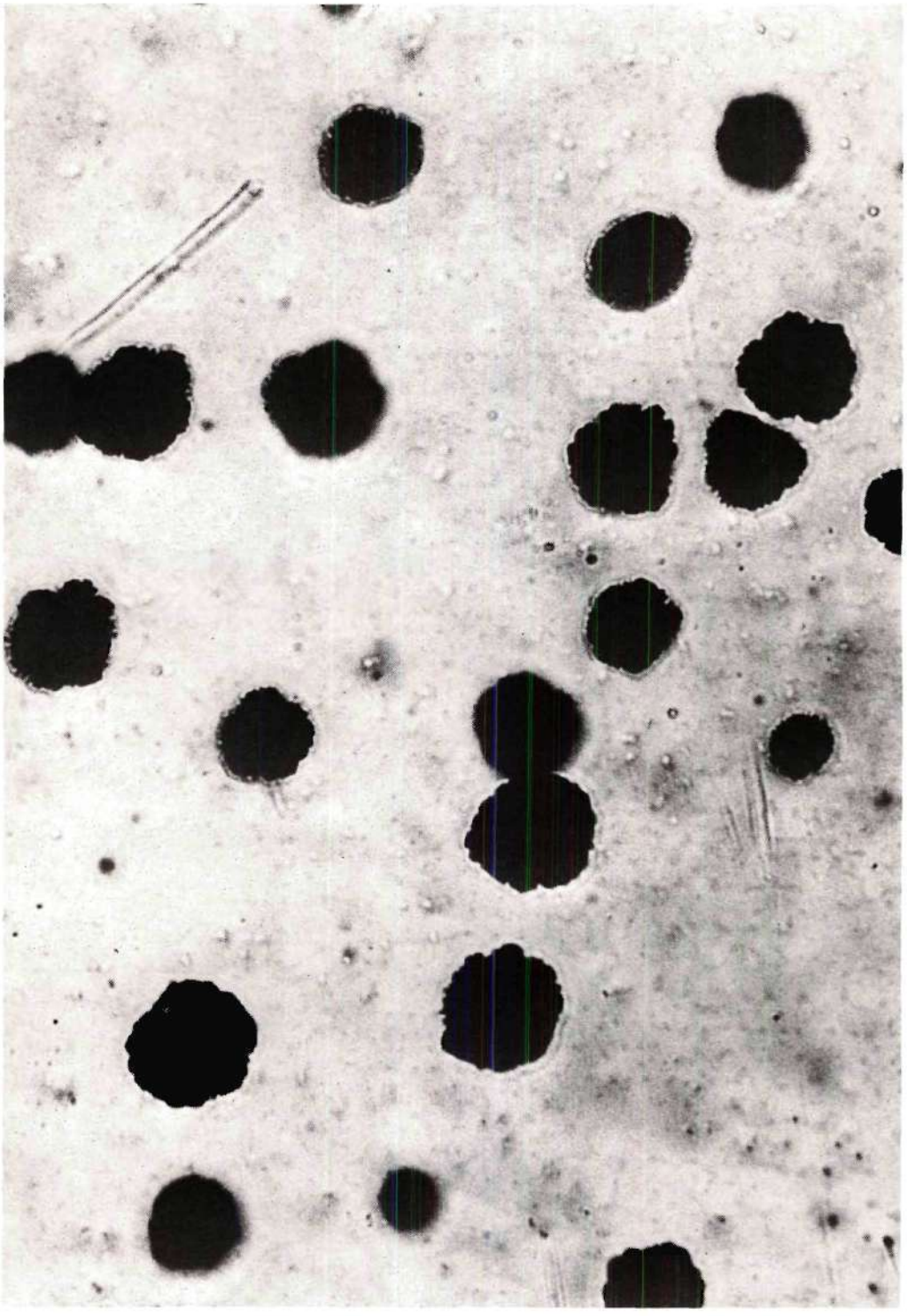

Figure 35. Fission-Neutron-Induced Recoil Particle Tracks in 250 μm Polycarbonate Foils Etched in 45% KOH Solution at 25°C Applying 1 kV at 2 kHz for 4 Hours

5.4.3 The Etchant Temperature

The undamaged surface etching rate (μm/hr) and mean track diameter (μm) are both strongly dependent on etchant temperature. For example, when conventional etching has been applied, the bulk etching rate in silicone polycarbonate etched at 97°C was about 200 times higher than that at 30°C (Fleischer et al., 1972). Furthermore, fission fragment track diameters etched in cellulose acetobutyrate in 6.25 N NaOH at 60°C were about 10 times larger than those at 30°C (Blanford et al., 1970).

Temperature of the etchant enhances both bulk etching rate and track diameter when electrochemical etching is applied. It also reduces the required etching time considerably. For example, as observed in these investigations the etching time was reduced from four hours to about 47 minutes when 250 μm polycarbonate foils were etched at 60°C instead of 25°C. This reduction depends significantly on the foil material and thickness, etchant composition, concentration, voltage, frequency, etc.

Both sensitivity (track/cm^2·rad) and mean track diameter increase linearly with the etchant temperatures as indicated in Figure 36. In this case the best fit equations are:

$$S = 9.5\ T - 228$$

$$D = 1.47\ T - 35$$

in which S = sensitivity (track/cm^2·rad), T = temperature (°C), and D = track diameter (μm). Figure 37 shows optical density as a function of etchant temperature for three different fission neutron doses for an etching time of 47 minutes. Although etching time is significantly reduced using higher temperatures, low temperatures such as 25°C are more conven-

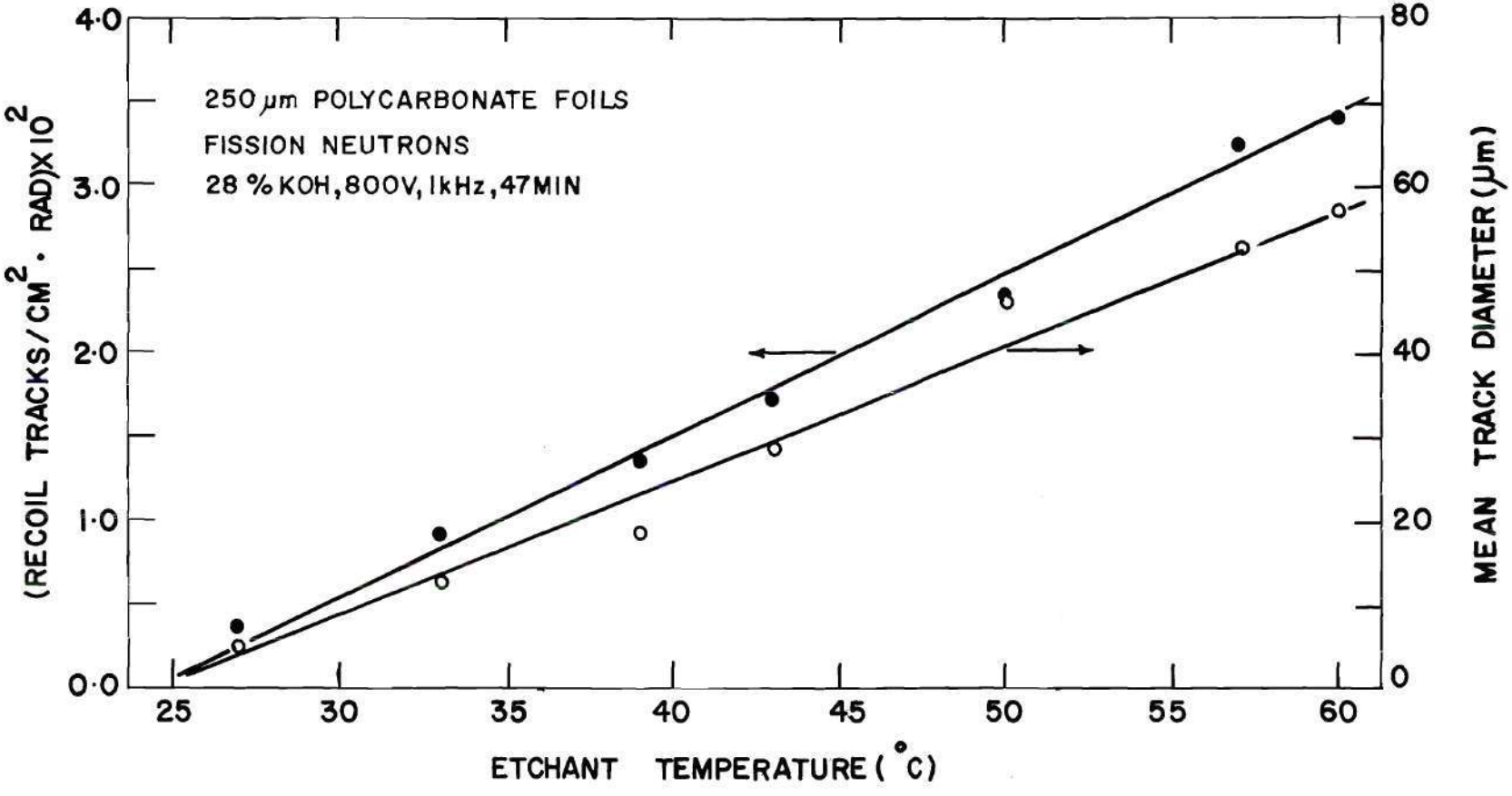

Figure 36. Recoil Track Density per Rad of Fission Neutron and Mean Track Diameter in 250 μm Polycarbonate Foils Etched in 28% KOH Solution Applying 800 V at 1 kHz for 47 Minutes

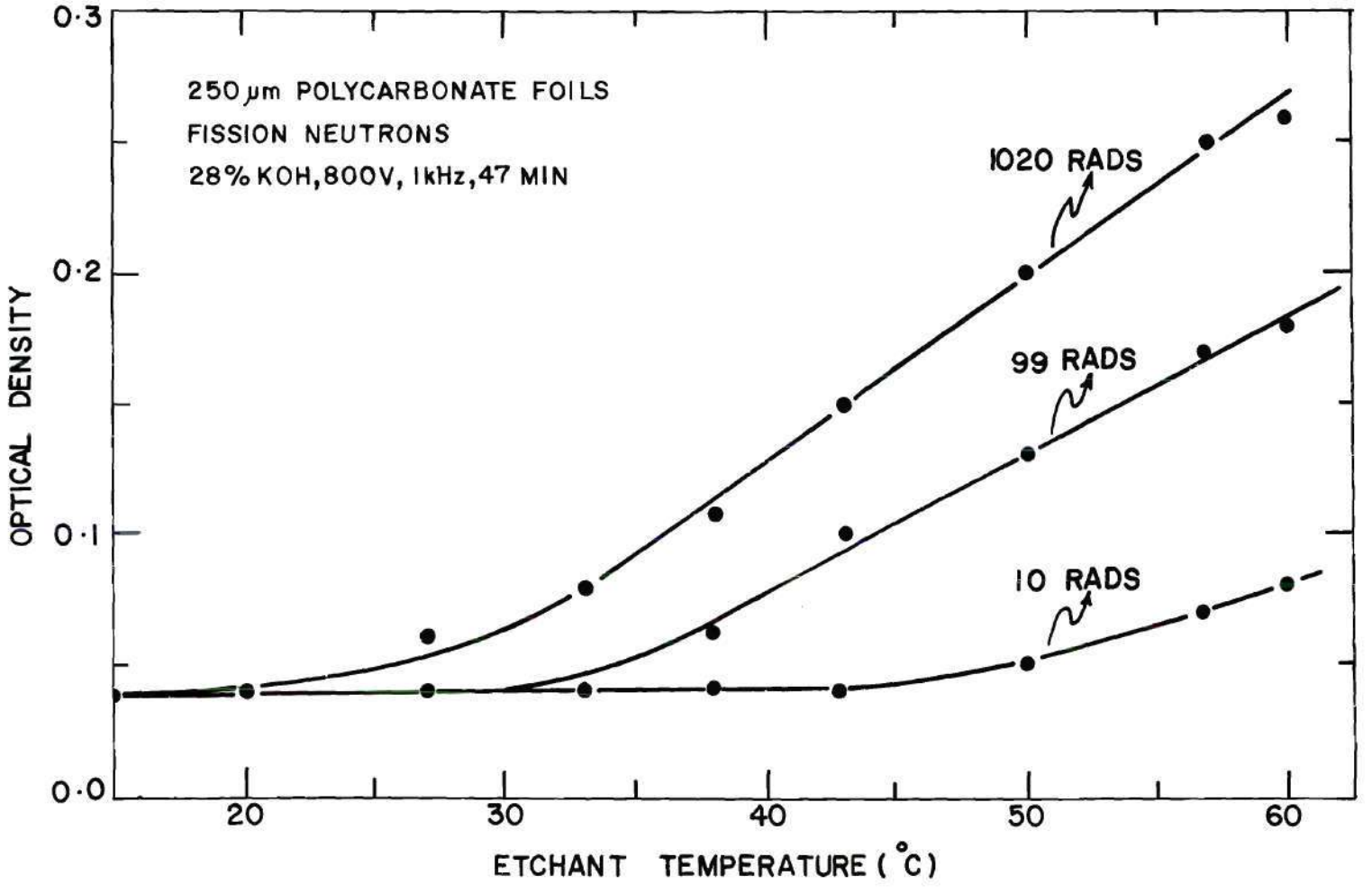

Figure 37. Optical Density as a Function of Etchant Temperature for Different Fission Neutron Doses in 250 μm Polycarbonate Foils Etched in 28% KOH Solution Applying 800 V at 1 kHz for 47 Minutes

ient and thus preferred for the remainder of our studies. Electrochemical etching operations at 25°C provide simplicity, convenience, no need for heating equipment, no need for temperature adjustment after each etching, more confidence in etching without breakdown through the foils, low etchant evaporation and as a result stability of etchant concentration. However, if low etching times are of interest, higher concentrations (e.g. 45 percent KOH) or the use of thinner foils (e.g. 125 μm) can compensate for etching times.

5.5 Dependence on the Distance Between the Electrodes

One of the factors which might seem to be crucial at first glance is the distance between the electrodes. However, since the current through the foil will not change appreciably with electrode position, no change in sensitivity is expected. Nevertheless since there are minor changes in the electrical characteristics with distance between the electrodes, some changes in track etching can be expected. Table 6 shows sensitivity (tracks/cm^2·rad), mean track diameter, and optical density at different distances between the electrodes when 125 μm polycarbonate foils were etched in 45 percent KOH solution at 25°C applying 800 V at two kHz for 90 minutes.

As indicated in the table, no significant changes other than experimental variations have been observed in sensitivity as the electrode distances are increased. However, mean track diameter and obviously optical density have decreased slightly with increase in distance. Therefore, minor changes in the distance and angle between the electrodes do not cause significant changes in the results.

Table 6. Sensitivity, Mean Track Diameter, and Optical Density of Fission-Neutron-Induced Recoil Particle Tracks in 125 μm Polycarbonate Foils Etched in 45% KOH Solution at 25°C Applying 800 V at 2 kHz for 90 Minutes at Different Distances Between the Electrodes

Distance Between the Electrodes (cm)	Sensitivity (tracks/cm^2·rad)	Mean Track Diameter (μm)	Optical Density (%) 10	100 (rads)	1000
3.5	$(8.86 \pm 0.28) \times 10^2$	26.1	0.05	0.13	0.30
8.5	$(8.17 \pm 0.36) \times 10^2$	24.98	0.05	0.12	0.27
13.5	$(9.20 \pm 0.38) \times 10^2$	21.53	0.05	0.11	0.26
18.5	$(8.48 \pm 0.29) \times 10^2$	20.9	0.05	0.09	0.23

5.6 Dependence on Particle Type and Bombardment Conditions

Based on a discussion given in section 3.1, high LET heavy ions such as fission fragments produce high damage densities along their paths which can be easily amplified by an etching method. Fission fragments and heavy ions from an external source bombarding a polymer foil form tracks on the surface layer. Therefore, etching conditions such as using 28 percent KOH solution at 25°C and applying 800 V at two kHz for a time which depends on the foil thickness can be applied. On the other hand, fast-neutron-induced recoil particle tracks are distributed throughout the foil and are formed by particles with different LET's. Therefore, etching conditions should be applied so that more tracks from deeper layers can be amplified to increase sensitivity for fast neutron detection. For example, using 45 percent KOH solution (when the other parameters are the same as above) will increase the sensitivity by a factor of two, as previously stated. The track diameter after an etching process depends on the damage density caused by the particle and it increases as this damage density increases.

CHAPTER VI

NEUTRON DOSIMETRY APPLICATIONS

Some detailed results on the optimization of electrochemical etching parameters for the amplification of fast-neutron-induced recoil particle tracks in Lexan polycarbonate were presented in Chapter V. Despite the physico-chemical results obtained, the characteristics of the foils as dosimeters need to be investigated. This chapter presents the results of dosimetry applications such as personnel dosimetry, fast neutron contamination measurements of some high energy x-ray beams, and depth dose studies near biological interfaces. The foils used in the following applications were all from Rowland Products, Inc.

6.1 Fast Neutron Personnel Dosimetry

Some studies on the applications of track etch methods as alternatives to the NTA films for fast neutron personnel dosimetry were given in a previous investigation (Sohrabi and Becker, 1971). Fission fragment registration methods employing ^{232}Th or ^{237}Np-10 μm polycarbonate (Kimfol) combinations were reported. The ^{237}Np demonstrated superior characteristics in terms of sensitivity and lower neutron energy threshold. Fission fragment track counting by a spark counting method also simplifies this process. However, the use of fissionable materials for neutron dosimetry adds to the cost, complexity, and likely administrative problems. On the other hand, although recoil particle track registration in polymers (i.e. no fission radiator) provides attractive features, it was

not seriously considered as feasible for routine fast neutron personnel dosimetry applications for reasons such as small size of the tracks obtained by conventional etching methods which make track counting methods difficult and neutron dosimetry in the range of interest in routine dosimetry impractical.

It has been shown that spark counting of recoil particle tracks in conventionally etched foils is not efficient (Johnson and Becker, 1970). Also the preliminary results on the amplification of these tracks by electrochemical etching have not lent encouragement to the immediate application of this technique (Sohrabi and Becker, 1971). Recently, spark counting of recoil particle tracks in 10 μm polycarbonate foils by extended etching (Becker and Abd-el Razek, 1974) and in six μm aluminized polycarbonate foils (as studied in the early stage of this investigation) has been possible, as was reported in section 4.4. However, our experience based on some preliminary investigation reveals difficulties in this spark counting approach for large-scale neutron dosimetry. These include mainly the necessity for carefully controlled etching conditions, difficulty in handling the etched foils having thickness of about two to four μm during the washing and drying processes, and during spark counting. Also spark count density will increase by successive spark counting and by movement of the etched foils on the electrode between each counting process.

The findings and improvements made on the electrochemical etching of recoil tracks have overcome many shortcomings associated with this dosimetry approach for many fast neutron dosimetry applications especially for fast neutron personnel dosimetry.

Figure 38 is a photograph of recoil particle tracks in 375 μm thick polycarbonate foils (RP) which have been exposed to different doses of

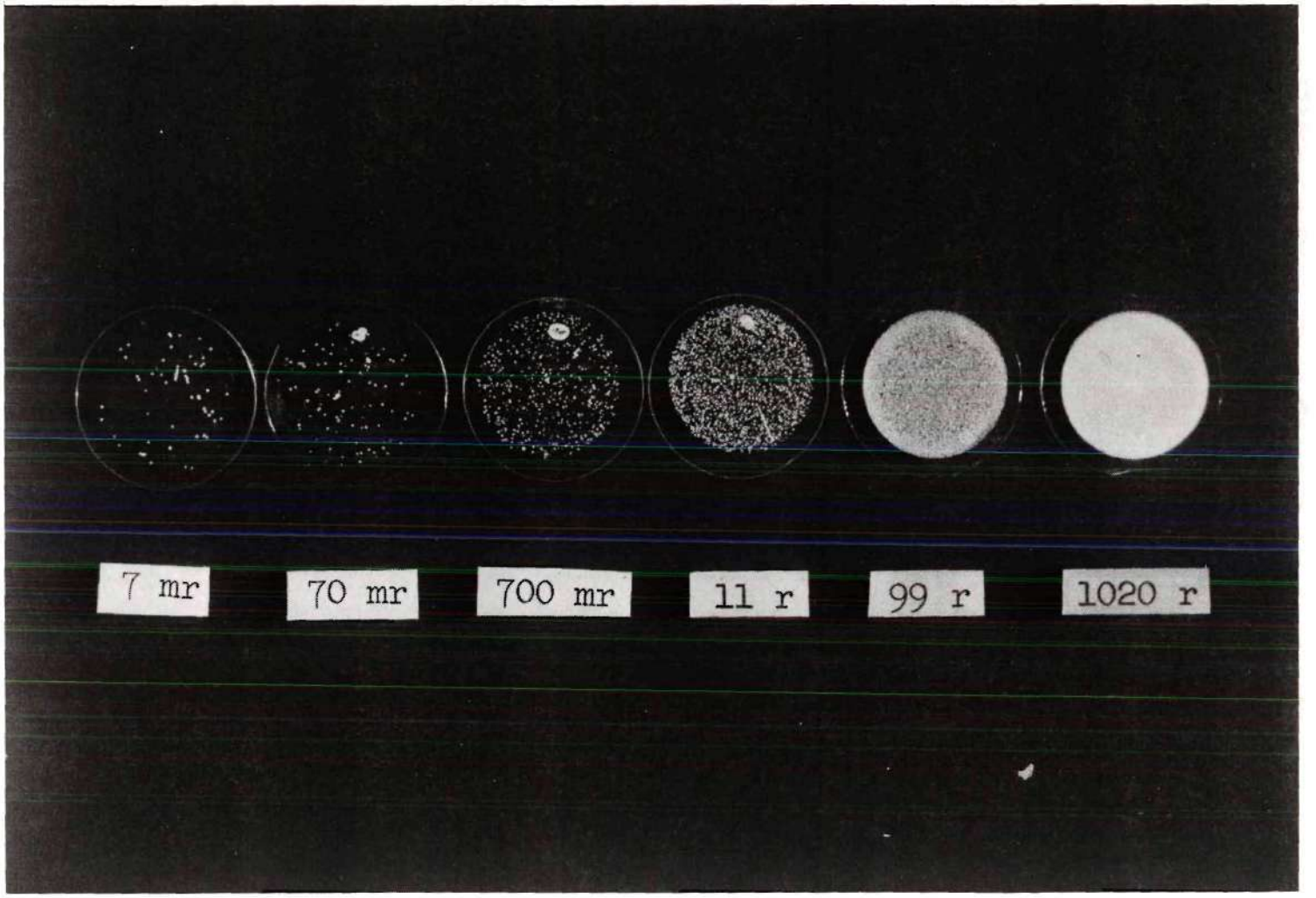

Figure 38. Photograph of Fast-Neutron-Induced Recoil Particle Tracks in 375 μm Thick Polycarbonate Foils Exposed to Different Doses of Fission Neutrons and Etched in 28% KOH Solution at 25°C Applying 700 V at 1 kHz for 14 Hours

fission neutrons, etched in 28 percent KOH at 25°C applying 700 V at one kHz for 14 hours. This photograph makes evident the characteristics which simplify the task of describing the encouraging possibilities of applying this system for neutron dosimetry; the amplification of the tracks is so pronounced that one can easily sort visually a number of foils according to the neutron dose they have received. The wide dose range of this dosimeter is apparent from the photograph, covering one mrad to 1000 rads or higher if desired and it can be used for both routine and accidental dosimetry cases. The large size of the tracks also simplifies track density evaluation methods.

It can be seen in Figure 39 that the sensitivity of recoil particle track registration in Lexan polycarbonate after electrochemical etching covers quite adequately the wide dose range required for personnel dosimetry. The sensitivity can be adjusted also by choosing the proper foil thickness and etching conditions, for example the responses of two different thicknesses such as 125 μm polycarbonate foils (upper curve) and 250 μm (middle curve) are shown in Figure 39 when different electrochemical etching conditions are applied. The results are compared also to spark count densities of ^{232}Th and ^{237}Np-10 μm polycarbonate (Kimfol) combinations (Sohrabi and Becker, 1971). The track density obtained by microscopic counting in 250 μm foils etched in 28 percent KOH solution at 25°C applying 800 V at two kHz for five hours is more than twice as large as when using a thick ^{232}Th-10 μm polycarbonate combination. In 125 μm foils etched for only 94 minutes in 45 percent KOH solution at 25°C applying 800 V at two kHz the sensitivity is equal to that of the 2.8 mg/cm^2 ^{237}Np-10 μm polycarbonate combination and about five times higher than

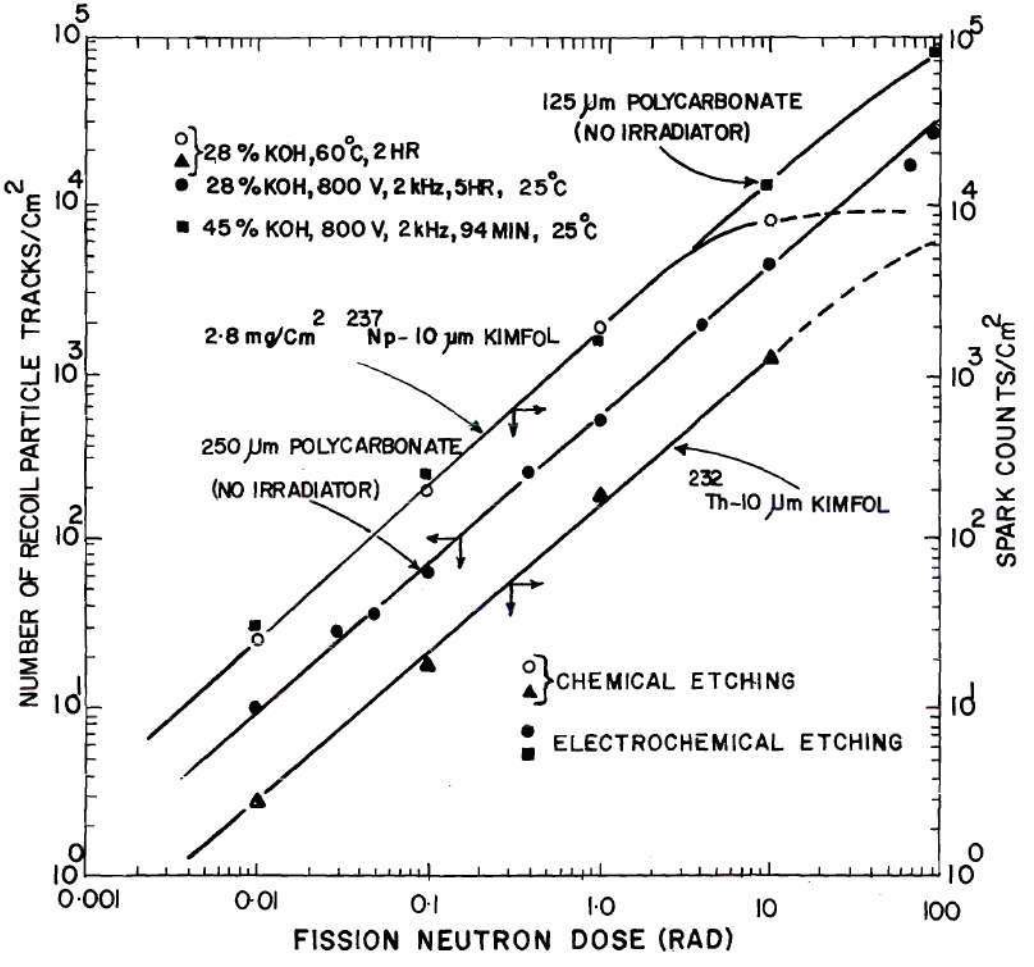

Figure 39. Recoil Particle Track Density in 125 and 250 μm Polycarbonate Foils (electrochemically etched) and Fission Fragment Spark Densities (conventionally etched) as Functions of Fission Neutron Dose

when the 0.1 mg/cm^2 Np-Au alloy/10 μm polycarbonate combination is used (Cross and Ing, 1975a).

Up to a few rads of fission neutrons, which is the range usually encountered in routine personnel dosimetry, track density can be determined simply by projecting the tracks on a microfilm screen. Up to about 100 rads with foils etched under the above mentioned etching conditions track density determination can be carried out by microscopic counting. Above 100 rads of fission neutrons track density determination under a microscope becomes difficult because of the large size of tracks in thicker foils. However, by lowering the etching time, the linearity can be extended up to higher doses if visual counting is being applied. At doses greater than 10 rads the visible change in optical appearance of foils becomes so pronounced that optical densitometry or other similar methods can be applied. Figure 40 shows optical density as a function of the HPRR fission neutron dose in 125 μm thick polycarbonate foils etched from 0.5 to 3 hours. Similar response curves have been obtained also using thicker foils. Although simple optical densitometry (which is of value for patient monitoring and criticality accident cases) does not seem to indicate a sharp increase in optical density with increase in neutron dose, special lighting methods may improve the response.

Care should be taken in the selection of polycarbonate foils since some foils might result in high background track densities (e.g. 500 tracks/cm^2). This high background density seems to be due to many causes such as cosmic rays after a long term stocking period, mishandling of the foils during rolling and packaging by some vendors and during pre-etching processes such as punching the foils, etc. However, in the sheets used

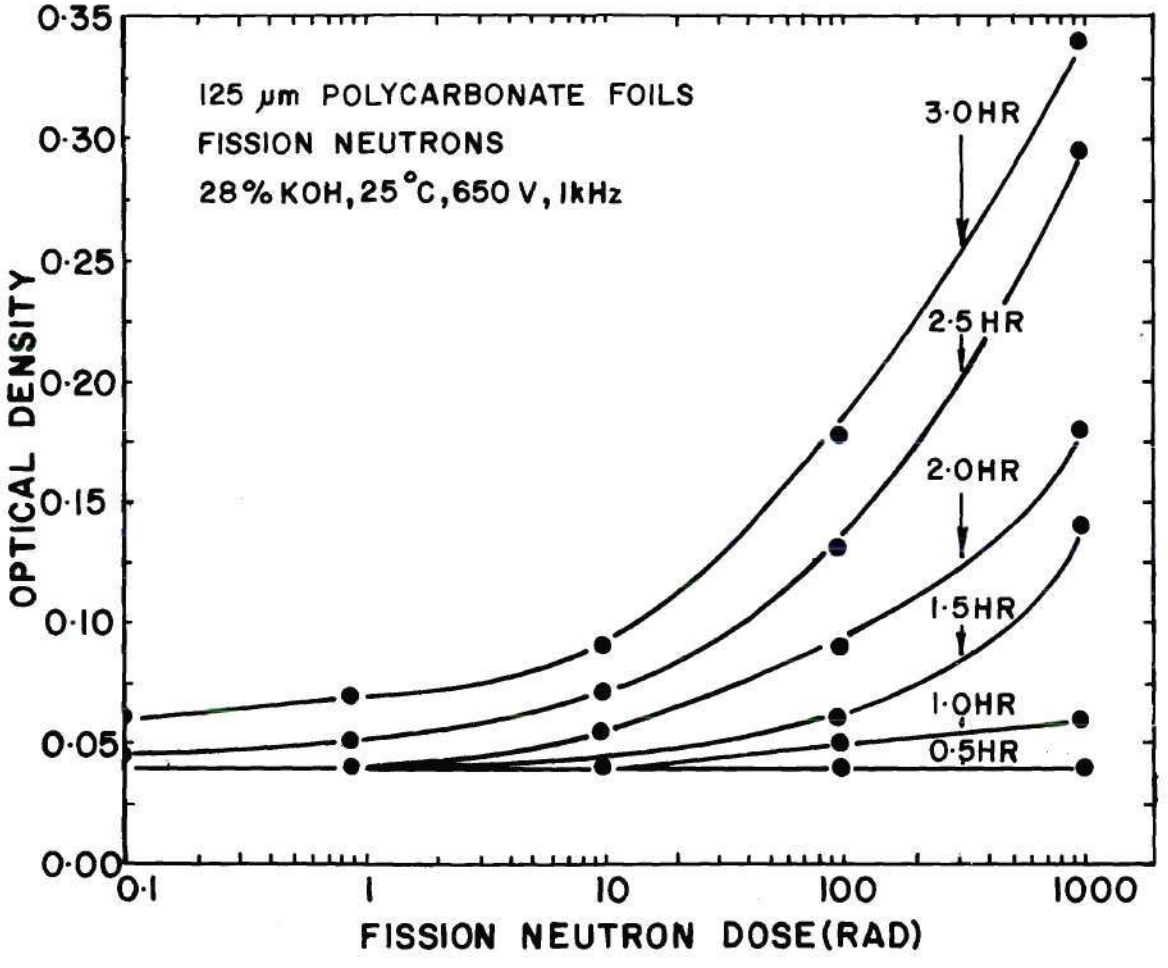

Figure 40. Optical Density as a Function of Fission Neutron Dose (rad) in 125 μm Polycarbonate Foils Etched for Different Etching Times in 28% KOH Solution at 25°C Applying 650 V at 1 kHz

in most of this application study the foils had very low background track density with reproducilibity from one sample to another, and good reproducibility (± 3 percent) was obtained. Nevertheless, for low neutron dose measurements in the lower part of the linearity range, foils of nil background track density are required to obtain high precision and accuracy so that each single track represents a meaningful measure of neutron doses at low neutron fluences. This does not seem to cause any serious problems since masked foils can be purchased or the foils can be especially manufactured, or the background tracks can be removed by special treatments.

An important factor in the use of fast neutron dosimeters if worn, as is usually the case, on the front side of the trunk is their directional response. Neutron absorption in the body changes the neutron flux and energy distribution and the inherent directional dependence of the detector will introduce an orientation dependence. The orientation dependence of polycarbonate foils used as a belt around a water filled elliptical thorax phantom was studied. This study was similar to a previous investigation (Piesch, 1970) except in our case electrochemical etching was applied. Foils were punched at different locations along the belt, etched and the responses were measured as a function of orientation to the neutron sources. Corrections were made for the varying distance by a computer program and the data were normalized.

Figure 41 shows the directional response of the recoil particle track method for 125 and 250 μm polycarbonate foils obtained on the mentioned phantom etched in 28 percent KOH solution at 25°C applying 800 V at two kHz for 2.5 and 5 hours, respectively.

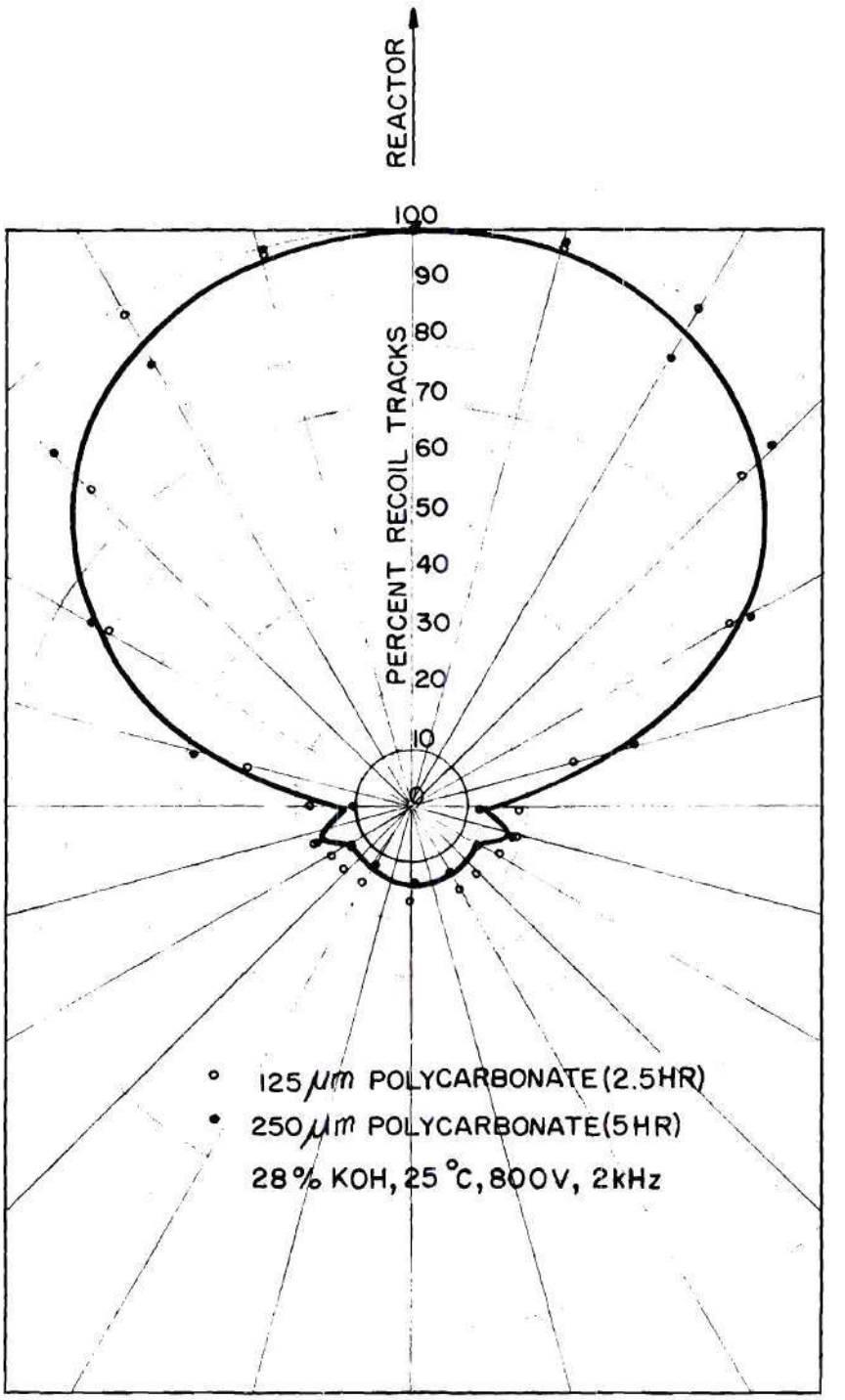

Figure 41. Directional Response of Recoil Particle Tracks in Polycarbonate Foils of Two Different Thicknesses (electrochemically etched) for Fission Neutrons

The results appear to be relatively independent of foil thickness except for angles. Figure 42 shows results of ^{237}Np and ^{232}Th on 10 μm polycarbonate (Kimfol) used in the same fashion on the same phantom exposed to fission neutrons and when conventionally etched (Sohrabi and Becker, 1971). As expected, the orientation dependence of recoil particle track registration is more pronounced than is the case for fission fragment registration as can be seen for example by comparing the responses at 90° in the two cases.

Directional dependence of recoil particle registration (Becker, 1967; Piesch, 1970) and fission fragment registration techniques (Cross and Ing, 1975) have been the subject of some previous investigations. Even the fission fragment registration method shows some sensitivity dependence on the direction of the incident neutron. The measured values of 0°/90° sensitivity were 1.15 ± 0.03 for ^{237}Np and 1.27 ± 0.06 for ^{232}Th foils for 14 MeV neutrons (Cross and Ing, 1975b). This ratio is more pronounced as indicated above for recoil particle registration, i.e. it is about 1.4 at the same energy (Becker, 1967). This ratio is energy dependent and increases as the neutron energy decreases.

Such directional dependence on the sensitivity is also very pronounced in NTA photographic films (Piesch, 1963; Krishnamoorthy and Ventakaraman, 1973). However, in the case of recoil particle track registration in polycarbonate foils, this directional dependence can be corrected or compensated by many means. For example, for radiotherapy applications such as beam measurements or patient monitoring in which the directions of neutrons are known, the response can be corrected by the use of data such as those given in Figure 41. Another correction method is to bend

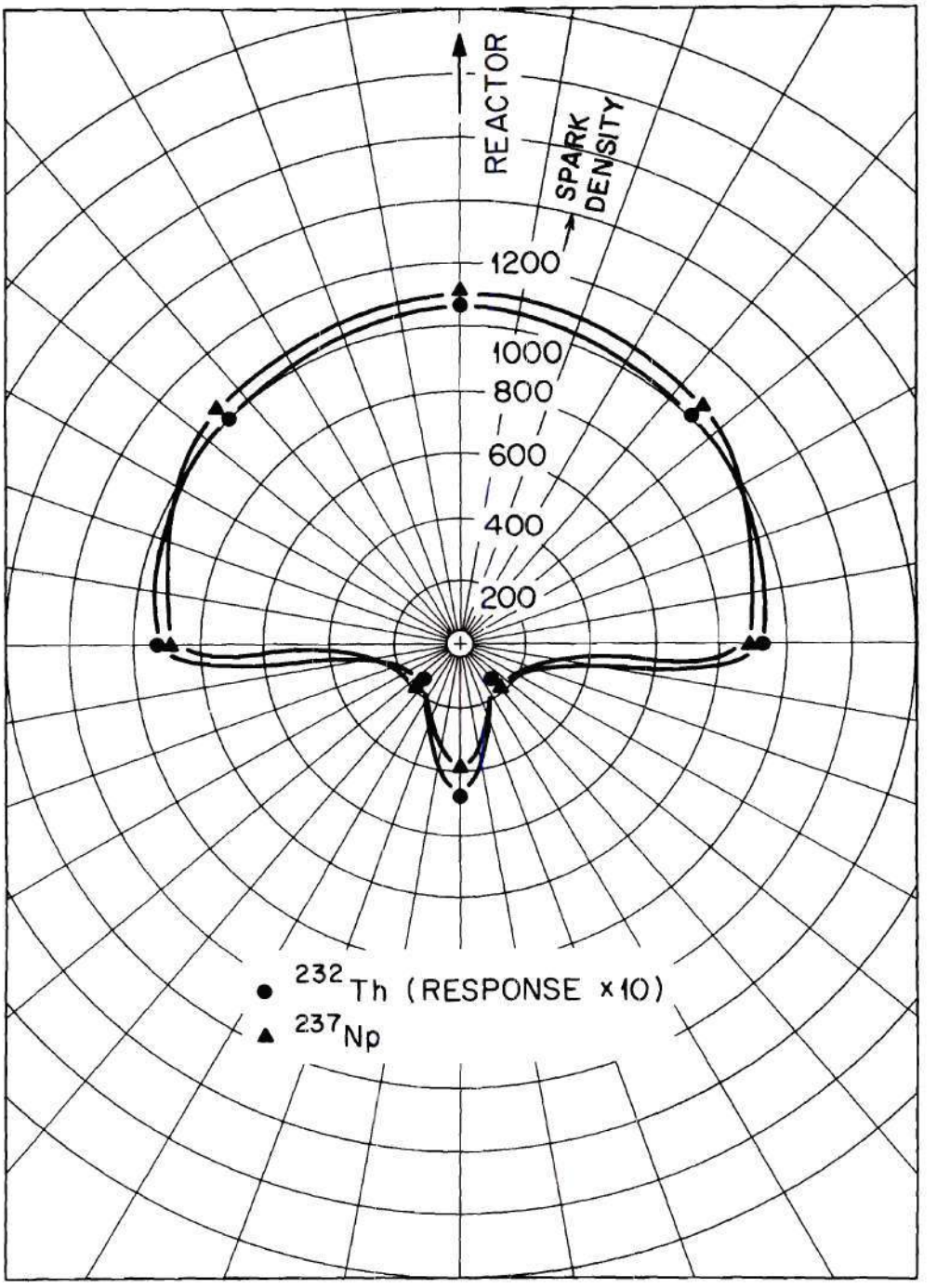

Figure 42. Directional Response of ^{232}Th and ^{237}Np-10 μm Kimfol Dosimeters for Fission Neutrons (after Sohrabi and Becker, 1971)

the foils in a circular or semi-circular fashion on a Lucite tube (e.g. one cm in diameter depending on the size of the foil). Figure 43 shows the percent sensitivity as a function of angle between the foil plane and the direction of incident neutrons for both rolled and unrolled foils. The straight line is obtained by counting the tracks on the foil strip facing the direction of the beam. Counting the whole area of the rolled foils leads to sensitivities varying by about 25 percent around the straight line. More precise rolling methods will minimize these variations. Furthermore, the diameter of the tube and the thickness of the foil are important factors relating to microscopic cracking which will be amplified by electrochemical etching. Other approaches such as mounting two, three, or four foils on the walls of a small cube may be applied also and prove more practical in special cases such as area monitoring.

Very little fading of "latent" recoil particles and fission fragment tracks can be expected to occur even under unfavorable working conditions and in tropical climates having high humidities (Becker et al., 1972; Piesch and Sayed, 1974; and this study). As can be seen in Figure 44, no fading of tracks has been detected at ambient room temperature for a period of one month (or even six months not shown on graph), and only 10 and 30 percent fading have been observed by storing the foils at 40°C and 60°C, respectively, for the same period of time, and 30 percent for 40 hour storage at 90°C. Piesch and Sayed (1974b) have also reported fading studies at different temperatures and humidities. Although it has been shown that 95 percent "latent" proton track fading occurs in NTA photographic film after 10 days storage at 5°C and 85 percent relative humidity (Piesch and Sayed, 1974b). Another example of high temperature

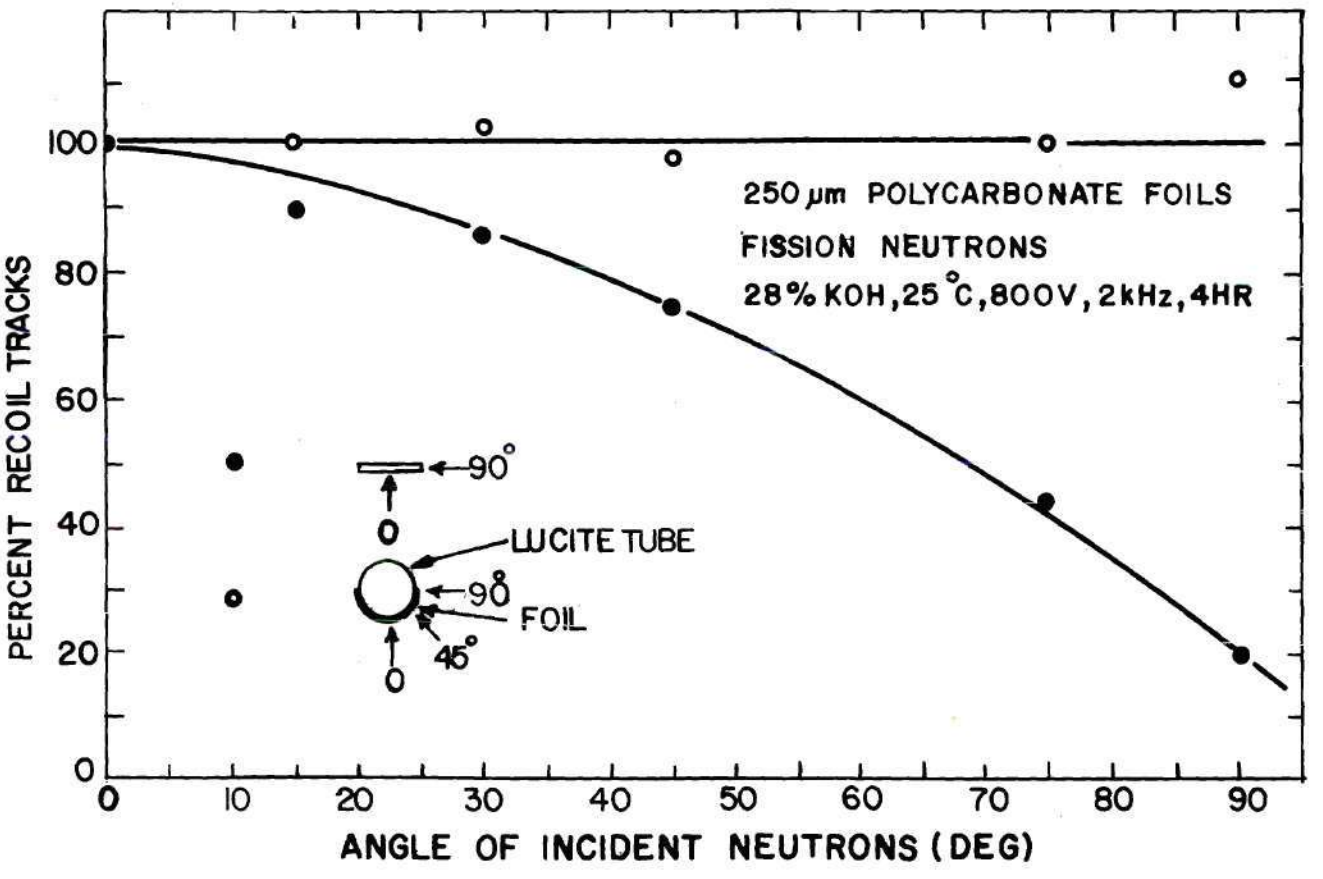

Figure 43. Percent Recoil Tracks as a Function of Angle of Neutron Incidence (deg) When Rolled and Unrolled 250 μm Polycarbonate Foils Etched in 28% KOH Solution at 25°C Applying 800 V at 2 kHz for 4 Hours

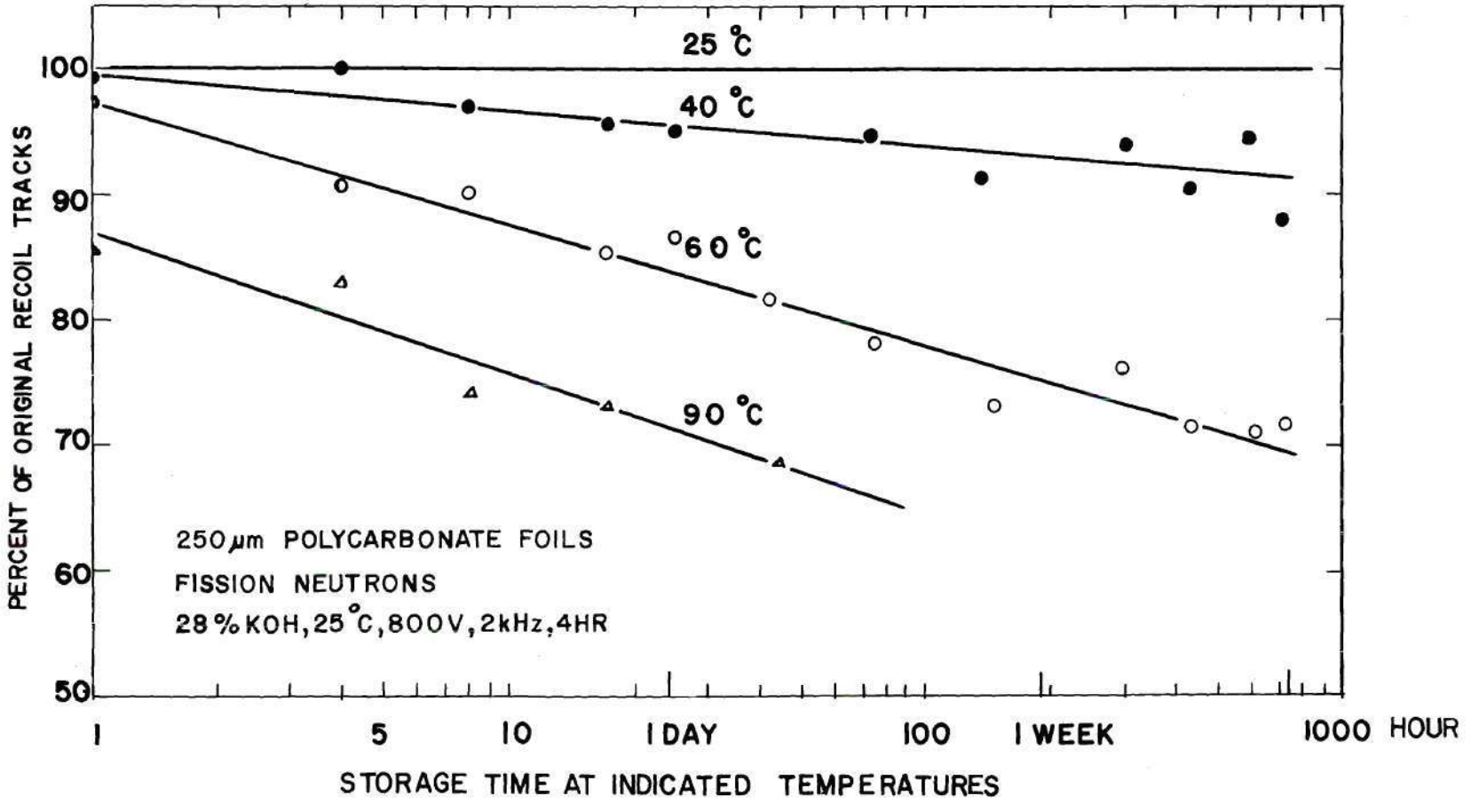

Figure 44. Percent of Original Recoil Particle Tracks as a Function of Storage Time at Different Storing Temperatures of 250 μm Polycarbonate Foils Etched in 28% KOH Solution Applying 800 V at 2 kHz for 4 Hours

fading indicates 80 percent fading in NTA films after nine days storage at 30°C and 76 percent relative humidity, while only 22 percent recoil particle track fading has been observed in polycarbonate after 21 days storage under the extreme conditions of 50°C and 97 percent relative humidities.

In Figure 45, sensitivity (tracks/n) of recoil particle registration is given as a function of neutron energy by three different investigations (Becker, 1967; Jozefowicz, 1973; and this research). The first two neutron energy dependence studies by Becker (1967), and Jozefowicz (1973) were carried out using conventional etching methods. In particular, Jozefowicz (1973) has placed more emphasis on the energy response around one MeV to verify the threshold energy for neutron detection which is about one MeV in this case. His data agree well with experimental values obtained by Becker (1967). As can be seen in Figure 45, the sensitivities obtained by electrochemical etching under the indicated etching conditions are lower by a factor of three to four (when 250 μm polycarbonate foils were used) compared to the values obtained by conventional etching. This was expected from the findings of this research, since as previously stated only recoil tracks registered on the surface layers are electrochemically etched under the non-equilibrium conditions applied. In conventional etching, however, which is usually carried out at a higher temperature (e.g. 60°C), etching is extended to a point where equilibrium is reached between disappearance of surface and near surface tracks and revealing of tracks from deeper layers. Fortunately, when electrochemical etching is applied, the sensitivity as previously stated can be further increased by increasing the etchant concentration from 28 percent to 45

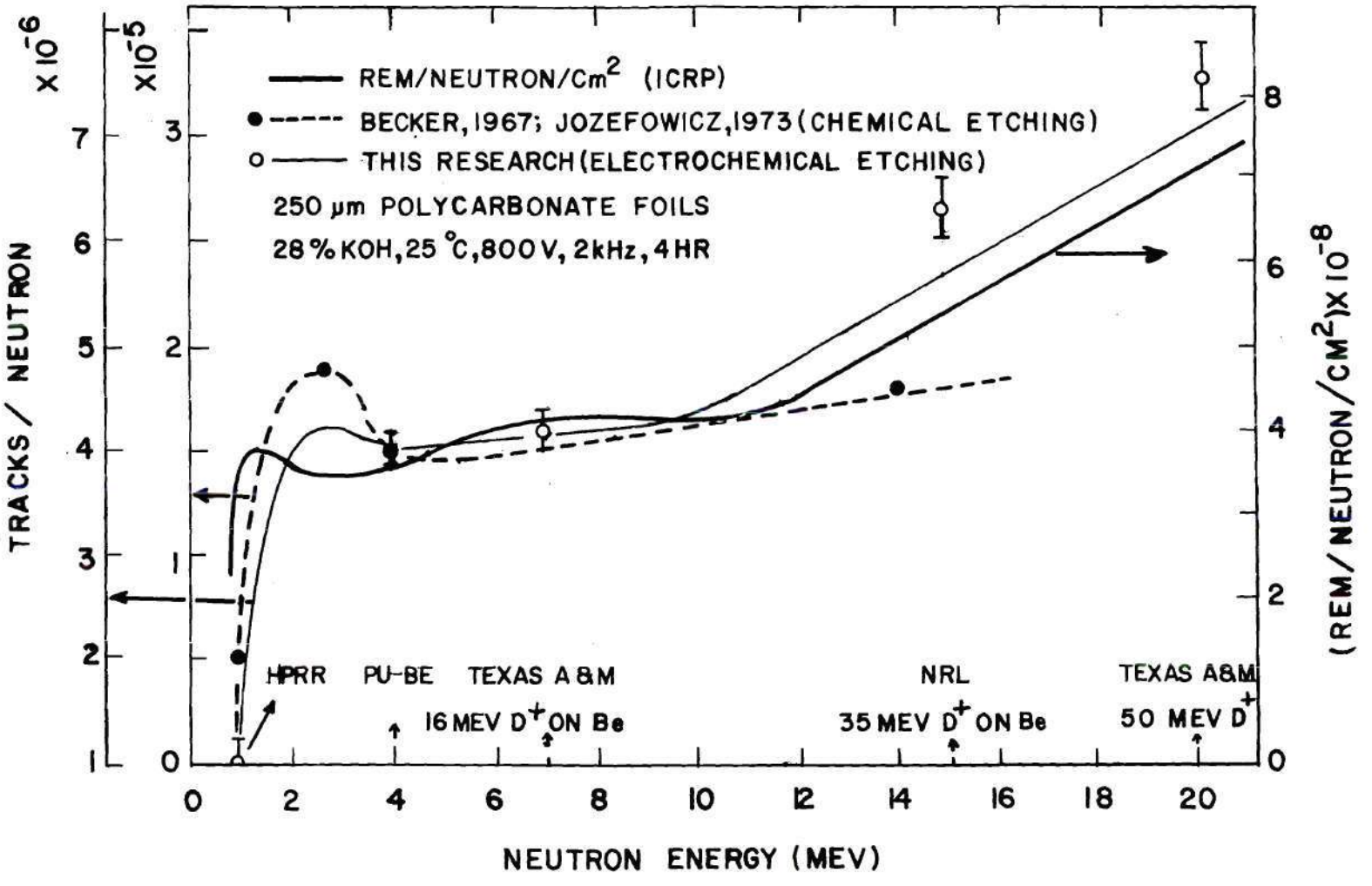

Figure 45. Neutron Sensitivity (tracks/n) as a Function of Neutron Energy Obtained in This Research in 250 μm Polycarbonate Foils (when electrochemically etched) Superimposed on Conventional Etching Data (dotted curve) Compared to ICRP Rem Curve (Becker, 1967; Jozefowicz, 1973; and this investigation)

percent KOH. The increased sensitivity is due to the appearance of more tracks from deeper layers.

The sensitivity response of recoil particle track registration follows approximately the rem response recommended by ICRP as stated by Becker (1967), even at the higher energies investigated in these studies. The sensitivity curve obtained by electrochemical etching in this research agrees well in the lower energy region with the other investigations but shows relatively higher sensitivity at higher energy where it matches the rem response. At the indicated etching conditions, a track density-to-rem conversion factor of 105 ± 7 tracks/cm^2·rem was obtained from about 1-20 MeV based on the data obtained from this study and shown in Figure 45. This factor can be increased by using other etchant concentrations or other alternatives.

Both theoretical and experimental results show a neutron threshold energy of about one MeV for fast-neutron-induced recoil particle track registration in polycarbonate when conventionally etched (Jozefowicz, 1971, 1973). This threshold can be concluded also from Figure 45. Part of the reason for this high energy threshold has been that proton tracks have been observed only in more sensitive polymers such as cellulose nitrate and cellulose acetate (Varnagy et al., 1971; Carpenter and LaFleur, 1972; Lück, 1974). In polycarbonate, only tracks due to recoil carbon and oxygen with a threshold energy corresponding to elastic scattering of neutrons of energy greater than one MeV have been observed. This threshold, however, depends on the etching method and the applied etching conditions. As previously stated, electrochemical etching relying on the conductive energy loss along the tracks behaves quite differently and

seems to amplify in polycarbonate tracks of carbon and oxygen of lower LET than those revealed by conventional etching methods and even proton tracks are revealed (Sohrabi and Morgan, 1975).

To investigate the possibility of proton track registration in polycarbonate, foils were irradiated by different broad beams of protons ranging from 100 to 900 keV in 100 keV intervals. Although the experiments were very crude, small tracks were observed spread over a large area in foil irradiated at 300 keV and higher. Figure 46 shows 500 keV proton tracks in 250 μm foils electrochemically etched in 28 percent KOH solution at 25°C applying 800 V at two kHz for four hours. There is a slight doubt about the mentioned proton threshold energies which needs to be clarified.

When urea pellets were used in contact with polycarbonate foils (as stated in Chapter IV) to produce protons under thermal neutron irradiation due to the $^{14}N(n,p)^{14}C$ reaction, clusters of tiny tracks were observed in certain spots only after foils were electrochemically etched under the mentioned etching conditions used above. Figure 47 shows clusters of expected 0.5 MeV proton tracks as well as a few scattered large tracks produced by fast neutrons. The small tracks as indicated on the figure were found only on the foil side facing the urea pellet. The larger tracks were found on both sides of the foils whether cadmium covered or not, while no small tracks of the above nature were found in cadmium covered foil combinations. The track density caused by fast neutrons under cadmium covered foils was found to be 105 tracks/cm^2·min corresponding to one rem/min of fast neutrons at the beam portal of the Biomedical Facility of the Georgia Tech Research Reactor while operating at one MW.

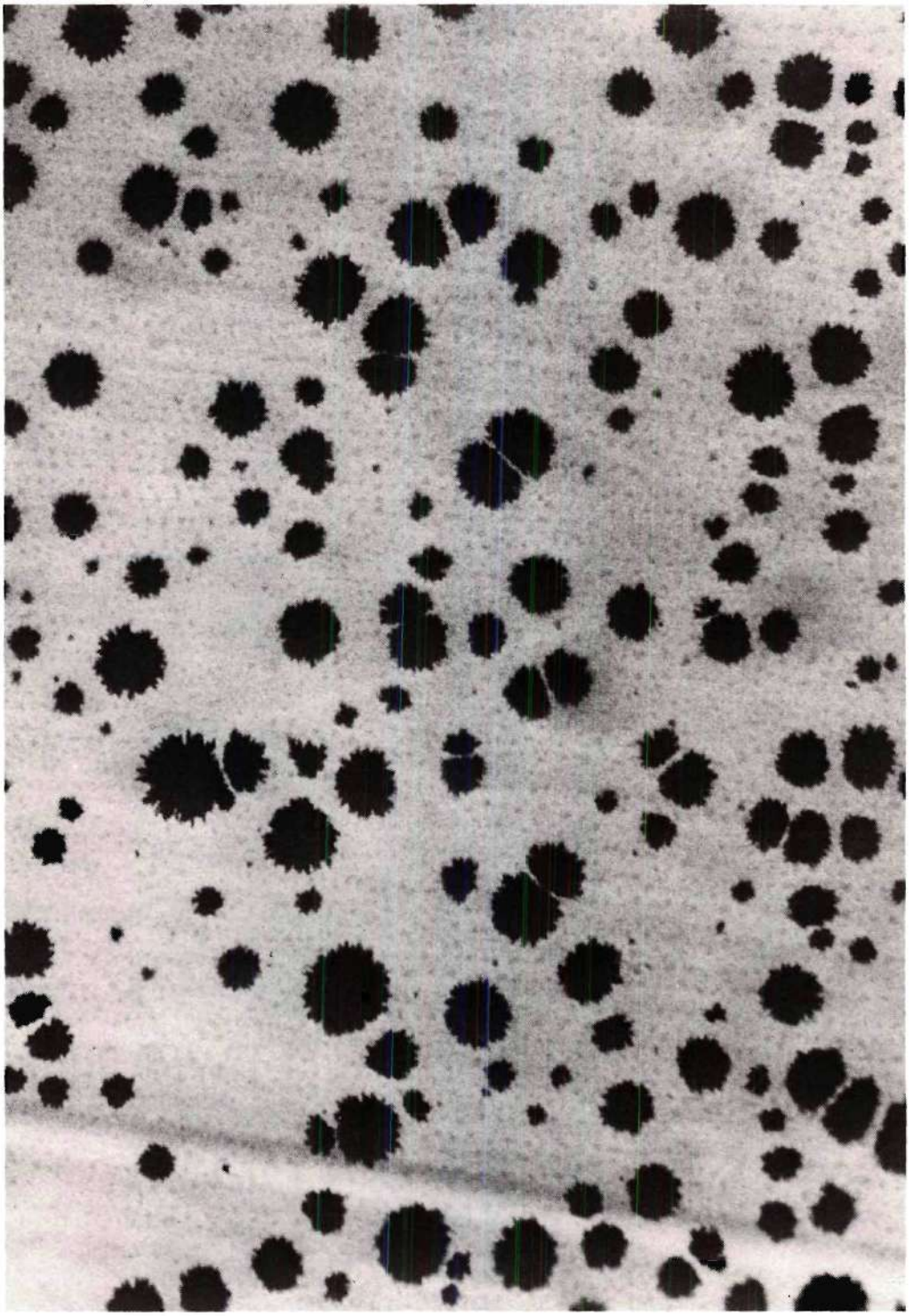

Figure 46. Tracks of 0.5 MeV Protons in 250 μm Polycarbonate Foils Etched in 28% KOH Solution at 25°C Applying 800 V at 2 kHz for 4 Hours

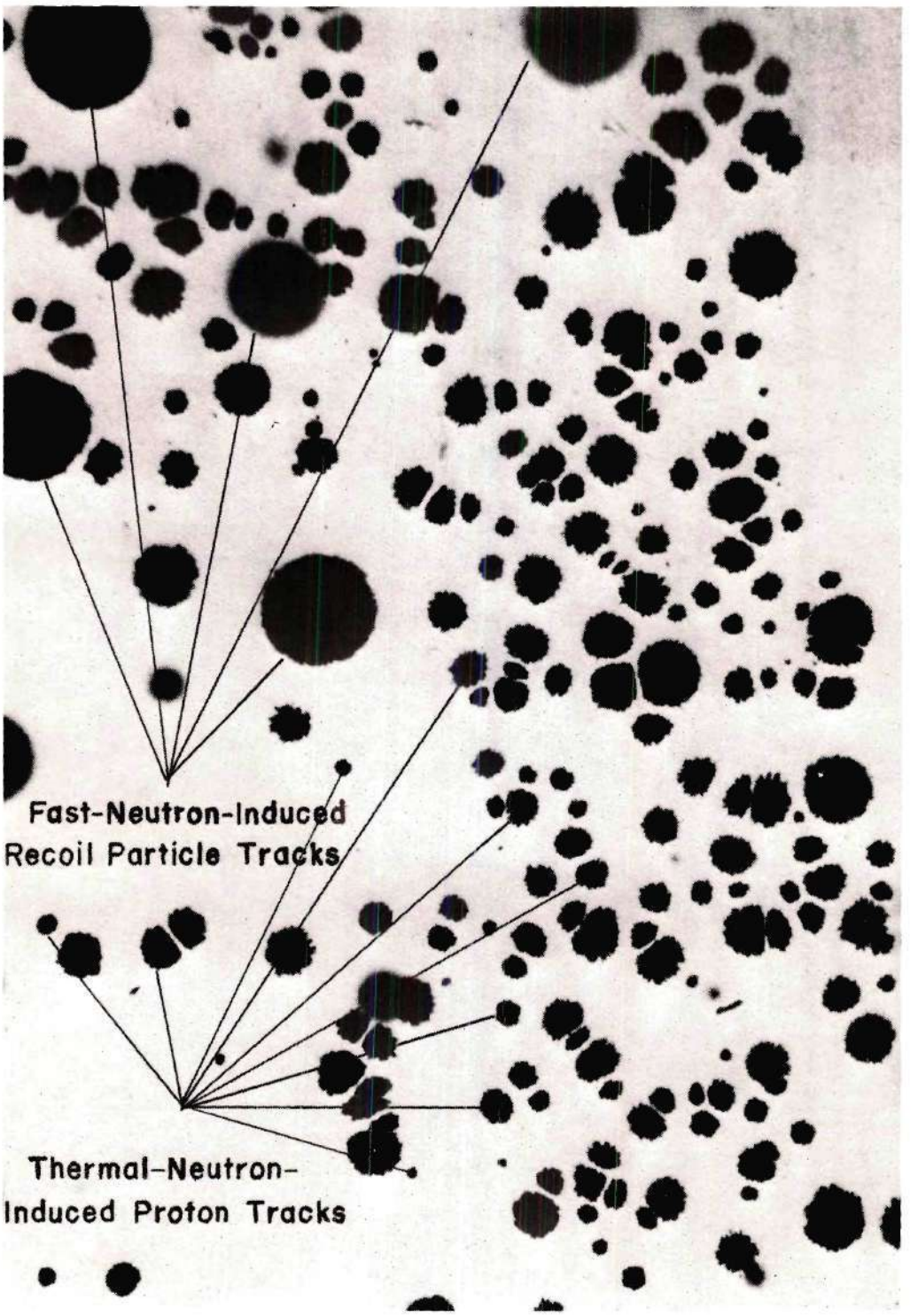

Figure 47. Tracks of 0.5 MeV Protons and Fast-Neutron-Induced Particles in 250 μm Polycarbonate Foils Etched in 28% KOH Solution at 25°C Applying 800 V at 2 kHz for 4 Hours

Further, very tiny tracks of protons were also observed under a light microscope in a red-dyed cellulose nitrate foil-urea combination when foils were etched conventionally in 28 percent NaOH at 25°C for 24 hours. Under these experimental conditions and the above mentioned observations, it may not be far from fact to expect that a portion of observed tracks is due to fast-neutron-induced recoil protons. More careful quantitative proton studies need to be performed to remove any doubt concerning registration of proton tracks and the threshold for their registration.

The size of tracks depends on type and energy of the incident charged particles, angle of incidence in the polymer, and the etching conditions applied. Since neutrons result in scattered recoil nuclei at preferred angles depending on the neutron energies, some investigations have been carried out to use this approach in obtaining an indication of the neutron spectrum (Tuyn, 1970). However, due to the small size of recoil tracks obtained by conventional etching the technique is very tedious for such an application. On the other hand, electrochemical etching, resulting in such large tracks, might make this technique much simpler. Figure 48 shows distributions of fast-neutron-induced recoil particle track diameters in polycarbonate for three different neutron spectra: a fission spectrum (HPRR), a Pu-Be spectrum, and a spectrum of neutrons produced by bombarding a Be target with 50 MeV d^+ ions. All data were obtained by visual measurements under a light microscope. Obviously, there are distinct differences in the distributions and the distributions are skewed more to the right as the neutron energy increases.

Pre-irradiations of unexposed foils to high doses of gamma rays from a ^{137}Cs source produced no increase in neutron sensitivity up to

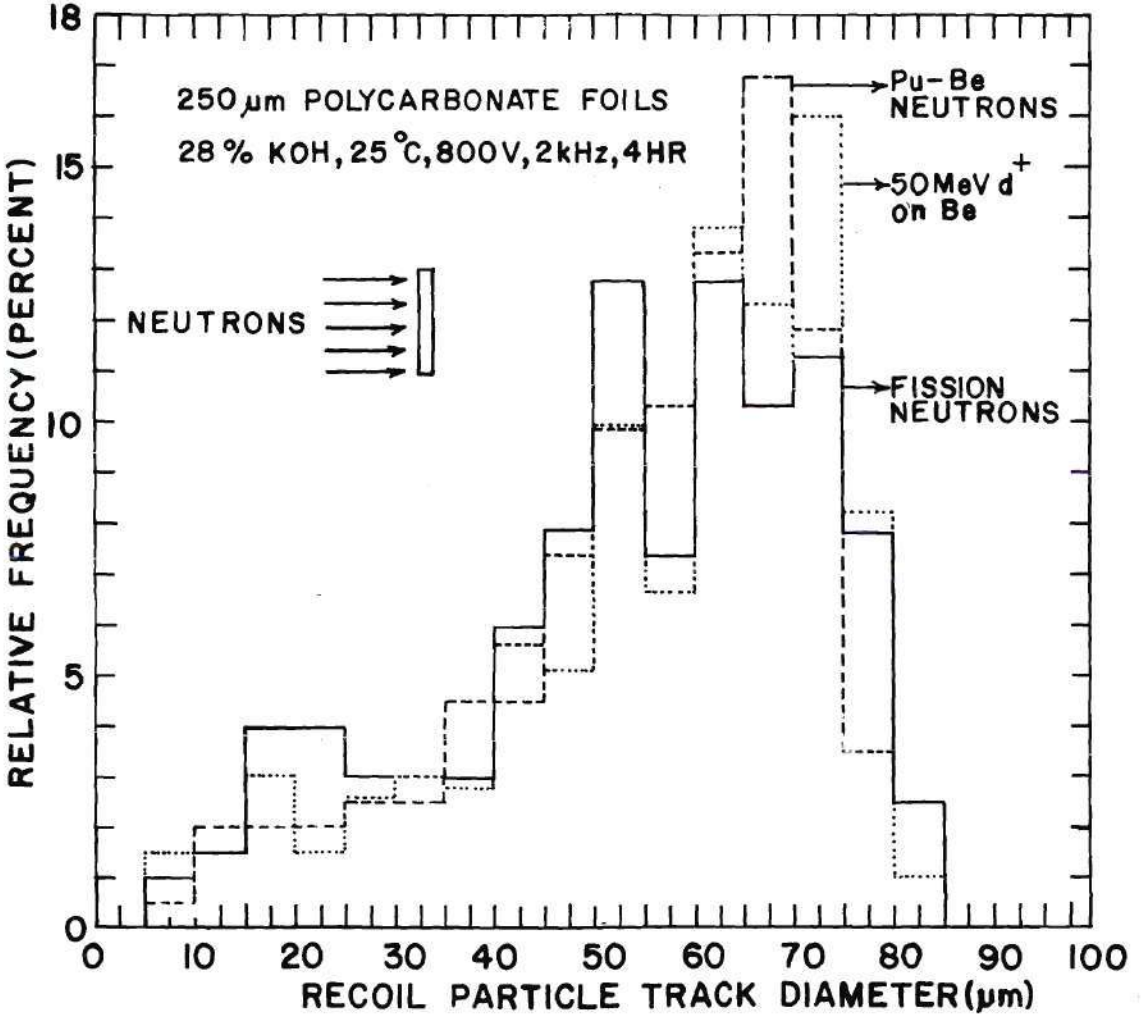

Figure 48. Fast-Neutron-Induced Recoil Particle Track Diameter Distributions in 250 μm Polycarbonate Foils Etched in 28% KOH Solution at 25°C Applying 800 V at 2 kHz for 4 Hours for Three Different Neutron Spectra

about 10^4 rads of gamma radiation after the foils were etched in a 28 percent KOH solution at 25°C applying 800 V at two kHz for four hours. Only a 25 percent increase in sensitivity was obtained for Pu-Be neutrons following gamma doses as high as six mrads. This increased sensitivity seems to be due to an increase in surface etching of polycarbonates. It appears that the electrochemical technique can be used for low fast neutron contamination measurements in the presence of high energy x-ray beams produced by medical betatrons and linear accelerators. This is an area of neutron dosimetry where the recoil particle track registration method appears to offer many advantages over other methods.

It was shown during this investigation that the neutron sensitivities are independent of the active area of the foils being etched. This result was obtained using 250 μm polycarbonate foils of 13 and 32 mm diameters. No difference was observed in the track densities in the two cases. This indicates that the reported data should be valid for foils having larger or smaller areas used in most of these experiments. Therefore, by using foils having larger areas better sensitivities can be obtained.

6.2 Fast Neutron Dosimetry in High Energy X-Ray Beams

Photoneutrons are produced whenever the photon energy exceeds a threshold value corresponding to the materials under irradiation such as target and collimator of medical betatrons and linear accelerators. Because neutrons are not effectively attenuated by shielding material provided for x-ray shielding and because of the higher biological effectiveness of fast neutrons, the measurement of this component of the high energy

photon beams is of some importance to prevent excessive irradiation of the patients under treatment and proper shielding of the radiotherapy rooms for the protection of employees. Therefore, fast neutron contamination measurement in high energy x-ray beams is of growing concern to medical physicists and companies supplying such machines for radiotherapy applications. Furthermore, the neutron energy spectrum and its flux depend on the photon energy and upon target and collimator materials.

Several investigations have been carried out to obtain neutron energy spectrum, dose, or dose equivalent in the beam of such high energy photon beams (Briden and Ice, 1972; Axton and Bardell, 1972; Wilenzick et al., 1973; and others). The measurements have consisted of activation of indium foils in spheres of different radii to obtain the neutron energy spectrum and the dose in the beam. Also measurements have been made by using fission fragment registration methods or the silicon diode technique (see the above references). Fission fragment registration itself has some sensitivity to photofission for which correction should be made (Wilenzick et al., 1973). Activation detectors such as indium are post-irradiation time-dependent which makes dosimetry by mail impracticable. Recoil particle registration methods with characteristics mentioned in the previous section, however, do not suffer from this defect so they can be used conveniently in a mail service. Fast neutron dose equivalents in a number of units (Clinac-18, Allis-Chalmers 25 MeV betatron, and Brown Boveri 45 MeV betatron) were under investigation by this particle registration method. This investigation was carried out to study the response of this dosimetry system under conditions where the neutron energy spectrum may not be known exactly and a low neutron dose is to be measured in the

presence of high doses of x-rays. Therefore, some preliminary results on neutron dosimetry of the two mentioned betatrons were obtained and are reported here with the expectation of conducting a much more extensive study during the continuation of this study.

The measurements were made along the central axis of each beam at the patient position, at the target-to-skin distances, and for field areas as were shown in Table 5 (Chapter IV). The polycarbonate foils of 250 μm thickness after irradiation to different doses in the beam were etched in 28 percent KOH solution at 25°C applying 800 V at two kHz for four hours. The track densities obtained were converted to rem by dividing them by the track density-to-rem conversion factor given in section 6.1. Figure 49 shows fast neutron dose equivalent (rem) as a function of high energy photon dose (rad) for a 25 MeV and a 45 MeV betatron as stated above. According to the data it can be concluded that the responses are linear functions of the photon dose strongly suggesting an insensitivity of the detection system to high doses of x-rays. It can be concluded also that for a patient treatment of 1000 rads of photons the ratios of fast neutron dose-equivalent to photon dose equivalent are 0.0066 and 0.0127 delivered along the central axis at TSD's of 100 and 110 cm, respectively, for the 25 and 45 MeV betatrons surveyed in this study. The measurement of the neutron contamination in these machines by other methods is under investigation and will be reported elsewhere (McGinley et al., 1976).

6.3 Neutron Depth Dose Studies

Experimental measurements and calculational treatments of neutron depth dose in homogeneous tissue media seem to have reached almost the

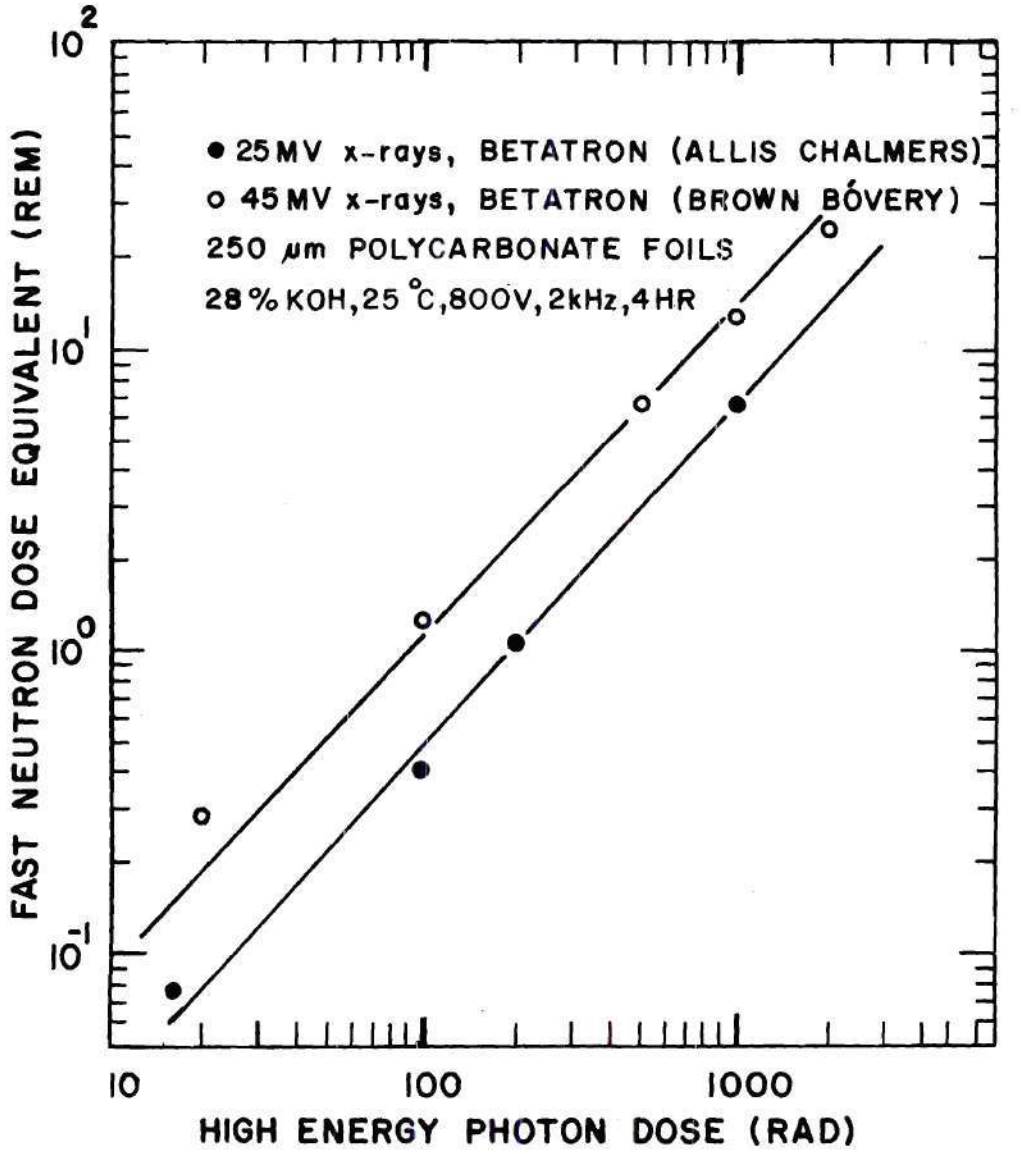

Figure 49. Fast Neutron Dose Equivalent as a Function of High Energy Photon Dose (rad) for 25 and 45 MeV Betatrons Obtained by Recoil Particle Track Registration in 250 μm Polycarbonate Foils (Measurements were made at the center of the primary beam at the patient position.)

level of saturation. Extensive calculational treatments of neutron depth dose by Snyder and Neufeld (1955); Auxier et al. (1968); Jones et al. (1971), and by many other investigators and experimental measurements employing various neutron beams and measurement conditions in terms of neutron energy, collimation arrangements, measurement methods, etc. (Mills and Hurst, 1954; Smith and Booth, 1962; Clifford, 1968; Lawson and Watt, 1964; Lawson et al., 1967; McGinley, 1971; Mijnheer et al., 1974; Hubbel et al., 1974; and others) have furnished much of the required information on homogeneous phantoms for neutron therapy and radiation protection purposes. Therefore, in recent years interest has shifted toward studying dose distribution in more realistic non-homogeneous phantoms, i.e. in media simulating the complexity and heterogeneity of a human body which is the object of interest in neutron therapy, human radiography, and radiation protection (Wilkie, 1971; Budinger et al., 1971; Bewley and Catterall, 1973). For example, presence of lungs has been shown to have a significant effect on neutron dose distribution (McGinley, 1971; Mijnheer et al., 1974). Presence of bone also causes deviations in neutron dose distribution. In particular, due to the presence of biologically important tissues in bone in terms of radiation damage, there has been a growing interest in performing neutron-depth dose distributions both by theoretical calculations (Lawson, 1967; ICRU, 1969; Prasad et al., 1971) and experimental measurements (Poston, 1971) at and near bone-tissue interfaces.

Lack of satisfactory localized experimental data at bone-tissue interfaces is due to poor spatial resolution of most dosimetry systems as was discussed in Chapter I. Extrapolation chambers are nearly ideal detectors for such conditions but are useful only in the hands of the

skilled researcher and require many adjustments and modifications if accurate data are to be obtained. Therefore, polymer track detectors provide some attractive features (as stated in Chapter I) for this type of application.

Before studying the distribution of dose near bone-tissue interfaces tissue-equivalent and bone-equivalent materials were investigated. Bone-equivalent plastic (B-100) has been an equivalent bone material used in many investigations both for construction of dosimeters and for incorporation into phantoms for studying heterogeneity due to the presence of bone imbedded in soft tissue (Poston, 1971; McGinley, 1971). In this material a high percentage of carbon has been incorporated to increase conductivity for construction of ionization chambers. Recently, a bone-equivalent liquid has been introduced for construction of bone structures in accordance with mathematical phantoms developed by Fisher and Snyder (1967). As tabulated in Table 3, Chapter IV, composition of this BE fluid matches closely the elemental content of the skeleton given by NCRP, No. 38 (1971). Therefore, it was of interest to us to verify experimentally neutron attenuation of BE plastic and BE fluid compared to TE fluid of Goodman (1969b) and to verify the possibility of using this fluid for bone-tissue interface studies. Furthermore, it seemed best to do this comparison along the central axis of an elliptical cylinder according to arrangements discussed previously in section 4.6.2.

Figure 50 shows percent recoil particle tracks as a function of depth in the three mentioned media, i.e. TE fluid, BE fluid and BE plastic, as obtained along the central axis of an elliptical cylinder exposed to HPRR fission neutrons. The fission neutron attenuation of the two BE

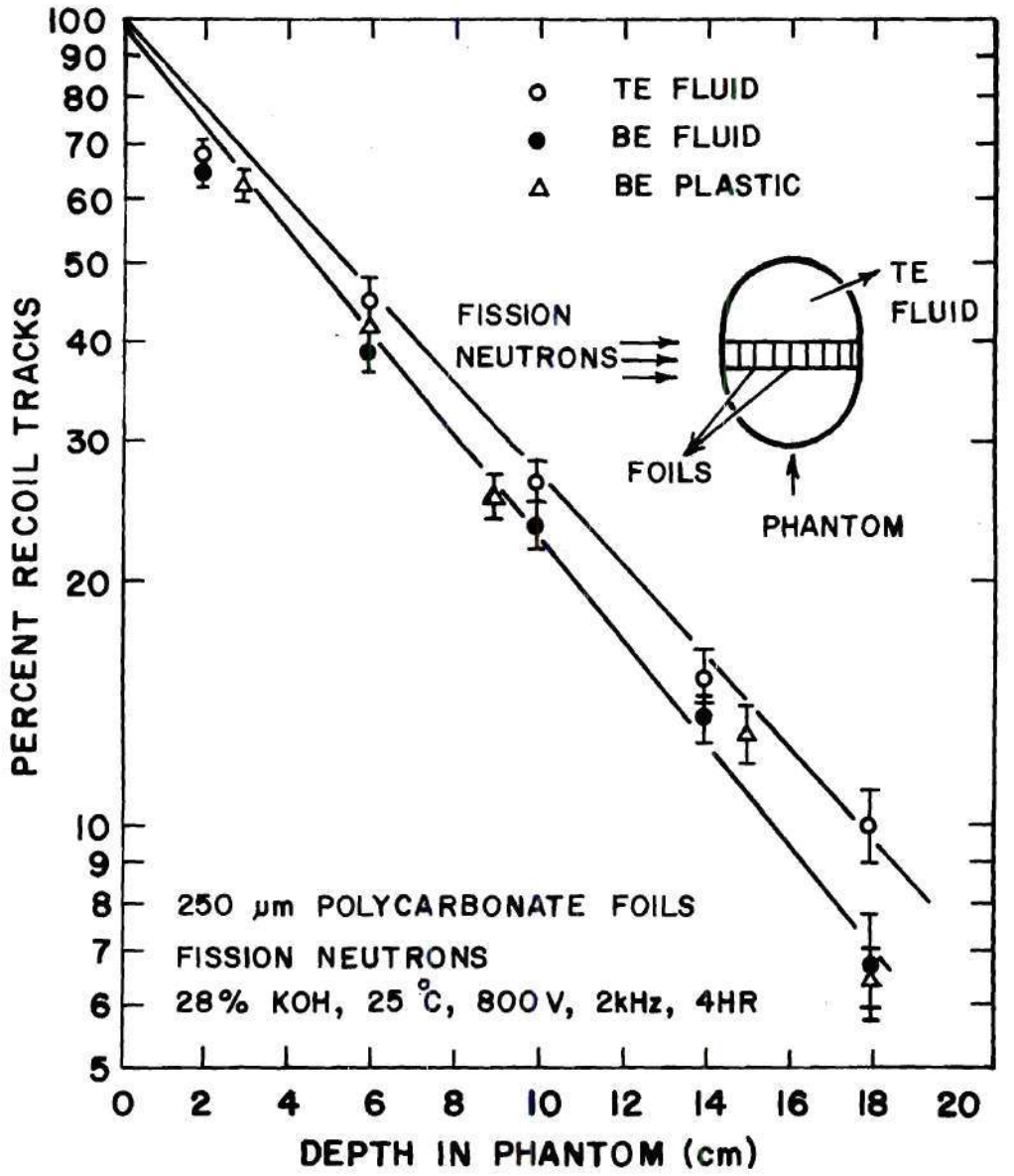

Figure 50. Percent Recoil Tracks as a Function of Depth in an Elliptical Phantom in Tissue- and Bone-Equivalent Materials for Fission Neutrons Using 250 μm Polycarbonate Foils

materials, $\mu \simeq 0.13\ cm^{-1}$, was more pronounced than in the TE fluid, $\mu \simeq 0.148\ cm^{-1}$. The responses in the two BE fluids matched perfectly well for this neutron spectrum. A similar comparison was made for higher energy neutrons ($\bar{E}$ = 15 MeV) using an extrapolation ionization chamber and a similar conclusion was obtained (McGinley and McLaren, 1976).

For bone-tissue and air-tissue interface studies the cubical phantom discussed in Chapter IV was used. It was constructed so that the central tube could be used to incorporate BE materials in TE fluid according to the procedure described before. Polycarbonate foils incorporated into the cylinder were supported parallel to each other and 250 μm apart so that the gap between could be filled by TE or BE fluid. Unlike most detectors, these sample holders could be placed right at the interface under study. Experiments were carried out for HPRR fission neutrons and a Pu-Be source. The source and phantom arrangements were discussed in Chapter IV. Some experimental results on these sources are given in the following.

Generally, all experimental and theoretical data available relative to the bone-tissue interfaces indicate that the neutron dose delivered to bone is lower than that to soft tissue because bone has a lower hydrogen concentration and hydrogen delivers a high percentage of the dose to these tissues. At the interface, the dose is higher on the tissue side than on the bone side and increases further when continuing beyond the interface into the tissue reaching a maximum as distance from the interface increases. The exact location of this maximum and its value depend on the neutron energy under consideration. The most relevant available data on these distributions are those of Poston (1971) carried out for

the HPRR fission spectrum, 14 MeV neutrons, and some isotopic neutron sources using an extrapolation ionization chamber. Therefore, they were used as a source of comparison in this investigation. Theoretical calculations of Lawson (1967) and Prasad et al. (1971) were valuable also in this study.

For fission neutrons Poston (1971) drew the conclusion from data of Lawson (1967) that the location of the maximum dose in soft tissue is at 2.6 mm from the bone-tissue interface having a value of five to six percent higher than the value at the interface. Figure 51 shows percent recoil particle tracks as a function of depth in soft tissue away from the interface according to the arrangement shown on the figure. The BE plastic used in this investigation was four cm thick and was placed at a depth of five cm in the phantom forming a bone-tissue interface at nine cm depth. From these very preliminary results, it is not simple to draw a very meaningful conclusion; however, there seems to be a maximum at a depth of one to three mm in soft tissue with a value about 10 percent greater than the interface value. Results obtained at the air-tissue interface using the same beam showed a slight increase in percent recoil particle tracks with depth in soft tissue of the order of 10 percent. Confirming these values requires further investigation.

Figure 52 shows percent recoil particle tracks as a function of depth in tissue away from the bone-tissue interface for a Pu-Be neutron spectrum. The BE plastic used in this investigation was also four cm thick and was placed at a depth of two cm forming the interface at six cm of depth in the phantom. The average energy of the neutrons is about 4.1 MeV and the maximum of the distribution is more pronounced in this

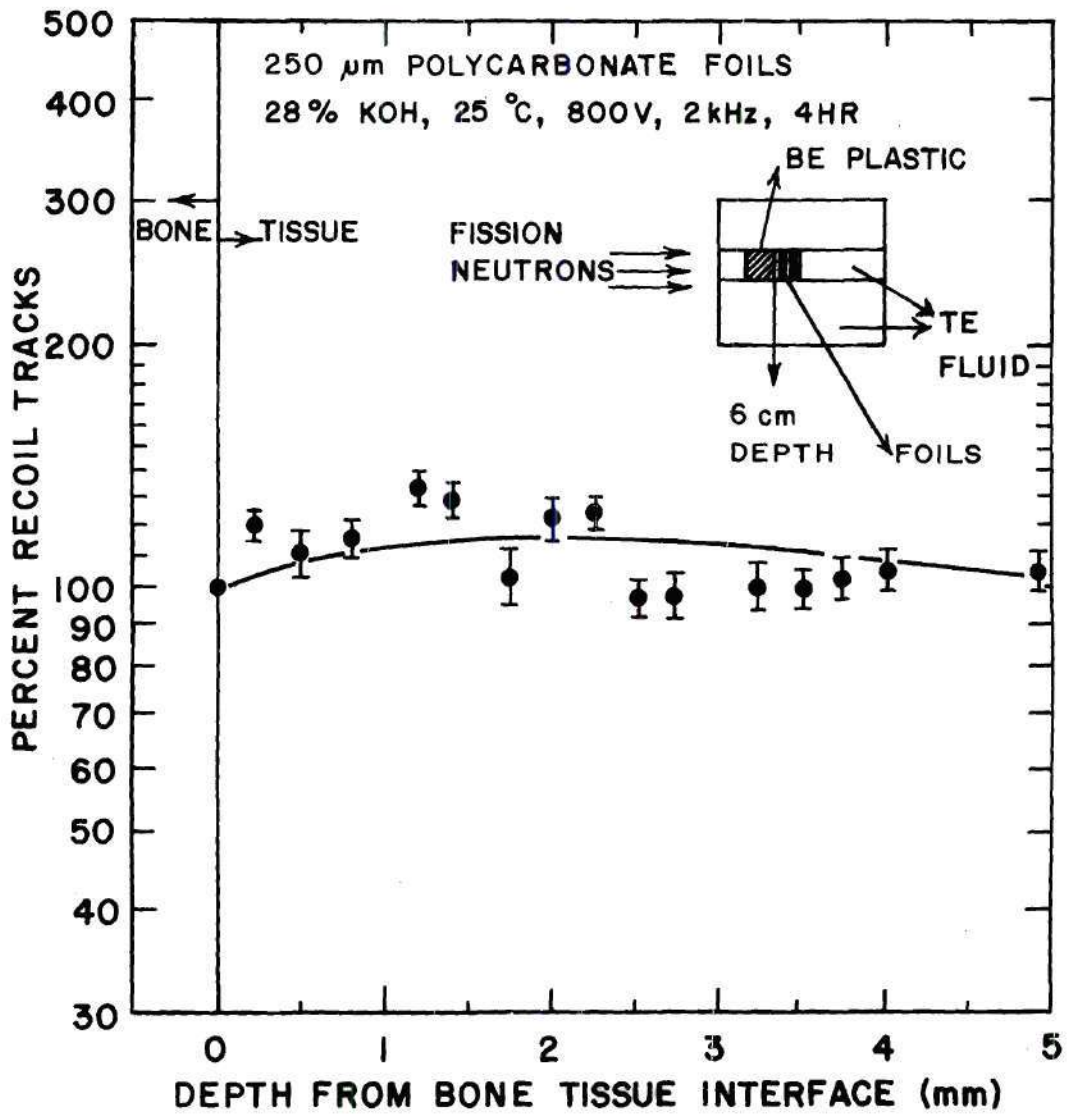

Figure 51. Percent Recoil Particle Tracks at a Bone-Tissue Interface for Fission Neutrons Using 250 μm Polycarbonate Foils

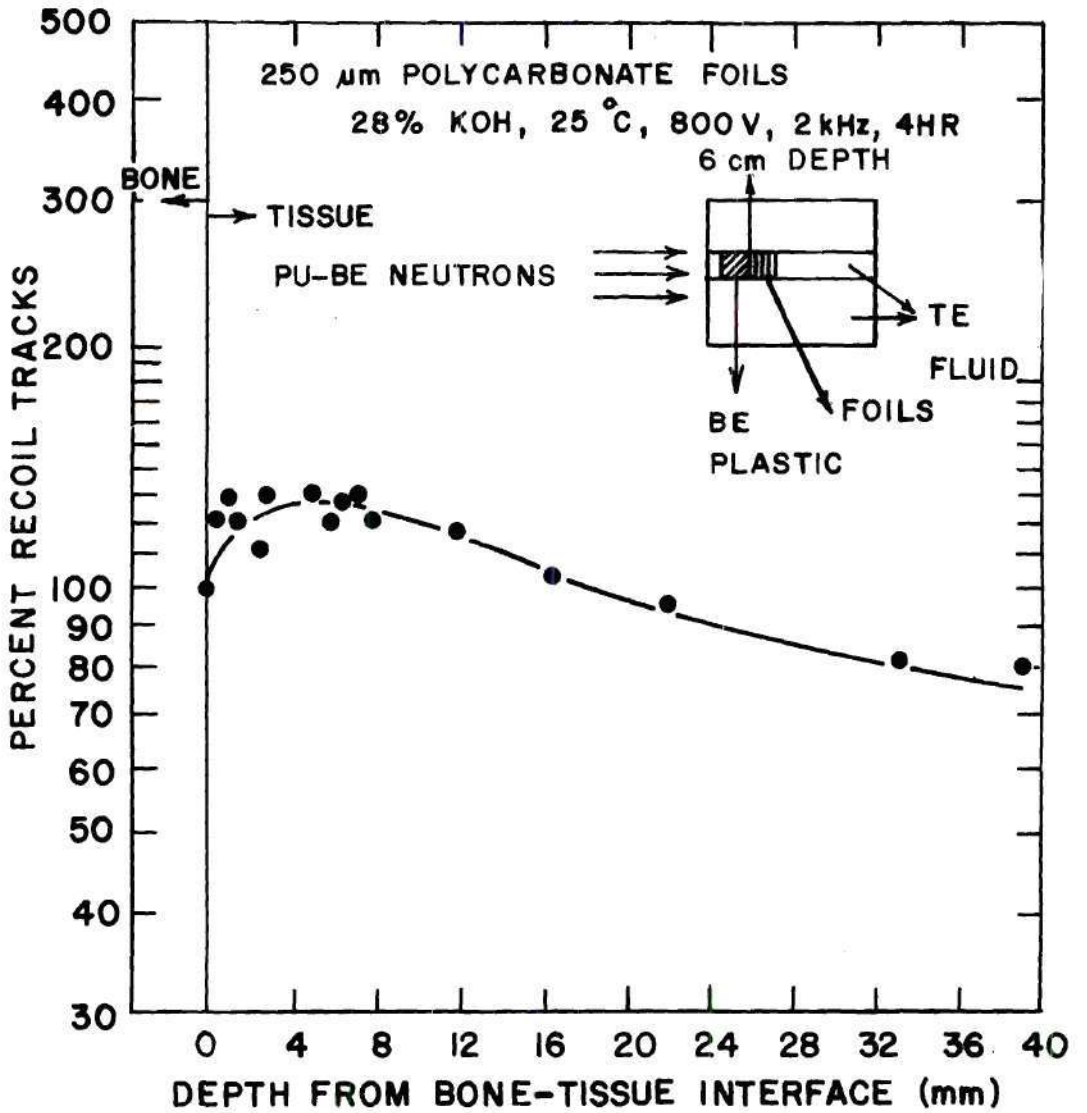

Figure 52. Percent Recoil Particle Tracks at a Bone-Tissue Interface for Pu-Be Neutrons Using 250 μm Polycarbonate Foils

case. The number of tracks at the maximum is about 25 ± 5 percent higher than at the interface; this maximum occurs at a depth of about four mm into the tissue and away from the bone-tissue interface. The general trend of this distribution is similar to that which Poston obtained for the same spectrum. However, the maximum value and location appear slightly different. Figure 53 shows percent recoil particle tracks as a function of depth in BE fluid placed in the same phantom at a depth of two cm. The BE fluid was contained in a sealed cylinder five cm in diameter and four cm long. The foils were placed in the BE fluid at different depths.

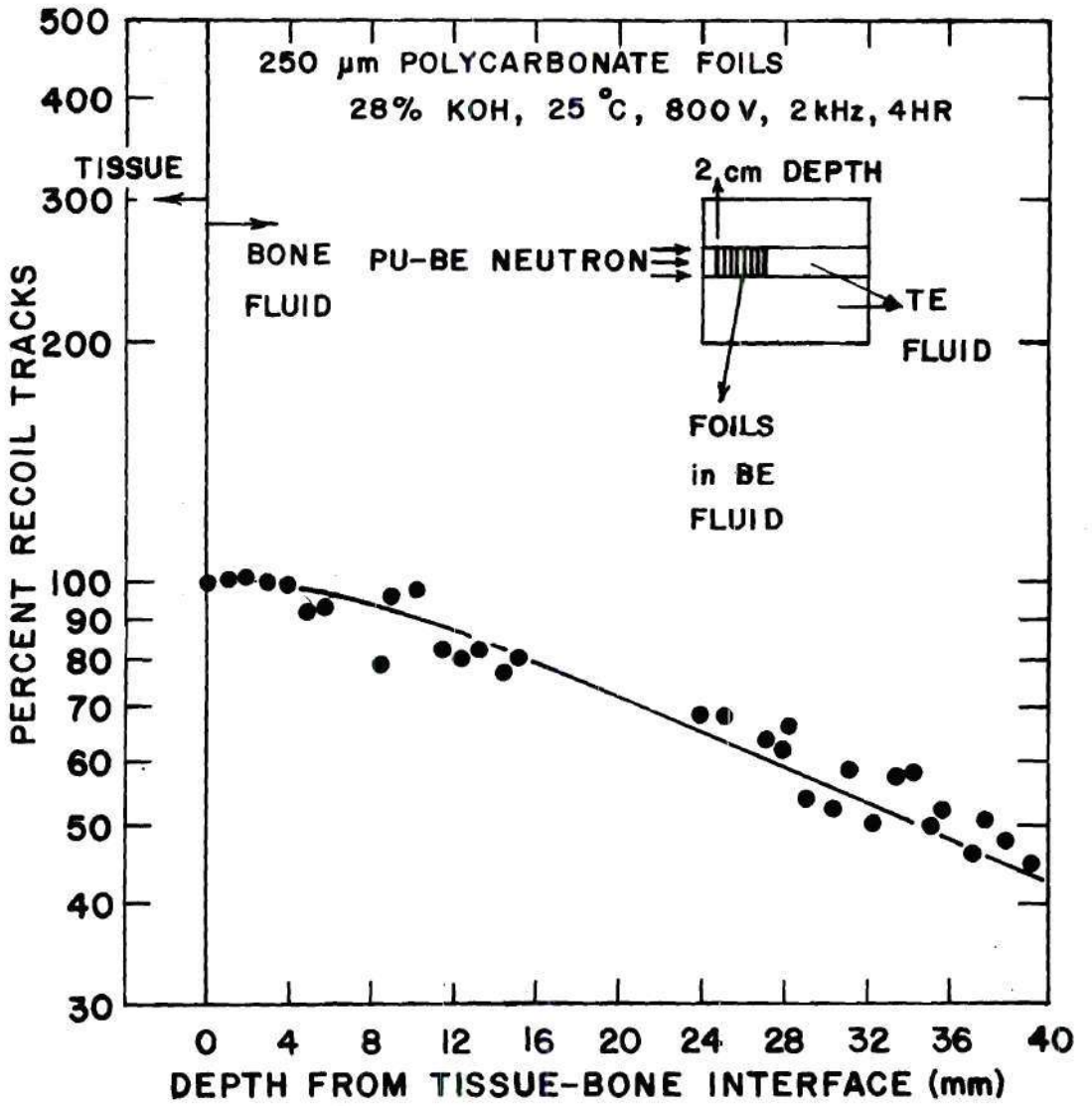

Figure 53. Percent Recoil Particle Tracks at a Tissue-Bone Interface for Pu-Be Spectrum Using 250 μm Polycarbonate Foils

CHAPTER VII

CONCLUSIONS AND RECOMMENDATIONS

7.1 Conclusions

Electrochemical etching amplification of fast-neutron-induced recoil particle tracks registered in polymers was investigated to obtain information on the physico-chemical characteristics of the technique controlling the amplification results and its feasibility for large-scale applications. The investigation included problems ranging from design and fabrication of an electrochemical etching system feasible for multiple-foil processing to studying electrochemical etching parameters controlling the etching results, and finally to the application of the developed dosimeters to fast neutron personnel dosimetry, fast neutron dose measurements in high energy x-ray beams, and a study of neutron dose at biological interfaces.

Electrochemical etching systems were designed and constructed to have the capacity of simultaneous multi-foil processing. They were successfully tested and improvements were made during the course of this investigation in terms of the etching chamber and the high voltage system.

Two high voltage systems were developed that would supply the necessary voltage, frequency, and power capacity and each was found to give completely satisfactory results. It can be concluded from these studies that such a technique can be easily adapted to process a large number of foils simultaneously. This finding should be of immediate interest to

many laboratories and companies supplying neutron personnel monitoring services.

Electrochemical etching parameters affecting the etching results were studied in considerable detail for the amplification of fast-neutron-induced recoil particle tracks in polymers. In particular, it was found that the recoil tracks in polycarbonate foils can be amplified with sharp contrast against background so that each single track can be observed easily with the unaided eye. This amplification was sufficient that one can easily sort a number of foils according to the neutron dose they received, ranging from one mrad to 1000 rad or higher. Lexan polycarbonate was chosen as the material of interest for the present investigation and to study parameters affecting the sensitivity (tracks/n·rad) and track diameter because it excelled in desirable characteristics for dosimetric applications.

The effectiveness of electrochemical etching in terms of maximum sensitivity and minimum etching time was found to be highest in the thinner foils. As foil thickness increases, sensitivity decreases and the time for optimum etching increases significantly. In thick foils (e.g. 500 μm), the electrochemical etching is practically ineffective in the present electrochemical etching system regardless of the voltage and frequency applied across the chamber, i.e. only a few tracks were developed in 500 μm foils.

In general, increasing etching time in a foil of a certain thickness, when other parameters were kept constant, increased the track density which eventually reached a plateau. This plateau seems to be different from the one obtained when conventional etching techniques are applied.

In conventional etching (usually in 28 percent KOH solution at 60°) extended etching leads to a plateau where equilibrium exists between the appearance of the new etched tracks from deeper layers and disappearance of the overetched tracks near the surface. However, in electrochemical etching (for example, when 250 μm polycarbonate foils were etched in 28 percent KOH solution at 25°C applying 800 V at two kHz for four hours), it was found that general surface etching is low so that only tracks on the surfaces of the foils are amplified. Therefore, at first those tracks due to highest LET recoil particles amplified followed by gradual appearance of tracks of lower LET recoil particles reaching a point where all the tracks from the surface have been amplified; then a plateau is obtained. Measured mean track diameters were generally linear functions of etching time for electrochemical etching with different foil thicknesses and for different etching conditions that were applied.

Applied voltage has a distinct effect on the etching results. As it increases the sensitivity (tracks/cm^2·rad) and mean track diameter increase reaching a semi-plateau above 600-700 volts. Thereafter, above this voltage, small variations in the applied voltage do not cause any significant effect on the etching results. Sensitivity and track diameter both increased in the same fashion as a function of the applied voltage. The sensitivity and mean track diameter were complex functions of the frequency of the applied voltage. They formed bell-shaped curves with their maximum at about two kHz. The general shape of the curves was found to be independent of the two power supply systems applied and independent of the foil thickness. However, the response with frequency for 375 μm polycarbonate foils seemed much sharper than for 250 μm foils and slight dif-

ferences were obtained in foils having the same thickness but originating from different manufacturers. Therefore, for all practical purposes, regardless of the foil thickness applied, two kHz was chosen as the optimum frequency.

Etchant concentration was found to have a very distinct effect on the etching results. The effects of NaOH and KOH solutions used as etchants were compared as functions of etching time. For equal concentrations (28 percent by weight), KOH was more effective at a shorter etching time. However, in terms of sensitivity they both reach approximately the same level after an optimum etching time characteristic of the etching solutions. On the other hand, there was a distinct difference between mean track diameters as a function of etching time with potassium hydroxide showing much larger mean track diameters at shorter time periods. The effect of concentration of etchant was studied and it was found that the sensitivity can be considered approximately a linear function of etchant concentration. However, mean track diameter is a complex function and appears to have a cyclic variation with the concentration. Also, appearance and shape of the tracks are different for various concentrations.

The effect of increasing etchant temperature is to reduce the time to amplify the tracks. However, in terms of increased sensitivity, at least under the conditions applied in these studies, no significantly better results were obtained above room temperature so most of the studies were carried out at 25°C. Higher temperatures add to the complexity of the etching system and require more carefully controlled etching conditions. Moreover, etching at 25°C provides convenience such as no requirement to heat the etchant and keep the evaporation low so that it can be

reused with reproducible results. However, if low etching times should be of considerable interest in routine applications, using thin foils (e.g. 125 μm) an optimized etching time of one to one and one-half hours provides good sensitivity (tracks/cm^2.rad).

Electrochemical etching results were found to be independent of the foil size used. Distance between the electrodes had no significant effect on sensitivity when other parameters were fixed. Only slight decrease in track diameter was observed as the distance between the electrodes increased. Therefore, the volume of the chamber could be minimized, i.e. use a chamber of short length to minimize the amount of etchant required. Also slight variations in the angle between the electrodes do not affect the reproducibility of the etching results; however, it is wise to keep the electrodes parallel to the plane of the foils. Due to our time restrictions, the effect of electrode sizes was not studied, but the size of the electrodes was kept the same as the area covered by the foils in order to obtain a uniform field across the foils.

It can be concluded from these experimental results that the applicability of this technique for large-scale uses is evident. The parameters affecting the etching results can be controlled easily and the effectiveness of the technique is far superior to conventional etching methods. The optimized etching conditions for most of the dosimetric applications which follow are using 125 or 250 μm polycarbonate foils etched in 28 or 45 percent KOH solutions at 25°C applying 800 V at two kHz for an etching time which depends on the foil thickness. As previously stated, sensitivity increases with etching time reaching a plateau which in this case corresponds to the appearance of all surface tracks. Operation of the

etching on this plateau makes the sensitivity relatively independent of the etching time. However, track diameter continues to increase linearly with etching time in this plateau region so that if track evaluation methods (such as optical densitometry) are being applied, the etching time must be carefully controlled. It should be further mentioned that the applied electrochemical conditions are not necessarily the ultimate choice of parameters for these may vary according to the application and type of output information required.

One of the main objectives of applying such advanced and elaborate etching methods was amplification of fast-neutron-induced recoil particle tracks in the hope of overcoming some of the shortcomings of recoil particle track etching using conventional methods. One of the most important shortcomings that we overcame was the small size of the tracks which had made track density evaluation methods difficult and neutron detection at low neutron fluxes impractical. Furthermore, the results were compared to existing data on the fission fragment registration methods using the spark counting technique and our results revealed that this method provides many advantages over fission fragment registration which is in the process of being used in many laboratories for their routine personnel monitoring as a replacement for the unsatisfactory NTA film method.

Some advantages of fast-neutron-induced recoil particle track amplification in polymers, in particular Lexan polycarbonate by electrochemical etching, for fast neutron dosimetry and personnel monitoring include the following:

1. The detector is fast neutron sensitive and insensitive to high doses of x, beta, and gamma radiation (e.g. insensitive up to 10^4 rads).

Therefore, the detector can be used even for fast neutron contamination measurements in high energy x-ray beams produced by betatrons and linear accelerators.

2. A wide dose range can be covered from 0.001 to 1000 rads or higher provided that freshly prepared polycarbonate foils are used in the low dose range.

3. Track density evaluation can be carried out easily by microscopic counting, projection methods (for example, on a microfilm screen), optical densitometry, etc. Furthermore, if large areas (e.g. two cm^2 or larger if desired) are scanned, extremely high sensitivity can be obtained.

4. Polycarbonate is a hard and usually homogeneous material thus providing good reproducibility in the measurements.

5. Polycarbonate with excellent latent track stability is suitable for long term integral dose measurements.

6. High quality polycarbonate sheets are commercially available in different thicknesses at reasonably low cost so that the cost per foil is nil, thus two or more foils can be incorporated in a badge to improve the statistics.

7. There is no need for fissionable materials such as ^{232}Th or ^{237}Np.

8. The sensitivity of the technique is comparable to the fission fragment registration technique and was found to be even equal to that of ^{237}Np on 10 μm polycarbonates.

9. There is no need for darkroom processing as is required under nuclear track emulsion processing. (However, it requires electrochemical processing.)

10. The dosimeters are small, rugged, and inexpensive which together with the no fading of tracks make dosimetry intercomparisons by mail both practicable and desirable.

11. The sensitivity (tracks/n) as a function of neutron energy was found to follow the ICRP rem curve.

The principal characteristic of this foil dosimeter system which might lower the accuracy of the neutron dose measurement appears to be directional dependence of recoil particle track registration. Unfortunately, this seems to be a fault which is common to some extent in all personnel monitoring systems. The directional dependence is not much greater (if any) than that observed in the NTA film system and the fission fragment registration methods show some directional dependence. However, in the recoil particle registration approach this directional dependence can be corrected or compensated by many means such as rolling the foils around a Lucite tube or the use of a special calibration procedure.

The threshold neutron energy detected by recoil particle track registration using conventional etching techniques is one MeV according to the existing data. This energy threshold when using electrochemical etching appears to be lower than one MeV; however, further research is necessary to obtain the exact value.

Some preliminary results on the performance of the dosimetry system developed under this investigation were obtained. The dose equivalents of fast neutron contamination of two high energy x-ray beams from medical betatrons were measured and found to be in good agreement with other methods of measurement.

Because this system of dosimetry offers exceptionally good spatial

resolution, it was used in some depth dose studies at bone-tissue interfaces. Comparisons were made also between the attenuation of neutrons in BE plastic and BE fluid. The results obtained for BE equivalent materials were in good agreement. The results of bone-tissue interface studies indicated a build up region to the rear of bone near the bone-tissue interface. This buildup was more pronounced in the case of neutrons from the Pu-Be source than for fission neutrons. It was concluded that the high spatial resolution of these dosimeters makes them ideal for this type of study.

7.2 Recommendations

While conducting this research and some concomitant studies, a number of related, new, and interesting ideas developed which deserve refinement and need to be further investigated. Additionally, these investigations would be consonant with the objectives of this research for the completion and improvement of this dosimetry technique as a standard method with high accuracy and precision for low neutron doses of interest.

In this study, electrochemical etching systems were constructed and applied for etching six foils simultaneously. However, for large-scale dosimetry etching systems to process simultaneously many more foils is necessary. The present study has shown the feasibility of a chamber for multi-foil processing. Such an electrochemical etching system is of interest not only for laboratory research but to vendors of film badge services, National Laboratories, and others concerned with large-scale dosimetry programs.

Studies of electrochemical etching parameters affecting the amplification of recoil tracks provided many interesting and in some cases

tantalizing observations. To answer these questions with more confirming confidence requires that additional detailed experiments be conducted. Furthermore, having 10 different parameters affecting the etching results allows many alternate approaches some of which are believed to lead to additional improvements.

Although the present study indicates the feasibility of this technique for immediate applications, background counts in some batch of polymers used will limit the accuracy of the method for low neutron dose measurements. Therefore, in this case methods must be developed to remove the background tracks before use or to purchase freshly prepared or especially treated foil materials. If the background tracks were removed or the polymer were completely free from the background tracks, then any single track caused by cosmic radiation or other low neutron dose (e.g. around nuclear facilities) could be detected with high accuracy and precision in the measurements.

Direct interaction of fast neutrons with polymers shows an inherent directional dependence as is the case with many other dosimeters. Fortunately this drawback in this case can be compensated by wrapping the foils around a Lucite bar or by the application of other approaches as mentioned in the text. Some improvements were obtained but further work ought to be carried out to optimize the size of the foils and the diameter of the Lucite tube to prevent any microscopic cracks in the foil. If such approaches are being applied in routine use, then a special badge should be designed for this configuration.

So far, there has been some question as to whether or not Lexan polycarbonate is sensitive to registration of proton tracks. It is

commonly believed that only carbon and oxygen recoils and alpha particles resulting from interaction of fast neutrons are recorded. There is no question but that recoils causing damage density greater than a critical value are recorded and these correspond to a certain neutron energy. Both theory and experiment seem to provide a neutron energy threshold of one MeV. Based on some preliminary results obtained in this study, it is believed that even proton tracks can be registered in Lexan polycarbonate. Therefore, as a result of these studies, there remains little doubt that there is a neutron threshold energy lower than one MeV when electrochemical etching is applied. However, there is need of further experimental investigation because of immediate interest in employment of this technique to fast neutron personnel dosimetry and the desirability of this dosimetry having an energy threshold below one MeV.

Some preliminary results are given on the performance of the dosimeters developed in this research as applied in dose equivalent measurements of fast neutrons in high energy x-ray beams from medical betatrons and linear accelerators. More studies should be carried out in the distribution of the dose equivalent in and outside the mentioned beams.

Experiments were carried out to compare the performance of bone-equivalent plastic and liquid in the attenuation of neutrons in comparison with the attenuation in tissue-equivalent fluid in phantoms as a function of depth using fission neutrons. Such experiments should be carried out at high neutron energies of interest for neutron therapy. Further, calculational treatments should be carried out in the comparison of the two mentioned bone-equivalent materials, especially in the case of bone-equivalent fluid which shows good flexibility for more sophisticated

heterogeneity studies in phantoms as a replacement for human bone. Further experiments are recommended also at bone-tissue interfaces for 14 MeV neutrons and those produced by medical cyclotrons that are used for neutron therapy.

The above constitute only a few of the observed problems and areas where additional research is recommended. Some of these are under investigation in a renewal contract we have with the U.S. Energy Research and Development Administration and the results will be reported in the scientific literature.

APPENDIX A

VARIATIONS OF OPTICAL DENSITY WITH ETCHING TIME AND NEUTRON DOSE FOR DIFFERENT POLYCARBONATE THICKNESSES

Figures 54, 55, and 56 show optical density as a function of etching time in 125, 250, and 375 μm polycarbonate foils, respectively, exposed to various doses of fission neutrons and etched in 45 percent KOH solution at 25°C applying 800 V at two kHz. After the initial starting times, the optical densities are all linear functions of etching time and follow the same general trend. The optical densities obtained in each foil thickness exposed to the same neutron dose have approximately the same value. As was discussed in section 5.2, when foil thickness increases the sensitivity (tracks/n) decreases and mean track diameter increases so that these compensate for each other in the optical density measurements. Further, comparing these values to those shown in Figure 18 obtained for 125 μm thick foils etched in 28 percent KOH solution at 25°C applying 650 V at one kHz will show no distinct differences in terms of optical density for the different etching conditions applied.

Figures 57, 58, and 59 show optical density as a function of fission neutron dose in 125, 250, and 375 μm polycarbonate foils, respectively, etched for several etching times under the above mentioned etching conditions. These curves are not linear at the lower neutron doses. However, in certain thicknesses (Figure 58) linearity is obtained above 10 rads indicating that conditions can be adjusted to obtain such linearity.

Although this optical dosimetry approach by regular densitometers does not provide the most sensitive reading method, it provided enough sensitivity to optimize the parameters studied and could be used for large-scale dosimetry when there is interest only in the high dose range (e.g. above 10 rads). It also shows the feasibility of how best to control responses when other reading methods are applied.

Figure 60 shows variations of optical density in 250 μm polycarbonate foils with neutron doses for different applied voltages. A similar family of curves has been obtained by varying the etchant concentration, frequency, etc. Such conditions may be changed to obtain the desired response curve as a function of dose.

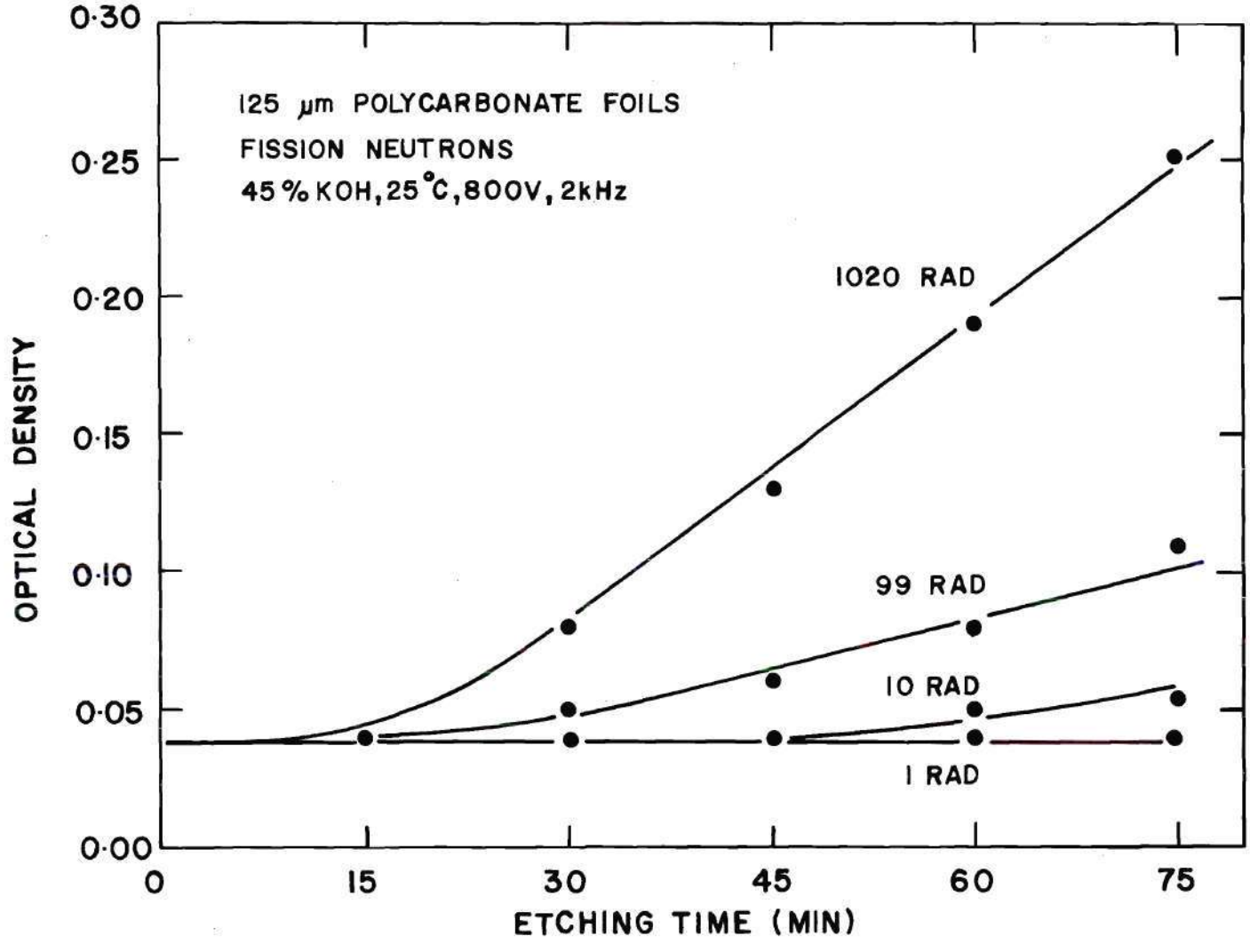

Figure 54. Optical Density as a Function of Etching Time in 125 μm Polycarbonate Foils Irradiated to Different Neutron Doses and Etched in 45% KOH Solution at 25°C Applying 800 V at 2 kHz

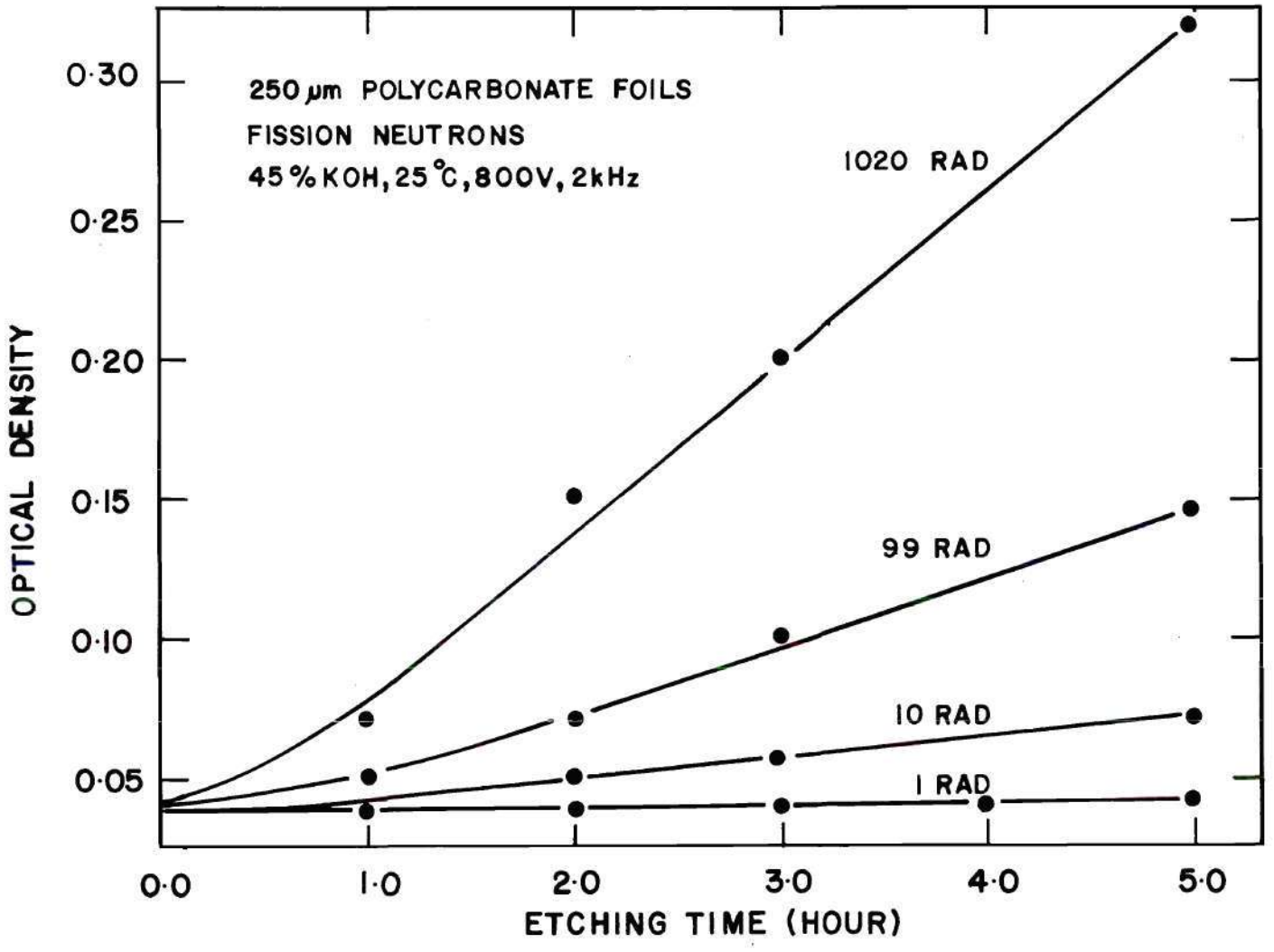

Figure 55. Optical Density as a Function of Etching Time in 250 μm Polycarbonate Foils Irradiated to Different Neutron Doses and Etched in 45% KOH Solution at 25°C Applying 800 V at 2 kHz

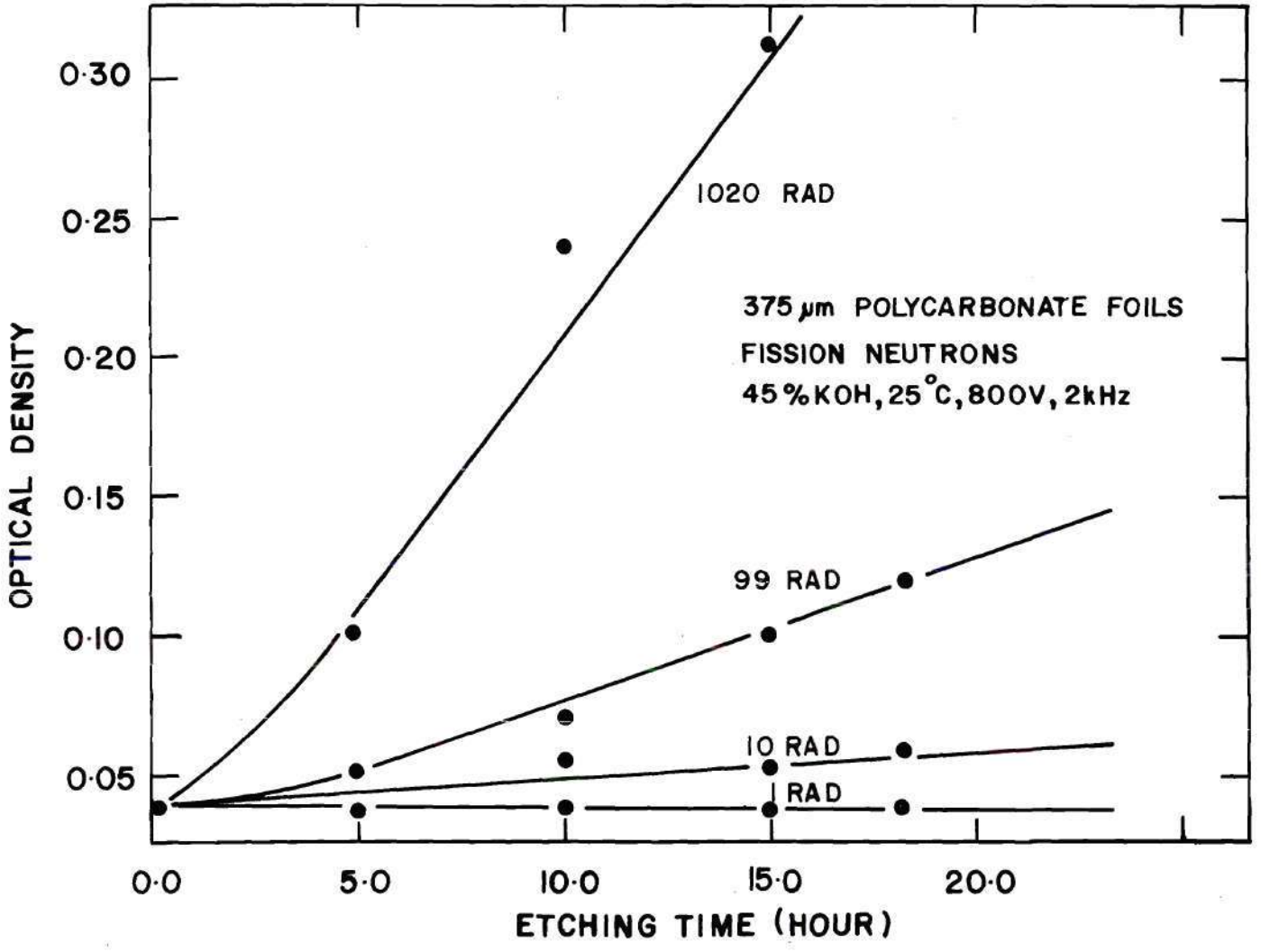

Figure 56. Optical Density as a Function of Etching Time in 375 μm Polycarbonate Foils Irradiated to Different Neutron Doses and Etched in 45% KOH Solution at 25°C Applying 800 V at 2 kHz

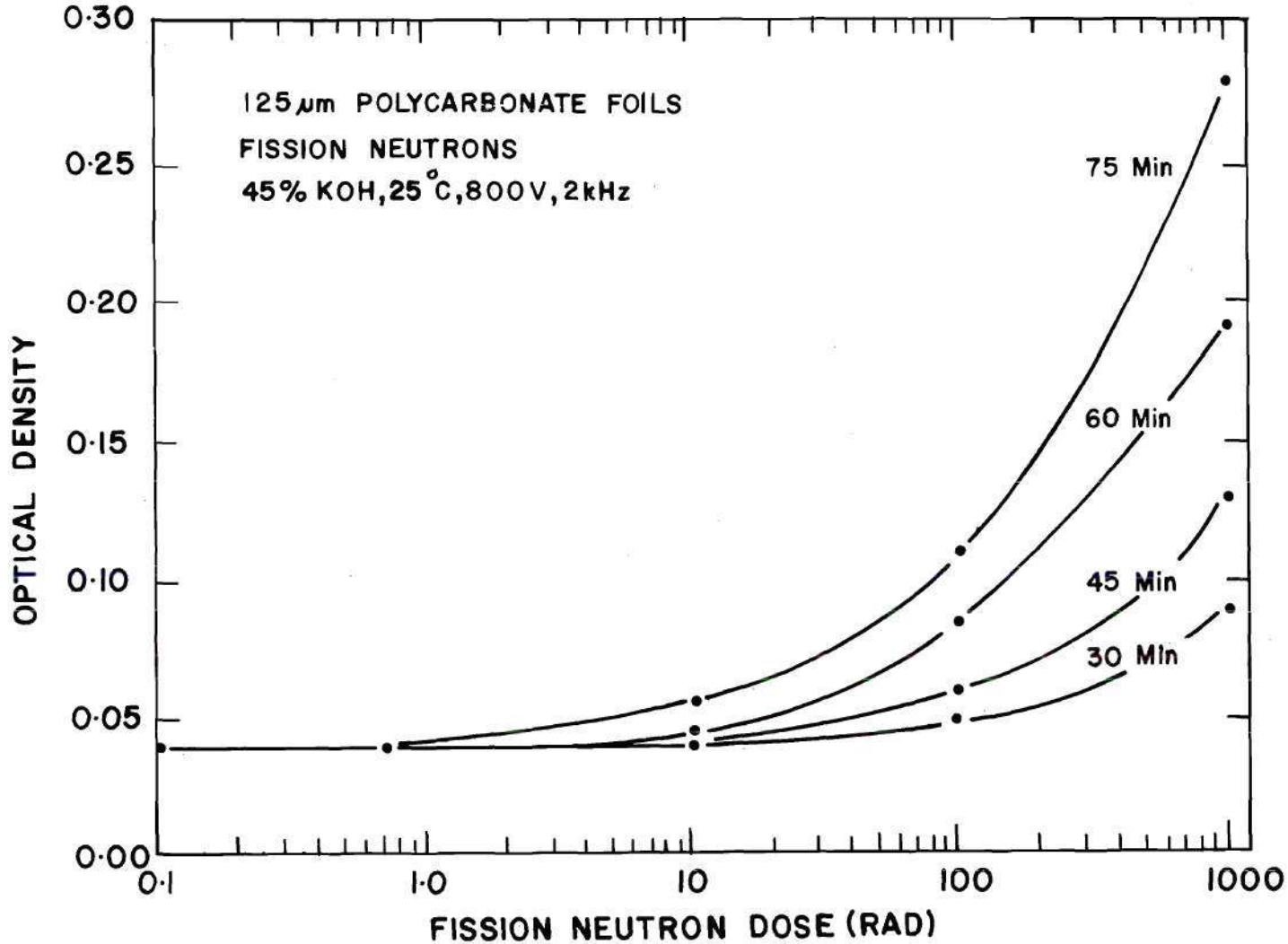

Figure 57. Optical Density as a Function of Fission Neutron Dose (rad) in 125 μm Polycarbonate Foils Etched in 45% KOH Solution at 25°C Applying 800 V at 2 kHz for Different Etching Times

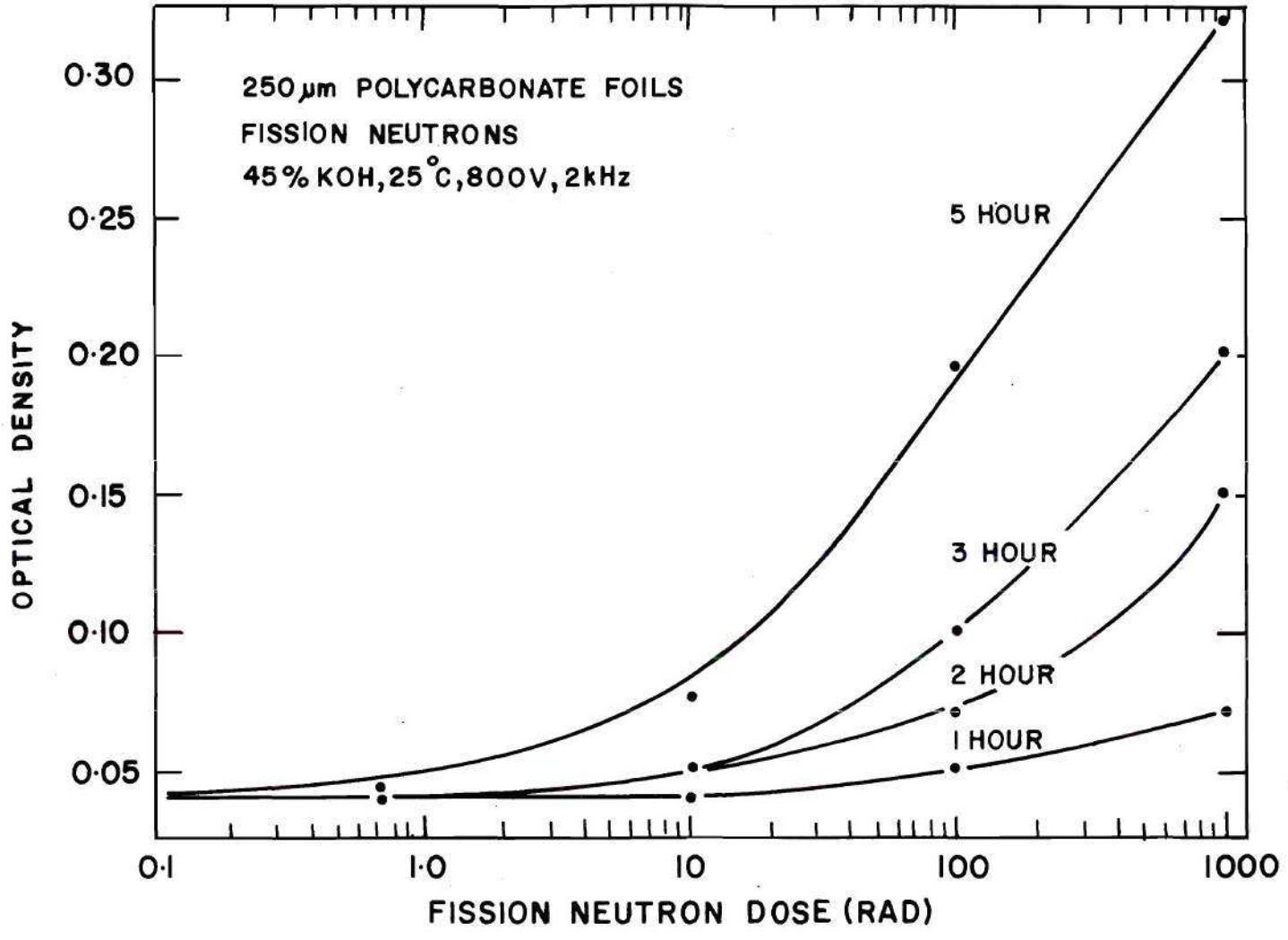

Figure 58. Optical Density as a Function of Fission Neutron Dose (rad) in 250 μm Polycarbonate Foils Etched in 45% KOH Solution at 25°C Applying 800 V at 2 kHz for Different Etching Times

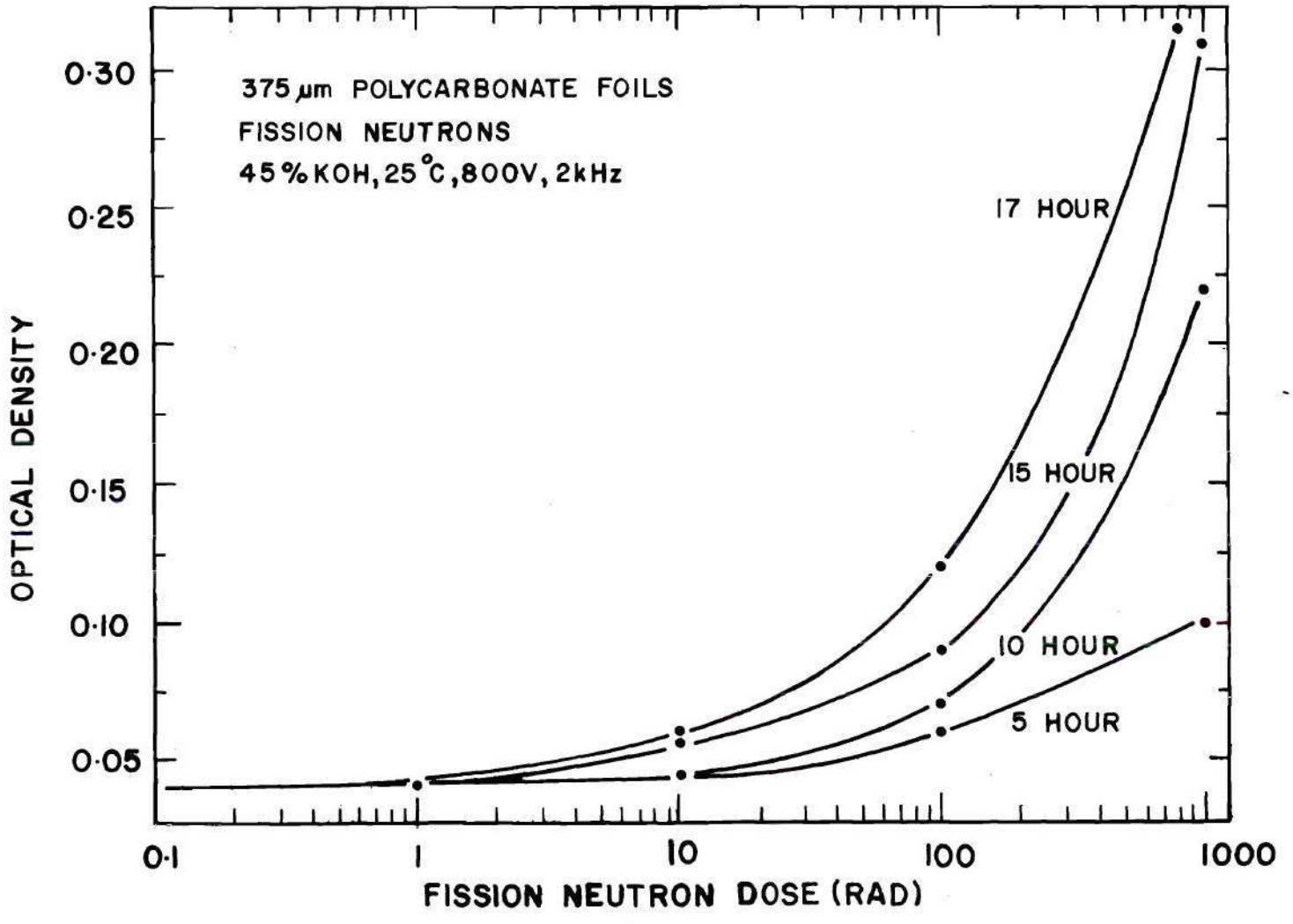

Figure 59. Optical Density as a Function of Fission Neutron Dose (rad) in 375 μm Polycarbonate Foils Etched in 45% KOH Solution at 25°C Applying 800 V at 2 kHz for Different Etching Times

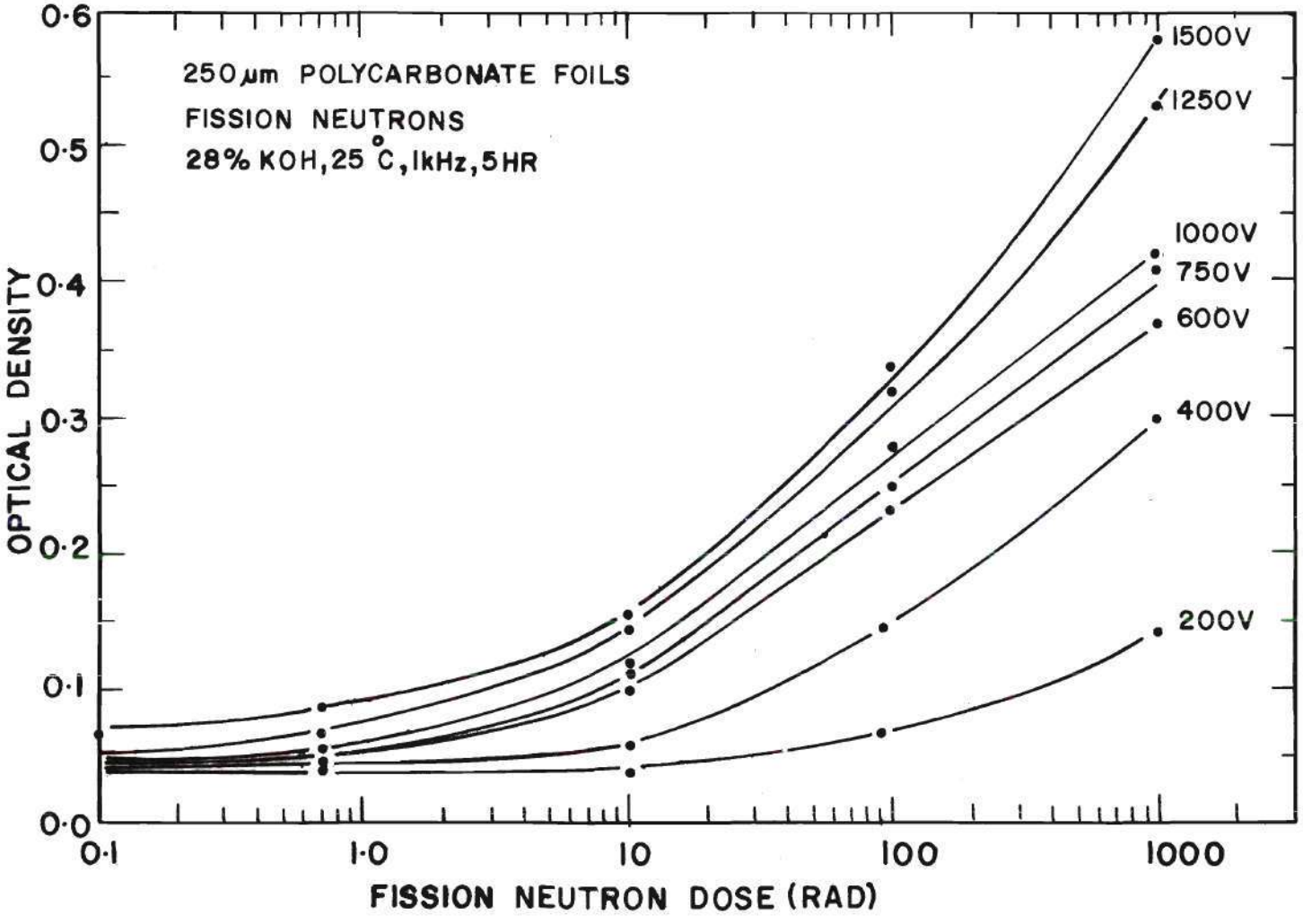

Figure 60. Optical Density as a Function of Fission Neutron Dose (rad) in 250 μm Polycarbonate Foils Etched in 45% KOH Solution at 25°C Applying Different Voltages at 1 kHz for 4 Hours

BIBLIOGRAPHY

Attix, F. H., Roesch, W. C., and Tochilin, E., Editors, Radiation Dosimetry, Vol. I, II, III; Academic Press, New York, 1966, 1968, 1969

Attix, F. H., Theus, R. B., Shapiro, P., Surratt, R. E., Nash, A. E., and Gorbics, S. G., "Neutron Beam Dosimetry at NRL," Phys. Med. Biol., 16, 4, 497 (1973).

Auxier, J. A., "The Health Physics Research Reactor," Health Physics, 11, 89 (1965).

Auxier, J. A., "Special Methods in Radiation Dosimetry," Chapter 7 in Principles of Radiation Protection, K. Z. Morgan and J. E. Turner, Editors; Robt. E. Krieger Publ. Co., Huntington, N. Y., reprinted 1973.

Auxier, J. A., Becker, K., Robinson, E. M., Johnson, D. R., Boyett, R. H., and Abner, C. H., "A New Radon Progeny Personnel Dosimeter," Health Physics, 21, 126 (1970).

Auxier, J. A., Snyder, W. S., and Jones, T. D., "Neutron Interactions and Penetrations in Tissue," Chapter 6 in Radiation Dosimetry, Vol. I, F. H. Attix, W. C. Roesch, and E. Tochilin, Editors; Academic Press, New York, 1968.

Axton, E. J. and Bardell, A. G., "Neutron Production from Electron Accelerators Used for Medical Purposes," Phys. Med. Biol., 17, 293 (1972).

Barr, T. A. and Hurst, G. S., "Fast Neutron Dose in a Large Tissue-Equivalent Phantom," Nucleonics, 12, 955 (1954).

Barbier, J., "Contrast Improvement of Image Obtained in Cellulose Nitrate Film by Track Etching Methods," Trans. ANS, 13, 530 (1970).

Becker, K., "Neutron Personnel Dosimetry by Non-photographic Nuclear Track Registration," Proc. ENEA Symp. Rad. Dose Measurements, Stockholm (1967).

Becker, K., "The Effect of Oxygen and Humidity on Charged Particle Registration in Organic Foils," Rad. Res., 56, 107 (1968).

Becker, K., "Alpha Particle Registration in Plastics and Its Applications for Radon, Thermal, and Fast Neutron Dosimetry," Health Physics, 16, 113 (1969a).

BIBLIOGRAPHY (Continued)

Becker, K., "Direct Fast Neutron Interactions with Polymers," ORNL-4446, p. 226, Oak Ridge National Laboratory (1969b).

Becker, K., "Dosimetric Applications of Track Etching," Chapter 2 in Topics in Radiation Dosimetry, Suppl. 1, F. H. Attix, Editor; Academic Press, New York, 1972.

Becker, K., Solid State Dosimetry, CRC Press, Cleveland, Ohio, 1973.

Becker, K., "A Simple Method for the Automatic Evaluation of Particle Tracks in Mica," Nucl. Inst. Methods, 126, 553 (1975).

Becker, K. and Abd-El Razek, M., "Automatic Spark Counting of Fast-Neutron-Induced Recoil-Particle Tracks in Polymer Foils," Nucl. Inst. Methods, 124, 557 (1975); see also ORNL-TM-4460 (1974).

Becker, K., Nagpal, J. S., Cheka, J. S., and Sohrabi, M., "Fading Characteristics of Various Film and Solid State Dosimeters in a Warm and Humid Climate," Paper 58, 17th Annual Meeting, Health Physics Society, Las Vegas (1972).

Benton, E. V., "A Study of Charged Particle Tracks in Cellulose Nitrate," USNRDL-TR-68-14 (1968).

Benton, E. V., "Method for Development of Volume Tracks in Dielectric Nuclear Track Recorders," Nucl. Inst. Methods, 92, 37 (1971).

Bewley, D. K., "Physical Characteristics of Fast Neutron Beams," Europ. J. Cancer, 7, 99 (1971).

Bewley, D. K. and Catterall, M., "Medical Radiography with Fast Neutrons," Brit. J. Radiol., 46, 24 (1973).

Bewley, D. K. and Parnell, C. J., "The Fast Neutron Beam from the MRC Cyclotron," Brit. J. Radiol., 42, 281 (1969).

Bichsel, H., "Charged Particle Interactions," Chapter 4 in Radiation Dosimetry, Vol. I, F. H. Attix, W. C. Roesch, and E. Tochilin, Editors; Academic Press, New York, 1968.

Blanford, G. E., Jr., Walker, R. M., and Wefel, J. P., "Track Etching Parameters for Plastics," Rad. Effects, 3, 267 (1970a).

Blanford, G. E., Jr., Walker, R. M., and Wefel, J. P., "Enhancement of Track Etching by a Spark Discharge," Rad. Effects, 3, 263 (1970b).

BIBLIOGRAPHY (Continued)

Blanc, D., Radioprotection, 5, 37 (1970).

Bleaney, Betty, "The Radiation Dose-Rates Near Bone Surfaces in Rabbits After Intraveneous or Intramuscular Injection of Pu-239," Brit. J. Radiol., 42, 51 (1969).

Block, J., Humphrey, J. S., and Nichols, J. E., "Hole Detection in Polymer Films and in Plastic Track Detectors," Rev. Sci. Insts., 40, 509 (1969).

Boot, S. J. and Dennis, J. A., "Flux Density Distributions in and Around a Man Sized Phantom Irradiated with Thermal Neutrons," Phys. Med. Biol., 13, 573 (1968).

Boyett, R. H., Johnson, D. R., and Becker, K., "Some Studies on the Chemical Damage Mechanisms Along Charged-Particle Tracks in Polymers," Rad. Res., 42, 1 (1970).

Bramlett, R. L., Ewing, R. I., and Bonner, T. W., "A New Type of Neutron Spectrometer," Nucl. Inst. Methods, 9, 1 (1960).

Brennan, J. T., Hendry, G. O., Herring, D. F., Hilton, J. H., Kim, J., and Quam, W. M., Correspondence, Brit. J. Radiol., 46, 233 (1973).

Briden, D. W. and Ice, R. D., "Neutron Measurements in Medical Betatron X-ray Beams," p. 124, 17th Annual Meeting, Health Physics Society, Las Vegas (1972).

Budinger, T. F., Phys. Med. Biol., 17, 303 (1972).

Budinger, T. F., Howerton, R. J., and Plechaty, E. F., "Neutron Radiography and Dosimetry in Human Beings: Theoretical Studies," Phys. Med. Biol., 16, 439 (1971).

Burlin, T. E., "Cavity Chamber Theory," Chapter 8 in Radiation Dosimetry, Vol. I, F. H. Attix, W. C. Roesch, and E. Tochilin, Editors; Academic Press, New York, 1968.

Burger, G., Grünauer, F., and Paretzke, H., "The Applicability of Track Detectors in Neutron Dosimetry," SM-143/17, Proc. IAEA Symp. on New Radiation Detectors (1970).

Carpenter, B. S. and LaFleur, P. D., "Observing Proton Tracks in Cellulose Nitrate," Int. J. Appl. Rad. Isotop., 23, 157 (1972).

Cassarett, A. P., Radiation Biology; Prentice-Hall, Inc., New Jersey, 1968.

BIBLIOGRAPHY (Continued)

Chadwick, J., "The Existence of Neutrons," Proc. Roy. Soc., London, A136, 692 (1932).

Charlton, D. E. and Cormack, D. V., "Energy Dissipation in Finite Cavities," Rad. Res., 17, 34 (1962).

Cheka, J. S., Phys. Rev., 71, 836 (1947).

Cheka, J. S., "Recent Developments in Film Monitoring of Fast Neutrons," Nucleonics, 12, 6, 40 (1954).

Clifford, C. E., "Dose Distributions in Phantoms Exposed to 2.95 MeV Neutrons," Health Physics, 15, 572 (1968).

Cohn, C. E. and Armani, R. J., "Automatic Scanning of Mica Track Recorders," Rev. Sci. Inst., 26, 1, 18 (1974).

Cole, A., Simmons, D. J., Cummins, H., Congel, F. J., and Kastner, J., "Application of Cellulose Nitrate Films for Alpha Autoradiography of Bone," Health Physics, 19, 55 (1970).

Costa-Ribeiro, C. and Lobão, N., "Testing of the LR-115 Kodak-Pathé Red Dye Cellulose Nitrate for Alpha Particle Detection," Health Physics, 28, 162 (1975).

Cross, W. G. and Ing, H., "The Use of ^{237}Np in Personal Dosimeters for Fast Neutrons," Health Physics, 28, 511 (1975a).

Cross, W. G. and Ing, H., "Directional Dependence of Fast Neutron Fission Track Dosimeter," P/44, 20th Annual Meeting, Health Physics Society, Buffalo, New York (1975b).

Cross, W. G. and Tommasino, L., "The Electrical Detection of Fission Fragment Tracks for Fast Neutron Dosimetry," Health Physics, 15, 196 (1968).

Cross, W. G. and Tommasino, L., "A Rapid Reading Technique for Nuclear Particle Damage Tracks in Thin Foils," Rad. Effects, 5, 85 (1970).

DePangher, J. and Tochilin, E., "Neutrons from Accelerators and Radioactive Sources," Chapter 23 in Radiation Dosimetry, Vol. III, F. H. Attix, W. C. Roesch, and E. Tochilin, Editors; Academic Press, New York, 1969.

Dutrannois, J., Proc. Int. Congr. Protection Against Accelerators and Space Radiation, CERN-71-16, Vol. 1, Cern, Geneva (1971).

Eenmaa, J., Personal Communication, University of Washington, Seattle (1975).

BIBLIOGRAPHY (Continued)

Eichholz, G. G., Personal Communications, Georgia Institute of Technology (1975).

Elias, H. and Pauly, J. A., Human Microanatomy; F. A. Davis Co., Philadelphia, 1966.

Enge, W., Grahisch, R., Beaujean, R., and Bartholmä, K. P., "Etching Behavior of a Cellulose Nitrate Plastic Detector Under Various Etching Conditions," Nucl. Inst. Methods, 115, 263 (1974).

Ennow, K., Some TSEE Measurements of Dose Gradients at Interfaces, Dosimetry in Agriculture, Industry, Biology, Medicine; IAEA, 179, 1973.

Failla, G., "The Measurement of Tissue Dose in Terms of the Same Unit for All Ionizing Radiations," Radiology, 29, 202 (1937).

Fain, J., Monnin, M., and Montret, ., "Spatial Energy Distribution Around Heavy Ion Paths," Rad. Res., 57, 379 (1974).

Field, S. B. and Parnell, C. J., "The Use of Threshold Detectors to Determine Changes in Fast Neutron Energy Spectrum with Depth in a Phantom," Brit. J. Radiol., 38, 618 (1965).

Fisher, H. L., Jr. and Snyder, W. S., Oak Ridge National Laboratory Report, ORNL-4168, 245 (1967).

Fitzgerald, J. J., Brownell, G. L., and Mahoney, F. J., "Neutron Tissue Dosimetry," Chapter 7 in Mathematical Theory of Radiation Dosimetry; Gordon & Breach Science Publishers, Inc., New York, 1967.

Fleischer, R. L. and Hart, H. R., Jr., "Fission Track Dating," G.E. Report No. 70-C-328 (1970).

Fleischer, R. L. and Price, P. B., "Tracks of Charged Particles in High Polymers," Science, 140, 1221 (1963).

Fleischer, R. L., Price, P. B., and Walker, R. M., "Tracks of Charged Particles in Solids," Science, 149, 383 (1965a).

Fleischer, R. L., Price, P. B., and Walker, R. M., "Ion Explosion Spike Mechanisms for Formation of Charged Particle Tracks in Solids," J. Appl. Phys., 36, 2645 (1965b).

Fleischer, R. L., Price, P. B., and Walker, R. M., "Simple Detectors for Neutrons and Heavy Cosmic Ray Nuclei," Rev. Sci. Inst., 37, 525 (1966).

BIBLIOGRAPHY (Continued)

Fleischer, R. L., Price, P. B., and Walker, R. M., "Nuclear Tracks in Solids," Sci. Am., 220, No. 6, 30 (1969).

Fleischer, R. L., Price, P. B., and Walker, R. M., Nuclear Tracks in Solids; University of California Press, 1975.

Fleischer, R. L., Price, P. B., Walker, R. M., and Hubbard, E. L., "Track Registration in Various Solid-State Track Detectors," Phys. Rev., 133, A1443 (1964).

Fleischer, R. L., Price, P. B., Walker, R. M., and Hubbard, E. L., "Criterion for Registration in Dielectric Track Detectors," Phys. Rev., 153, 353 (1967).

Fleischer, R. L., Viertte, J. R. M., and Price, P. B. (1972); see Becker, K. (1973).

Fowler, J. F., "Fast Neutron Therapy-Physical and Biological Considerations," Chapter 8 in Modern Trends in Radiotherapy, Vol. I, T. J. Deely and C. A. P. Wood, Editors; Appleton-Century-Crofts, New York, 1967.

Fox, W. B., Personal Communication, Oak Ridge National Laboratory (1974).

Frank, A. L. and Benton, E. V., "High Energy Flux Detection with Dielectric Plastics," Rad. Effects., 3, 33 (1970).

Garry, S. M., Stansbury, P. S., and Poston, J. W., "Measurement of Absorbed Dose for Photon Sources Distributed Uniformly in Various Organs of a Heterogeneous Phantom," ORNL-TM-4411, Oak Ridge National Laboratory (1974).

Gold, R., Armani, R. J., Rusch, G. K., and Yule, Th. J., "Fast Neutron Personnel Dosimetry with Solid-State Track Recorders," Nucl. Inst. Methods, 118, 383 (1974).

Goodman, L. J., "Neutron Dosimetry with Tissue-Equivalent Chambers," Symp. on Neutrons in Radiobiology, CONF-691106 (1969a).

Goodman, L. J., "A Modified Tissue-Equivalent Liquid," Health Physics, 16, 763 (1969b).

Gray, J. H., Conger, A. D., Ebert, M., Hornsey, S., and Scott, O. C. A., "The Concentration of Oxygen Dissolved in Tissue at the Time of Irradiation as a Factor in Radiotherapy," Brit. J. Radiol., 26, 638 (1953).

Gray, L. H. and Read, J., "Measurement of Neutron Dose in Biological Experiments," Nature, 144, 439 (1939).

BIBLIOGRAPHY (Continued)

Griffith, R. V., "Particle Registration in Dielectric Materials. A Bibliography," USAEC, Cont. No. W-7405-Eng-48, Lawrence Livermore Laboratory (1974).

Gupton, E. D. and Davis, D. M., "Health Physics Instruments," Chapter 15 in Principles of Radiation Protection, K. Z. Morgan and J. E. Turner, Editors; Robt. E. Krieger Publ. Co., Huntington, New York, reprinted 1973.

Hankins, D. E., "Progress in Personnel Neutron Dosimetry," Proc. Third Int. Cong. of Int. Rad. Prot. Assn., Washington, D. C., CONF-730907, p. 515 (1973).

Haywood, F. F., Burson, Z. G., and Banta, H. E., "A Self-replenishing Tritium Target for Neutron Generators," ORNL-TM-3397, Oak Ridge National Laboratory (1972).

Henke, R. P., Benton, E. V., and Heckman, H. H., "Sensitivity Enhancement of Plastic Track Detectors through Photo-oxidation," Rad. Effects, 3, 43 (1970).

Hollinshead, W. H., Textbook of Anatomy; Harper and Row Publishers, New York, 1967.

Hoy, J. E., "An Albedo-Type Personnel Neutron Dosimeter," Health Physics, 23, 385 (1972).

Hubbel, H. H., Jr., Chen, W. L., Shinpaugh, W. H., and Jones, T. D., "Measured and Calculated Dose Distributions from Neutrons Incident on a Tissue-Equivalent Phantom," Health Physics, 27, 289 (1974); ORNL-TM-3425 (1971), Oak Ridge National Laboratory.

Hurst, G. S., "Ionization Methods of Mixed Radiation Dosimetry," Chapter 6 in Principles of Radiation Protection, K. Z. Morgan and J. E. Turner, Editors; Robt. E. Krieger Publ. Co., Huntington, New York, reprinted in 1973.

Hurst, G. S. and Ritchie, R. H., "Fast Neutron Dosimetry," Radiology, 60, 864 (1953).

Hurst, G. S. and Ritchie, R. H., "Radiation Accidents: Dosimetric Aspects of Neutron and Gamma-Ray Exposures," ORNL-2748 (Pt. A), Oak Ridge National Laboratory (1959).

ICRP, A Review of the Radiosensitivity of the Tissues in Bone, Report No. 11, The International Commission on Radiological Protection, 1967.

ICRU, Neutron Fluence, Spectra, and Kerma, Report No. 13; International Committee on Radiological Units and Measurements, 1969.

BIBLIOGRAPHY (Continued)

ICRU, Radiation Quantities and Units, Report No. 19; International Committee on Radiological Units and Measurements, 1971.

Ing, H. and Cross W. G., "A Criticality Neutron Dosimeter Using the $^{103}Rh(n,n)^{103m}Rh$," Health Physics, 25, 291 (1973).

Jasiak, J. and Piesch, E., "Use of Kodak NTA Personnel Neutron-Monitoring Film as Track Etching Detector," Nucl. Inst. Methods, 125, 545 (1975).

Jee, W. S. S., Dell, B., and Miller, L. G., "High Resolution Neutron-Induced Autoradiography of Bone Containing ^{239}Pu," Health Physics, 22, 761 (1972).

Johnson, D. R. and Becker, K., "Mechanisms and Applications of Nuclear Track Etching in Polymers," ORNL-TM-2826, Oak Ridge National Laboratory (1970).

Jones, T. D. and Auxier, J. A., "Neutron Dose, Dose Equivalent and Linear Energy Transfer from ^{252}Cf Sources," Health Physics, 20, 253 (1971).

Jones, T. D., Snyder, W. S., and Auxier, J. A., "Absorbed Dose, Dose Equivalent and LET Distributions in Cylindrical Phantoms Irradiated by Collimated Beam of Monoenergetic Neutrons," Health Physics, 21, 253 (1971).

Jozefowicz, K., "Energy Threshold for Neutron Detection in Makrofol Dielectric Track Detectors," Nucl. Inst. Methods, 93, 369 (1971).

Jozefowicz, K., "Energy Dependence of the Efficiency of Neutron Detection in Polycarbonate by Recording Atom Recoil Tracks," Paper SM-167/36, Proc. Symp. Neutron Monit. Rad. Prot. Purposes, IAEA, Vienna (1973).

Katz, R. and Kobetich, E. J., Phys. Rev., 170, 397 (1968).

Kerr, G. D. and Strickler, T. D., "The Application of Nuclear Track Detectors to the Hurst Threshold Detector Systems," Health Physics, 12, 1141 (1966).

Khan, H. A., "Semi-Automatic Scanning of Tracks in Plastics," Rad. Effects, 8, 135 (1971).

Khan, H. A., "The Usefulness of Mica and Quartz Track Detectors at High Environmental Temperatures," Nucl. Inst. Methods, 114, 61 (1974).

Khan, H. A., "Enhancement of the Fast-Neutron Detection Efficiency of Solid State Nuclear Track Detectors," Nucl. Inst. Methods, 126, 557 (1975a).

BIBLIOGRAPHY (Continued)

Khan, K. H., "The Effects of Pre-Irradiation Annealing on the Track-Development Properties of Solid-State Nuclear Track Detectors," Nucl. Inst. Methods, 125, 419 (1975b).

Khan, K. H. and Durrani, S. A., "Electronic Counting and Projection of Etched Tracks in Solid State Nuclear Track Detectors," Nucl. Inst. Methods, 101, 583 (1972).

Kortüm, G., Treatise on Electrochemistry; Elsevier Publishing Company, New York, 1965.

Krishnamoorthy, P. N. and Venkataraman, G., "Comparison of Various Neutron Personnel Dosimeters," Paper SM-167/78, Proc. Symp. Neutron Monit. Rad. Prot. Purposes, IAEA, Vienna (1973).

Lark, N. L., "Spark Scanning for Fission Fragment Tracks in Plastic Foils," Nucl. Inst. Methods, 67, 137 (1969).

Lawson, R. C., "The Recoil Proton Dose at a Bone-Tissue Interface Irradiated by Fast Neutrons," Phys. Med. Biol., 12, 551 (1967).

Lawson, R. C., Clare, D. M., and Watt, D. E., "(D,D) and (D,T) Neutron Depth-Dose Measurements in a Tissue-Equivalent Phantom," Phys. Med. Biol., 12, 201 (1967).

Lawson, R. C. and Watt, D. E., "Neutron Depth Dose Measurements in a Tissue-Equivalent Phantom for an Incident Pu-Be Spectrum," Phys. Med. Biol., 9, 487 (1964).

Lück, H. B., "Diameter Evolution of Proton Tracks in Cellulose Nitrate Detector," Nucl. Inst. Methods, 116, 613 (1974).

Lück, H. B., "Investigation of Energy Resolution in Detecting Alpha Particle Tracks Using a Cellulose Nitrate Detector," Nucl. Inst. Methods, 124, 359 (1975).

Maurette, M., "Track Formation Mechanisms in Minerals," Rad. Effects, 3, 149 (1970).

Mayofis, M. I., Plastic Insulating Materials, Van Nostrand, Inc., New York, 1966.

McGinley, P. H., "Fast Neutron Therapy Treatment Planning," Ph.D. Dissertation, Georgia Institute of Technology (1971).

McGinley, P. H. and McLaren, J. P., "Distortion of Fast Neutron Dose Distribution by Bone," Medical Physics, 3, 3 (1976).

BIBLIOGRAPHY (Continued)

McGinley, P. H., Sohrabi, M., Wood, M., Mills, M., Rodriguez, R., "Dose Levels Due to Neutrons in the Vicinity of High Energy Photon Beams from Medical Accelerators," to be presented at 9th Mid Year Topical Symp., Health Physics Soc., Denver, Colorado (1976).

Medveczky, L. and Somogi, G., "Fast Neutron Flux Measurements by Means of Plastics," Paper 6, Int. Conf. Corpuscular Photography, Florence (1966); see also Atomki Kozlem, 8, 226 (1966).

Mijnheer, B. J., Broers-Challiss, J. E., and Broerse, J. J., "Measurements of Radiation Components in a Phantom for a Collimated d-T Neutron Beam," 2nd Eur. Symp. Neut. Dos. in Biol. Medicine, Neuherberg/Munchen (1974).

Mills, W. A. and Hurst, G. S., "Fast Neutron Dosimetry in a Small Tissue-Equivalent Phantom," Nucleonics, 12, 17 (1954).

Monnin, M., "Mechanisms of Track Formation in Polymers," Rad. Effects, 5, 69 (1970).

Monnin, M. and Blanford, G. E., Jr., "Detection of Charged Particles by Polymer Grafting," Science, 181, 743 (1973).

Morgan, K. Z., "The Responsibilities of Health Physics," The Scientific Monthly, 62, 93 (1946).

Morgan, K. Z., Personal Communication, Georgia Institute of Technology (1973).

Morgan, K. Z. and Turner, J. E., Principles of Radiation Protection; Robt. E. Krieger Publ. Co., Huntington, New York, reprinted 1973.

Murray, R. L., Introduction to Nuclear Engineering; Prentice-Hall, Inc. New Jersey, 1961.

NCRP, Protection Against Neutron Radiation, Report No. 38; Recommendation of the National Council on Radiation Protection and Measurements, 1971.

Neufeld, J., "Absorbed Dose and Tissue Dose," Health Physics, 24, 101 (1973).

Nishiwaki, Y., Kawai, H., and Morishina, H., "Techniques of Spark Counting Etched Nuclear Tracks on Plastic Foils for Neutron Monitoring," Paper SM-167/22, Proc. IAEA Symp. Neutron Monit. Rad. Prot. Purposes, IAEA, Vienna (1973).

Piesch, E., Atompraxis, 9, 179 (1963).

BIBLIOGRAPHY (Continued)

Piesch, E., "Development for the New Neutron Detectors for Accidental Dosimetry," Symp. New Dev. Phys. Biol. Rad. Detectors, SM-143/131 (1970).

Piesch, E., "Developments in Radiophotoluminescence Dosimetry," Chapter in Topics in Radiation Dosimetry, Suppl. 1, F. H. Attix, Editor Academic Press, New York, 1972.

Piesch, E. and Burgkhardt, B., "LiF Albedo Dosimeters for Personnel Monitoring in a Fast-Neutron Radiation Field," Paper SM-167/8, Proc. IAEA Symp. Neutron Monit. Rad. Prot. Purposes, IAEA, Vienna (1973).

Piesch, E. and Sayed, A. M., "Depth Dose Distribution Measurements and Attenuation for a Cf-252 Source," 2nd Eur. Symp. Neutron Dos. in Biol. Medicine, Neuherberg/Munchen, 30.9 (1974a).

Piesch, E. and Sayed, A. M., "Latent Track Fading in Solid-State Track Etching Detectors," Nucl. Inst. Methods, 119, 367 (1974b).

Prasad, M. A., Sundaraman, V., and Venkataraman, G., "The Recoil Proton Dose Across a Bone-Tissue Interface Due to Fast Neutrons," Phys. Med. Biol., 16, 461 (1971).

Poston, J. W., "Neutron Depth Dose Distributions in Heterogeneous Phantoms," Ph.D. Dissertation, Georgia Institute of Technology (1971).

Prêtre, S., "Personnel Neutron Dosimeter, Based on Automatic Fission-Track and Spark Counting, for Routine and Emergency Use," Paper SM-167/14, Proc. Symp. Neutron. Monit. Rad. Prot. Purposes, IAEA, Vienna (1973).

Prêtre, S., Tochilin, E., and Goldstein, N., "A Standardized Method for Making Neutron Fluence Measurements by Fission Fragment Tracks in Plastics--A Suggestion for an Emergency Neutron Dosimeter with Rad-Response," Proc. 1st Int. Cong. IRPA, Part I, p. 491 (1968).

Price, P. B. and Walker, R. M., "Chemical Etching of Charged Particles," J. Appl. Physics, 33, 3407 (1962).

Price, P. B., Walker, R. M., and Fleischer, L., "Method of Measuring Fast Neutrons by Observing Multiprolonged Tracks of Charged Particles Formed in Cellulose Nitrate," U.S. Patent No. 3,356,250 (1971).

Rago, P. F., Barral, R. G., and Carter, T. G., "A Sensitive Fast Neutron Monitor Using Fission-Foil Lexan Detectors," Health Physics, 26, 102 (1974).

BIBLIOGRAPHY (Continued)

Randolph, M. L., "First Collision Doses Produced by Fast Neutron Fluxes of Wide Energy Distributions," Rad. Res., 19, 492 (1963).

Roesch, W. C., "Dose for Non-equilibrium Conditions," Rad. Res., 9, 399 (1958).

Roesch, W. C. and Attix, F. H., "Basic Concepts of Dosimetry," Chapter 1 in Radiation Dosimetry, Vol. I, F. H. Attix, W. C. Roesch, and E. Tochilin, Editors; Academic Press, New York, 1968.

Rossi, H. H. and Failla, G., "Tissue-Equivalent Ionization Chambers," Nucleonics, 14, 32 (1956).

Rossi, H. H. and Rosenzweig, W., "Measurements of Neutron Dose as a Function of Linear Energy Transfer," Rad. Res., 2, 417 (1955).

Schultz, W. W., "Track Density Measurements in Dielectric Track Detectors with Scattered Light," Rev. Sci. Insts., 39, 1893 (1968).

Shapiro, J., Radiation Protection - A Guide for Physicists and Physicians; Cambridge Harvard University Press, 1972.

Shapiro, P., Personal Communication, Naval Research Laboratory (1975).

Silk, E. C. H. and Barnes, R. S., "Examination of Fission Tracks with an Electron Microscope," Phil. Mag., 4, 920 (1959).

Sinclair, W. K., "Radiobiology Dosimetry," Chapter 29 in Radiation Dosimetry, Vol. III, F. H. Attix, W. C. Roesch, and E. Tochilin, Editors; Academic Press, New York, 1969.

Smathers, J. B., Personal Communication, Texas A&M University (1974).

Smith, J. W. and Boot, S. J., "The Variation of Neutron Dose with Depth in a Tissue-Equivalent Phantom," Phys. Med. Biol., 7, 45 (1962).

Snyder, W. S. and Neufeld, J., "Calculated Depth Dose Curves in Tissue for Broad Beams of Fast Neutrons," Brit. J. Radiol., 28, 342 (1955).

Sohrabi, M., "Electrodeposition of ^{238}U and Its Application in Fast Neutron Dosimetry by Fission Fragment Registration in Silver Activated Phosphate Glasses," Tehran University Nuclear Center (1969).

Sohrabi, M., Unpublished Data (1971).

Sohrabi, M., "The Amplification of Recoil Particle Tracks in Polymers and Its Application in Fast Neutron Personnel Dosimetry," Health Physics, 27, 598 (1974).

BIBLIOGRAPHY (Continued)

Sohrabi, M. and Becker, K., "Some Studies on the Application of Track Etching in Personnel Fast Neutron Dosimetry," ORNL-TM-3605, Oak Ridge National Laboratory (1971); see also Sohrabi, M., M.S. Thesis, University of Tennessee (1971).

Sohrabi, M. and Becker, K., "Fast Neutron Personnel Monitoring by Fission Fragment Registration from Np-237," Nucl. Inst. Methods, 104, 409 (1972).

Sohrabi, M. and Morgan, K. Z., "Recent Progress in Fast Neutron Personnel Dosimetry Using Track Etch Methods," Paper I4, Proc. Third Eur. Cong. of Int. Rad. Prot. Assn., Amsterdam (1975); see also, Sohrabi, M., Trans. ANS Student Conf., Georgia Institute of Technology, p. 24 (1975).

Somogi, G., "Influence of Thermal Effects on the Track Registration Characteristics of Plastics," Rad. Effects, 16, 233 (1972a).

Somogi, G., "Effect of Ozone Atmosphere on the Detecting Properties of Plastic Track Recorders," Rad. Effects, 16, 233 (1972b).

Spiers, F. W., "Dose in Soft Tissue and Bone," Brit. J. Radiol., 24, 365 (1951).

Spiers, F. W., "A Review of the Theoretical and Experimental Methods of Determining Radiation Dose in Bone," Brit. J. Radiol., 39, 216 (1966).

Spiers, F. W., "Transition Zone Dosimetry," Chapter 32 in Radiation Dosimetry, Vol. III, F. H. Attix, W. C. Roesch, and E. Tochilin, Editors; Academic Press, New York, 1969

Stone, R. S. and Larkin, J. C., "Treatment of Cancer with Fast Neutrons," Radiology, 59, 608 (1942).

Sweeting, O. J., Editor, The Science and Technology of Polymer Films, Vol. II; Wiley-Interscience, New York, 1971.

Theus, R. B., Bondelid, R. O., Attix, F. H., August, L. S., Shapiro, P., Surratt, R. E., and Rogers, C. C., "Physical Characteristics of the NRL Fast Neutron Beam for Radiation Therapy," Cancer, 34, 1, 17 (1974).

Tochilin, E. and Shumway, B. W., "Dosimetry of Neutrons and Mixed Neutron Fields," Chapter 22 in Radiation Dosimetry, Vol. III, F. H. Attix, W. C. Roesch, and E. Tochilin, Editors; Academic Press, New York, 1969.

BIBLIOGRAPHY (Concluded)

Watt, D. E., Lawson, R. C., and Clare, D. M., An Experimental Appraisal of the Validity of Neutron Dosimetry Theory in Radiation Protection Neutron Monitoring; IAEA, Vienna, p. 27, 1967.

Wilenzick, R. M., Almond, P. R., Oliver, G. D., and DeAlmeida, C. E., "Measurements of Fast Neutrons Produced by High Energy X-Ray Beams of Medical Electron Accelerators," Phys. Med. Biol., 18, 3 396 (1973).

Wilkie, W. H., "Theoretical Image-Forming Quality of Fast Neutron Radiography," Ph.D. Dissertation, Georgia Institute of Technology (1970).

Williamson, F. S., Jordan, D. L., and Hundnut, D., "The Janus Reactor. I. Preliminary Dosimetry in the Exposure Rooms," Rep. ANL-7136, Argonne National Laboratory (1965).

Wingate, C. L., Gross, W., and Failla, G., "Experimental Determination of Absorbed Dose from X Rays Near the Interface of Soft Tissue and Other Materials," Radiology, 79, 284 (1962).

Young, D. A., "Etching of Radiation Damage in Lithium Fluoride," Nature (London), 182, 375 (1958).

Zirkle, R. E., Marchbank, D. F., and Kuck, K. D., "Exponential and Sigmoid Survival Curves Resulting from Alpha and X Irradiation of Aspergillus Spores," J. Cellular Comp. Physiol., 39, Suppl. 1, 75 (1952).

Zolotukhin, V. G., Obatov, G. M., Prokoviera, Z. A., Kerim-Markus, I. B., Kochetov, O. A., and Tzvetov, V. I., "Influence of Incidence Angle of Monoenergetic Neutrons on Dose Equivalent Distribution for Recoil Nuclei in Man's Phantom," Health Physics, 20, 205 (1971).

VITA

Mehdi Sohrabi was born in Tehran, Iran on April 16, 1944. He received a Bachelor of Science degree in Physics from the Faculty of Sciences of the University of Tehran in 1965. After graduation, he participated in a training program in Mechanics offered by the National Iranian Oil Company. Following this program, he served as a Second Lieutenant in the Imperial Army of Iran for 18 months.

In April 1967, Mr. Sohrabi was employed as a staff member by the University of Tehran. In this position, he was active in operational health physics and dosimetry research especially in neutron dosimetry. After the opening of the Research Reactor of Tehran, a five MW pool-type reactor, he was placed in charge of reactor health physics. In 1969, he received a Master of Science degree in physics from the University of Tehran.

In 1970, Mr. Sohrabi was awarded an International Atomic Energy Agency Fellowship to do research in the Health Physics Division of Oak Ridge National Laboratory. While at ORNL, he was interested in operational health physics and dosimetry for human exposures and radiobiology and he did some research in this area. His simultaneous work at the Graduate School of the University of Tennessee, Knoxville, was completed with another Master of Science degree in Physics in 1971.

In 1972, Mr. Sohrabi joined Georgia Institute of Technology to pursue his graduate studies towards a Doctor of Philosophy degree in Nuclear Engineering. In 1973, under the guidance of Dr. Karl Z. Morgan,

he established this research program, and since then has received two research grants from the U. S. Energy Research and Development Administration. He served as a co-principal investigator in these projects.

He is the author or co-author of the following papers, publications and reports:

1. "Electrodeposition of U-238 and Its Application in Fast Neutron Dosimetry by Fission Fragment Registration in Silver Activated Phosphate Glasses," M.S. Thesis, University of Tehran (1969).

2. "Some Studies on the Application of Track Etching in Fast Neutron Personnel Dosimetry," M.S. Thesis, University of Tennessee, Knoxville (1971); see also ORNL-TM-3605 (1971), with Klaus Becker.

3. "Fast Neutron Personnel Monitoring by Fission Fragment Registration from Np-237," Nucl. Inst. Methods, 104, 409 (1972), with Klaus Becker.

4. "Fading Characteristics of Various Films and Solid State Dosimeters in a Warm and Humid Climate," Paper 58, 17th Annual Meeting, Health Physics Society, Las Vegas (1972), with others.

5. "Electrochemical Amplification of Recoil Particle Tracks in Polymers and Its Application in Fast Neutron Personnel Dosimetry," Health Physics, 27, 598 (1974).

6. "Recent Developments in Fast Neutron Personnel Dosimetry Using Track Etch Methods," Paper I4, 3rd European Congress IRPA, Amsterdam, The Netherlands (1975), with Karl Z. Morgan; see also Trans. Am. Nucl. Soc. Student Conf., p. 24 (1975). (This paper received an award as the best paper of the Health Physics Session at the American Nuclear Society Student Conference.)

7. "Development and Application of Some Fast Neutron Dosimetry Techniques Utilizing Plastic Track Detectors for Therapy and Health Physics," USERDA Contract No. AT-(40-1)-4814 (1975), with Karl Z. Morgan.

8. "Thickness Dependence of a Simple Fast Neutron Dosimeter," Paper CB7, Southeastern Section, American Physical Society, November 13-15, Auburn, Alabama (1975), with Karl Z. Morgan.

Mr. Sohrabi has many years of teaching and research experience in the institutions and universities with which he has been associated. He has been active in some social and scientific groups and he is a member

of the Health Physics Society, the International Radiation Protection Association, the Society of Sigma Xi, and the Iranian Radiation Protection Society.